THE INTERACTION OF FILLERS AND LUBRICANTS IN RIGID PVC COMPOSITIONS

by

STEPHEN THOMAS PEPPER

A DOCTORAL THESIS submitted
in partial fulfilment
of the requirements for the
award of Doctor of Philosophy of the
Loughborough University of Technology

1988

Supervisor: M. Gilbert, PhD

Institute of Polymer Technology
and Materials Engineering

CERTIFICATE OF ORIGINALITY

This is to certify that I am responsible for the work submitted in this thesis, that the original work is my own except as specified in acknowledgements, and that neither the thesis nor the original work contained herein has been submitted to this or any other institution for a degree.

S. T. Pepper

ACKNOWLEDGEMENTS

I am deeply indepted to my supervisor, Dr Marianne Gilbert, for her invaluable assistance and unceasing encouragement.

I wish to acknowledge the Science Engineering Research Council and Cookson Group plc for the joint financial support throughout this research project.

My thanks also go to: -

Dr Andrew Craig, Cookson Industrial Materials Ltd, for enthusiastic support and discussions as my collaborative supervisor.

Dr Michael Hancock and Dr Robert Higgs, ECC International Ltd, for advice and suggestions during a number of joint meetings.

The technical staff at Cookson Research laboratories for the genuine desire to help during my visits to their laboratories.

The technicians at IPTME, especially Mr Ray Owens and Mr Tony Davies, who never refused a request.

I am especially grateful to Miss G. A. Hunt for her assistance and patience during the preparation of this thesis

ABSTRACT

The physical properties of rigid PVC products can be related to formulation, preblending and processing characteristics. A fuller understanding between these interrelations involves investigation of a complete processing system from powder additives to end product. A knowledge of these relationships can lead to a optimisation of formulation aspects and processing conditions.

Fillers and lubricants have often been incorporated into PVC compounds on a empirical basis, however in this investigation a wide range of compositions were carefully chosen and included a calcium carbonate filler at levels upto 40 phr. These were dry blended and then characterised by bulk density and filler content. The premix was processed using an instrumented twin screw extruder, a wide processing 'window' being chosen to provide a product range with large variations in fusion level. Further compounds were extruded, incorporating two different impact modifiers.

The extrudates was assessed for degree of fusion by differential thermal analysis, solvent immersion and microscopy. The filler distribution, surface appearance and residual grain structure was observed using a range of microscopy techniques and the results related to operating conditions. A measure of fusion level was obtained from master curves of heat of fusion versus 'processing temperature'. The filler level did not influence the degree of fusion.

Various mechanical properties of the pipe were assessed. Impact performance was measured using an instrumented falling weight impact tester and the subsequent fracture behaviour depended on the composition and fusion level. Impact properties were dramatically reduced at a critical filler content and ductile-brittle transition temperatures were obtained for the extrudates by testing at low and high temperatures. Tensile properties did not follow the trends observed during impact testing but indicated a progressive reduction in tensile properties with increasing filler content.

LIST OF SYMBOLS

A	-	Endothermic area of A peak
	-	Tensile specimen overall length
	-	Cross sectional area
B	-	Time base setting
	-	Tensile specimen width
	-	Endothermic area of B peak
$\bar{\gamma}$	-	Average shear strain
C	-	Length of narrow portion of specimen
ΔH_A	-	Energy of endotherm A
ΔH_B	-	Energy of endotherm B
ΔH_F	-	Heat of fusion
ΔH_P	-	Heat of fusion for polymer
ΔH_{MAX}	-	Maximum heat of fusion
ΔP	-	Extrusion pressure
ΔP_{ENT}	-	Pressure loss due to entrance effects
ΔP_{VISC}	-	Viscous pressure loss
Δq_s	-	Y axis sensitivity
D	-	Capillary diameter
	-	Width of narrow portion of specimen
ε_B	-	Elongation at break
ε_Y	-	Elongation at yield
E	-	Cell calibration constant
	-	Small radius
E_F	-	Impact failure energy
E_0	-	Available impact energy
E_{TOT}	-	Total energy available
F	-	Large radius
F_B	-	Tensile force at break
F_Y	-	Tensile force at yield
g	-	Acceleration due to gravity
G	-	Distance between reference lines
h	-	Test height
H	-	Distance between sample grips
I	-	Thickness (preferred)
K_{IC}	-	Fracture toughness

l_B	-	Extension at break
l_o	-	Initial guage length
l_Y	-	Extension at yield
L	-	Capillary length
m	-	Sample mass
	-	Impact mass
$\dot{m}$	-	Extruder mass output
v	-	Velocity
n	-	Viscous loss term
ϕ_F	-	Volume fraction of filler
P	-	Pressure
P1	-	Metering zone pressure
P2	-	Adaptor pressure
P3	-	Pipe head pressure
Q	-	Specific energy consumption
R	-	Capillary radius
σ_B	-	Ultimate tensile stress
σ_{REL}	-	Relative tensile stress
σ_Y	-	Yield stress
s.d	-	Sample standard deviation
S	-	Stress concentration function
S_R	-	Recoverable shear strain
SS	-	Screw speed
τ	-	Shear stress
$\bar{\tau}$	-	Average shear stress
T_G	-	Glass transition temperature
TM1	-	Adaptor temperature
TM2	-	Pipe head temperature
TM3	-	Screw temperature
TQ	-	Measured torque
TQ_o	-	Torque under no load conditions
y	-	Predicted head pressure
y_P	-	Multiple regression value for pressure

TABLE OF CONTENTS

CHAPTER ONE

LITERATURE REVIEW

1.1 INTRODUCTION

1.1.1 POLY(VINYL CHLORIDE)

Poly(vinyl chloride) (PVC) is a large tonnage thermoplastic which has been commercially available since the beginning of the last war. Its wide acceptance has been attributed to the scope of additives which enable a host of compositions to be formulated and these additives have to a large extent overcome the inherent processing problems of PVC. The versatility of this polymer can be highlighted by its range of material properties and applications which result in both flexible and rigid products.

1.1.2 CONSUMPTION AND APPLICATIONS OF PVC

The consumption of PVC has dramatically increased since the war with the notable exceptions of the oil crisis in 1974 and the discovery that VCM is a major health hazard. The current importance of PVC can be shown in the table 1.1 depicting the UK consumption of plastics.

The major application areas for PVC are vast and can be highlighted by considering the breakdown of PVC consumption in Western Europe [2] as shown in table 1.2.

Table 1.1 and 1.2 illustrate that PVC is a large tonnage commodity plastic with a wide number of product ranges. The material has obtained an important market share by its competitive material cost, versatility and low conversion costs [3]. The future expected growth areas include UPVC pipe, UPVC windows, biaxially blown bottles, rigid foams and crosslinked plasticised PVC [3, 4].

TABLE 1.1

UK consumption of plastics [1]

('000t)	1985	1986
Low density PE+LLDPE	580	610
High density PE	250	275
Polypropylene	330	370
PVC	450	484
Polystyrene	148	156
Expandable Polystyrene	30	33
Polyamides	22	23
ABS copolymer	55	58
Acetals	11	12
PET/PBT	41	45
Acrylics	28	29
Polyester film	24	24
Phenolic resins	50	49
Amino resins	125	131
Polyester resins	51	53
Epoxides	18	19
Urethanes	94	100
Others	295	265
TOTAL	2602	2736

TABLE 1.2

PVC Market in Western Europe

MARKET	1986 ('000t)	% Total
Rigid PVC		
Bottles	342	8·3
Film and Sheet	436	10·5
Injection moulding	81	2·0
Pipe and Conduit	990	23·9
Profile Extrusion	536	12·9
Records	77	1·9
Miscellaneous	93	2·2
TOTAL RIGID	2555	61·7
Plasticised PVC		
Coated Fabrics	161	3·9
Film and Sheet	338	8·2
Flooring	210	5·1
Tubing and profiles	167	4·0
Wire and Cable	394	9·5
Miscellaneous	162	3·9
TOTAL PLASTICISED	1432	34·6
Other applications	153	3·7
TOTAL CONSUMPTION	4140	100·0

1.1.3 MANUFACTURE OF PVC

1.1.3.1 VINYL CHLORIDE MONOMER PRODUCTION

The modern production of vinyl chloride monomer (VCM) does not depend upon acetylene as a raw material, since the growth of the petrochemical industry has provided a ready supply of ethene. Ethene is converted to VCM via two distinct processes [5].

A) The traditional ethene conversion process involves two main stages :-

Stage One:

$$CH_2{=}CH_2 + Cl_2 \xrightarrow[30\text{-}50\,^{\circ}C]{\text{Ferric Chloride}} CH_2Cl{-}CH_2Cl$$

Ethene + Chlorine → Ethylene dichloride

Stage Two:

$$CH_2Cl{-}CH_2Cl \xrightarrow[500\,^{\circ}C\ @\ 3\ Atms]{\text{Kaolin Catalyst}} CH_2{=}CHCl + HCl$$

Ethylene dichloride → VCM + Hydrogen chloride

B) A one stage conversion process has been recently introduced using a balanced oxychlorination process.

$$CH_2{=}CH_2 + HCl + \tfrac{1}{2}O_2 \xrightarrow[250\text{-}315\,^{\circ}C]{\text{Cupric Chloride}} CH_2{=}CHCl + H_2O$$

Ethene + Hydrogen chloride + oxygen → VCM + Water

VCM is a sweet smelling gas (B.Pt -13°C) which may be stored as a liquid under pressure without a polymerisation inhibitor.

1.1.3.2 TOXICITY OF VCM

VCM was not originally considered a health hazard, although hazards of fire, explosion and narcosis were appreciated, until the mid 1960's when some PVC plant operators contracted various diseases including acro-

osteolysis, Raynaud's syndrome and scleroderma [6]. Further work using animals to elucidate the causes and connection of VCM to these diseases revealed a rare fatal cancer of the liver named as angiosarcoma of the liver. The indications of this work [7] and many others suggested that VCM was a human carcinogen and these preliminary investigations were confirmed with the discovery of a number of cases where plant operators had contracted angiosarcoma. The new hazards of VCM resulted in radical changes in plant design, plant operation and removal of residual VCM. These improvements were introduced in 1974 and reduced plant VCM levels from approximately 300 ppm (parts per million) to less than 5 ppm. The present EEC directive has stipulated a technical long term limit value (TLTLV) of less than 3 ppm.

1.1.3.3 POLYMERISATION OF VCM

PVC is commercially polymerised by four techniques: -

i) Suspension
ii) Bulk or Mass
iii) Emulsion
iv) Solution

Suspension polymerisation predominates over bulk and emulsion techniques in terms of tonnage, approximately 80% of world nameplate capacity [8], while solution polymerisation is mainly used for copolymers and speciality applications. Suspension and mass polymers are generally characterised by their coarse particle size (100-150 μm diameter), high bulk density and good free flowing properties while emulsion polymers are finer in size (0·1-2 μm diameter) and have good plasticiser absorption properties [9].

The typical product applications for the grades of PVC produced via the differing polymerisation techniques are highlighted in the following table.

TABLE 1.3

Ranges of application of PVC [10]

PVC-types / processing	rigid-PVC			plasticized-PVC		
	E	S	B	E	S	B
	K-values			K-values		
calendering	(60-65)	57-65	57-65	70-80	65-70	70
thermal refined films	75-80	-	-	-	-	-
floor covering	-	-	-	60-80	50-70	
extrusion of rigid PVC						
pressure pipes	70	67-68	67-68			
profiles	65-70	65-67	57-68			
sheets and flat films	60-65	60	60			
blown films	60	57-50	60			
extrusion of plasticized-PVC						
general				65-70	65-70	65-70
cable materials				-	65-80	
mainly				-	70	70
blow moulding	-	57-60	58-68		65-80	60-65
injection moulding	-	55-60	56-60	-	55-70	55-60
processing of pastes	-	-	-	70-80	70-80	

1.1.4 CLASSIFICATION OF PVC

The requirements of PVC depend upon the exacting nature of its application, however an ASTM publication lists the major criteria for the classification of PVC [11].

Molecular Weight

Molecular weight can be assessed via solution viscometry to yield a viscosity number (0·5% solution of PVC in cyclohexanone at 25°C) or related to a 'K' value (Fikentscher 'K' value). The molecular weight of PVC has an important bearing upon the processability and physical properties of the polymer, in general a compromise is taken between a high level of mechanical performance (high 'K' value) and easier processing (low 'K' value). The previous table, table 1.3, demonstrated that low 'K' values were generally used for intensive processing operations such as

injection moulding while in heavily plasticised applications, such as pastes, a high 'K' value is advisable in order to retain the level of physical properties.

The molecular weight distribution of PVC can be assessed by gel permeation chromatography (GPC) to yield important processing information.

Sieve Analysis

The PVC polymer may be sieved and the percentage retained measured to ensure that no large grains are present, alternatively the particle size distribution may be measured via a bank of sieves or other techniques such as a Coulter counter, microscopy etc. The particle size, particle distribution and particle shape have a significant influence upon processing techniques and bulk handling equipment.

Bulk Density

Bulk density is a measure of the weight per unit volume of PVC particles and can be related to the spherical shape and particle size distribution of PVC. A high bulk density indicates a high packing efficiency and is preferred for maximum output from processing equipment.

Plasticiser Absorption

The amount of plasticiser absorbed is a function of particle size, surface area and porosity of the PVC grains. The ability of a particular grade of PVC to absorb a plasticiser is important in assessing the dry blend characteristics of plasticised compositions. The porosity of PVC grains may be examined by techniques such as light microscopy and mercury intrusion porosimetry [12].

Dry Flow

The ability of PVC powder to flow through restrictions and hoppers is important for many processes and can be assessed by the flow of the powder through a standard funnel.

Electrical Conductivity

The electrical properties of PVC can be considerably reduced by impurities such as surfactant residues etc and thus a measure of electrical conductivity can be used to assess the purity of the PVC material.

Other tests which may be useful to characterise PVC include percentage heat loss, heat stability, 'fish-eyes' content (ungelled PVC in a milled sheet), transparency and, of course, processing studies.

1.2 ADDITIVES FOR PVC

1.2.1 INTRODUCTION

PVC, unlike its main competitors, is unique in that a technology has been borne to overcome the poor inherent processing stability of the polymer. Thus PVC technology usually involves the introduction of additives to facilitate acceptable processing, extend material properties, reduce cost etc. The range of additives is vast but in general the main additives can be listed as follows [14] :-

Stabilisers	Fillers
Plasticisers	Pigments
Impact modifiers	Lubricants
Polymeric Processing Aids	Extenders

Miscellaneous additives include :- Blowing agents, dyes, fire retardants, antistatic agents, fungicides, light stabilisers, brighteners, viscosity depressants etc.

1.2.2 STABILISERS

The processing of PVC usually involves a temperature and shear history and since PVC is notoriously susceptible to decomposition under these conditions, then the

introduction of stabilisers is commonplace.

The effects of degradation include :- colour change due to polyene formation, acidic gas (HCl), voids due to gaseous byproducts, streaks of degraded material during processing, dramatic reduction in mechanical/electrical performance and attack of corrosive gas upon processing machinery and personnel.

The actual mechanisms of degradation and associated theory of stabilisation have not be universally agreed, however the generally accepted requirements of an effective 'ideal' stabiliser might be as follows [14, 15, 16]:

i) The reaction with hydrogen chloride.
ii) The replacement of structural weaknesses with more stable groups.
iii) The rendering of pro-degradent substances innocuous.
iv) The interruption of conjugated polyene structures.
v) The neutralisation or removal of resin impurities or contaminates.

A PVC stabiliser may be expected to comply to one or more of these requirements but it is unlikely that a stabiliser will be effective in all of these criteria. PVC stabilisers may be categorised into three main classes [12, 16]:

Primary Heat Stabilisers

Lead salts, heavy metal salts and organotin compounds

Secondary Heat Stabilisers

Organic compounds, organophosphites and epoxy compounds

Light Stabilisers

Cadmium compounds, tin compounds, organophosphites etc.

Primary stabilisers can be combined with the less effective secondary stabilisers and in some circumstances a synergistic behaviour has been noted. In this project lead salts were exclusively used; these primary stabilisers are, in general, powerful, low cost and versatile and some lead salts have a dual purpose as a lubricant. However lead compounds are: toxic (restrictive legalisation in certain applications), sulphur staining, restricted by a safe lead content otherwise voiding may occur and lastly PVC compositions containing lead compounds are generally opaque due to the tinctorial power of the stabiliser.

1.2.3 LUBRICANTS

1.2.3.1 INTRODUCTION

Lubricants are primarily used in PVC compounds to facilitate easier processing, greater output, lower heat and shear history and better surface finish. Unfortunately the interaction of these materials is not well understood and poor formulation can lead to products which are under or overfused, possess poor physical properties and possibly have a poor aesthetic appearance. The incorporation of lubricants is further complicated by the available commercial range, contrasting literature and the requirement that lubricants should be tailored to specific formulations and processing machinery.

1.2.3.2 LUBRICATION MECHANISMS

Lubricants are generally classed into two differing groups: internal and external.

EXTERNAL

These materials provide a lubricating layer between a polymer melt and hot metal surface, their lubricating efficiency in this manner depends upon low compatibility

especially at operating conditions and a strong boundary film. Poor formulation or excessive lubrication can result in 'plate-out', poor fusion, possible reduction in properties, melt slippage and poor surface finish.

INTERNAL

These additives are fundamentally different to external lubricants since lubrication occurs by a reduction in the internal friction of the melt at the processing temperature. The characteristics of internal lubricants are increased compatibility with PVC and little affinity for the hot metal surface. They reduce heat-build up of the melt and lower melt viscosity. While external lubricants are commonly referred to as fusion retarders, these materials have little effect upon fusion rates or are deemed mild fusion promoters.

1.2.3.3 CLASSIFICATION OF LUBRICANTS

The commercial range of additives classed as lubricants is vast and their chemical formulation equally varied, however lubricants can be considered as a member of one of the following groups [17]:

a) Straight chain carbon molecules: paraffin and hydrocarbon waxes.

b) Straight chain carbon molecules with polar end groups: fatty acids and fatty acid esters.

c) Polar centre molecules with long carbon chains attached: metal stearates.

Although the chemical nature of common lubricants can be classed into well defined groups, their action is far more difficult to generalise. The efficiency and nature of lubricants have been considered by an array of techniques:

Chemical structure and polarity [18-20].
Torque rheometry [21-25].
Optical properties such as haze [20, 23, 26-27].
Capillary rheometry [28-29].
Glass transition temperature [19, 27].
'Fluidity' test [18, 26].
Optical wetting and penetration [30].
Frictional forces through extrusion die [31].
Mechanical properties [18, 26, 32-34].
Processing studies [17, 22, 34-36].

Most studies have attempted to relate the action of a lubricant with a measurable property such as torque rheometry or have observed the relationship between the role of a lubricant and its chemical structure. For example Marshall and Jacobsen [26, 18] identified the optical property, haze, as a measure of the lubricant's function in PVC, poor haze representing poor compatibility and thus a more external nature.

Hartitz [23] considered the Brabender™ torque rheometer as a tool which could class a lubricant into two groups; the first group had little or no effect upon fusion time at any concentration ('internal') while the second group of lubricants significantly delayed fusion time ('external').

King and Noël [19] conducted a fundamental study using differential scanning calorimetry to detect slight changes in the glass transition temperature (T_G) of PVC when blended with lubricants. The level of T_G reduction indicates lubricant compatibility and effectiveness as an internal lubricant.

A simplified overview of the publications concerning single component lubricated compositions suggest that straight chain carbon lubricants are mainly external in processing behaviour. Straight chain carbon molecules with polar end groups are possibly intermediate and lastly polar groups with long chain carbon molecules can be grouped as

internal lubricants. Formulation studies using the aforementioned techniques have led to contrasting views on a number of well known commercial lubricants, for example a number of workers [24, 30] have suggested that calcium stearate behaves as an external lubricant, while other processing studies [17, 22, 25, 37] have categorised calcium stearate as a fusion promoter which thus should be classed as an internal lubricant.

The understanding of these additives is further complicated since many UPVC compositions incorporate combinations of differing lubricants; the composition of these systems is, in general, based upon empirical knowledge rather than scientific appraisal.

1.2.3.4 MULTIPLE-COMPONENT LUBRICANT SYSTEMS

The interaction of various lubricant combinations have been assessed [23, 25, 27, 29, 32, 36, 38, 39] and a number of these studies have revealed a synergistic influence between commercial combinations. Rabinovitch [27] assessed the combination of calcium stearate with paraffin wax and reported a synergistic response at intermediate levels upon toughness, surface finish and extruder power requirements. An 'ideal' model was proposed which was based upon a mobile layer of calcium stearate adhering to PVC primary particles and the hot metal surface, with a interlayer within the calcium stearate film of paraffin wax molecules. Thus the interaction of these components at a specific ratio provides a better boundary layer.

Hartitz [23] blended a number of metal soaps with lubricants of an external nature and noted a synergistic delay in fusion time as measured on a Brabender plastograph. Yu *et al* [38] propounded a delay in fusion behaviour for certain combinations of paraffin wax and calcium stearate; this phenomenal delay could not be explained on the basis of the work within the paper.

1.2.4 FILLERS

PVC has been filled, at some period of time, with almost every variety of filler available, and the extent of the filler range can shown in the following figure [40, 41]:

FIGURE 1.1

Fillers for PVC

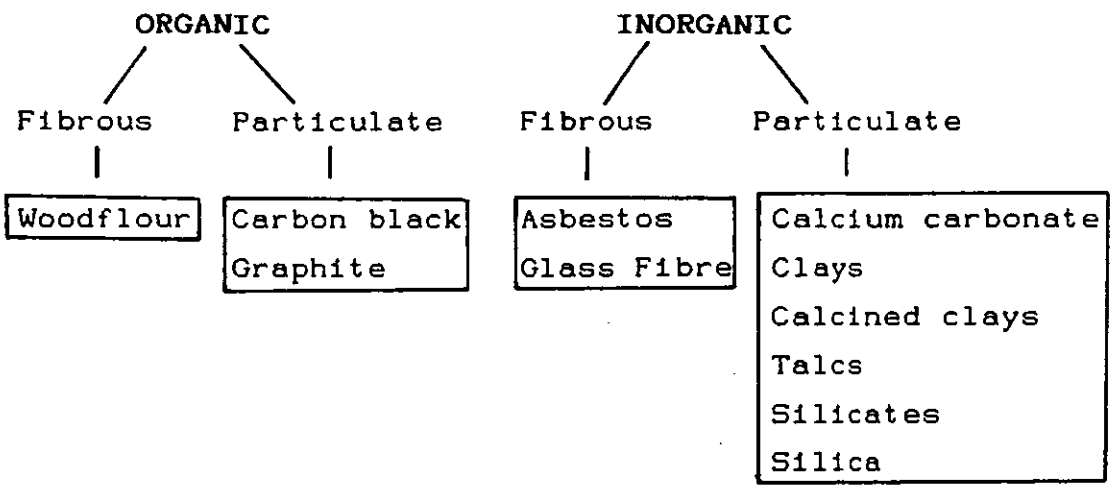

Although the range of fillers is vast, the main commercial filler is predominantly calcium carbonate obtained by natural or synthetic routes. Calcium carbonate is incorporated in most opaque UPVC formulations and far outstrips all the other fillers in terms of application and tonnage, for example the Western Europe consumption of calcium carbonate is approximately 100,000 tonnes per annum [42].

1.2.4.1 GENERAL REQUIREMENTS OF A PVC FILLER

The desirable characteristics of a PVC filler depend to a large extent upon the intended application, however, the basic criteria may be listed as follows [40, 41, 43]:

i) Maximum improvement *or* no deleterious effect upon properties
ii) Low moisture content
iii) Good wetting of polymer matrix
iv) Freedom from impurities
v) Appropriate specific gravity
vi) Low cost and good availability
vii) Non-flammable
viii) Absence of odour and good colour
ix) Chemical resistance and heat resistance
x) Available in range of controlled particle size and particle size distribution
xi) Good processing and dispersion characteristics
xii) Low water solubility and low plasticiser uptake

It is unlikely that a filler candidate will be ideal in each of the above performance criteria, but generally a compromise is taken between amount, type, characteristic of the filler and the properties of the filled compound.

The properties which can characterise a filler and have a direct bearing upon selection criteria can be reviewed as follows [15, 40, 43, 44];

a) Particle shape, size and distribution
b) Surface area
c) Oil absorption
d) Bulk density
e) Specific gravity
f) Refractive index, opacity and colour
g) Hygroscopicity and moisture content
h) Hardness and modulus
i) Surface treatment
j) Chemical composition and impurities

1.2.4.2 CALCIUM CARBONATE AS A FILLER FOR PVC

A coated calcium carbonate filler was used throughout this program. The popularity of the filler can be related to its low cost, abundance, non-toxicity and

versatility in terms of particle criteria. A number of technical advantages have been proposed for the prudent incorporation of calcium carbonate fillers:

Advantages

Low cost
Non toxic, non irritating, odourless
White, low refractive index and easily coloured
Softness (Mohs hardness of ≈3)
Abundant raw material from natural minerals
Synthetic production from calcium salts
Wide range of particle size and distributions
Easily coated in dry form
Antiplate agent
Acid acceptor
Pigment
Reduction in shrinkage problems
Stability over wide temperature range

Disadvantages

Attacked by acids
At high temperatures, calcium carbonate decomposes
Little/zero reinforcing of properties
Relative high moisture content
Processing of filled compounds may prove difficult
Low stiffness filler
Final specific gravity of compound increased

1.2.4.3 MANUFACTURE OF CALCIUM CARBONATE FILLERS

Calcium carbonate can be obtained via three main techniques to produce: purified ground calcium carbonate, dry processed coarse calcium carbonate and precipitated calcium carbonate [41, 44-47].

Dry processed calcium carbonate grades are not widely used since the dry grinding of natural minerals produce a coarse particle size distribution and inherent

impurities which can lead to dark and inferior products in terms of mechanical properties.

Precipitated calcium carbonate fillers can produce high quality grades which are considered to infer the best combination of properties upon PVC. These grades are produced synthetically by a recarbonation process which regenerates calcium carbonate by precipitation from calcium hydroxide. The mean particle size can be of a very low order, for example 0·2-2·0 μm.

Purified calcium carbonate grades have gained recent commercial interest and involve the wet grinding of purified natural minerals such as chalk deposits. The median particle is intermediate between the two other types, approximately 1-10 μm.

1.2.4.4 SURFACE TREATED CALCIUM CARBONATE FILLERS

The possible advantages of coating calcium carbonate fillers have been known for some time [45] and the typical coating agents are stearic acid and calcium stearate, although other coatings have been tried [48-49]. The coatings can be applied by dry blending in high speed mixers. The main reasons for the coating of purified grades of calcium carbonate are considered as follows [48,50]:

a) Lower oil/plasticiser absorption
b) Less hydrophilic nature
c) Increased thermal stability due to stabilising effect of coating
d) Reduced problem of filler agglomeration
e) Processing aid
f) Better 'wetting' of PVC matrix

1.2.4.5 PROPERTIES OF CALCIUM CARBONATE FILLED SYSTEMS

There are few publications concerning the properties of calcium carbonate filled systems, especially at levels

greater than 20% and the vast commercial range adds to the ambiguity of the situation. The studies have tended to highlight the importance of dispersion and particle size/distribution.

The 'top cut' of a filler grade, namely the upper 10% of the particle size distribution, can have a dramatic effect upon properties such as notched impact resistance, surface appearance, tear resistance and machine wear on processing equipment [46,51]. Similarly coarser grades of calcium carbonate can produce substantially inferior products since relatively large particles (in excess of 10 μm) can act as zones whereby concentration of stresses occurs [50,52]. Alternatively, fine particle size calcium carbonate fillers have been known to provide enhancement to properties such as notched impact resistance [34,46,51,53-54]. The fine grades of calcium carbonate provide large filler surface areas and thus many bonding sites for interaction with the polymer matrix, hence the retention and possible enhancement of some mechanical properties [51].

An important feature in the use of filler additives is dispersion; poorly dispersed filler is similar in behaviour to the presence of oversized or large particles. The effect of poor dispersion was unintentionally observed by various workers [53,55].

Chauffoureaux and fellow colleagues [53] prepared a joint report upon calcium carbonate filled PVC from a number of companies. The investigative study considered two coated fillers (mean particle sizes: 0·07 and 2·4 μm) at two loadings, 10 and 20%. The first stage of the work involved the production of sheets by extrusion and testing the respective samples between 'houses' for a large number of properties. Impact performance, drop ball and tensile impact, clearly demonstrated that the fine particle size filled grades were significantly inferior when compared to unfilled and coarse filled extrudates. These results were linked to poor dispersion as observed by scanning electron microscopy. The micrographs illustrated the gross

agglomeration of the finer particle sized filler and this poor dispersion was accepted as the main contributory factor for the poor impact behaviour. The second stage of work produced samples of the same formulations by two roll milling and then compression pressing, this mixing procedure removed any agglomerates greater than 1 μm. In this case the impact performance of the samples were significantly improved by the addition of 10-20% of the fine particle size coated calcium carbonate, an improvement of approximately 2 and 6 fold respectively being observed.

The dispersion of fine particle size filler may be aided by the coating which is considered to act as a lubricant surrounding the filler particles to prevent agglomeration and aid mixing.

Specific properties such as tensile, tear, fatigue and low temperature are generally lowered, while physical criteria including tensile creep behaviour, fracture toughness (K_{Ic}), moduli (tensile, Young's, flexural), weathering and shrinkage are enhanced. Impact behaviour depends upon filler specification and processing conditions.

Thus filler loading, dispersion, grade, coating and particle size characteristics have a important bearing upon the properties of filled PVC products [51-53, 56].

1.2.5 IMPACT MODIFIERS

The impact performance of UPVC can be substantially improved by the addition of modifiers. Although the fracture behaviour of PVC is not considered brittle, the general pattern of usage demands more resilient products. Outdoor applications such as cladding, window profiles and rainwater products specify adequate impact retention even at sub-zero temperatures. The impact performance of many PVC products is critically dependant upon slight changes in formulation and/or processing conditions. The use of modifiers can provide a well balanced composition which does not respond dramatically to these minor alterations.

1.2.5.1 IMPACT MODIFIER CLASSIFICATION

Modifiers are generally semi-compatible with PVC and are based upon rubbery-type materials, although it can be argued whether certain fillers, such as fine precipitated calcium carbonate, should be considered as impact modifiers in a separate class. However the major additives which are termed impact modifiers can be listed as follows:

Acrylonitrile/butadiene/styrene (ABS)
Methyl methacrylate/butadiene/styrene (MBS)
Acrylics; All acrylics or modified acrylics (ACR)
Ethylene vinyl acetate (EVA)
Chlorinated polyethylene (CPE)

These additives can be melt blended or, in the case of EVA and CPE, grafted to PVC by adding the preformed modifier to the PVC prepolymerisation ingredients. The level of addition is typically between 5 and 15%.

MBS and ABS are not recommended for outdoor applications due to poor UV stability associated with the butadiene segment of the terpolymer, while the other generic materials offer good weathering stability. All acrylic type modifiers are widely used in United States of America while Europe has traditionally used CPE and EVA for certain applications.

This project investigated two different impact modifiers, namely a CPE and an all acrylic (ACR). A brief summary of the general attributes of each type is given in table 1.4 [57]:

TABLE 1.4

Performance of CPE and ACR impact modifiers

Impact Modifier	Advantages	Disadvantages
CPE	1. Outdoor applications (esp in Europe) 2. Good low temperature properties, better ductility at low temperatures than acrylics 3. Good impact retention and efficiency 4. Good melt elasticity	1. Can be over-processed 2. Yellowing in white products 3. Low heat deflection temperature 4. Poor hot strength 5. Higher specific gravity than ACR
ACRYLIC	1. Outdoor applications 2. Wide processing window 3. Excellent colour, impact efficiency and retention 4. Low die swell	1. Low heat deflection temperature 2. Moderate low temperature performance

1.2.5.2 MECHANISMS OF IMPACT MODIFICATION

The enhanced behaviour of modified PVC under very high strain rates can be explained by two distinct mechanisms; firstly the modifier is dispersed as discrete particles within a continuous PVC network and secondly the modifier forms a continuous phase which encapsulates PVC primary particles.

Acrylic modifiers

The modifier in a blend with PVC forms discrete particles within the PVC matrix; an improvement in impact is visualised by deformation/cavitation of the rubber particles during a high speed stress wave [58-59] and the lowering of yield stress permitting cold drawing which can also act as an additional mechanism of energy absorption [59-60].

The all-acrylic system is based upon a saturated acrylic rubber which is not prone to weathering problems and the extent of impact improvement is related to: i) evenly dispersed particles ii) particle-matrix adhesion iii) particle size distribution iv) viscoelastic nature of rubber v) rubber content and lastly vi) modifier level [61]. The particle size distribution of the modifier is generally not affected by processing conditions, since the crosslinked discrete particles are determined during polymerisation and thus acrylic modified grades are less susceptible to 'over-processing' [62].

CPE and EVA modifiers

These modifiers are considered to produce a 'honey-comb' type of structure [63-68], where an elastomeric network is formed in which primary PVC particles are embedded. The improvement in impact can be related to the blend's irreversible deformation behaviour. Siegmann *et al* [59] observed that in the case of unmodified PVC the failure behaviour during tensile deformation was predominantly crazing, followed by shear banding and then finally voiding until failure. However CPE modified systems differed from this sequence since shear banding followed by voiding were seen as the mode of failure. Although these conclusions can not be directly linked to failure in an impact test, they do provide an insight to the possible mechanisms involved.

A number of studies [62, 65-68] have mentioned the importance of mechanical processing upon the honey-comb structure of network systems. The optimum condition for impact enhancement is observed when a elastomeric network encapsulates the primary particles. In the case of higher temperatures or an increased shear history the primary particles are destroyed which also leads to the destruction of the network, resulting in the formation of discrete globules in a continuous PVC matrix. The resultant spherical inclusions do not conform to the ideal particle size distribution required for good impact efficiency [61] and thus inferior impact performance, when compared to the original blend, is observed.

Menges *et al* [67] produced a high impact grade of PVC (via copolymerisation with EVA) and examined compression moulded and extruded samples by electron microscopy, impact, tensile and sorption techniques. The study revealed the dramatic dependence of processing temperature upon impact strength; at a temperature of 188°C the optimum impact performance was observed. At higher temperatures the performance was progressively reduced and this was associated with the destruction of the network system to produce discrete particles of the modifier. A model was introduced, as shown in figure 1.2, which could account for the reduction in impact properties.

FIGURE 1.2

Influence of processing upon EVA modified PVC

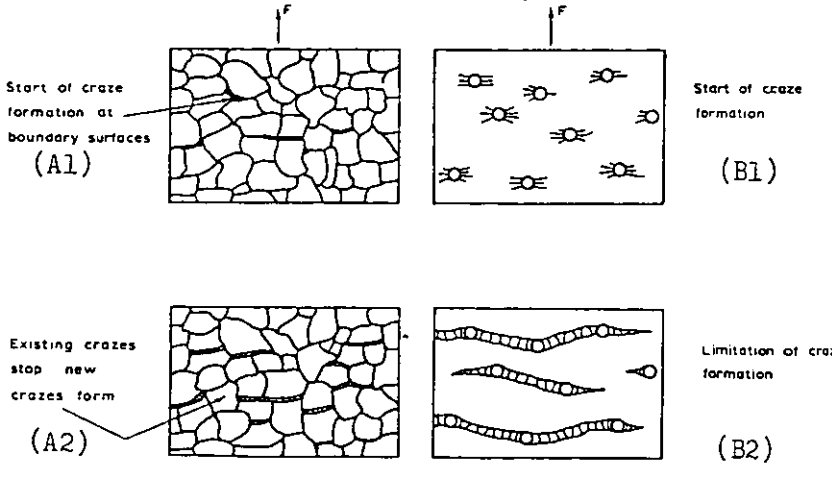

Case A: Modified PVC processed at low temperatures

In the early deformation of modified PVC (A1), small crazes develop at the primary particle interface which are perpendicular to the direction of applied stress. Craze formation acts as a source of energy absorption, the craze continuing to propagate until it encounters a perpendicular boundary interface where continued growth is prevented (A2) and further crazes are initiated at other convenient boundary interfaces.

Case B: Modified PVC processed at high temperatures

The situation after phase transformation, ie destruction of network structure, suggests that in the early stages of deformation crazing occurs around these globules of modifier (B1). Further deformation leads to craze propagation and interconnection of crazes until a critical length is reached whereby growth is stopped (B2).

Rabinovic [62] impact tested milled UPVC blends of EVA, CPE and all acrylic modifiers and confirmed the sensitivity of CPE and EVA to over-processing when compared to the all acrylic modifier.

1.3 MORPHOLOGY AND MOLECULAR STRUCTURE OF PVC

The particulate nature of PVC was highlighted by earlier studies including Berens and Folt [69] and Hori [70], and the influence of this unique morphology has wide ranging ramifications upon processing and subsequent properties. The origins of the particulate nature of PVC can be related to the mechanism of polymerisation.

1.3.1 SUSPENSION POLYMERISATION

The conversion process which produces PVC from vinyl chloride monomer involves suspending the monomer, as liquid droplets, in a continuous water phase by a combination of

vigorous agitation and in the presence of a protective colloid. The batch mixture is continually agitated and maintained at a specific polymerisation temperature (≈50-75°C) until the required conversion is achieved, whereby the resultant slurry is 'stripped' of residual VCM, dried and then finally coarse screened to remove extraneous large particles [71]. The rate of agitation, polymerisation temperature and level of colloid protection are the main variables involved in the control of molecular weight and grain characteristics such as porosity and shape.

The conversion process proceeds by a series of aggregation steps [71-73] and an schematic representation [72] is shown in figure 1.3.

FIGURE 1.3

Mechanism of suspension polymerisation

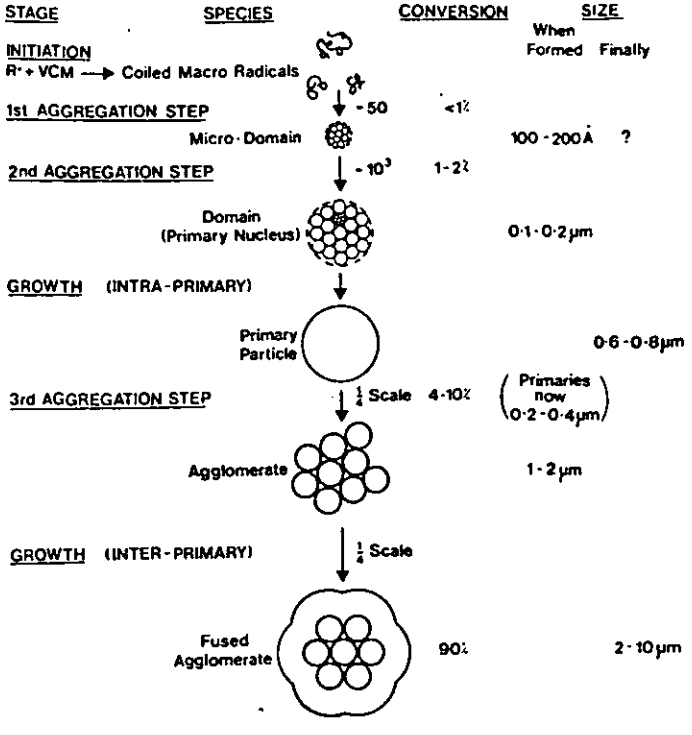

The polymerisation mixture is quickly warmed to the reaction temperature and decomposition of the initiator occurs. Also a skin or pericellular membrane encapsulating the polymerising droplet occurs at a very low rate of conversion [71] and is formed by the graft copolymerisation of poly(vinyl chloride) on to the poly(vinyl acetate) protective colloid. Coalescence of a number of monomer droplets can often occur at conversion levels of 5-15% to produce particles which are termed grains.

Within the monomer droplet the growing polymer chain soon precipitates out of the monomer since PVC is insoluble in VCM, agglomeration of a number of polymer chains (≈50 maximum) form the product of the first aggregation step, namely microdomains. Microdomains are stable only for a short time and after a brief growth stage, microdomains coagulate to form the next identified species: domains or primary particle nuclei (≈1000 microdomains). The domains remain stable and continue to grow to produce primary particles until at approximately 3-10% conversion the domains become unstable and flocculate to form the third aggregate species; agglomerates. Agglomerates increase in size with increasing conversion rate due to further growth of the primary particles to produce an agglomerate diameter of approximately 2-10 μm.

The final irregular appearance of PVC grains is attributed to the reduction in internal grain pressure at high conversion rates leading to partial collapse of the grain.

1.3.2 PVC NOMENCLATURE

The particulate nature of PVC has been identified or observed by a large number of workers [71-82], however Geil [82] summarised a discussion held at an International Symposium (Lyon Villeurbanne, 1976) upon the preferential terminology for the morphology of PVC. Table 1.5 lists the preferred nomenclature, origin of species and approximate

size range. Allsopp [72] has applied this classification to the proposed mechanism of polymerisation as outlined previously.

TABLE 1.5

PVC NOMENCLATURE

Term	*Approximate size* Range (μm)	Average (μm)	*Origin or description*	*Previous terminology (with references)*
Grain	50–250	130	Visible constituents of free flowing powders, made up of more than 1 monomer droplet.	Granule[2] Cellular grain[3]
Sub-grain	10–150	40	Polymerised monomer droplet.	Sub-granule[2] Unicell[3]
Agglomerate	2–10	5	Formed during early stage of polymerisation by coalescence of primary particles (1–2 μm). Grows with conversion to size shown.	Aggregate[2] Cluster[3] Macro-globule[4]
Primary particle	0·6–0·8	0·7	Grows from domain. Formed at low conversion (less than 2%) by coalescence of micro-domain: grows with conversion to size shown.	Microgranule Primary particle[2] Granule[3] Micro-globule[4]
Domain	0·1–0·2	0·2 (200 nm) (2000 Å)	Primary particle nucleus. Contains about 10^3 micro-domains. Only observed at low conversion (less than 2%) or after mechanical working. Term only used to describe 0·1 μm species; becomes primary particle as soon as growth starts.	Primary nucleus[2] Granule[3]
Micro-domain	0·01–0·02	$\simeq$0·02 (20 nm) (200 Å)	Smallest species so far identified. Aggregate of polymer chains—probably about 50 in number.	Basic particle[2] Particle[3]

Notes
1. The domain is not a feature of PVC morphology in high conversion polymer samples since a growth of this species with conversion obliterates all memory of it. It may only be 'regenerated' and observed after subsequent processing.
2. As soon as formation of the domain is complete and growth is registered it is preferable to call it a primary particle. Therefore, the term domain is often ignored in favour of primary particle even at the point of morphogenesis of the 0·2 μm primaries at low conversion.
3. The reason for a separate identity for the domain is that it may be shown in future to contain an atypical morphological or molecular feature, e.g. higher level of crystallinity.

The application of standard terms to describe the particulate structure observed by many investigators [70, 72–73, 76, 78, 80] has lead to an overall idealised model which provides a universal approach to the understanding of PVC particulate structure.

1.3.3 MOLECULAR STRUCTURE OF PVC

The previous section considered the particulate nature of PVC and a general idealistic model of PVC grain morphology can be presented (figure 1.4).

FIGURE 1.4

PVC grain morphology

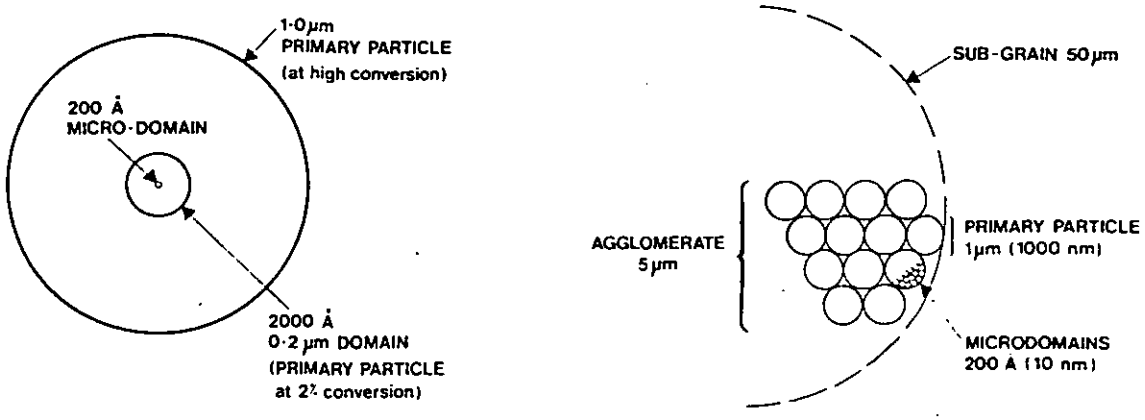

However the molecular structure of PVC has also been the subject of much debate and thus far a general agreement has not been reached.

Vinyl polymers have a general repeat unit $-CH_2-CHX-$, where the substituent X is a chlorine atom in the case of PVC. A consequence of a substituent group is that configuration isomers can occur, whereby the substituent can be placed in a number of distinct positions with respect to the backbone. The domination of a particular isomer depends to a large degree upon energetic considerations during polymerisation, if a particular substituent placement is favoured then a stereoregular polymer will be produced. Figure 1.5 depicts the three tactic placements of the substituent chlorine atom for PVC [83].

The first two placements are regular, while the final tactic placement is irregular. Commercial polymerisation techniques generally favour syndiotactic polymers with a syndiotactic value of approximately 55% [60, 84-85]. The degree of syndiotacticity can be increased by the use of effective chain transfer agents or low polymerisation temperatures. The regularity of a polymer is dependant upon tacticity, degree of branching and other

structural defects such as head to head/tail to tail monomer addition, unsaturation, peroxide/hydroperoxide groups etc.

FIGURE 1.5

Tactic placements for PVC

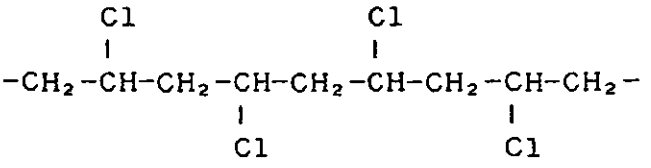

Syndiotactic (rrr)

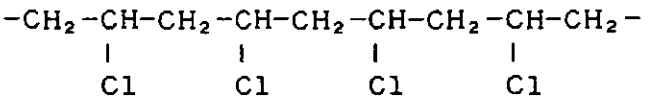

Isotactic (mmm)

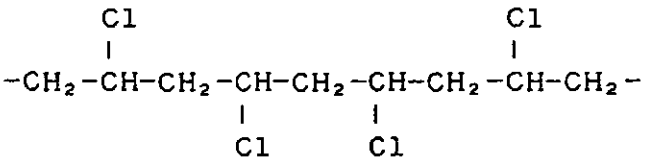

Heterotactic (rmr)

1.3.3.1 PVC CRYSTALLINITY

The crystalline nature of PVC has been studied by a wide range of techniques including wide/small angle X-ray diffraction (WAXS/SAXS), differential thermal analysis, density, infra-red and recently small angle neutron scattering (SANS). The implications of these studies are that crystallinity is related to the presence of short syndiotactic sequences [60, 67, 86-87] and increasing levels of syndiotacticity produces a more crystalline polymer [60, 88]. It is also suggested that the microdomains contain a crystalline nucleus surrounded by constrained amorphous material [89-90].

The crystalline nucleus was first investigated by Natta and Corradini [91], who proposed that the unit cell was orthorhombic with a-, b- and c- dimensions of 10·6, 5·4 and 5·1 Å respectively and that the chains, two per unit cell, were planar syndiotactic. Wenig [90] concluded that the crystals grow in a lamella-like manner, although rod-like structures may be present due to deformation of the lamellae. Summers [92] considered a platelet crystal structure (figure 1.6) in which the crystals are held together by tie molecules (figure 1.7) to produce a three dimensional network.

FIGURE 1.6

PVC platelet crystal

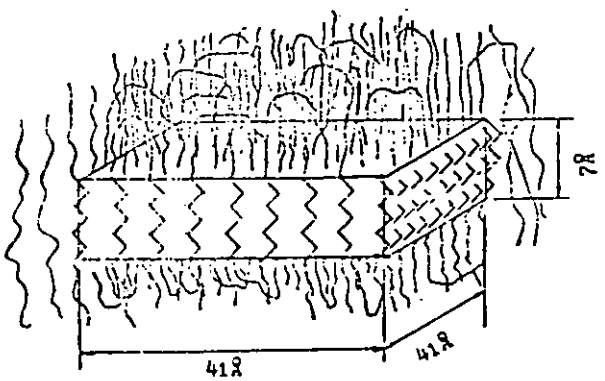

FIGURE 1.7

The microdomain structure of PVC

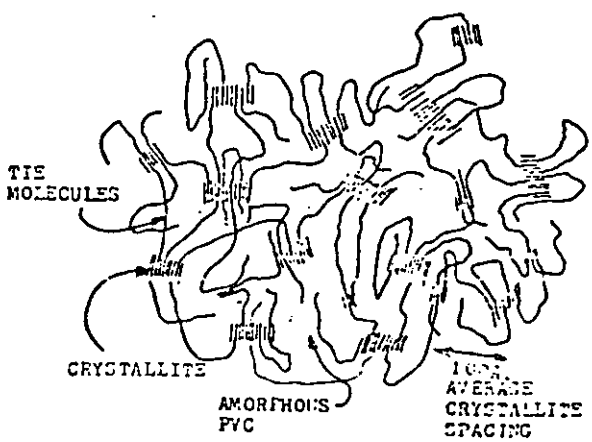

The level of crystallinity in commercially polymerised PVC is usually reported to be between 5-10% [77, 67, 86-87, 88, 93-94]; although Straff *et al* [95] did not obtain a SAXS peak for UPVC and thus stated that PVC is not crystalline. Similarly Singleton *et al* [96] did not obtain a SAXS peak for UPVC but were able to observe a peak for plasticised PVC. These examples highlight the inherent problems in ascertaining the crystallographic nature of PVC, since low levels of crystallinity are involved and results are often complicated by large background scatter, e.g. WAXS diffractogram of PVC. A recent study , Ballard *et al* [97], applied a SANS technique to plasticised PVC (10% deutoero-di-n-octylphthalate). The investigators suggest that i) SANS is a more sensitive technique than WAXS/SAXS, ii) the crystallinity of PVC is approximately 15% and iii) the technique could assess the melting characteristics of PVC.

There is considerable evidence [84, 98-100] to suggest that annealing or drawing of PVC results in the development of a two-dimensional order perpendicular to the chain (nematic mesomorphic phase). One of the observations of this secondary crystallinity is a broad melting endotherm which may be related to a network of imperfect crystallites [84].

1.4 FUSION OF PVC

The fusion of PVC has been studied by many workers and, no doubt, will continue to be the source of further research. It is generally appreciated that the 'quality' of PVC products is critically dependent upon the level of fusion, however the precise fusion mechanism is not easily attained. Since the pioneering work of Berens and Folt [69], many workers have attempted to relate the development of fusion to the observed particulate nature of PVC. The investigative tools include optical and electron microscopy, torque rheometry, capillary rheometry, differential thermal analysis and property measurements.

1.4.1 FUSION MECHANISMS

Sieglaff [77] and Krzewki and Collins [81] in separate publications proposed that fusion of PVC could be achieved by three different routes:

a) PVC grains are broken down into sub-micron particles which are then compacted. These structures interdiffuse to produce a fused material.

b) Breakdown of the grains produces micro-particles which are compacted and undergo internal fusion. The microparticles interdiffuse to complete fusion.

c) The grains do not rupture to yield sub-grain structures, the grains are compacted and internal fusion occurs. Again these units interdiffuse to obtain a fused network.

These general routes account for the majority of mechanisms observed by a large number of workers [67, 75, 79, 101], however experimental evidence and specific mechanisms were detailed for a better understanding of the fusion mechanisms. Sieglaff [77] also postulated that in commercial processing techniques, a combination of all three routes may be appropriate.

An early study by Hattori *et al* [73] observed the inner structure of extrudate specimens which were embedded in a methyl methacrylate material. The extrudate specimens were obtained between a processing range of 160-210°C and the ultramicrotomed section observed via a transmission electron microscope. At low processing temperatures (160-170°C) the inner particulate structure seems unaffected, while at extrudate temperatures of approximately 180°C the micron particles (≈1 μm primary particle) are loosened and form a continuous network . A further increase in processing temperature (>190°C) leads to a breakdown of this network

and the inclusion of fine threads or fibrils (ca. 300 Å). Network disintegration is complete at 200°C and no further morphology transitions were noted. A fibrillar structure was also described by Vidyikina *et al* [102] during a study of roll milling. A higher screw speed resulted in an increase in processing temperature before the various phase changes occurred. In the same study, Hattori *et al* also observed that this particle breakdown to fibrils was still possible by the application of heat alone but was only induced at high temperatures (ie. 3 minutes @ 220°C). Thus they concluded a fusion mechanism involving particle breakdown to form fibrils and that a shear regime had an additive effect to processing temperature.

Faulkner [80] applied a Brabender plasticorder™ to postulate a particle breakdown mechanism for PVC, the various features of a typical temperature-torque trace [103], figure 1.8, were associated with specific particle transitions.

FIGURE 1.8

Brabender temperature-torque trace

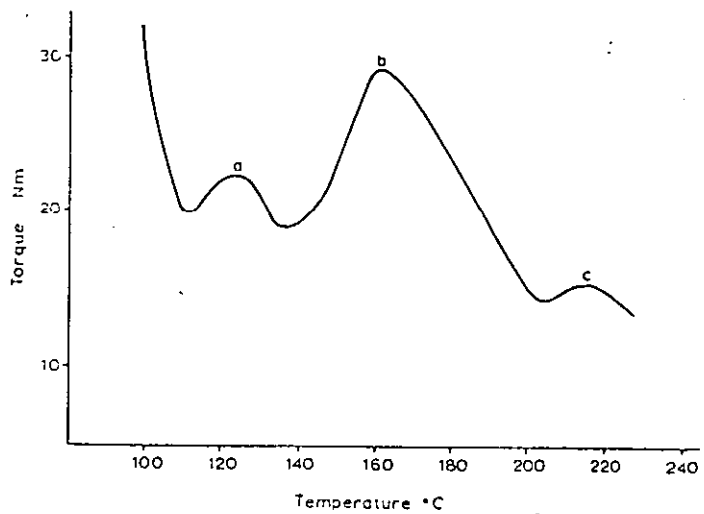

Faulkner conducted an extensive study by collecting small samples at intervals throughout the rheometer trace and assessing the particle hierarchy via scanning and transmission electron microscopy. He attributed the following inferences to the characteristic peaks shown in figure 1.8; peak (a) was reported to contain a compacted mixture of whole grains and ruptured grains. At peak (b) the micrographs reveal a deformed fibrillated material which still retains a primary particle nature. At the final torque peak (c) the material has undergone molecular deformation and primary particles are not evident, although a domain structure might be present. The author suggested that the processing history of a compound could be assessed by re-determining its temperature-torque trace. Also Rabinovitch [104] conducted a temperature-torque rheometer study and confirmed the previous study, however the effect of Brabender conditions and polymer characteristics upon the position of the aforementioned peaks was emphasised.

An overview of fusion based upon various publications [80, 105-106] was presented by Portingell [107]; he inferred that the fusion mechanism can be divided into two components. Firstly a supra-molecular component, where progressive breakdown of particulate structure occurs from stage III particles to a mixture of stage II and III and of stage II and I to a true melt with possibly a few surviving stage I's (Stage III, II and I particles refer to grains, primary particles and domains respectively). The second component involves a parallel molecular activity; here it is acknowledged that even in the predominantly particle flow region there is a level of molecular deformation across the surface layer of the particles [105]. Thus a degree of interdiffusion and entanglement of chain segments across the particle boundaries invokes a level of fusion. As the processing temperature increases the crystallites melt and molecular chain mobility increases, while the effect of particle breakdown is to permit molecular diffusion across boundaries and promote chain entanglement. The greater the

particle breakdown and processing temperature then the greater the molecular mobility and thus entanglement (upto a degradation limit). On cooling the crystallites reform and a new network is obtained. Thus the level of fusion depends upon the degree of particle breakdown coupled with crystalline melting and molecular diffusion. Benjamin [108] suggested a similar scheme.

A pictorial model was presented by Summers [92, 109-110] which involves a crystal structure, as shown in figure 1.6, and the assumption that primary particles are the main flow units. A low processing temperature (typically 160-170°C) yields primary particle flow with poor particulate interaction, the particles are being held together by the three dimensional network structure shown in figure 1.9.

FIGURE 1.9

Primary particles in a low temperature melt

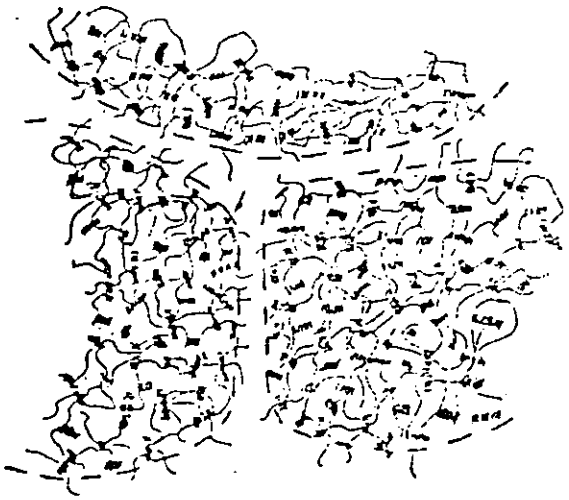

At a higher processing temperature (>177°C), some of the crystallites melt and thus interaction between the particles is increased (figure 1.10). The particulate structure is not completely destroyed and upon cooling recrystallisation takes place which can link the particles together by newly formed crystallites (figure 1.11). These crystallites cause a fibrillation effect when the material

is acetone sheared between two glass plates [110]. Summers could therefore account for the anomalous flow behaviour of PVC as described by Collins and Metzger [111] i.e. the two activation energies for PVC flow behaviour could be assigned to the different interactions shown in figure 1.9 and 1.10. The low activation energy value is due to low melt temperature flow behaviour when the primary particles are discrete and a higher flow activation energy is associated with increased interparticle diffusion.

FIGURE 1.10

Primary particles in a higher temperature melt

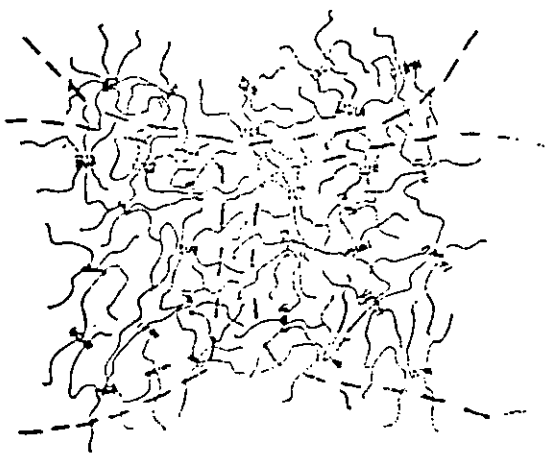

FIGURE 1.11

Primary particles after cooling and recrystallisation

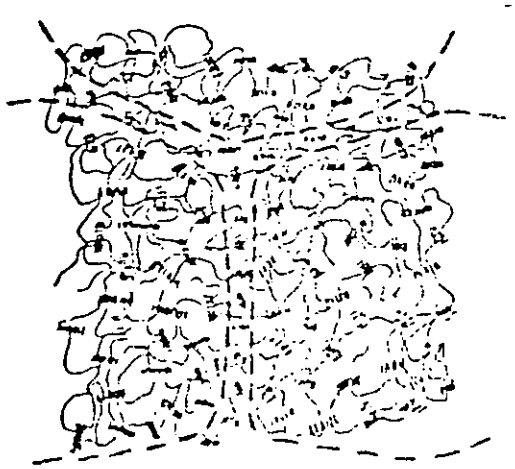

Lastly Allsopp [112] conducted an extensive study which assessed the effect of different processing equipment upon the particulate nature of PVC. He revealed that grain breakdown was not the normal mechanism in the case of extrusion and accounted for previous publications by suggesting that PVC studies generally involved sample preparation via high shear equipment such as the Brabender plasticorder™ and laboratory Banbury™ mixers. Thus two fusion routes were identified (figure 1.12):

a) Comminution mechanism; the grains are broken down into finer structures such as primary particles.
b) 'CDFE' mechanism; the less aggressive conditions do not induce grain attrition but instead the grains are compacted, densified, and fused before appreciable shear forces are present, and finally due to a high directional shear stress the grains are elongated.

FIGURE 1.12

Fusion mechanisms during processing

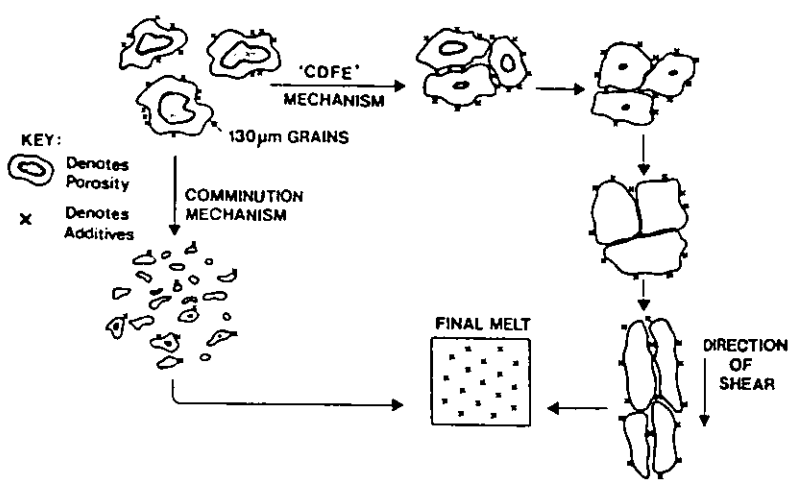

This proposal has received recent support from a number of workers [113-116]. Allsopp ranked common laboratory and processing equipment in an attempt to predetermine the possible route of fusion (figure 1.13).

FIGURE 1.13

Comminution/densification mechanisms of fusion

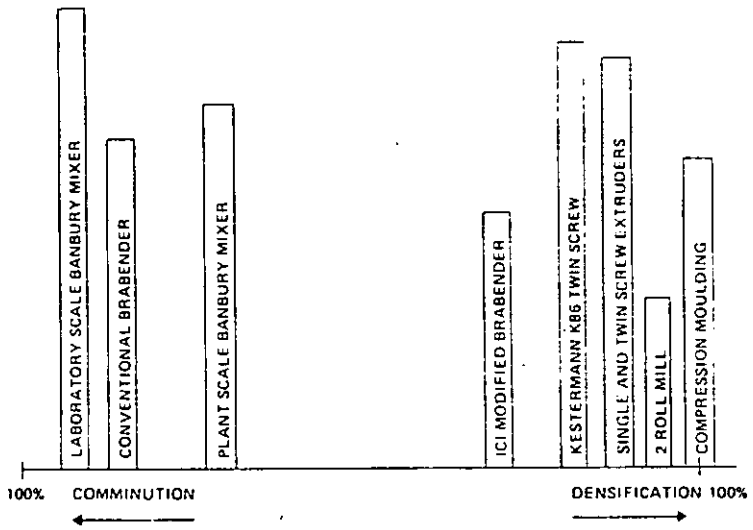

Gilbert *et al* [114] confirmed a CDFE route for extrusion and further extended the mechanism by postulating a primary crystalline melting mechanism which on recrystallisation leads to a network formation consisting of secondary crystallites.

1.4.2 ASSESSMENT OF FUSION

It is evident that the complex particle hierarchy and subsequent fusion mechanism are critically dependant upon the type of processing equipment and conditions used. Thus in order to evaluate these processing effects and to relate fusion levels to properties a method of fusion assessment is required. There are a number of established techniques available which have been extensively reviewed in

the literature [107, 114, 117], it is therefore intended in this section to discuss, in detail, those techniques which are relevant to this project.

1.4.2.1 MICROSCOPY

Particle breakdown can be qualitatively evaluated by microscopy techniques. Light microscopy can detect the grain nature of PVC and the possible breakdown into primary particles, while more powerful electron microscopes can view much smaller units. The previous section, 1.4.1, cited various publications which have used the high resolution power of electron microscopes to yield conclusions upon possible fusion mechanisms [73, 77, 80, 81, 108, 116, 118]. However as a technique for quantifying the level of fusion, these instruments are problematic since: a value for fusion level is not easily obtained, careful and reproducible sample preparation is essential, a small area is viewed which is deemed to be representative of the specimen, and lastly the equipment is not recommended as a quality control test because of high capital cost and operator expertise. It is therefore common to use these microscopes to confirm observations from other fusion tests.

Other microscopy techniques can distinguish between fusion levels, for example, differential interference contrast (DIC) and use of a Jamin-Lebedeff interferometer [114, 119]; these techniques can detect refractive index fluctuations with thermal history.

1.4.2.2 SOLVENT TESTING

Solvent tests are convenient and are widely used as a quick appraisal of fusion. Solvent attack (e.g. acetone or methylene chloride) depends upon the extent of a cohesive molecular network; a poorly fused specimen will contain areas where a fusion network exists and also particles that are not restrained by the molecular network. The swelling of

these particles could lead to partial disintegration and thus severe visual attack [107]. A well fused product can be visualised as a network of high integrity and thus few 'free' particles which could lead to gross solvent attack. Poorly fused articles can show quite dramatic failure during these tests, but discrimination between quite highly fused specimens is more subjective [114]. International standards have been introduced for this type of test [120-121]. Solvent uptake has also been related to the thermal history of PVC [113, 116, 122] although the application of this phenomenon has yet to be fully evaluated.

Summers *et al* [109-110] measured the acetone uptake in PVC and concluded that acetone at room temperature only enters the amorphous phase, the crystallites are not destroyed and thus continue to act as crosslinks. The shearing of swollen acetone samples, as viewed by optical microscopy, could differentiate between levels of fusion. Poorly fused products disintegrated into discrete particles, while more highly fused specimens lead to a network linked by fibrils. This solvent test again provides a qualitative result and the discriminating power between moderately fused specimens is limiting.

1.4.2.3 TORQUE RHEOMETRY

A temperature-programmable torque rheometer can be used to assess the processing history of a PVC compound, Faulkner [80] developed a testing procedure which compared a torque/temperature curve (figure 1.8) for a ground crumb of the processed composition with that of a reference curve from a dry blend of the same composition. Figure 1.14 illustrates the relationship between a well and a poorly fused compound using this test. The results can be difficult to interpret and again provide a comparative analysis.

FIGURE 1.14

Temperature programmed Brabender curves

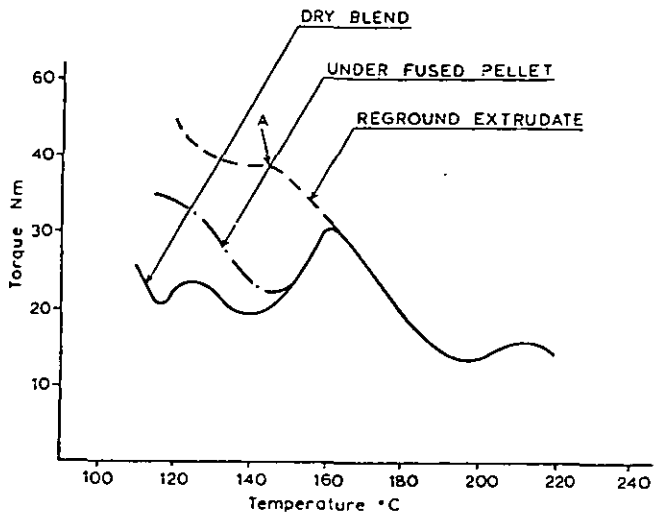

1.4.2.4 CAPILLARY RHEOMETRY

Gonze [103] and Lamberty [123] published a method of determining the level of fusion of a processed PVC composition. The rheological method measures the elastic pressure loss in a short capillary at low temperatures (typically 130-150°C). The widely reported technique [81, 108, 124-126] can provide a measurable fusion value providing the following assumptions apply [77]: a) changes in the particulate structure can be assessed by corresponding changes in the elastic behaviour of the material; b) melt elasticity increases with increasing network interaction; c) capillary entrance pressure loss is indicative of melt elasticity. The technique measures the pressure necessary to extrude the material through a short capillary (small length/diameter ratio), ΔP is defined as:

$$\Delta P = \tau\ (2n + S_R) + \tau\ \frac{4L}{D} \qquad (1.1)$$

Where
- ΔP - Extrusion pressure
- τ - Shear stress at capillary wall
- n - Viscous loss term
- S_R - Recoverable shear strain
- L - Capillary length
- D - Capillary diameter

The first term of the above equation accounts for the entrance pressure loss, and the second term represents viscous behaviour, i.e. ΔP can be rewritten;

$$\Delta P = \Delta P_{ENT} + \Delta P_{VISC} \qquad (1.2)$$

Where ΔP_{ENT} - Pressure loss due to entrance effects

ΔP_{VISC} - Viscous pressure loss

Lamberty demonstrated that if a low L/R capillary is used ('Zero-length' capillary) then the entrance pressure term, (ΔP_{ENT}), predominates. The total entrance pressure loss can be further divided into viscous and elastic components. Han [127] has shown that the viscous component is only 10% of the total pressure drop and so for practical purposes, entrance pressure losses are a measure of melt elasticity.

A plot of capillary pressure versus processing temperature can produce a 'S' shaped curve (figure 1.15).

FIGURE 1.15

Capillary fusion curve [103]

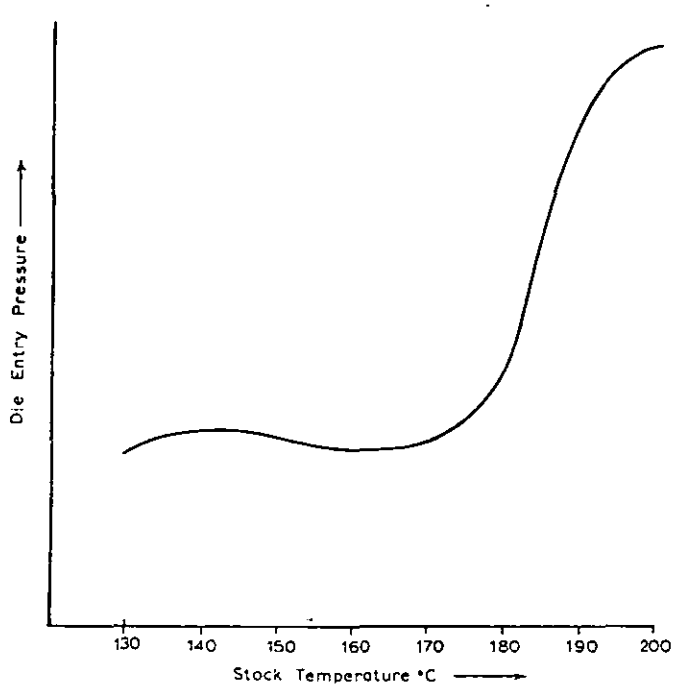

The initial decrease in entry pressure is related to grain breakdown, followed by the gradual increase in molecular network formation. The production of a standard reference curve then enables further results to be quoted as a percentage [108];

$$\text{Gelation level } \% = \frac{P_{SAMPLE} - P_{MIN}}{P_{MAX} - P_{MIN}} \times 100 \qquad (1.3)$$

The test provides a quantifiable result, although the main limitation seems to be the production of a reference curve for every composition and processing technique.

1.4.2.5 THERMAL ANALYSIS

Thermal analysis techniques, i.e. differential scanning calorimetry, can provide useful information upon thermal transitions such as: glass transition temperature (T_G), crystalline melting point and so forth. The thermal analysis of PVC has been shown to produce a more complex trace than might be expected from an essentially amorphous material [69, 94, 128-129]. Gilbert and Vyvoda [128] accounted for the complex pattern and suggested a relationship between observed endothermal peaks and processing history. Figure 1.16 depicts the effect of compression moulding temperature (value quoted on right-hand side of trace) upon DSC thermograms for the processed samples.

A DSC trace of virgin PVC and dry blends of limited heat history show a T_G of approximately 80°C and a broad melting endotherm for primary crystallinity ranging from about 155 to 195°C. If the dry blend is subsequently processed then T_G remains unchanged, however the broad endothermic peak is replaced by two endothermic peaks ('A' & 'B') as shown in the above figure. The sharper higher temperature endotherm 'B' represents the melting of crystallites of various sizes and degrees of perfection. An increase in processing temperature leads to the melting of

FIGURE 1.16

DSC thermograms of processed PVC

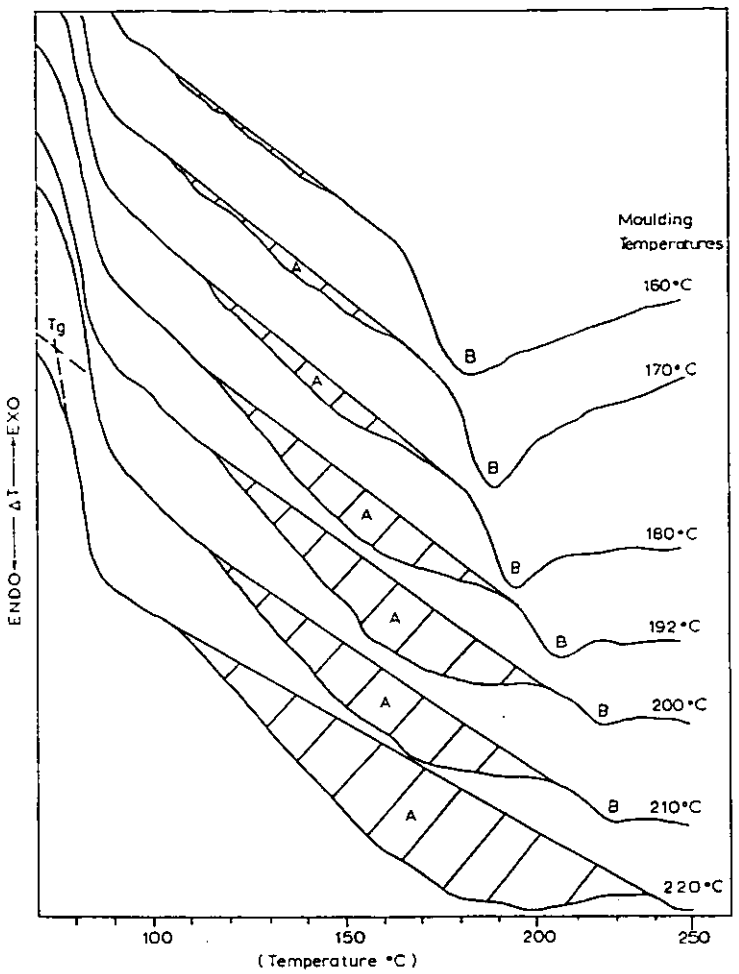

lower temperature crystallites and the annealing of higher temperature crystallites. Thus the 'B' endotherm, observed at higher processing temperatures, decreases in size while shifting to a higher temperature. If the processing temperature exceeds ≈160°C a second endotherm peak, 'A', appears, a further increase in processing temperature produces a larger and broader peak range from approximately 110°C to the onset of the 'B' endotherm. This endothermic peak is attributed to recrystallisation of the primary crystallites to produce secondary crystallites of a lower order. If the energy of this endotherm (ΔH_A) is plotted against processing temperature, a 'S' shaped curve is produced which resembles a reference curve obtained from capillary rheometry studies. Therefore Gilbert *et al* [128] proposed a potential method for determining the fusion level

of processed PVC. It was also concluded that the 'B' onset temperature corresponds to the mass processing temperature and is analogous to the effect of annealing temperature upon the position of the 'B' endothermic peak [94, 129]. The above method has been used to assess samples produced via a number of processing techniques and the results suggest that the technique differentiates between equipment types and may elucidate the fusion mechanism involved.

A recent study by Terselius *et al* [116] has provided support for the application of differential thermal analysis to measure fusion levels of processed PVC samples. The study produced samples by roll milling and extrusion and assessed the process of fusion via thermal analysis, capillary rheometry and transmission electron microscopy. A correlation of breakdown of primary particles and formation of secondary cooling crystallites was observed, the onset of breakdown occurs at a lower temperature for roll milling (166-174°C) as opposed to extrusion (190-194°C). The findings provided further evidence to support the concept of a thermomechanical mechanism of fusion.

Patel *et al* [130] produced a 'master curve' which related capillary rheometer pressures to endothermic energy (ΔH_A) values. The master curve combined results of three types of processing equipment and it was suggested that a measure of fusion can be quoted for an unknown sample irrespective of its thermomechanical history.

Covas [131] used thermal analysis to measure the progression of fusion within single and twin screw extruders. The technique was particularly useful for this study since only a small sample is needed and information upon primary and secondary crystallinity is available. The results provided complementary evidence to support an extended version of the fusion mechanism proposed by Allsopp [112].

Although thermal analysis is a relatively new method for the assessment of fusion the suggested advantages are: small test specimen, less dependence upon composition,

'internal' estimate of processing temperature and fusion gradients can be investigated. The small test specimen can present problems when a representative value is required from a bulk product.

1.4.2.6 MISCELLANEOUS TECHNIQUES

Physical properties:- The relationship between physical properties and the level of fusion is far from established and the literature will be reviewed in a later section, 1.5.3. Physical testing as an indirect method of assessing fusion may be difficult since a large number of test specimens is required and the test shape may not be easily obtained from the physical form of the product.

Melt flow index (MFI):- Krüger and Menges carried out modified MFI tests upon PVC samples at different stages of processing and concluded that the MFI is a measure of the ratio of fused to non-fused primary particles. Therefore a quantitative measure of processing can easily be obtained with a simple and readily available MFI unit [132].

Extrudate appearance:- An increase in fusion level leads to an increase in melt elasticity which can result in a decrease in the quality of the extrudate appearance due to 'melt fracture' [107, 124, 133-134]. Therefore the extrudate appearance under extreme shear conditions, for example; 'zero length' die, can provide a qualitative assessment of fusion.

Viscoelastic methods:- Elongational flow rheology [134] and dynamic oscillatory testing [106] have been used to observe the effect of fusion level upon viscoelastic response: however the techniques are sophisticated and difficult to interpret so do not lend themselves to quick and easy measurements.

1.5 PROCESSING AND PROPERTIES OF UPVC

1.5.1 DRY BLENDING

Powder feedstock is commonly prepared via a high speed blending unit consisting of a high speed heater mixer linked to a larger, jacketed cooler mixer. The additives are distributed in the heater mixer by a centrifugal action of a high speed impellor to form a fluid vortex. High shearing forces invoke a significant increase in charge temperature until a blend temperature of about 120°C is reached, when the premix is discharged to the cooling mixer. The possible consequences of high speed mixing include: dispersion of additives, densification of PVC grains, grain comminution, and liquids/low melting point additives adsorbed onto PVC grains [136].

The continual widespread use of powder feedstock as a precursor to UPVC processing (particularly pipe extrusion) has lead to a number of dry blending studies [42, 107, 119, 136-139]. The studies have monitored the effects of dry blending variables upon premix characteristics such as additive adsorption/absorption, bulk density, free flowing behaviour, additive dispersion and processing stability.

Miadonye [139] correlated high speed mixer variables, such as rotor speed, mix time and charge weight, to the aforementioned premix characteristics. It was therefore proposed that an optimum operating window could be ascertained for a particular type of high speed mixer.

1.5.2 EXTRUSION OF UPVC

1.5.2.1 SINGLE VERSUS TWIN SCREW EXTRUDERS

Single and twin screw extruders are both used to process UPVC; however the extruders operate via different principles. The single screw generates high shear and high

temperatures with minimum amount of residence time. The efficiency of single screw extrusion depends upon shear heating, backflow and, possible screw mixing sections within the screw design. Alternatively, the twin screw extruder is a low shear, high volume positive pump and its mixing mechanism depends upon a rolling, kneading action with heat input via induction [140].

Twin screw extruders dominate the market in Europe for the extrusion of UPVC dry blends, while single screws are still widely used in the U.S.A.

A conical counter rotating intermeshing twin screw extruder was used in this project and therefore further discussion bears this configuration in mind.

1.5.2.2 TWIN SCREW EXTRUDERS

These extruders are designed to have positive conveying characteristics, the material being forced in a forward motion by the action of intermeshing screws to produce discrete chambers of material ('C' shaped packets). The output from such machines are not significantly affected by the extruder temperature profile [141-142], while output increases linearly with increasing screw speed [142-143]. Also the characteristics of the powder feedstock are known to influence the extrusion rate of a twin screw [36, 137-138]; a high bulk density results in increased mass output. Over-feeding can result in excessive screw torque and 'melt' pressures and thus feeding mechanisms are recommended [142-144].

The melting mechanism of UPVC in twin screw extruders has been reported in a number of publications [112, 131, 141, 145-146]. A generalised view suggests that the majority of the barrel length involves compaction and heating of the powder, while the melting process takes place, rapidly, during the last section of the screws (melting complete over several turns, possibly one). A molten film is produced at the barrel wall which is

introduced to a compacted solid bed of powder, and due to a violent tumbling action a melt pool of distorted shape is produced. Further melting quickly develops, due to shear and heat transfer, at the solid bed/melted material interface. Processing conditions are reported to have little effect upon the melting mechanism [131] although the position of melt formation may alter [139, 141].

1.5.3 INTERRELATION BETWEEN PROCESSING, FUSION AND PROPERTIES

There are few reported studies which attempt to correlate the relationships between the processing of a UPVC composition, a measured fusion value, and the consequences of a processing history upon physical properties.

Benjamin [108] extruded a series of pipes under controlled conditions to provide four gelation levels. A fusion level was determined by a 'zero length' capillary rheometer method and the pressure results related to a reference curve prepared by roll milling (32, 44, 68, 90% gelation levels). The pipes were subjected to a wide range of tests including: solvent attack, tensile, impact, crack formation and hydrostatic water pressure. Solvent testing revealed that the samples with high levels of fusion resisted attack while the poorly fused pipes (32 and 44%) were affected. Tensile results (stress at yield) suggested a constant maximum value at a higher gelation level of 68%, while ductility tests, such as tensile impact, tensile strain at break, resistance to crack formation, produced an optimum value at approximately 44-68% gelation level. Bejamin concluded that a gelation level of approximately 60-70% would provide the best balance of properties for the particular pipe and composition chosen. The results confirmed his earlier hypothesis based upon experience in pipe extrusion (figure 1.17). Berndtsen [147] and Menges *et al* [67] also observed a maximum in ultimate strain at an appropriate processing level.

FIGURE 1.17

Pipe properties versus gelation level

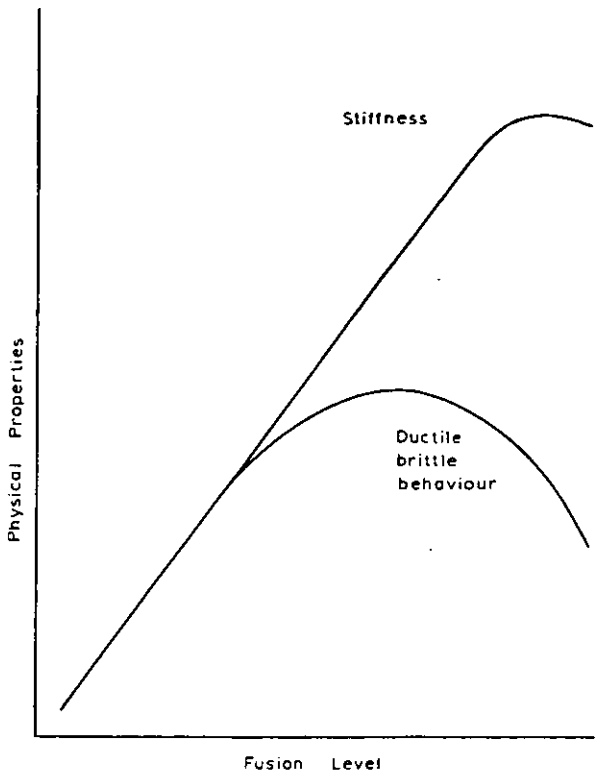

Marshall *et al* [113] produced a wider range of gelation levels than Benjamin with a die set temperature range from 170-227°C. The strip extrudates were assessed for fusion level by a range of techniques; capillary rheometry, differential thermal analysis (DTA) and solvent absorption. Capillary rheometry and DTA results provided broad agreement with a maximum in test value at approximately 215°C. Solvent absorption was also shown to produce a standard fusion curve and thus was established as a quantitative method for the assessment of fusion in a processed sample. Screw speed was also studied and its effect upon capillary rheometer pressure values was negligible except at low profile temperatures. An instrumented pendulum impact tester was used to assess Izod impact specimens of the extruded strip after removal of the extrudate surface. The impact results

generally support Benjamin's hypothesis of short term ductility at mid fusion levels, i.e. maximum in impact strength at approximately 60% fusion level. A possible explanation for this impact behaviour was discussed as the processing condition whereby grain structure is destroyed in favour of a inhomogeneous 'melt'.

Summers *et al* in a series of papers [109, 148-149] considered the effect upon impact performance by plotting dropped dart impact strength versus extrusion temperature. A distinct peak at an approximate melt temperature of 190°C was obtained for a low output rate, while a higher output rate resulted in lower overall impact strength with a peak at a higher temperature (≈195°C). The extrudates were assessed for fusion level by the acetone shearing test (§1.4.2.2) and the micrographs confirmed a steady progression in fusion level with increasing processing temperature. An explanation for these results was postulated as a consequence of melt fracture or 'lubrication' failure, leading to poor surface finish and thus poor impact retention. A higher processing temperature tends to promote this melt phenomenon due to higher melt elasticity and, similarly, a high extrusion rate would induce the likelihood of melt fracture and consequently a overall decrease in impact properties. In order to confirm this postulation, the product surface was press polished at the original extrusion melt and then impact tested. The press polished specimens did not yield a maximum, instead a monotonic 'S' shaped curve which did not differentiate between extrusion rate was observed. Therefore the presence of surface stress concentrators produced during melt fracture was proposed as the possible cause for reduced impact performance at higher processing temperatures.

Terselius *et al* published a number of papers [116, 125, 150-152] which discussed the physical properties of a pipe series. The pipe series was extruded at different extrusion temperatures ranging from 180-204°C and had a corresponding fusion range of 10-75% (measured by capillary

rheometry). A initial study [125] illustrated a distinct maximum in a falling weight impact test (B50 test: ISO/DIS 3127), however other impact tests, such as double 'V' notch and tensile impact, produced a monotonic increase with processing temperature until a levelling off at the upper temperature region. The initial conclusion of this work cited a similar mechanism to the behaviour of impact modified grades (§1.2.5.2: CPE and EVA modifiers). A later study [150] reaffirmed a maximum during falling weight tests for both instrumented and B50 type tests. Also, this study in contrast to Summers *et al* [149] did not observe the disappearance of a maximum when the samples were press polished. It was concluded that the most efficient resistance to crack initiation is found in pipes of moderate gelation level and that this may be attributed to enhanced post-yield deformation [60].

Terselius *et al* [151], also, evaluated the aforementioned pipes for tensile properties. Yield properties were concluded to be insensitive to a change in gelation level, while post-yield deformation behaviour was suggested as a discriminating test for gelation levels. Further post-yield tensile tests at different test temperatures revealed a maximum at the approximate T_G for PVC. The yield results were explained by considering that a 'yield flow unit' is a small entity which is unaffected by the network formation. Alternatively, post-yield parameters were related to an increase in cold drawing and thus a dependence on the development of a load bearing network of entanglements and crystallites. These tensile results are supported, in whole or part, by a number of workers [75, 105, 153].

Covas [131] provides a recent correlation between processing, structure and properties. This processing study considered both a single and a twin screw extruders, and a mechanism of fusion was conjectured based upon the 'CDFE' proposed by Allsopp [112]. Tensile properties were evaluated by producing families of stress-strain curves with different

gelation levels at different test rates and test temperatures. Yield properties were, again, seen to be unaffected by fusion level and were attributed to a molecular relaxation mechanism, however elongation at break and stress at break were dependant upon gelation level. A maximum value occurred between fusion levels 40-65% as observed by Benjamin [108]. This fusion range corresponds to a processing temperature of 193-203°C and the optimum tensile properties were related to the existence of a network morphology with possible residual primary particles. Testing above T_G showed that increasing gelation level leads to increased post-yield parameters which may be accounted by a continuing development of network coherence. Impact performance using an notched Izod specimen on an instrumented pendulum impact tester produced another maximum when impact strength is plotted against gelation level. The occurrence of this broad peak was reported at a fusion range of 40-50%, similar to results obtained for post-yield ductility tests; this result was related to the introduction of a network with residual primary particles.

1.5.3.1 INTERACTION OF ADDITIVES

The interaction of additives, such as lubricants, fillers and impact modifiers, is not well understood in terms of the complete extrusion process i.e. additive preparation, extrusion and, finally, product performance.

Lubricants have been thoroughly investigated by laboratory tests such as the Brabender™ rheometer and roll mill in order to evaluate the behaviour of the lubricant in terms of lubricant mechanism, i.e. external or internal or mixed (§1.2.3.3). Processing studies have suggested that external type lubricants delay fusion while lowering the effective melt viscosity [22, 33-34, 36, 142, 154], however the effect upon specific fusion levels and properties is rarely discussed. Marshall *et al* [113] showed that a higher level of external lubricant produced a delay in fusion as measured

by capillary rheometry studies, the delay in fusion resulted in a delay in attaining maximum impact properties and an overall lowering of impact properties. Ditto [155] discussed an empirical approach which can be applied to the introduction of lubricants. The paper cites a series of case studies whereby extrusion problems are overcome by the addition of selective ingredients determined by experience. The overall conclusion suggests that the balance between gelation promoters and gelation retarders can be adjusted to solve melt quality problems.

The introduction of appreciable amounts of mineral fillers have been evaluated to some extent (§1.2.4.5) although little work has been published as to the consequences of processing conditions and/or formulation aspects.

Finally the effect of processing conditions upon impact performance of impact modified grades have been assessed by a number of publications (§1.2.5.2).

1.6 PROJECT AIMS

A considerable amount of work has been carried out in the general area of structure, processing and properties of PVC compounds at the Institute of Polymer Technology, and this project aims to continue this theme, *albeit*, in a different direction.

The overall objective of this project is to provide a fuller understanding of the relationships between blending, formulation, extrusion conditions and product properties for filled UPVC compositions. A knowledge of these relationships can, hopefully, lead to a optimisation of formulation aspects and processing conditions.

The literature review presented in this chapter has identified a number of relevant conclusions:

a) The mechanism of fusion for a given processing machine is still not fully understood.

b) The level of fusion can have a significant effect upon properties, however poor agreement is observed between workers.

c) A number of experimental techniques have been established which can provide a quantitative assessment of fusion levels for processed PVC.

d) Little work is published upon filler incorporation and, particularly, the effect of processing filled grades upon fusion characteristics and properties.

e) Formulation studies have not attempted to overview a complete extrusion process from additive incorporation to product testing.

f) The introduction of low cost additives is economically desirable since material costs in a process, such as extrusion, accounts for 70% [156] of the product costs.

The objectives of this project were therefore sub-divided as follows:

i) Incorporate appreciable amounts of a mineral filler into a base composition and monitor any effects upon processing parameters.

ii) Process the filled grades within a broad processing window in order to establish a fuller understanding of processing filled systems.

iii) Evaluate the pipe extrudate for degree of fusion, filler dispersion, surface appearance and relevant mechanical properties.

iv) Analyse possible relationships between properties and processing conditions with particular reference to filler addition.

v) Alter the balance of the lubricant system by addition of specific lubricants and observe the effects upon processing and properties.

vi) Consider the effect of introduction of impact modifiers into unfilled and filled compositions.

Figure 1.18 presents a schematic layout of the project objectives and experimental techniques applied.

FIGURE 1.18

Schematic layout of project

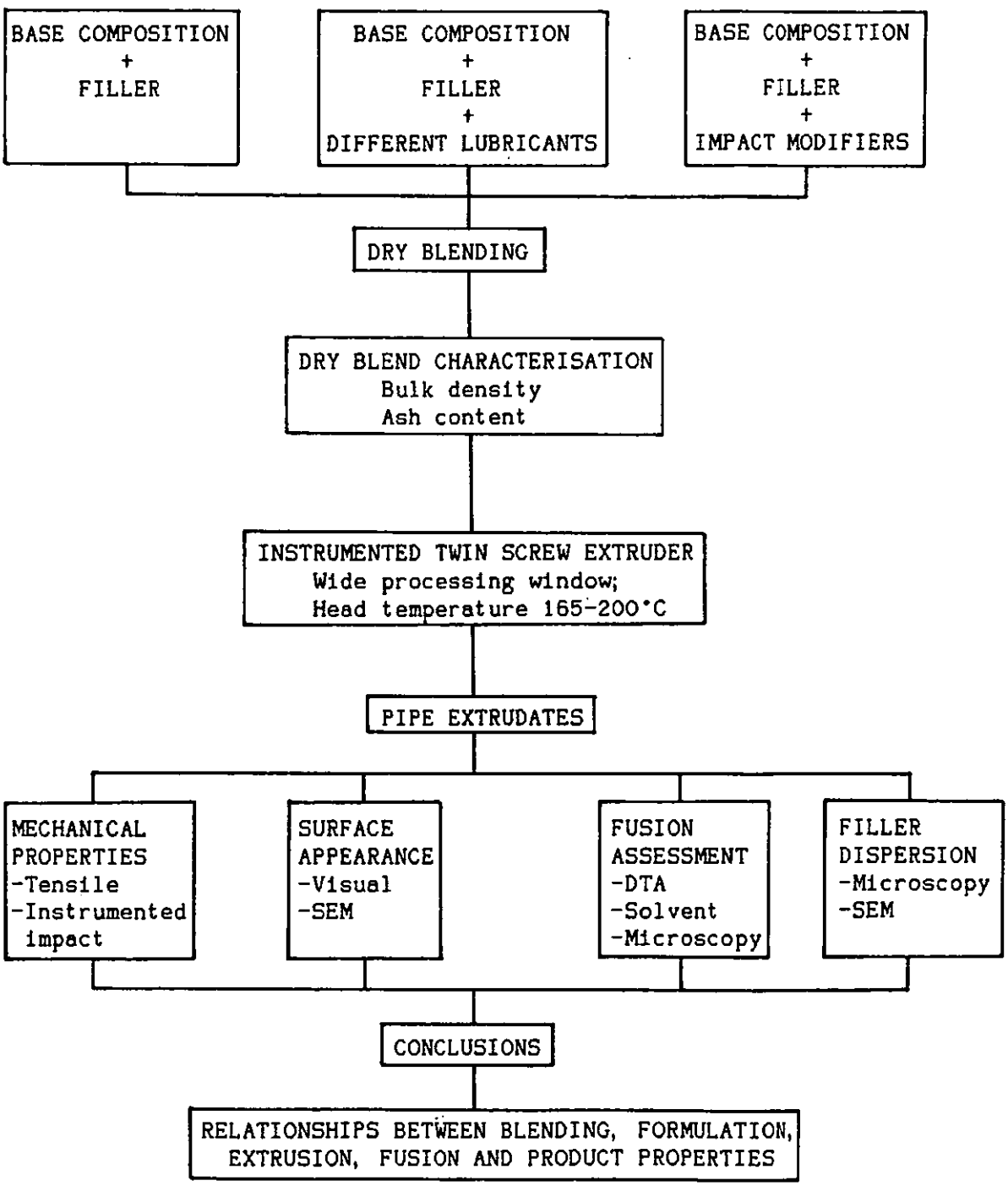

CHAPTER TWO

EXPERIMENTAL PROCEDURE

2.1 INTRODUCTION

The project objectives defined two main areas of interest: i) effect of filler upon processing, fusion and properties and ii) effect of additives, such as lubricants and impact modifiers, upon unfilled and filled systems. Therefore samples were prepared for subsequent testing in two stages.

2.2 PVC FORMULATION

A general purpose UPVC pipe formulation, supplied by Cookson group plc, was used as the basis for processing and formulation studies (table 2.1).

TABLE 2.1

PVC formulation

	phr
Polymer 'Corvic' S68/173	100
Filler Polcarb S	0⇒50 †
Stabiliser/lubricant system	
Tribasic lead sulphate	2·0
Normal lead stearate	1·2
Calcium stearate	0·4
Primary lubricant: Sasol H1	0·1

† Increments of 10 phr

These compositions were used exclusively in the first stage of this project and were coded 0⇒5 inclusive.

2.2.1 PVC POLYMER

A suspension PVC polymer, particularly suited to rigid PVC twin screw extrusion, was produced by ICI plc. The technical specification for this grade can be listed in the following table [157]:

TABLE 2.2

Technical specification for 'Corvic' S68/173

Grade	S68/173
Viscosity No (ISO R174: 1974)	116
'K' Value (from Visc No)	68
Apparent density (g/ml)	0·56
Relative density	1·40
Particle size (%)	
less than 250 μm	>99
less than 75 μm	< 5
Volatiles content (%)	< 0·3

2.2.2 FILLER

A stearate coated fine calcium carbonate manufactured and supplied by E.C.C international was used as a representative material and the technical specification for this common filler can be listed as shown in table 2.3 [158].

2.2.3 COMPOSITE STABILISER/LUBRICANT SYSTEM

The main heat stabiliser in this system was tribasic lead sulphate (TBLS: $3PbO.PbSO_4.H_2O$), which is a powerful and versatile stabiliser, commonly used in twin screw extrusion.

Normal lead stearate (NLSt: $Pb(CH_3(CH_2)_{16}COO_2)$) is generally used in conjunction with other lead salts and its

intended application is as a moderate external lubricant in a well balanced lead stabilised system.

Calcium stearate (CaSt: $Ca(CH_3(CH_2)_{16}CO_2)$) is not very effective as a heat stabiliser but is primarily used as a 'internal' lubricant.

The last component of this combined stabiliser/ lubricant system was a primary lubricant. The lubricant for this section of the study was Sasolwaks H1, which is a high melting point, crystalline, paraffin wax (average formula: $C_{50}H_{102}$) and is predominantly classed as an external lubricant.

Detailed technical data on the above ingredients is provided in Appendix A.

TABLE 2.3

Technical data for Polcarb S

Brightness (ISO)	85 ± 1·0
Particle size (%)	
greater than 53 μm	0·01 (max)
greater than 10 μm	0·5 (max)
less than 2 μm	86·0 ± 3
Surface area (m^2g^{-1})	7·0
Oil absorption (g/100g)	18
Moisture (%)	0·2 (max)
Chemical analysis (%)	
calcium carbonate	97·0
acidic residues	1·8
stearate addition	1·0

2.3 LUBRICANT/MODIFIER STUDY

The second stage of this study investigated the effect of lubricants and impact modifiers upon the processing and properties of an unfilled and a heavily

filled UPVC pipe. The base composition, shown in table 2.1, was altered by the replacement of the primary lubricant with a series of other lubricants and, secondly, the addition of impact modifiers. Table 2.4 lists the type and level of additives used.

TABLE 2.4

Description of lubricants and modifiers

Additive reference	Description	phr	Sample code
Lubricant			
Sasol H1	High M.pt paraffin wax	0·1	-
Oletec 6009	Low M.pt paraffin wax	0·2	A
Oletec 6009	Low M.pt paraffin wax	1·0	B
Loxiol G12	Fatty acid ester of glycerine	1·0	C
Loxiol G15	Hydrogenated castor oil	1·0	D
PE 520	Polyethylene wax	0·2	E
Pristerene 4903	Stearic acid	1·0	F
Modifier			
Dow 3615	Chlorinated polyethylene	10·0	G
KM 323B	All-Acrylic	10·0	H

Further information is provided in Appendix A.1.2.

These additives were incorporated in the formulation containing 30 phr of Polcarb S and also in an unfilled composition.

2.4 DRY BLENDING

Two high speed mixers were initially investigated: a 8 litre T.K.Fielder and a 40 litre Henschel. A previous study [168] reported severe problems of filler segregation during the dry blending of highly filled calcium carbonate compositions, and therefore further experimentation was necessary in an attempt to attain a representative filled premix. All the main blending parameters for the Fielder intensive mixer was varied (i.e. batch weight, jacket temperature, rotor speed and batch sequence) and no significant improvement in filler distribution was obtained.

Thus the geometry and size of the mixer was not considered appropriate to provide highly filled dry blends.

The operating conditions of the Henschel mixer were also studied, and the optimum conditions determined. In this case an increase in batch weight (increase in fill factor) aided the production of highly filled compositions.

Figure 2.1 illustrates the basic layout of a dry blending process [107]: a batch weight of 18 kg was premixed by hand and then placed in a pre-warmed heater mixer (45°C), the heater mixer is started and the impellor speed was preset at 1500 rpm. The dry ingredients were mixed to 120°C, where the material was automatically dumped to the stationary cooler mixer by a pneumatic discharge valve (the cooler mixer was started after hot material was dumped to minimise filler loss). The lower speed of the cooler mixer impellor (low frictional heating) and the cooled jacket quickly cooled the dryblend (3-5 mins) to a handling temperature of 30-40°C. The cooled premix was then discharged and reweighed. The blending time varied between 9 mins ± 55 secs for the blends and the cycle time between batches was carefully controlled at 5 mins to ensure consistent heater mixer temperature before mixing (45-50°C).

2.5 ASSESSMENT OF DRY BLENDS

2.5.1 ASH CONTENT

A small amount of dry blend (6 ± 0·2 g) was sampled, accurately weighed, and then ashed in a furnace at 900°C for a period of one hour. The remaining ash was reweighed and the percentage ash retained calculated, this value was then related to a calibration graph, as shown in Appendix B, to yield a filler content (phr). The calibration graph was prepared by ashing filled blends which had been accurately weighed and hand mixed. An average of three results were taken and an accuracy of better than 1 phr was achieved in all cases.

FIGURE 2.1

Dry blending process

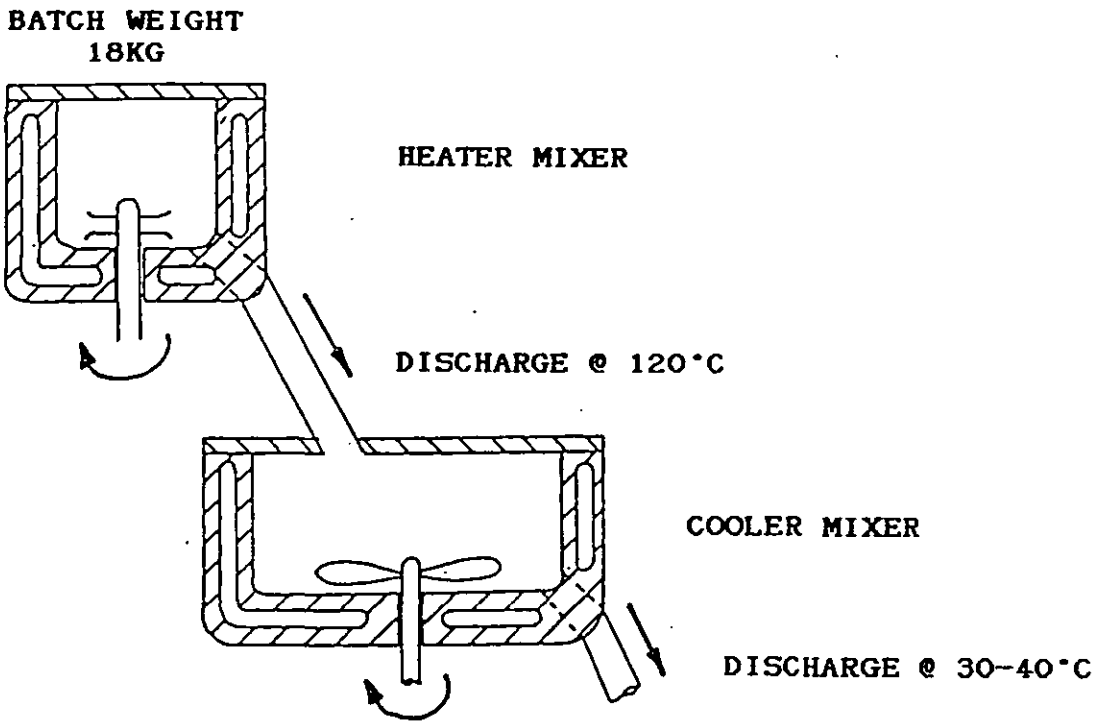

2.5.2 BULK (TAP) DENSITY

Approximately 100 g of the dry blend was poured into a tall graduated cylinder and vibrated using a Tap-pack volumeter™ at a rate of one drop per second until the volume equilibrated. The tap density was reported as the ratio of powder weight to final volume. Two measurements were taken and an accuracy of 1 cm^3 was noted, equivalent to a tap density of 0·01-0·02 g/cm^3.

2.6 TWIN SCREW EXTRUSION

A Krauss Maffei KMDL-25 twin screw extruder at Cookson group central laboratories was used to produce pipe specimens from the Henschel blends. The intermeshing conical counter-rotating machine has been fully described in the literature [131, 142, 154]; a standard head was fitted with an

approximate overall diameter of 32 mm and an annulus gap of 1·8 mm. Table 2.5 lists the salient technical specifications for this extruder [154]:

TABLE 2.5

Machine details of KMDL-25

Screw diameter tip	25 mm
feed	50 mm
Screw length	400 mm
Screw speed	5·05-50·5 rpm
Screw torque (max)	5·19 Nm
Dc motor rating	0·265-2·65 kW
Output capacity (max)	≈18 kg/hr

The screw configuration is shown in figure 2.2 [169].

FIGURE 2.2

KMDL-25 Screw design

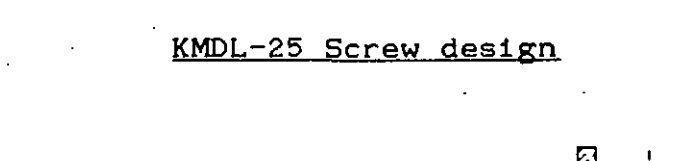

The laboratory extruder was instrumented to provide information at all stages within the extrusion process. Figure 2.3 illustrates the KMDL-25 and the positions where temperature and pressure probes are located [142]:

FIGURE 2.3

Instrumentation of KMDL-25

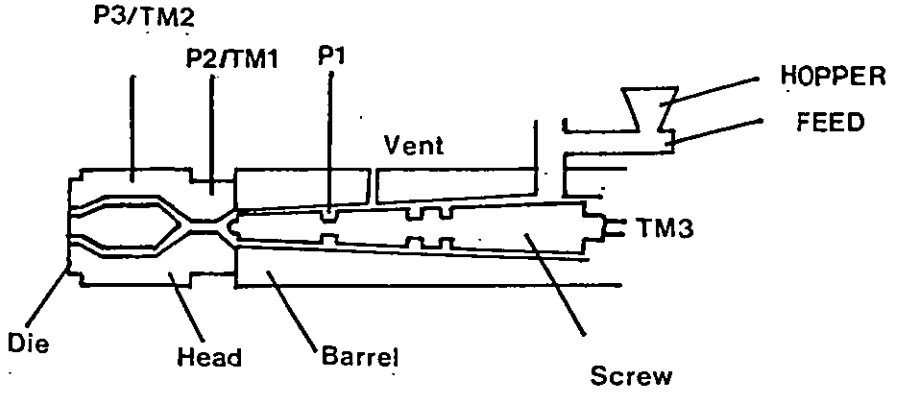

Where: TM1 = Adaptor temperature (°C)
TM2 = Pipe Head temperature (°C)
TM3 = Screw temperature (°C)
P1 = Metering zone pressure (Bar)
P2 = Adaptor pressure (Bar)
P3 = Pipe head pressure (Bar)

The pipe head has an electrical heater band around the body and tip while the screw and barrel is heated by oil jackets; both systems are carefully monitored by proportional controllers and thermocouples. The attached hardware provides a continuous hardcopy of the above measurements and, in addition, indicates torque (TQ: % of maximum torque) and screw speed (SS: rpm).

2.6.1 OPERATION OF EXTRUDER

The conditions under which the premixes were processed were determined by an extensive trial study, the conditions were chosen to allow a wide processing 'window' of vastly different compositions.

TABLE 2.6

Extrusion conditions

VARIABLE		EXTRUDER PROFILE CODE						
		A†	B†	C	D	E	F	G‡
Screw speed	(rpm)	25	25	25	25	25	25	25
Volumetric feeder	(rpm)	38	38	38	38	38	38	38
Zone 1 temperature	(°C)	165	165	165	180	180	200	210
Zone 2 temperature	(°C)	165	165	165	180	180	200	210
Screw temperature	(°C)	150	150	150	150	150	150	150
Head temperature	(°C)	165	170	180	180	190	200	210
Die tip temperature	(°C)	165	170	180	180	190	200	210

† Unable to produce 'acceptable' pipe

‡ Degradation streaks; included for 0 phr as reference only

The above table indicates a wide processing range and each extruder profile was used for each filler increment. The pipe specimens were key coded with respect to filler content and extruder conditions; the filler code 0⇒5 (increments of 1 representing 10 phr of Polcarb S) was followed by the extruder profile code shown above. Thus a pipe code of 3E represents a 30 phr composition extruded at conditions E.

The experimental procedure was largely influenced by the incorporation of substantial quantities of filler and low extrusion temperatures. The extruder was starve fed since flood feeding tripped the machine torque limit for higher levels of filler and a relatively low screw speed was also necessary. The feeding of heavily filled compositions led to severe handling problems; the material would bridge the hopper and adhere to the volumetric screw feeder and thus, ultimately, lead to surging. These problems were largely overcome by ensuring that the screw feeder remained as cool as possible and implementing a multi-pronged stirrer in the feed hopper. The feeding of these problem materials was also aided by alternating the extruder runs between a

heavily filled dry blend and a lightly filled dry blend rather than a progression of lightly filled to heavily filled. The occurrence of surging or reduction in output was carefully monitored by the graphical output of torque and head pressure; a steady reduction in torque indicated a reduction in feed rate. However, after applying the above remedies, a steady state situation was quickly obtained (15-20 mins) and pipe samples were taken when the instrumented values levelled off. Pipe section was produced via a sizing and water trough unit and the section was monitored for eccentricity. The pipe output was measured as mass and length per unit time and a small length of pipe was subjected to a methylene chloride test (MCT: 15 minutes immersion at room temperature).

Pipe specimens could not be obtained for extrusion profiles A and B due to poor melt extensibility and at the highest profile code considered, G, degradation/'burn up' was evident, and thus this profile was only used for 0 phr as an indicator of the maximum processing temperature possible for the composition used.

2.6.2 PROCESSING OF LUBRICANT/MODIFIER COMPOSITIONS

The processing of these compositions was similar to the experimental procedure noted above, except that only one extrusion condition, profile E, was chosen since this profile provided a pipe with acceptable processability and extrudate appearance. The resultant pipes were labelled 0 or 3 (0 or 30 phr Polcarb S: §2.3) followed by the extrusion code E and then lastly a lubricant/modifier code as described in table 2.4.

2.7 SURFACE APPEARANCE

The surface appearance of pipes was qualitatively assessed by:

i) Visual observation: the pipes were ranked in order of roughness.

ii) Scanning electron microscopy: small samples of the pipe, representative of the complete pipe, were mounted onto aluminum specimen stubs, sputter coated with gold and viewed under a Cambridge Stereoscan 2A electron microscope. The surface appearance was photographed at various levels of magnification.

2.8 ADDITIVE DISPERSION

Additive dispersion was observed by optical microscopy: 3-5 μm sections were microtomed using a Leitz 1400 microtome with a 'D' profile steel blade. The section was mounted between a glass slide and glass cover slip using cedarwood oil as a suitable mounting fluid. The sections were viewed using a Zeiss universal transmission microscope with various objectives (Zeiss 6·3/0·16 & 16/0·35) in common light, phase contrast and dark field modes.

Sections were taken in the direction of extrusion as well as transverse to the machine direction.

A number of the thin sections prepared above were also observed via UV fluorescence microscopy. If PVC is degraded then the formation of an conjugated species will lead to primary fluorescence in the visible region. Similarly poor distribution of stabilising additives could lead to regions of fluorescence [112, 170] during processing. Thus this technique provides an indication of processing history, additive dispersion and residual grain content. The Zeiss microscope was fitted with a Zeiss III RS fluorescence attachment incorporating a 50 watt HBO high pressure mercury

vapour lamp. The attachment also housed a G365 exciter filter for maximum visible light emission at 365 nm and a barrier filter, LP 420, for transmission of the visible spectrum only [170]. The sections were focussed and photographed using a special UV objective; Plan-Neufluor 16/0·50.

2.9 ASSESSMENT OF FUSION

2.9.1 ACETONE SHEARING TEST

Summers *et al* [109] described a optical microscopy technique using sheared acetone swelled samples to provide a better discriminating power then traditional solvent immersion tests. Therefore small specimens (approximately 2 mm cube) were cut from the pipe samples and immersed in glass stoppered tubes of acetone for 5 hours. The treated samples were sheared between glass slides and viewed via common light microscopy (Zeiss universal microscope: 6·3/0·16) under dark field illumination.

2.9.2 DIFFERENTIAL THERMAL ANALYSIS

The application of thermal analysis as a tool for measuring fusion levels of processed PVC has already been discussed in §1.4.2.5. The instrument used was a Du Pont 990 Thermal Analyser with a Du Pont DSC cell. An aluminium sample pan and a reference pan (empty) are placed on their respective positions on a constantan disc. The disc is embedded within a silver heating block and a silver lid caps the complete unit; the block is heated at a constant rate and heat is efficiently transferred through the constantan disc to the separate pans. The differential heat flow between the sample pan and empty reference pan is measured by chromel-constantan thermocouples positioned underneath the pan location. This signal response can be amplified and recorded on a x-y plotter versus sample temperature. The

cell was accurately calibrated by thermal analysis scans of known materials, such as tin and indium; these materials have sharp melting points with precise heat of fusion values, and thus the cell can be calibrated for energy measurements of unknown materials. A purge gas (nitrogen) is used to maintain the cell and prevent corrosion by noxious gases.

Figure 2.4 illustrates a typical DSC thermogram of a 'moderately' processed UPVC pipe with the salient features noted.

Small samples of pipe (10-12 mg) are scanned from room temperature to 240°C at a heating rate of 20°C/min and an Y axis sensitivity of 1 and 2 mV/cm. A minimum of three samples were taken each pipe specimen and no skin effects was observed for the thin pipe section. The nitrogen purge gas was pumped throughout the scanning period at a rate of 60 cc/min.

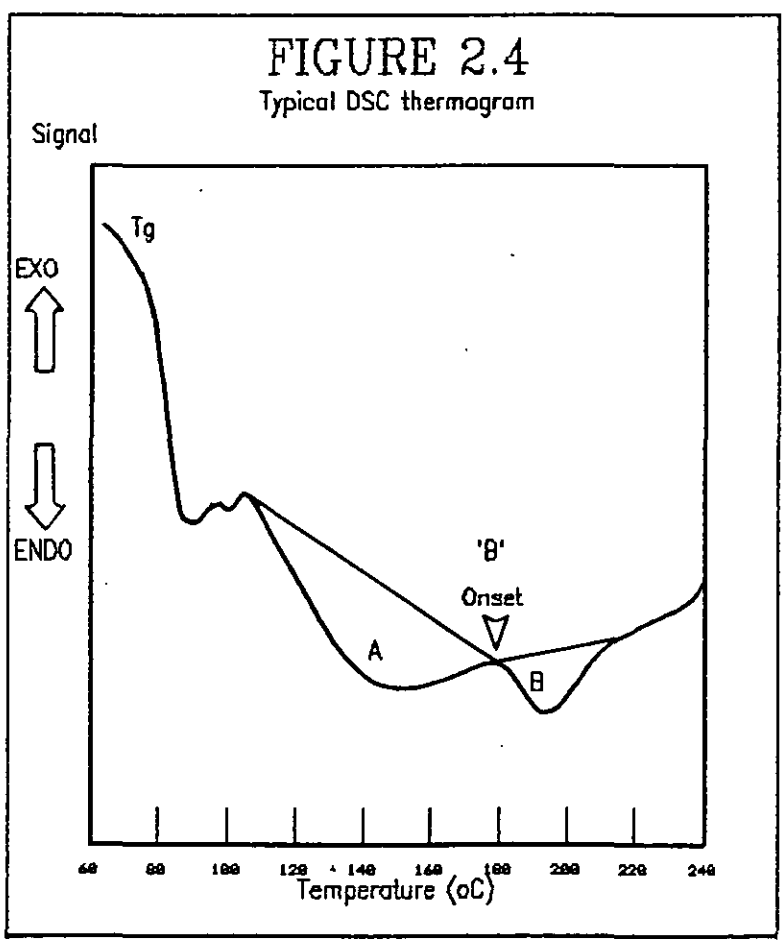

The area of peaks 'A' and 'B' can be determined by a planimeter and converted into heats of fusion by the following relationship:

$$\Delta H_F = \frac{A}{m} (60\ B\ E\ \Delta q_s) \qquad (2.1)$$

Where ΔH_F = Heat of fusion (J/g)
A = Endothermic area (cm^2)
m = Sample mass (g)
B = Time base setting (0·5 min/cm)
Δq_s = Y axis sensitivity (1 & 2 mV/cm)
E = Cell calibration constant (0·25 & 0·22 mW/mV)

2.10 MECHANICAL PROPERTIES

2.10.1 TENSILE TESTING

Tensile specimens were prepared from the pipe samples and uniaxial tensile properties evaluated using a J.J Lloyd universal testing machine (T5002) fitted with an infra-red extensometer. The dumb-bell test pieces were prepared by cutting, parallel to the extrusion direction, with a press die and the test pieces conformed to the dimensions of type 1 of BS 903 : Part A2 : (1971) standard [171] (figure 2.5).

FIGURE 2.5

Tensile specimen: Type 1

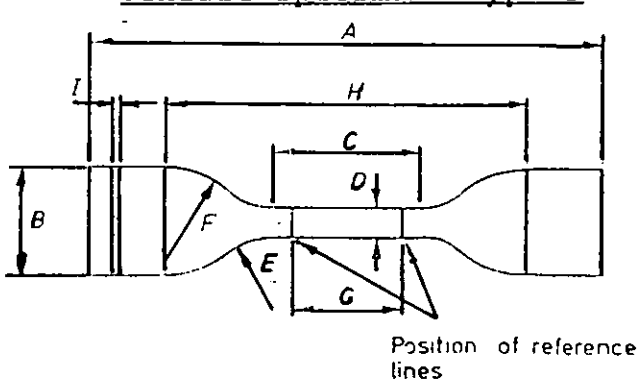

Where	A	=	Overall length (minimum)	75
	B	=	Width at ends	12·5 ± 1
	C	=	Length of narrow portion	25 ± 1
	D	=	Width of narrow portion	4·0 ± 0·1
	E	=	Small radius	8·0 ± 0·5
	F	=	Large radius	12·5 ± 1·0
	G	=	Distance between reference lines	20
	H	=	Distance between sample grips	40 ± 5
	I	=	Thickness (preferred)	2·0

All dimensions are in millimetres

Five test pieces were tested at a crosshead speed of 50 mm/min and at room temperature conditions. An initial gauge length of 20 mm was marked with graphite tape and the infra-red extensometer positioned to follow these markers.

The resultant force-extension graphs were used to determine the following tensile parameters:

$$\text{Ultimate tensile stress} = \sigma_B = \frac{F_B}{A} \qquad (2.3)$$

$$\text{Yield stress} = \sigma_Y = \frac{F_Y}{A} \qquad (2.4)$$

$$\text{Elongation at yield} = \varepsilon_Y = \frac{(l_Y - l_0)}{l_0} \times 100\% \qquad (2.5)$$

$$\text{Elongation at break} = \varepsilon_B = \frac{(l_B - l_0)}{l_0} \times 100\% \qquad (2.6)$$

Where	F_B	=	Force at break	(N)
	A	=	Cross-sectional area of waisted portion of dumb-bell	(mm^2)
	F_Y	=	Force at yield point	(N)
	l_Y	=	Extension at yield point	(mm)
	l_0	=	Initial gauge length	(mm)
	l_B	=	Extension at break	(mm)

2.10.2 IMPACT PROPERTIES

Impact testing is a widely used property measure for UPVC products and is covered by a large number of standards. Traditionally, evaluation has included Charpy, Izod and Gardner type tests where an impact failure energy or 50% failure rate is determined. More recently, instrumented impact tests have been used which can provide more information upon failure mechanisms, product testing and reduce the number of test pieces. The correlation between processing and impact properties is not well understood, and conclusions differ from the presence of a maximum to a monotonic increase with increasing fusion level (§1.5.3).

A Rosand instrumented falling weight impact tester (type 5A) was used to evaluate impact properties. The basic layout of the falling weight column is shown in figure 2.6 [172].

A Kistler™ transducer is positioned between the impactor probe and the impact weight; on drop release of this arrangement, the impactor probe accelerates, due to gravity, towards the sample holder. The probe assembly flags a optic trigger which activates a transient recorder to begin data collection of the force signal with time. The fracture event may be only a few thousandths of a second (typically <10 ms), however the 12 bit transient recorder can obtain 2000 data points during this period to provide an accurate account of the fracture behaviour. A microcomputer (modified BBC model B) receives the digitised force signal and provides data handling, storage, analysis and print-out facilities. The microcomputer can represent the fracture behaviour as force-time or force-deflection graphs and analysis of the trace yields detailed information, such as gradient, force or energy, at any given point. Energy values are obtained by integration of the trace upto the force/time co-ordinates. The salient features of the force-deformation trace are shown in figure 2.7 [174].

FIGURE 2.6

Instrumented impact tester

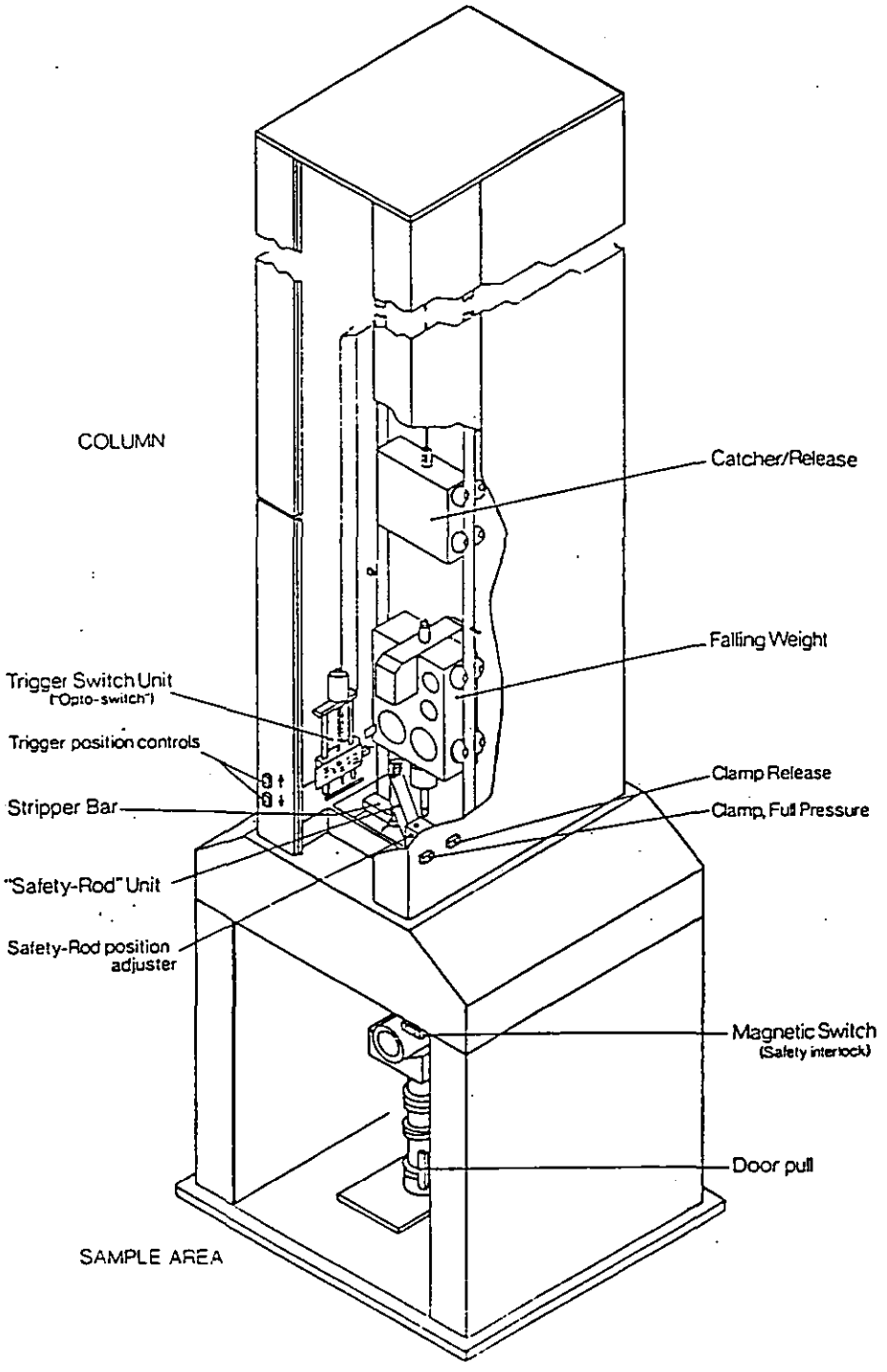

FIGURE 2.7

Force-deformation trace

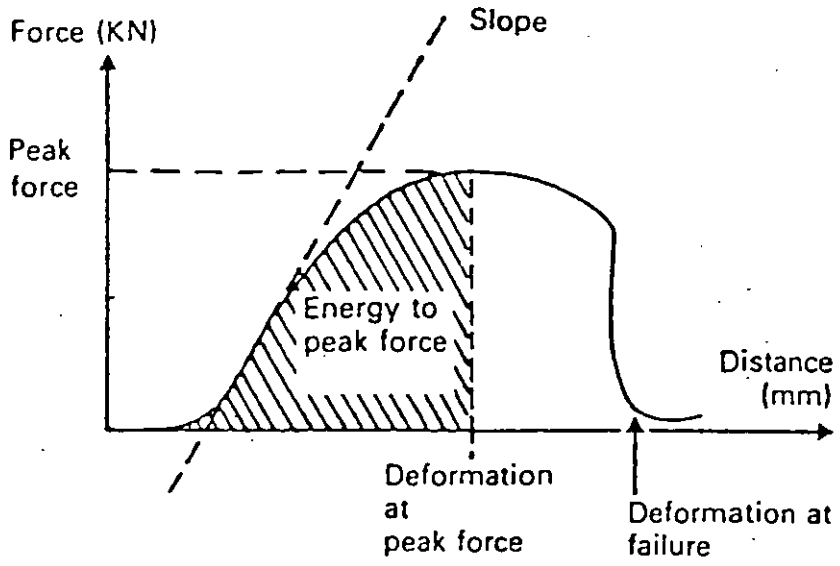

The type of fracture behaviour can be generalised as shown in figure 2.8. Ductile failure produces a broad peak with failure occurring beyond a yield. Brittle/ductile behaviour is suggested when failure occurs at a sharp yield peak and lastly brittle fracture produces low force and deformation values with difficulty in discerning between initiation and propagation characteristics. These terms are applied to pipe fracture and a number of intermediates are envisaged depending upon conditions.

2.10.2.1 EXPERIMENTAL PROCEDURE FOR IMPACT TESTING

IMPACT RIG

Pipe specimens are commonly tested using a 45° 'V' block which supports an unclamped length of pipe. However the geometry and ductility of a proportion of the pipes to be tested did not allow complete fracture of the pipe surface(s); instead, pipe collapse and deformation yielded a complicated trace which could not discriminate between the

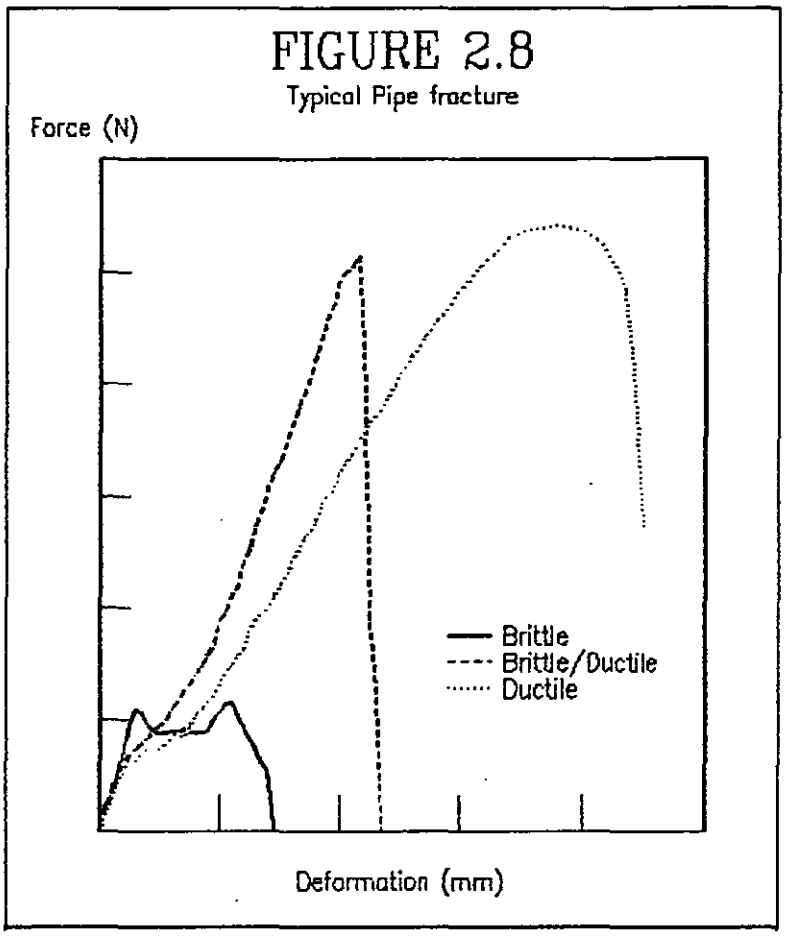

pipe walls. Thus further work considered a number of geometries and finally an impact rig was designed and used throughout the program (Appendix C). A minimum of ten split pipe samples were measured for pipe wall thickness, clamped in the rig and then tested.

IMPACT VELOCITY

The test speed is determined by the drop height:

$$v = \sqrt{(2gh)} \qquad (2.7)$$

Where υ = Velocity (m/s)

g = Acceleration due to gravity (9·81 m/s²)

h = Test height (m)

The drop height (>0·5 m) did not greatly affect test results and the chosen speed was suggested by a draft BSI proposal [173], i.e. 1 metre drop height corresponding to an impact velocity of 4·4 m/s.

The available impact energy can be determined at this height by the simple relationship in equation 2.8:

$$E_o = mgh \qquad (2.8)$$

Where E_o = Available impact energy (J)

m = Impact mass (25·35 kg)

g = Acceleration due to gravity (9·81 m/s²)

h = Test height (m)

Therefore the available impact energy at a test of one metre is 249 J. It must be ensured that the available impact energy is large in comparison with the absorbed impact energy; since a large reduction in impact velocity due to energy absorption can affect the characteristics of the force-deformation trace. A reduction of 20% is the maximum permitted [173] and the impact mass required to satisfy this criterion can be estimated by the following equation.

$$m \geq 3 \times \frac{E_{TOT}}{g.h} \qquad (2.9)$$

Where m = Impact mass (kg)

E_{TOT} = Total energy available (J)

g = Acceleration due to gravity (9·81 m/s²)

h = Test height (m)

In all cases the reduction in impact velocity was estimated to be less than 5% of original impact velocity.

FILTERING

The force signal of instrumented impact testers is invariably filtered to some degree by a low pass filter in an attempt to reduce adventitious vibration (especially for brittle materials). However excessive filtering can hide the true characteristics of the fracture behaviour or reduce peak values such as peak force. The Rosand impact tester incorporates non-resonant materials such as titanium and a digital filter which can 'post-filter' the signal; this digital filter allows an optimum filter to be chosen after testing and thus reduces the likelihood of spurious results. The maximum reduction in peak force observed for the filters chosen (1·5-4 kHz) was <3%.

BRITTLE-DUCTILE TRANSITIONS

The majority of testing was performed at room temperature. In addition the pipe series extruded at profile F (§2.6.1) was subjected to low and high temperature impact testing. The temperatures involved were -20, -10, 0, 10, 20, 41, 60, 80 and 100°C ± 1 °C. The cold temperature samples were conditioned in a cold finger bath of ethylene glycol for 8 hours while the high temperature samples were placed in a hot air oven for a minimum of 8 hours. Heat transfer during removal of sample from the medium to the specimen holder was considered insignificant since the complete test cycle was approximately 5 seconds and the impact rig was also conditioned at the prescribed test temperature.

SUMMARY OF TEST CONDITIONS

Impactor tip	10 mm hemispherical (ISO)
Impact speed	4·4 m/s
Impact height	1·0 m
Impact mass	25·35 kg
Number of specimens	10 (minimum)
Sweep time	5, 10 and 20 ms
Low pass filter	1·5, 2·0, 3·0 and 4·0 kHz
Test temperature	All pipes at room temperature Pipes processed at profile F: -20, -10, 0, 10, 20, 41, 60, 80, 100°C

EXTRUDER PROFILES: A & B

Pipes manufactured at these low temperature profiles did not produce a regular shaped pipe and thus could not be tested in the above manner. These extrudates were longitudinally split and placed in a hot upstroking compression press at 125°C, after a period of 10 minutes a pressure of 5000 kg was applied and held for 5 minutes. The pressed samples were then cooled by circulating cold water throughout the platens. The resultant sheets were impact tested using a DIN anvil (60 mm OD/40 mm ID) with a ring clamp pressure of 3000 N.

CHAPTER THREE

PROCESSING RESULTS

3.1 DRY BLENDING

The dry blending of highly filled compositions can lead to a severe problem of filler segregation. The optimum conditions were determined, as described in §2.4, and the results suggested that careful control on overall batch weight and blending sequence were necessary to obtain compositions containing representative amounts of filler. Blending time was unaffected by an increase in filler level except for blends 4 and 5 (representing filler levels of 40 and 50 phr respectively). The higher levels of filler produced a delay in mixing time as shown in table 3.1.

TABLE 3.1

High speed blending time

Blend code	Filler level (phr)	Discharge time (min)
0	0	8'5"
1	10	8'10"
2	20	8'5"
3	30	8'10"
4	40	8'45"
5	50	9'45"

All the blends (0,3E- to 0,3EH) produced for the additive study yielded a discharge time of approximately 8 min 10 s and thus the additives did not affect the blending time.

3.1.1 DRY BLEND CHARACTERISTICS

3.1.1.1 ASH CONTENT

The filler contents of the blends were determined by ashing a small quantity of the dry blend and comparing the percentage ash retained with a reference graph (§2.5.1). The results can be tabulated as follows:

TABLE 3.2

ASH CONTENT

Blend code	Ash content (phr)	Volume fraction (% Vol)
0	0·0	0·0
1	8·5	0·046
2	18·1	0·1208
3	27·1	0·163
4	35·6	0·2228
5	40·0	0·2569

A good agreement is obtained between the expected filler loading and ash content upto the higher filler loadings of 40 and 50 phr. The highly filled compositions result in a proportion of the filler being retained within the mixer chamber, i.e. mixer fouling. These results are supported by the blending results since high filler loadings and possible filler loss leads to a reduction in the effective mixing charge involved in the vortex type mixing action and thus a longer mix time.

The blends produced for the additive study were also assessed and yielded similar results to the above table, i.e. 30 phr compositions indicated a filler content of between 27-28 phr.

3.1.1.2 BULK (TAP) DENSITY

Tap density indicates the ability for a powder to pack efficiently and possibly the effect of the particle size distribution involved.

All the blends were tested and the results can be listed in table 3.3 and figures 3.1 and 3.2.

TABLE 3.3

Tap density of powder blends

a) Varying filler content:

Blend code	Filler content (phr)	Tap (Bulk) density (g/cm^3)
0	0·0	0·73
1	8·5	0·75
2	18·1	0·78
3	27·3	0·79
4	35·6	0·86
5	40·9	0·96

b) Varying additive type:

Filler code	BLEND CODE								
	-	A	B	C	D	E	F	G	H
	Tap density (g/cm^3)								
0	0·74	0·73	0·75	0·74	0·71	0·72	0·74	0·73	0·73
3	0·79	0·79	0·78	0·81	0·78	0·79	0·82	0·82	0·82

Figure 3.1 illustrates an approximate linear increase in tap density upto a filler content of approximately 30 phr, where a exponential increase is observed. Figure 3.2 suggests that additive type has little effect upon tap density of the base composition and that the effect of filler is more prominent.

FIGURE 3.1

Tap density versus Filler content

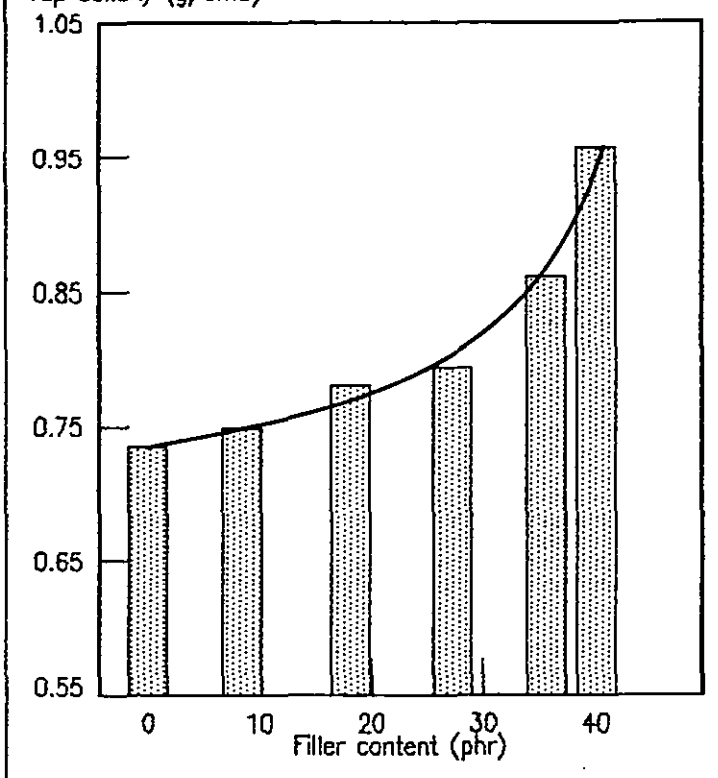

FIGURE 3.2

Tap density for Additive blends

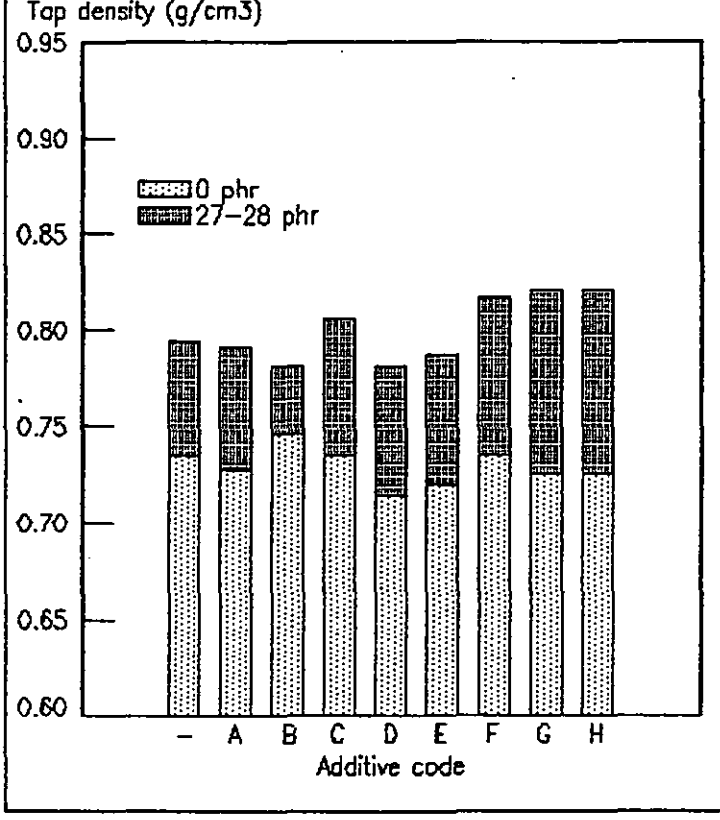

3.1.1.3 SCANNING ELECTRON MICROSCOPY OF POWDER BLENDS

Scanning electron micrographs of the dry blended powders were taken and a selection is shown in figures 3.3-3.8 inclusive. Figure 3.3 and 3.4 illustrate that the unfilled dry blend (0) resembles that of the virgin suspension polymer and the distinct irregular surface formed by the agglomeration of sub-grains can clearly be seen. The micrographs of the lightly filled dry blend, (1), suggest that the filler is located within the folds of the grain (figures 3.5 and 3.6) to form a more spherical shaped grain. The presence and position of the calcium carbonate filler can be detected by X-ray analysis to produce a calcium element map as illustrated in figure 3.7. The map is the same field of view as figure 3.6 and infers that the filler is preferentially situated in the fold of the particle rather than on the grain extremities. The blend containing a higher filler level, 18·1 phr, reveals a much more even coating of filler and a large proportion of the available grain surface is coated. A further increase in filler loading leads to a slight increase in the covering power of the filler, however it is evident that at a filler level of 18·1 phr the grain surface is almost completely covered by filler.

The micrographs presented can, to some extent, explain the difficulty observed in blending representative blends and the results obtained for the dry blend characteristics. A moderate level of filler coats the surface of the PVC grains and is therefore attached or possibly adsorbed onto the polymer surface. A higher level of filler will continue to coat the grain surface until the surface is completely covered; at this level there is 'free' or loosely attached filler particles and it can be envisaged that this free filler can be removed quite easily from the system. If the above results are considered then the dry blending procedure becomes more difficult at higher levels of filler (blends 4 & 5) and the ash content indicates that a higher proportion of filler is lost as fouling of the

FIGURE 3.3: Micrograph of powder blend O (×100)

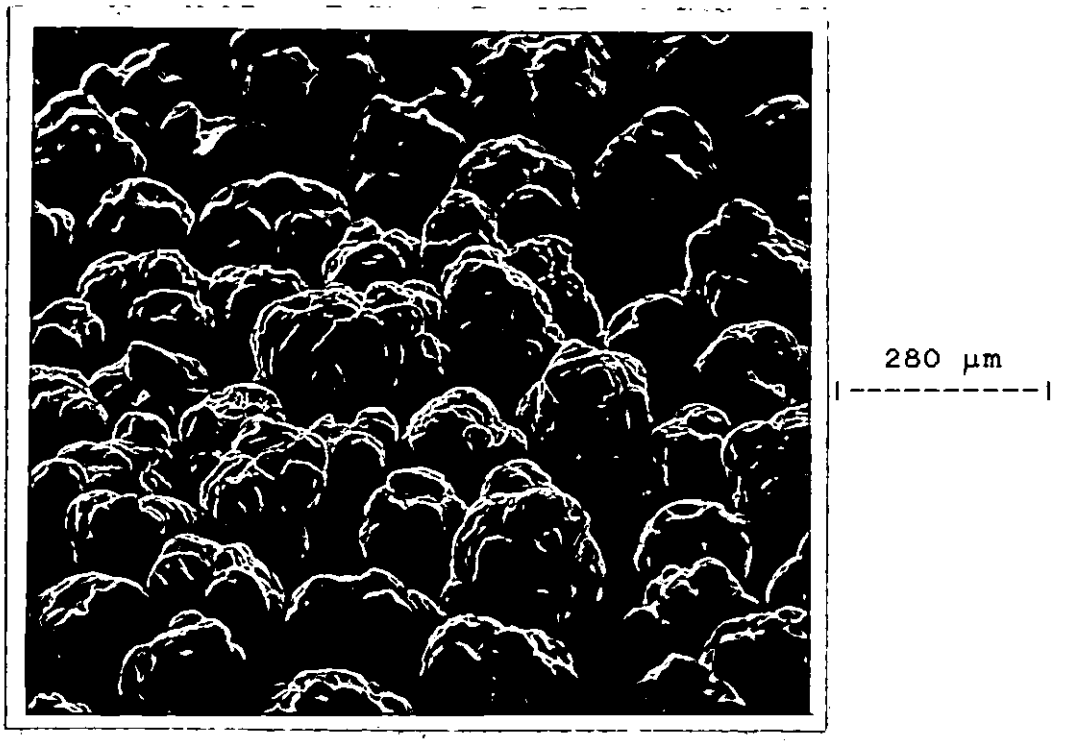

FIGURE 3.4: Micrograph of powder blend O (×1000)

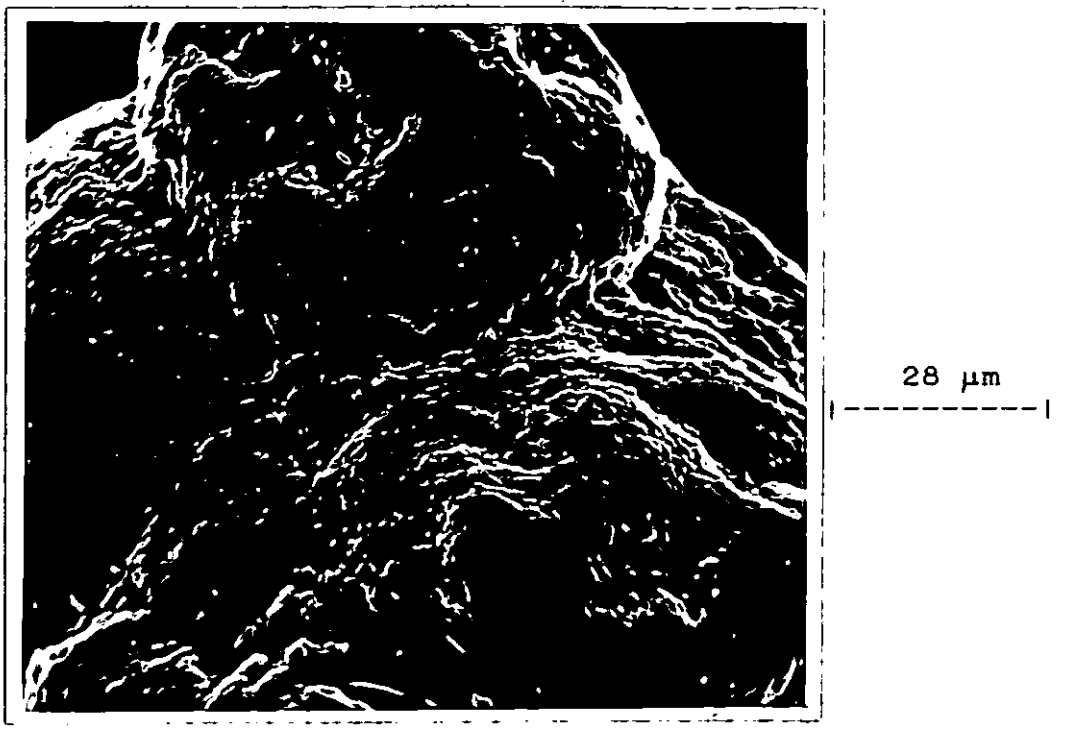

FIGURE 3.5: Micrograph of powder blend 1 (×100)

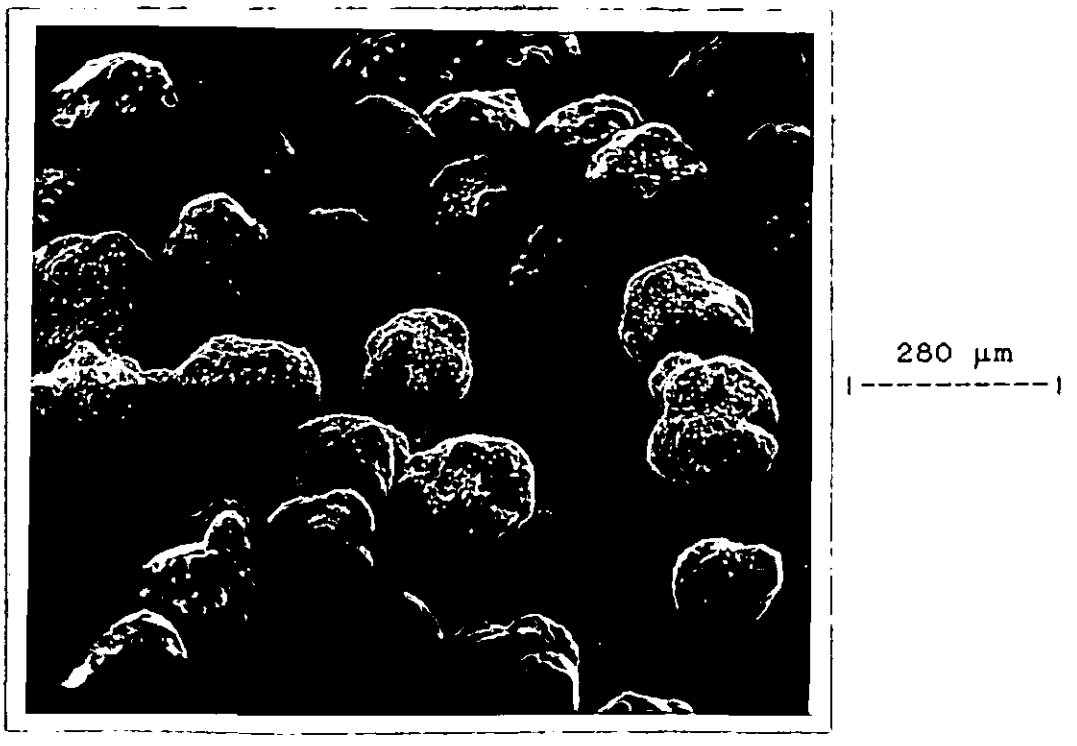

FIGURE 3.6: Micrograph of powder blend 1 (×1000)

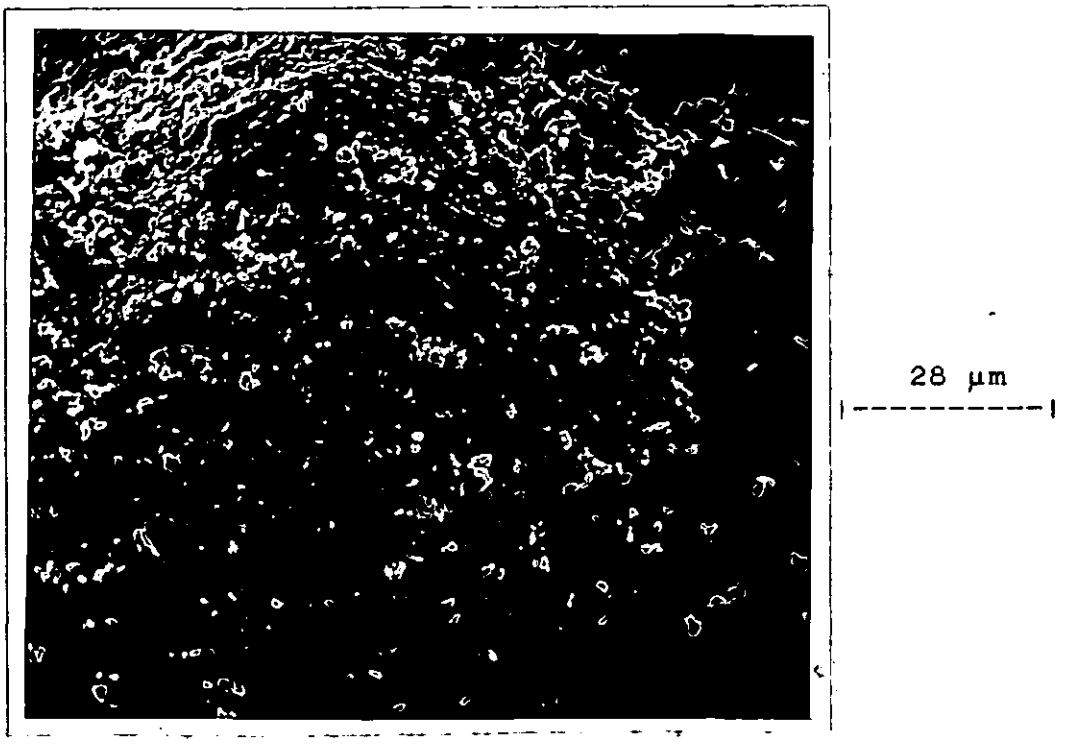

FIGURE 3.7: Ca micrograph of powder blend 1 (×1000)

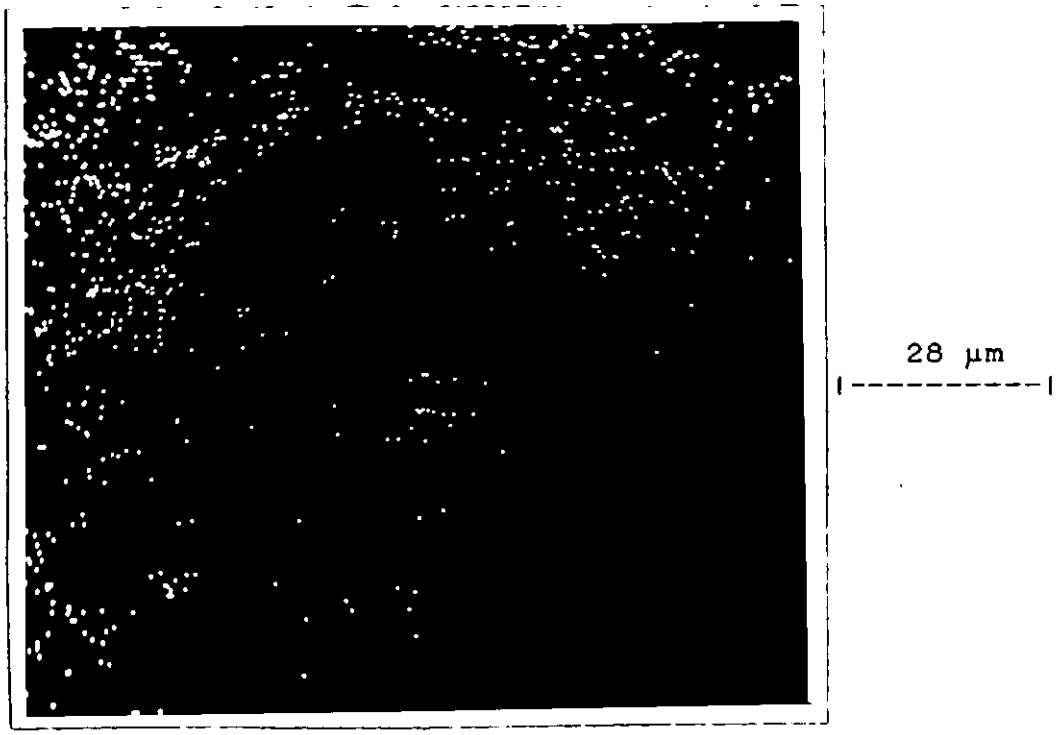

FIGURE 3.8: Micrograph of powder blend 2 (×1000)

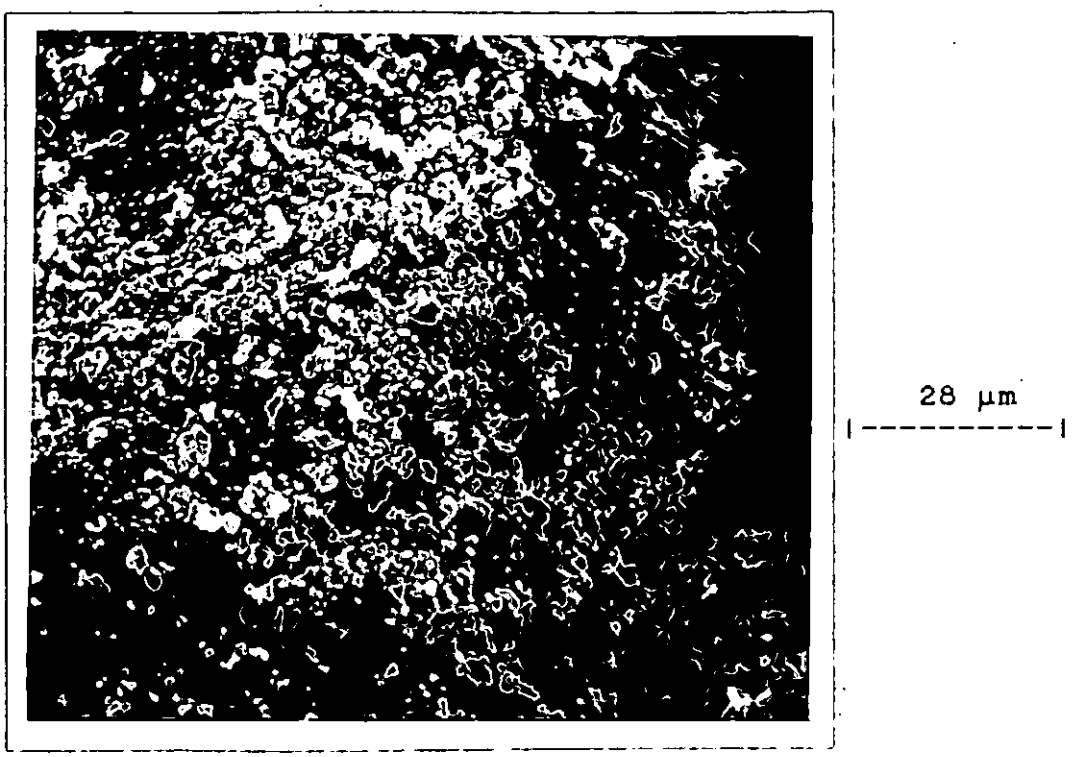

mixer i.e. a filler rich layer within mixer chamber).

Bulk density suggests a steady increase is observed due to the higher specific gravity of the filler and bi-modal particle size distribution, until an approximate filler level of 30 phr is reached. At this value, the tap density increases dramatically since the 'free' filler attempts to fill the interstices between the polymer grains and thus produce a more efficiently packed powder.

3.2 TWIN SCREW EXTRUSION

The instrumented KMDL-25 provides a large amount of data for each extruder profile and composition chosen, however some of this data is used to monitor the operating conditions of the extruder and not the processing characteristics of the material. These results, such as oil jacket temperatures, are given in Appendix D.1 and suggest that the oil jackets provide good, reproducible temperature control for a given extruder profile. Similarly the head and adaptor temperature values indicate the temperature of the extruder at that specific point rather than the 'melt' or material temperature. Thus it is difficult to assign a true melt temperature to a particular profile/composition run since the material temperature will not be wholly dependant upon the temperature of the surrounding metal and the inability to accurately calibrate the thermocouple/ transducer probes used in the Krauss Maffei.

The results which can be used to assess the processability of a material are listed into two main areas:

Mechanical/processing energy
Extrusion pressures

3.2.1 MECHANICAL ENERGY: FILLER CONTENT

The instrumented extruder continuously monitors screw torque as a percentage of the permitted maximum and

also torque can be related to the measured output by the following relationship [142, 175]:

$$Q = \frac{2\pi \cdot SS \cdot (TQ - TQ_o)}{\dot{m}} \qquad (3.1)$$

Where Q = Specific energy consumption (rev.%/g)
SS = Screw speed (20 rpm)
TQ = Measured torque (%)
TQ_o = Torque under no load conditions (20·5%)
$\dot{m}$ = Extruder mass throughput (g/min)

Specific energy consumption gives a measure of the mechanical energy supplied to the material per unit mass of material.

Appendix D.2 presents the data for the filled compositions extruded at profiles A-F inclusive, while figures 3.9 and 3.10 represents the data graphically.

It can be seen from the figures that a family of curves are produced and as might be expected there is a decrease in mechanical energy requirement from profile A to F and, generally, an increase in torque and Q with increasing filler content. Both figures are similar and the quadratic curves clearly differentiate between the profiles until a distinct deviation is observed at a approximate filler level of 30 phr for profiles D, E and F; a levelling off is observed instead of a sharp upward turn as seen for the other profiles. Since a true 'melt' temperature is not obtained from the extrusion data then it is difficult to fully characterise the effect of filler upon the extrusion process. An indirect method was therefore used to obtain the final processing temperature, (the DSC technique described in §1.4.2.5) and the interrelations will be discussed in §4.1.1.

FIGURE 3.9

Torque versus Filler content

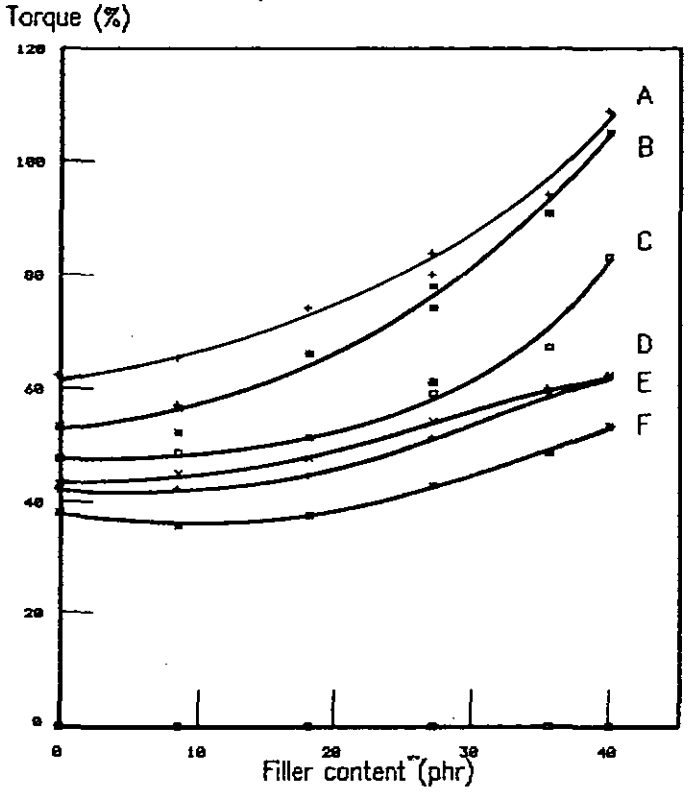

FIGURE 3.10

Mechanical energy versus Filler content

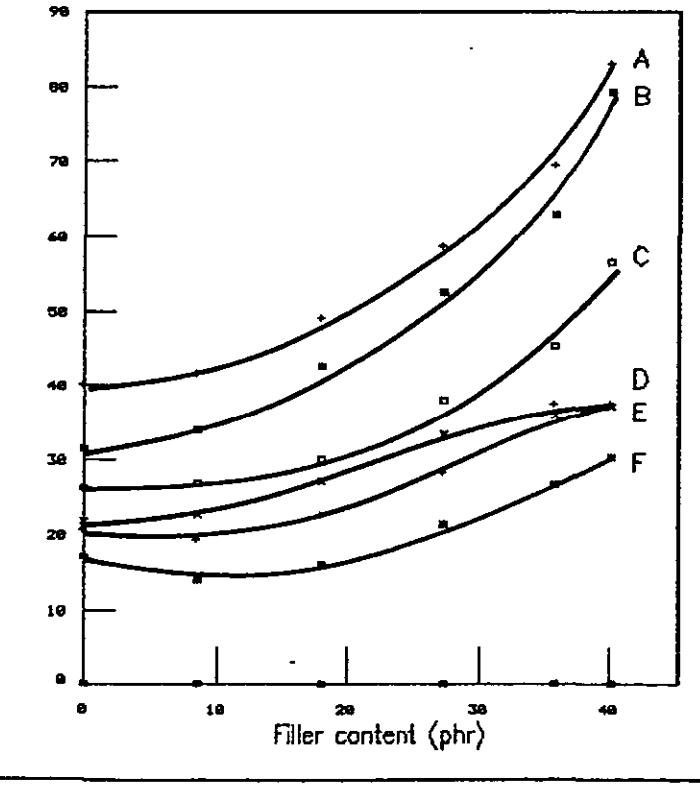

3.2.2 EXTRUSION PRESSURES: FILLER CONTENT

The extrusion pressures within the Krauss Maffei KMDL-25 are recorded via force transducers positioned in the pipe head and adaptor piece. The results for the P1, head and inlet pressures are given in Appendix D.3 and figures 3.11 and 3.12 illustrate head and inlet pressures respectively. The pressure at the start of the discharge zone, P1, is insignificant unless the pressures in the adaptor and head zones are relatively high for the particular blend, indicating that the length of the solid/ melted material has increased to the start of the discharge zone and thus producing a response at P1. Figure 3.11 illustrates a series of quadratic curves similar in appearance to the torque and Q measurements; clearly the curves show the dependence of the set head temperature upon head pressure. For instance profiles C and D differ in terms of barrel temperature and not the set head temperature; the resultant pressure curves for C and D are almost identical indicating the significant influence of head temperature upon head pressure.

Figure 3.12 represents the inlet pressure versus filler content and a linear relationship is observed for each profile. The lines are not parallel and again the influence of the set head temperature can be seen.

3.2.3 EXTRUSION RESULTS: ADDITIVE STUDY

The second stage of the processing work considered the interaction of lubricants and impact modifiers in filled and unfilled UPVC; the processing characteristics of these compositions can be monitored within the instrumented twin screw extruder. The results are listed in Appendix D.4 and these values can be represented in figures 3.13-3.16 inclusive. It can be seen from the results that although the main extrusion parameters remained constant the experimental values are significantly different from the original series

of extrudates which incorporated a wide processing window and wide filler range. These apparent differences can be attributed to the extruder being rebuilt after the first stage of processing; similarly the output rates for the two additive series (0 phr and 30 phr) are not identical which again can be related to a slight modification of the rebuilt extruder between the two additive trials. However the sets of data are reproducible within each distinct series and also the value of Q, which accounts for differing mass throughput, is similar for the processing of identical blends (0E- and 3E-) during each individual extrusion trial.

Pressure at the start of the discharge zone, P1, is not noted for the majority of the unfilled blends with the exception of 0EE and 0EH. No response was obtained for the filled blends.

Figures 3.13 and 3.14 demonstrate the significant effect of a small concentration change of an additive and additive type can have upon the processing characteristics of an unfilled pipe formulation. The bar charts generally reveal the same trend i.e. Q, head and inlet pressure produce a similar ranking order for the additives investigated. If the influence of lubricant amount and type is considered first then the pipe codes can be ranked in terms of mechanical energy and head pressure as follows:

	LOW ◄ ------ value ------- ► HIGH						
Q	0EB	0EF	0EA	0EC	0E-	0ED	0EE
Head pressure	0EB	0EF	0EA	0E-	0EC	0ED	0EE

It is, of course, difficult to provide a full explanation for the trend without details upon melt temperature and level of fusion which are not presented at this stage.

FIGURE 3.11

Head pressure versus Filler content

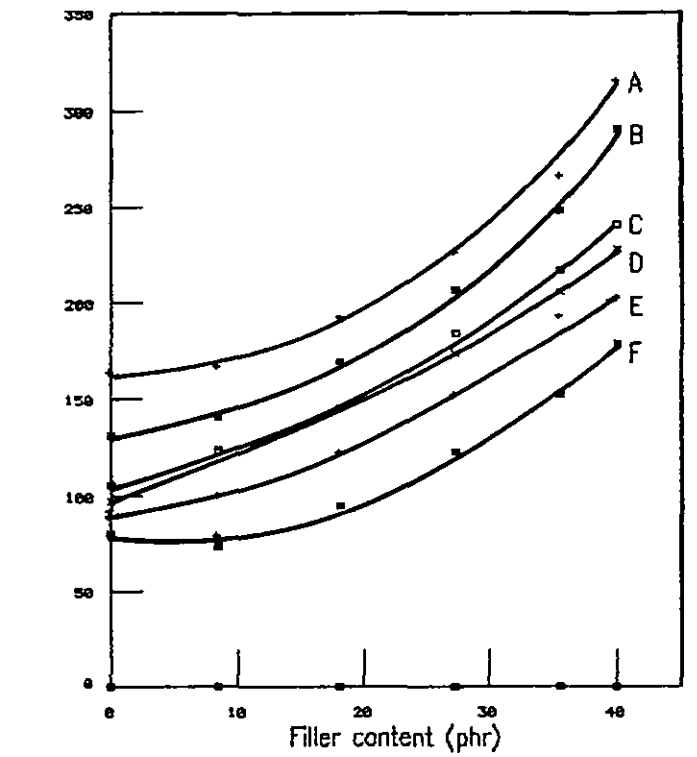

FIGURE 3.12

Inlet pressure versus Filler content

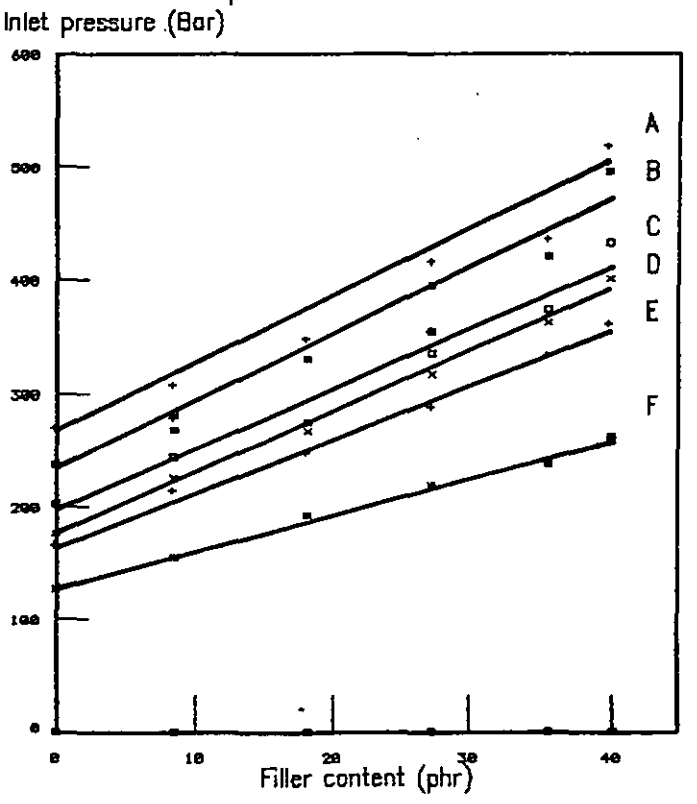

However it is interesting to note that a relatively high level of a low melting point paraffin wax (OEB) does produce a low Q and head pressure result; alternatively a high m.pt polyethylene wax (OEE) yielded high torque and pressure characteristics when compared to a low m.pt paraffin wax used in equal proportions (OEA). The incorporation of suggested 'internal' lubricants such as GMS (OEC) and castor oil (OED) resulted in a higher head pressure than a comparable level of, say, a paraffin wax.

The effect of incorporating a impact modifier (OEG & OEH) upon a unfilled composition (OE-) suggests that the CPE additive (OEG) does not affect the processing characteristics dramatically while the application of an all acrylic modifier leads to higher melt pressure values.

Figures 3.15 and 3.16 illustrate the processing results for the filled composition (30 phr) using the array of additives discussed for the 0 phr series. It can be seen from the bar charts that the processing characteristics are again dependant upon the additive and the lubricant systems can be ranked as follows:

	LOW ◄ ------ value ------- ► HIGH						
Q	3EB	3EF	3ED	3E-	3EC	3EE	3EA
Head pressure	3EF	3EB	3EE	3E-	3EC	3ED	3EA

In this series the effect of lubricant is not as dramatic as for the unfilled compositions with the exceptions of 3EB and 3EF, these lubricants again yielded low torque and head pressure results.

The effect of impact modifier addition differed from the unfilled system in that torque and Q values were largely unaffected, although a sizable reduction in head and inlet pressures (especially for 3EG) were noted.

This brief introduction to the extrusion results will be expanded in later chapters when discussion upon fundamental results, such as fusion level, is presented.

FIGURE 3.13

Torque and Q for Additive blends

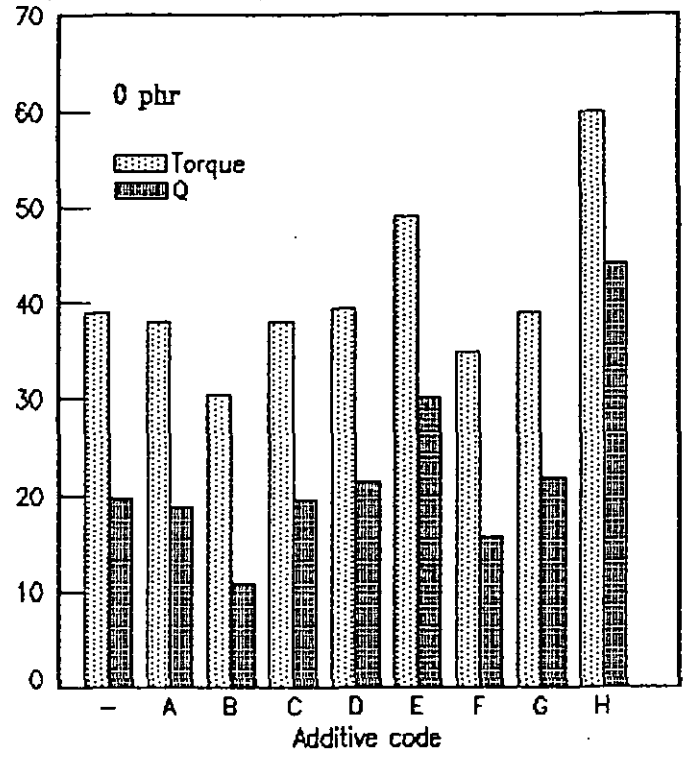

FIGURE 3.14

Extrusion pressure for Additive blends

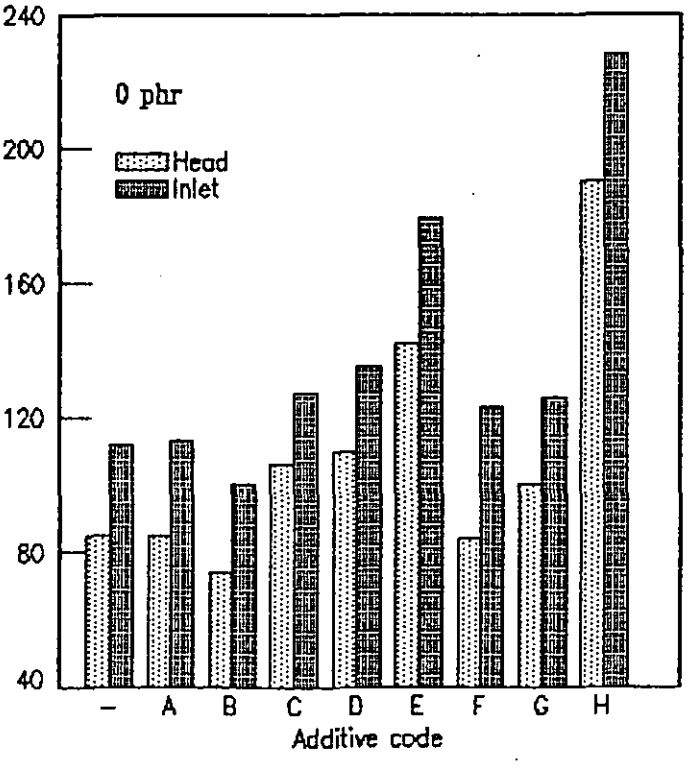

FIGURE 3.15

Torque and Q for Additive blends

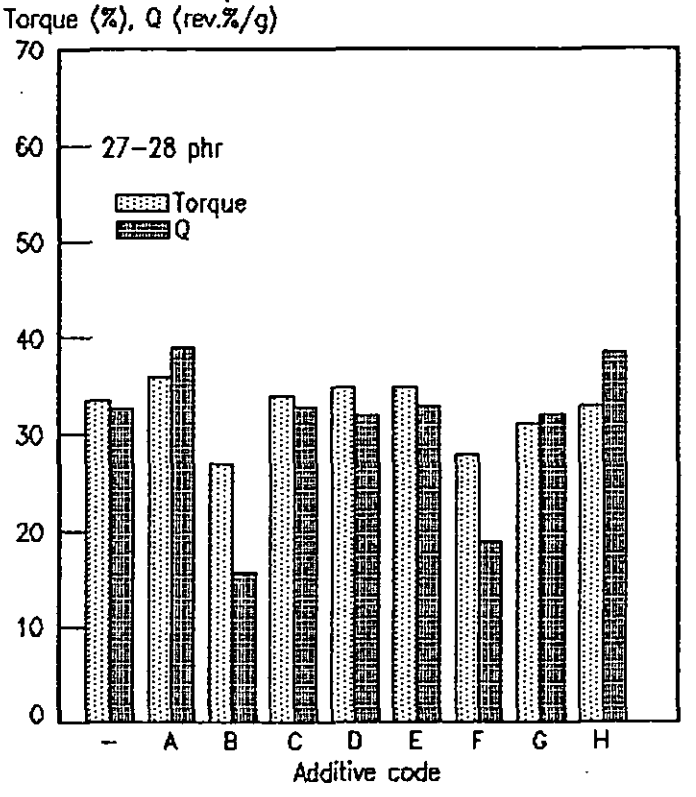

FIGURE 3.16

Extrusion pressure for Additive blends

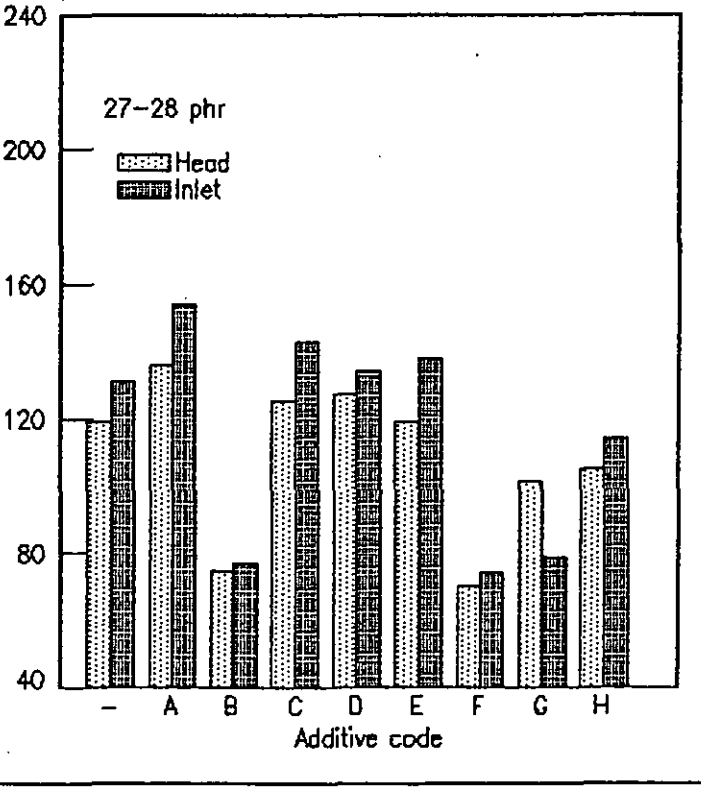

3.3 EXTRUDATE APPEARANCE

The aesthetic appearance of an extrudate is an important parameter in the extrusion process and an arbitrary assessment based upon visual examination is commonplace. All the extrudates were visually assessed for surface finish; both the outer and inner surfaces were examined and ranked in ascending surface quality. Obviously the arbitrary nature of such an assessment can present difficulties, however the pipes were relatively easily segregated in groups of similar surface texture and gloss.

3.3.1 APPEARANCE: OUTER SURFACE

The introduction of an appreciable amount of filler (20 phr) leads to a darker product i.e. brown tint due to the impurities associated with the filler. The outer surface of the pipe series containing a wide filler range can be ranked as shown in table 3.4:

TABLE 3.4

Outer surface of pipe series O-5

GROUP †					
I	II	III	IV	V	VI
5A,B	5C-F	3A-D	3E	3F	2F
4A,B	4C-F	2A,B	2C,D	2E	1F
		1A,B	1C,D	1E	0F
		0A,B	0C,D	0E	

† Where I = poor surface finish and VI = best

The above table indicates that an increase in the temperature of the extruder profile (A⇒F) leads to a better surface finish and the extrudate quality deteriorates beyond a filler level of approximately 30 phr. The texture and

gloss of the heavily filled systems remain poor even at the higher temperature profiles.

The extrudate appearance can also be ranked in a similar manner for the additive series (table 3.5):

TABLE 3.5

Outer surface of additive series

GROUP †		
IV	V	VI
OEA	OE-	3EH
OEF	OEB-E	OEH
3E-	OEG	
3EE, F	3EA-D	
	3EG	

† Where groups as per table 3.4

The additive variations seems to have little effect upon the surface finish with the exception of the acrylic impact modifier; in this case a clear improvement is observed.

3.3.2 APPEARANCE: INNER SURFACE

The inner surface is often considered in the evaluation of the processability of a composition and again the extrudates for this study can be ordered in terms of quality.

The inner surface did not discriminate between the processing and composition range particularly well and are more difficult to arrange into discrete groups. However it can be observed that the reverse of table 3.5 is obtained, that is, a high filler content/low temperature profile gave a better surface finish.

TABLE 3.6

Inner surface of pipe series 0-5

GROUP		
II	III	IV
0B-F	1C, D	0A
1E, F	2D, E	1A, B
	4C	2A-C
	4E, F	2F
	5C-F	3A-F
		4A, B
		4D
		5A, B

Table 3.7 presents the approximate ranking of the inner surface for the additive series:

TABLE 3.7

Inner surface of additive series

GROUP †					
I	II	III	IV	V	VI
0EG	0EA-F	3ED	3E-	0EH	3EG
			3EA	3EB, C	3EH
			3EE	3EF	

† Where groups as per table 3.6

The additive series requires extra groups since the inner surface quality has been extended upto group VI which is very smooth and glossy. It is interesting to note that the filled grades generally give a better finish.

3.4 METHYLENE CHLORIDE TEST

All the extrudates passed the methylene chloride test after 15 minutes immersion at room temperature with the exception of extrudates processed at profiles A and B. Other extrudates processed using low temperature profile showed signs of attack and swelling but in the context of the test did not fail. The pipes extruded at low processing temperature (A & B) showed excessive swelling and splitting.

CHAPTER FOUR

THERMAL AND MICROSCOPY RESULTS

4.1 DIFFERENTIAL THERMAL ANALYSIS

The technique of thermal analysis, as described in §1.4.2.5 and §2.9.2, has recently been applied to ascertain the processing history of PVC products. All the extrudates discussed in §2.6.1 were assessed for the following parameters: heat of fusion of peak 'A' (ΔH_A), heat of fusion of peak 'B' (ΔH_B) and the onset temperature of peak 'B' ('B' onset temperature). The values obtained for ΔH_A can then be related to a percentage fusion by the following expression.

$$\% \text{ Fusion} = \frac{\Delta H_A - \Delta H_P}{\Delta H_{MAX} - \Delta H_P} \times 100 \qquad (4.1)$$

Where ΔH_A = Experimental value for heat of fusion
ΔH_P = Heat of fusion for polymer (0·28 J/g)
ΔH_{MAX} = Maximum heat of fusion (10·53 J/g)

The area of the respective peaks can be related to a heat of fusion by the expression given in 2.1. A negligible value was obtained for the virgin polymer and this was included in the above expression (4.1) for completeness. The maximum heat of fusion was obtained for the pipe extrudate 3F and is used to represent 100% fusion. The heat of fusion values were calculated as an energy value per gram of PVC; therefore the values obtained for the filled compositions were corrected, using the measured ash content, on a weight basis to provide a comparable energy value.

Table 4.1 lists the results obtained for the filled compositions processed within a large processing window.

TABLE 4. 1

Thermal Analysis of filled compositions

Pipe code	'B' Onset temperature (°C)	ΔH_A (J/g)	ΔH_B (J/g)	% fusion
0A	170·3	0·43	1·93	1·4
0B	172·7	1·11	1·80	8·1
0C	175·2	2·55	1·66	22·1
0D	178·8	3·25	1·13	29·0
0E	187·2	5·37	0·49	49·6
0F	197·5	7·63	0·12	71·7
1A	175·7	3·69	1·25	33·3
1B	174·0	1·69	1·06	13·7
1C	184·0	5·91	0·74	54·9
1D	186·8	5·96	0·83	55·4
1E	193·2	7·57	0·13	71·1
1F	203·5	9·37	0·10	88·7
2A	175·7	1·68	1·35	13·7
2B	178·5	3·04	1·24	26·9
2C	185·8	5·27	0·75	48·7
2D	186·7	5·21	0·72	48·1
2E	195·3	8·41	0·27	79·3
2F	203·2	9·92	0·04	94·1
3A	174·2	2·13	1·29	18·0
3B	178·0	2·87	0·99	25·3
3C	186·2	5·69	0·77	52·8
3D	190·2	6·22	0·34	58·0
3E	195·2	8·16	0·28	76·9
3F	207·3	11·18	0·00	106·4
4A	175·8	1·97	1·42	16·4
4B	180·0	2·34	1·15	20·1
4C	192·8	7·63	0·42	71·7
4D	193·3	7·13	0·42	66·9
4E	194·8	7·96	0·36	74·9
4F	203·5	9·31	0·00	88·2
5A	179·7	3·15	1·41	28·0
5B	177·7	2·82	1·14	24·8
5C	188·2	5·92	0·51	55·1
5D	192·2	7·12	0·38	66·8
5E	195·8	7·35	0·25	69·0
5F	204·5	9·45	0·00	89·5

4.1.1 'B' ONSET TEMPERATURE

The onset temperature of the 'B' peak can be compared with the indicated extrusion temperature recorded via a thermocouple/transducer arrangement (table D.1) as shown in figure 4.1. It can be seen that generally an upward straight line relationship is observed, however the values for the 0 series are shifted to a higher recorded head temperature. The head temperature, as indicated in §3.2, is a measure of the local extruder temperature rather than the material temperature at that point. Also the inability to calibrate the transducer or the recording device suggests that the recorded head temperature value does not provide an accurate means to assess the processing regime. The problem of calibration can be observed for the 0 series of extrudates; these extrudates were processed during a different trial to the filled systems and the recorded head temperatures indicate a significantly higher value than the 'B' onset measurement although the energy values obtained for peak 'A' were in fact lower than the filled extrudates at their respective profile temperatures. It is therefore suggested, in this case, that an estimate of processing temperature is best indicated by the indirect method of thermal analysis.

Figure 4.2 illustrates the effect of the extruder profiles chosen for this study upon the estimated processing temperature ('B' onset). The unfilled extrudates differed from their filled counterparts and this observation can be related to the setting of the extruder rather than a material consideration. Little difference is seen between profiles A & B and C & D. These profiles differ in terms of barrel temperatures and thus it would seem that the head temperature is the major variable in controlling the effective processing temperature. Changing profiles from B to C, D to E and E to F resulted in a distinct increase in 'B' temperature, in fact an increase of 10°C is observed which can be related to the 10°C difference in set head

FIGURE 4.1

'B' Onset versus Head temperature

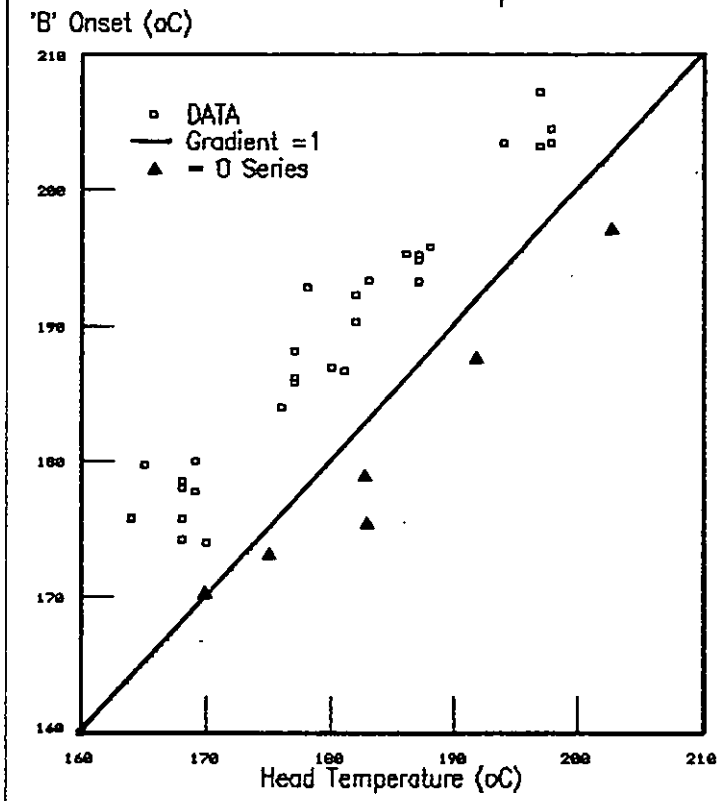

FIGURE 4.2

'B' Onset versus Extrusion profile

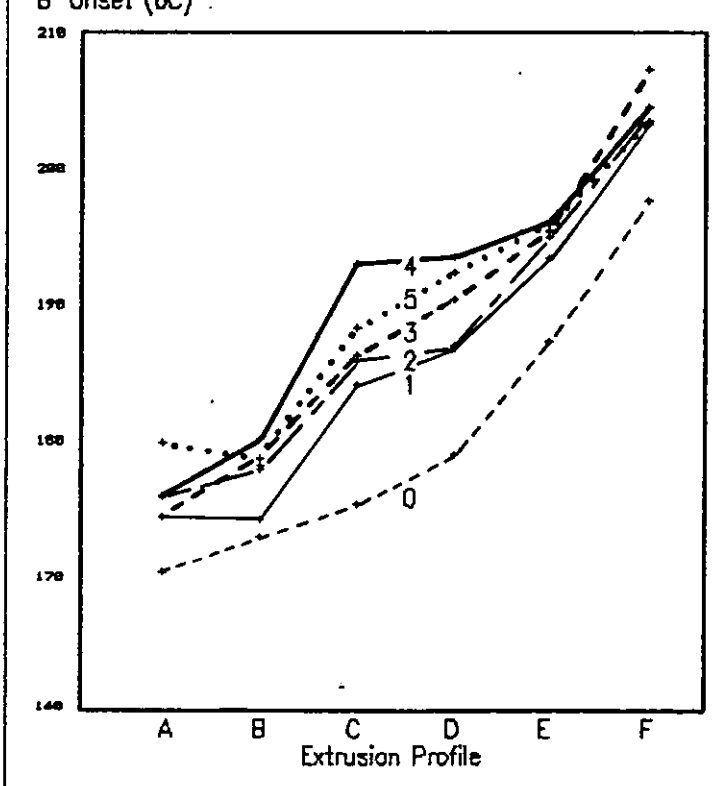

temperature. The effect of increasing filler content leads to a marginal increase in 'B' onset temperature at intermediate profile temperatures which could be related to the higher viscosity of filled systems. The higher profile temperatures do not differentiate between the filler levels since the proportion of mechanical energy is reduced due to the higher temperatures of the extruder.

4.1.2 PROCESSING OF FILLED SYSTEMS

Figures 4.3 and 4.4 represent the extrusion results presented in §3.2.1-3.2.2 versus 'B' onset temperature. A family of curves are produced which are similar and clearly distinguish between filler levels. The figures show a strong decrease in extrusion value (head pressure or Q) with an increase in processing temperature (especially at the lower end of the processing window). In order to evaluate the data further, linear multiple regression analysis was used to combine the components of filler content and processing temperature with a measured extrusion property. Expression 4.2 depicts the relationship between these components and the linear regression analysis, the coefficient of correlation suggests an acceptable model, however further transformation of the multiple regression analysis, via expression 4.3, yields a more accurate model.

$$y_P = 721{\cdot}523 + 3{\cdot}982(x_F) - 3{\cdot}416(x_B) \qquad (4.2)$$

Correlation (r) = 0·97
SD of errors = 14·73

Where y_P = multiple regression value for pressure (Bar)
x_F = filler content (phr)
x_B = 'B' onset temperature (°C)

FIGURE 4.3

Head pressure versus 'B' Onset

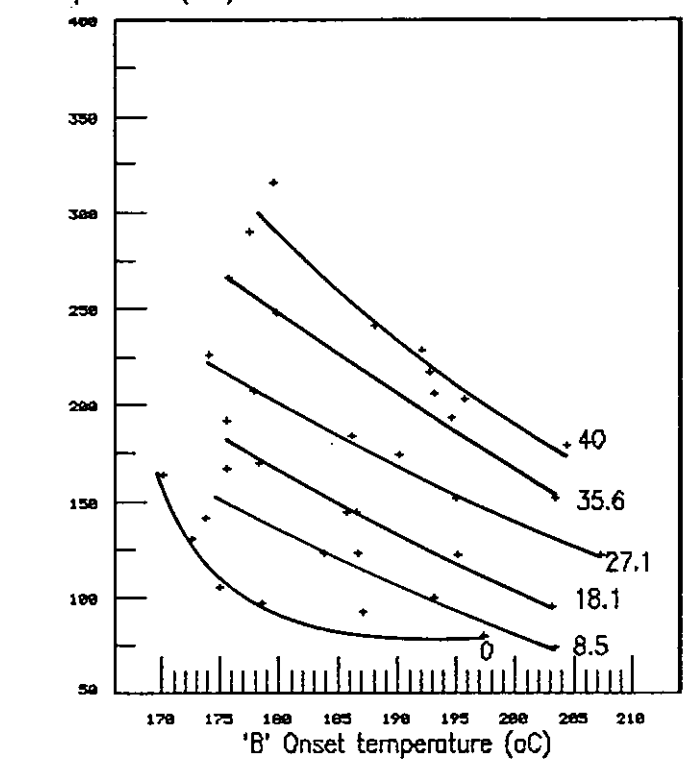

FIGURE 4.4

Q versus 'B' Onset

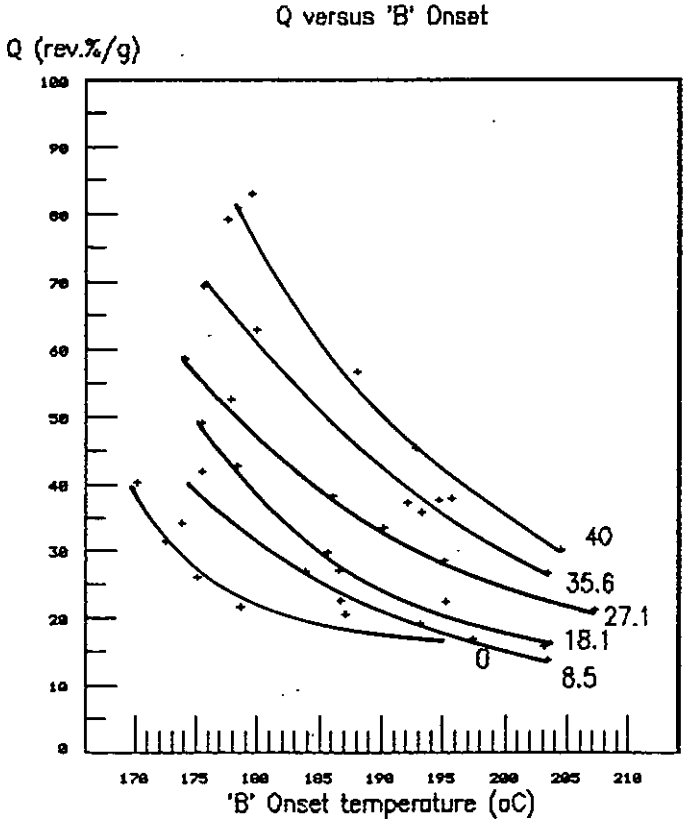

$$y = 73{\cdot}869 + 0{\cdot}00299(y_p)^2 \qquad (4.3)$$

Correlation (r) = 0·982
SD of errors = 11·39

Where y = predicted Head pressure (Bar)
y_p = multi-regression value (Bar)

Figure 4.5 depicts the relationship between the actual head pressure results and the predicted head pressure values using this type of analysis.

Thus from the above analysis there is a strong dependence on both filler content and processing temperature, which can be accounted for in expression 4.2 and 4.3, thus the significance of these dependant variables can be determined and combined to predict head pressure. Therefore the expression given in 4.2 condenses the family of curves shown in figure 4.3 to a single mathematical relationship.

4.1.3 ENDOTHERMIC ENERGY OF PEAK 'A'

The area of a peak obtained from a UPVC thermogram can be converted to an energy value by the relationship given in equation 2.1. Endothermic energies were calculated for peaks 'A' and 'B' as shown in table 4.1; these values are plotted against 'B' onset temperature and are presented in figure 4.6. The graph illustrates that an increase in 'A' peak is obtained with increasing processing temperature and that the points occur as groups according to the extrusion profiles chosen. A curve can be fitted to the scatter points which describes the observations well:

$$\Delta H_A = -115{\cdot}89 + 1{\cdot}018('B') - 0{\cdot}00197('B')^2 \qquad (4.4)$$

Correlation (r) = 0·9874
SD of errors = 0·4592

Where 'B' = 'B' onset temperature (°C)

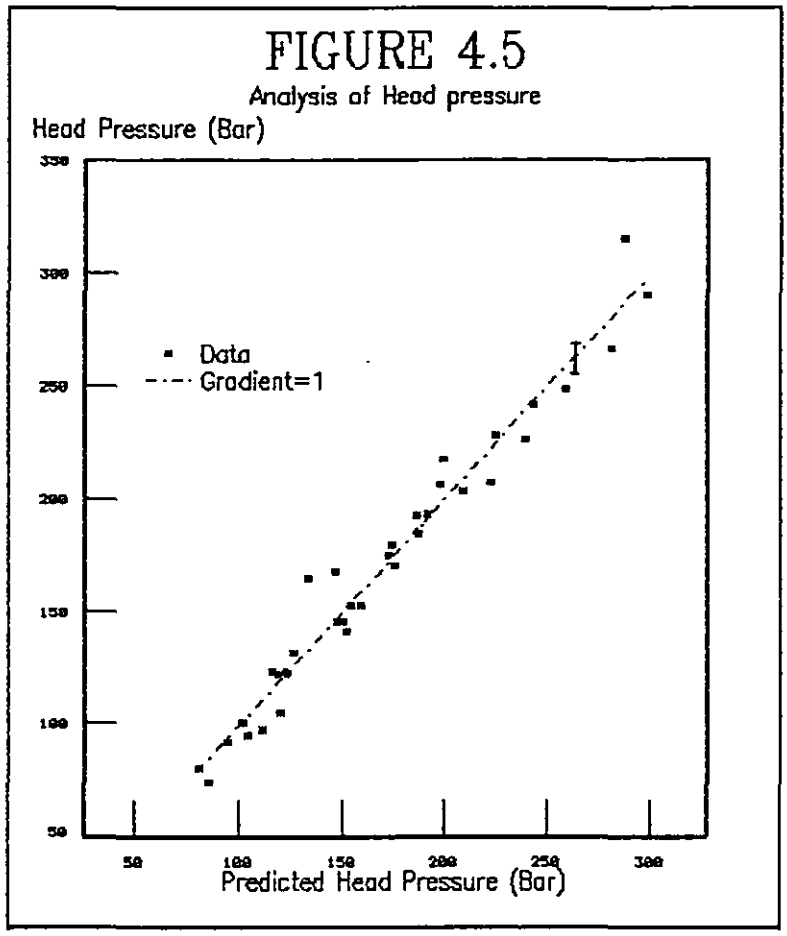

A very low energy value is measured for extrudates processed at profiles A & B, and the peak area increases rapidly with increasing 'B' onset temperature. The rate of increase in ΔH_A begins to diminish above an approximate temperature of 185°C leading to the observed curvature. It can be seen from the error bar (standard deviation of errors) that a low degree of scatter is obtained considering the wide processing window and filler loading. Since all the data points fit a single curve then the effect of filler loading upon ΔH_A appears negligible.

FIGURE 4.6

Master Fusion Curve

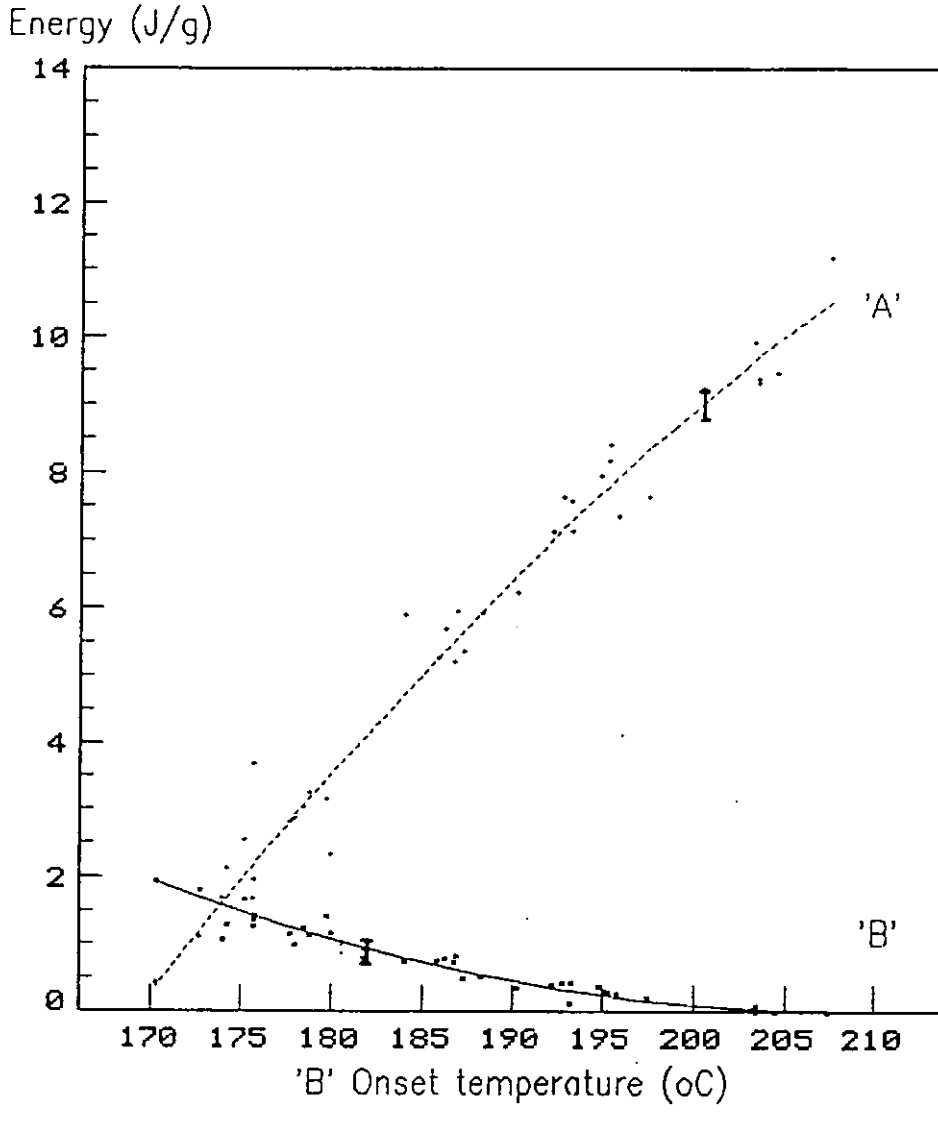

In the case of ΔH_B, a decrease in value is observed with increasing 'B' onset temperature and in a similar manner to ΔH_A the trend can be characterised by a polynomial curve:

$$\Delta H_B = 43{\cdot}954 - 0{\cdot}409('B') + 0{\cdot}00095('B')^2 \qquad (4.5)$$

Correlation (r) = 0·9633
SD of errors = 0·149

The trend again shows no dependence upon filler content and the value decreases to zero at approximately 202°C, although the ability to measure the ΔH_B at high processing temperatures is more difficult due to the small peak area and baseline definition.

A maximum of 10·53 J/g is obtained from the best fit curve of ΔH_A from the experimental value provided by pipe code 3F. This value was taken as an arbitrary 100% fusion level from which other ΔH_A values can be compared as a percentage (equation 4.1 and table 4.1).

If the calculated ΔH_A values are plotted against the extruder profile, then similar trends are noted to figure 4.2 ('B' onset temperature versus extrusion profile) which reaffirms the relationship seen in figure 4.6.

Figure 4.7 illustrates the master fusion curve for the filled compositions processed within a wide processing window. The graph is, of course, similar in appearance to the figure depicting ΔH_A and can be used to label a extrudate with a level of fusion. Again the scatter points can be characterised by a single curve with the following attributes:

$$\%\ \text{Fusion} = -1080{\cdot}09 + 9.4122('B') - 0{\cdot}01795('B')^2 \qquad (4.6)$$

Correlation (r) = 0·9842
SD of errors = 5·06

FIGURE 4.7

Master Fusion Curve

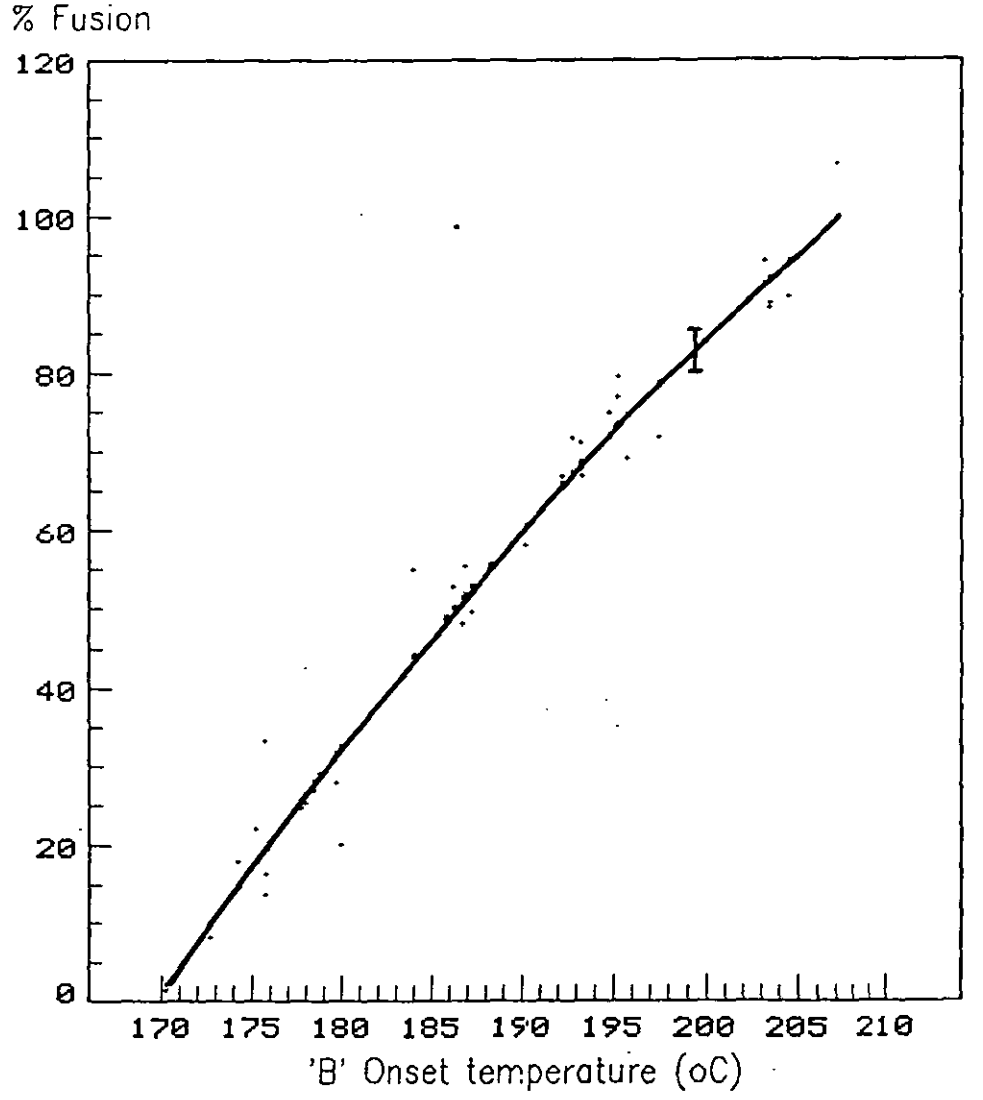

4.2 THERMAL ANALYSIS OF ADDITIVE BLENDS

In a similar manner to the filled compositions the extrudates incorporating a range of additives were assessed via thermal analysis. Table 4.2 presents the data obtained:

TABLE 4.2

Thermal Analysis of additive blends

Pipe code	'B' Onset temperature (°C)	ΔH_A (J/g)	ΔH_B (J/g)	% fusion	Predicted % fusion
0E-	188·7	5·27	1·19	48·6	56·9
0EA	189·0	5·56	0·28	51·5	57·6
0EB	188·0	5·81	0·52	53·9	55·0
0EC	186·0	5·83	1·20	54·1	49·6
0ED	187·5	5·46	0·19	50·5	53·7
0EE	185·3	6·19	0·37	57·7	47·7
0EF	186·8	7·38	0·18	69·3	51·7
0EG	190·8	6·45	0·19	60·2	62·3
0EH	192·0	8·69	0·20	82·1	65·4
3E-	190·8	7·50	0·45	70·4	62·3
3EA	189·8	6·24	1·14	58·1	59·7
3EB	193·0	9·43	0·17	89·2	67·9
3EC	192·7	7·12	0·32	66·8	67·1
3ED	189·0	8·11	0·48	76·4	57·6
3EE	190·7	6·94	0·38	65·0	62·0
3EF	190·0	6·60	0·34	61·7	60·2
3EG	190·8	5·29	0·50	48·9	62·3
3EH	195·7	8·44	0·22	79·7	74·4

Figure 4.8 presents the 'B' onset data as a bar graph; the variation within the 0 phr series is relatively low with the notable exception of 0EH. Similarly the filled compositions do not reveal any large differences with the exceptions that the overall values are slightly higher than for the zero series and 3EH yields a slightly higher result. It may not be acceptable to directly compare the two sets of data since the extrusion conditions are not identical (§3.2.3). However it is evident that the twin screw extruder

accurately controls the temperature build-up for the different compositions.

The second figure (4.9) demonstrates that the degree of fusion differs between additive types and since the processing temperature is similar for the blends then the observed variation must be accounted for by an alternative explanation. The last column in table 4.2 is the predicted % fusion using the measured 'B' onset temperature in the equation given for the filled compositions (equation 4.8). The predicted fusion level accounts, to some extent, for the slight variation in 'B' onset temperature and comparison between this value and % fusion indicates that the type/amount of additive has a significant bearing upon the size of the 'A' peak. These results will considered in full when compared with complementary evidence (§6.3.1.4).

4.3 MICROSCOPY OF FILLED EXTRUDATES

4.3.1 OPTICAL MICROSCOPY

Microscopy slides of extrudates containing 0⇒40 phr of filler were prepared as discussed in §2.8. The sections were taken parallel and transverse to the direction of extrusion; however little variation was observed between the direction of sampling. The results of the large number of sections can be summarised into the following relevant points:

The extrudates containing a relatively low level of filler (0 & 8·5 phr) revealed a distinct residual grain structure; the grain inclusions were clearly identified as dark spheres within a bright speckled matrix. The speckled effect may be attributed to the dispersion of particulate additives and since additives are not dispersed within residual grains the outline of the grain can be observed.

FIGURE 4.8

'B' Onset for Additive blends

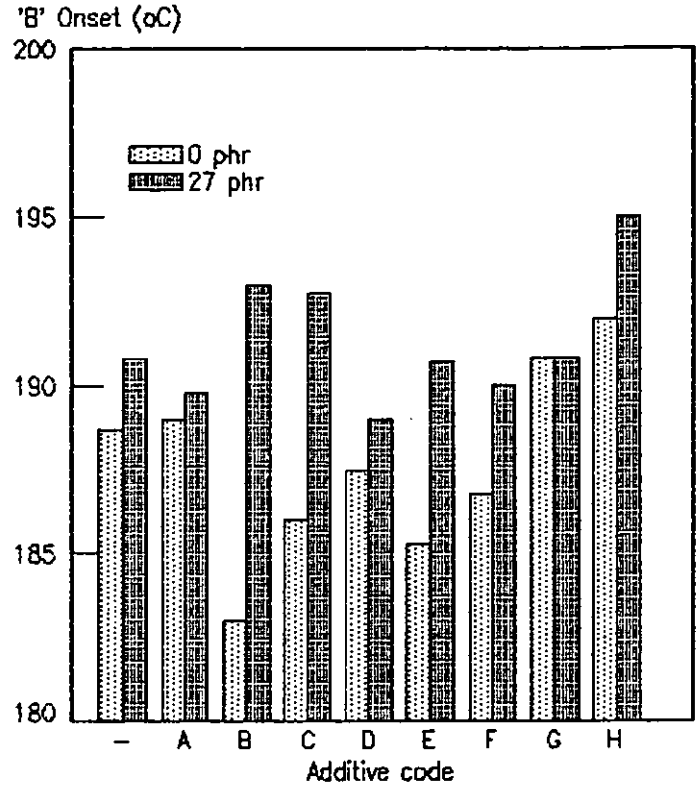

FIGURE 4.9

% Fusion for Additive blends

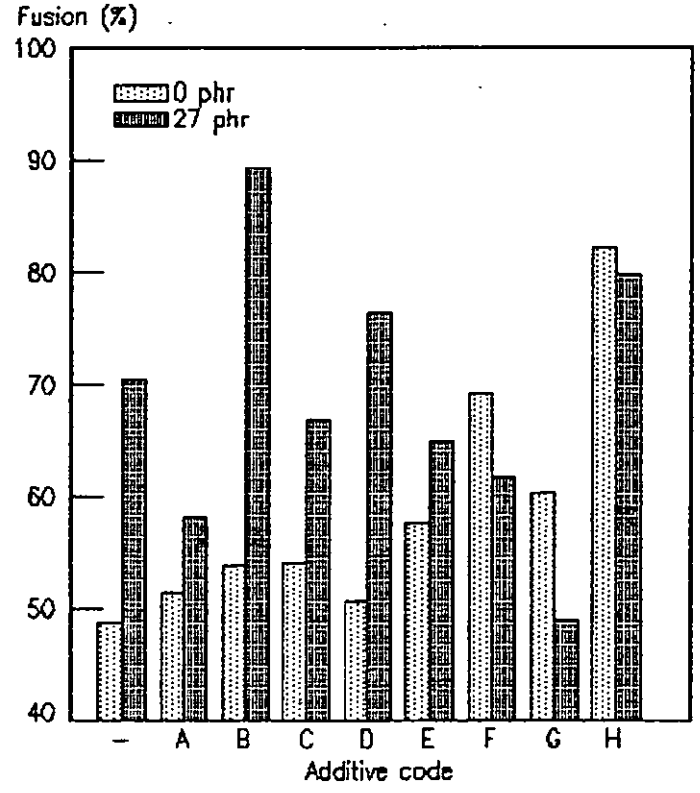

A dark field illuminated background was used for these sections so that the grains are seen as dark entities as opposed to near transparent spheres in an ordinary light background.

Figures 4.10-4.12 are shown to represent extrudates 0A-0F and 1A-1F; the first figure is an section of 0A which indicates a few residual grains and is similar in appearance to the section of 1A. Figure 4.11 is a section of 0B and indicates that the residual grain content of extrudates processed at profile A was far lower than extrudates produced at the higher process temperature B. The inclusions are spherically shaped and generally a higher grain content was observed for the 8.5 phr filler series (especially at the higher profile temperatures). The micrograph of 0B is representative of pipes; 0B-C and 1B-C where the spherical nature of the grains remains intact and distinct.

An increase in profile temperature did not result in the complete destruction of the grains but a progressive elongation of the grains in the direction of extrusion with increasing profile temperature. Figure 4.12 illustrates the elongation of the grains in section 0E which ultimately can be observed as streaks. The elongation of grains are clearly seen in sections 0D-F and 1D-F with the increased likelihood of 'streaking' in the high profile temperatures of 0F and 1F.

It is difficult to accurately measure the diameter of the original grains since a size distribution is envisaged and also the problems of sectioning a sphere must be appreciated, however an approximate diameter of 50-100 μm can be suggested from the large number of micrographs observed.

FIGURE 4.10: Microphotograph of section 0A

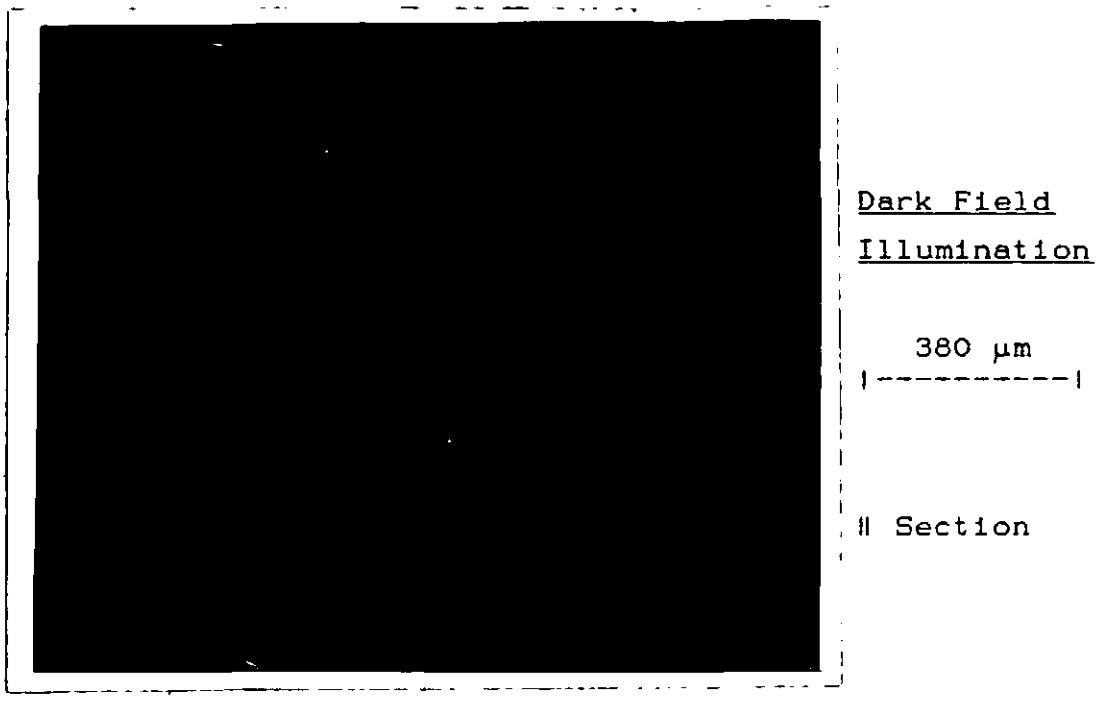

The second series of figures 4.13-4.15 depict the influence of a higher loading of filler (18·1 phr); the low profile temperature sections A, B & C indicate well dispersed blends (e.g. figure 4.13) which, unlike the lightly filled extrudates, do not contain significant traces of residual grains. (If residual grains are detected then the grains are highly elongated even at the low temperature profiles). Higher profile temperatures D, E & F result in intermediate stages of dispersion where traces of filler agglomeration can be seen (section 2D in figure 4.14) and finally quite distinct areas of agglomeration as shown in section 2E in figure 4.15 as white spherical patches. Thus the higher profile temperatures of E and F yielded extrudates with poorer filler dispersion.

FIGURE 4. 11: Microphotograph of section OB

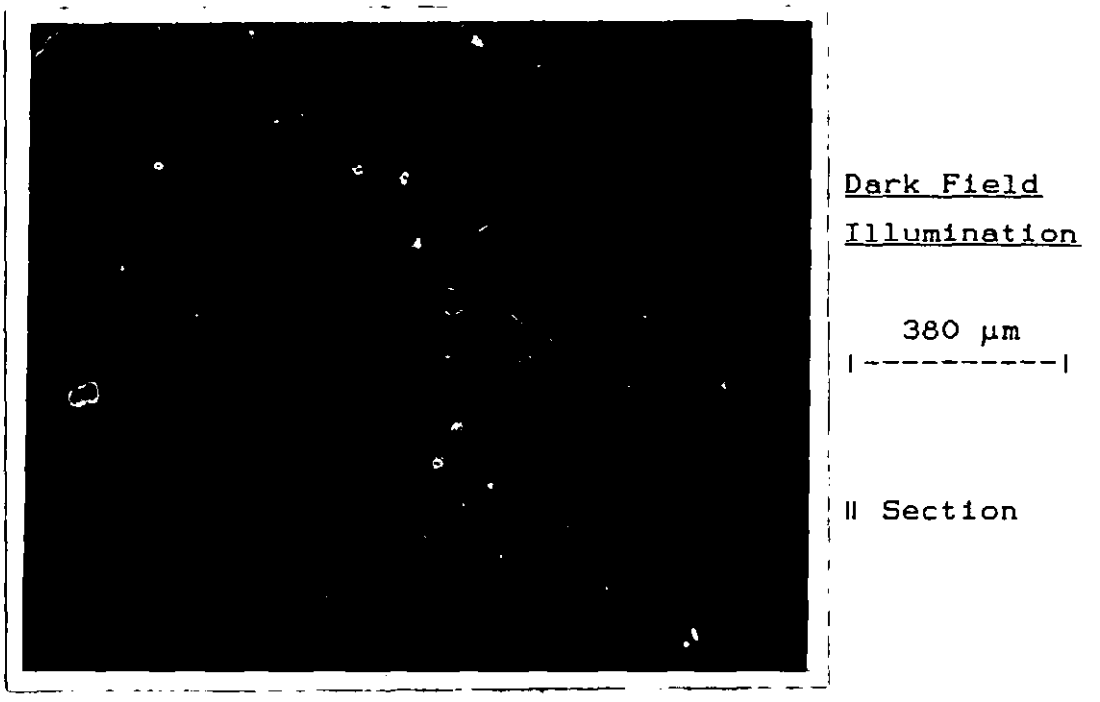

FIGURE 4. 12: Microphotograph of section OE

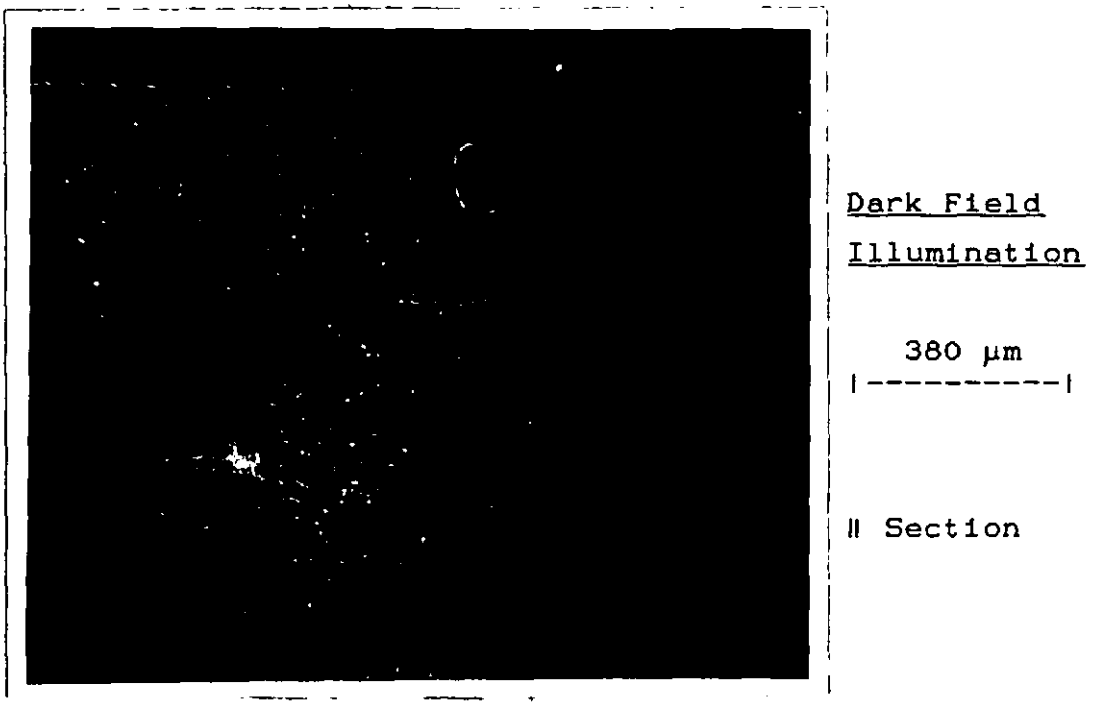

FIGURE 4.13: Microphotograph of section 2A

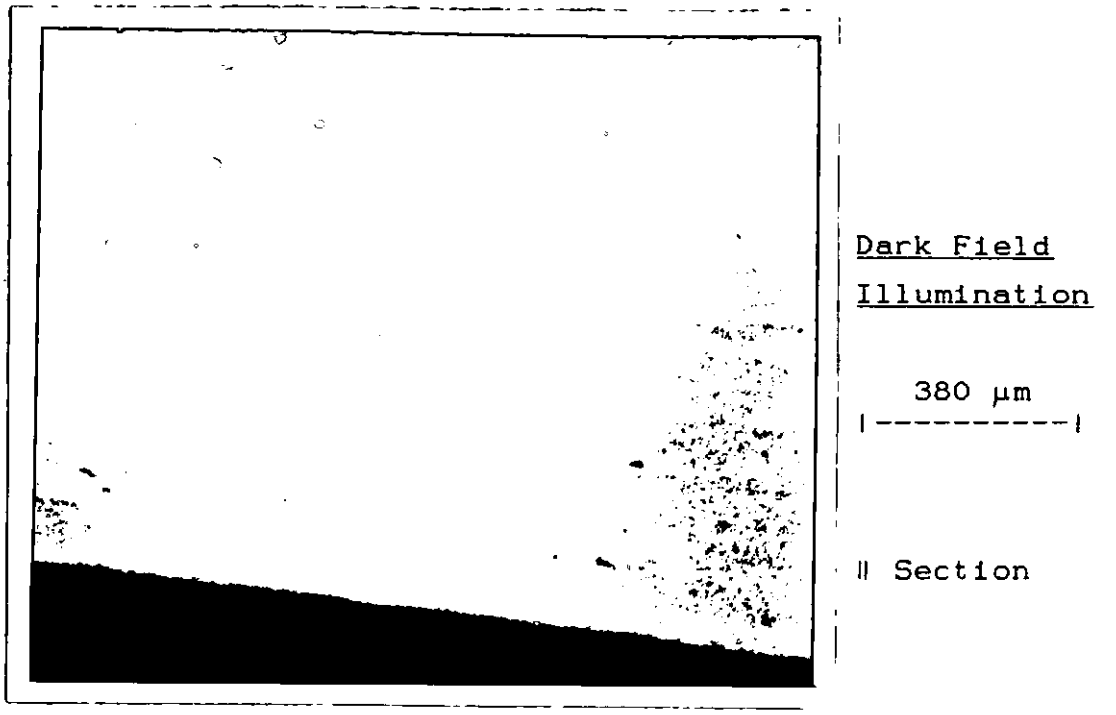

A further increase in filler loading results in extrudates which differ depending upon the extent of filler dispersion. The increases in filler loading can be clearly seen in the micrographs, however the dominant feature for all these highly filled extrudates (27·1, 35·6 and 40 phr) appears to be the level of filler dispersion. Some degree of mixing is evident at low temperature profiles (A & B) as shown by the micrograph of section 5A (figure 4.16), however poor dispersion can be seen at intermediate profiles (C & D eg. figure 4.17) and finally very poor dispersion is obtained for samples produced at the high extruder profiles (E & F) as illustrated by section 5F.

Poor dispersion of filler produces agglomerates of approximately 30-40 µm in diameter which on sectioning can lead to filler drop-out, the effect of filler drop-out being seen as dark voids as shown in micrograph 4.18. Residual grain content is not significant (with the exception of 3A where residual grains were detected), or is masked by the high filler content which prevents identification in the field of view.

FIGURE 4.14: Microphotograph of section 2D

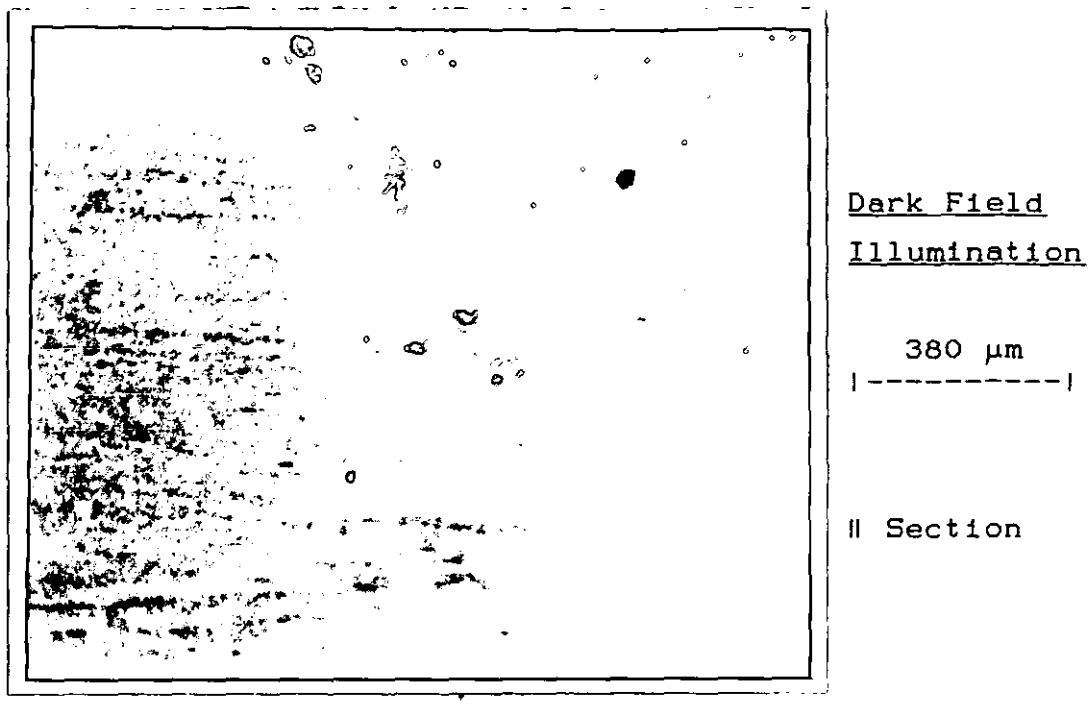

FIGURE 4.15: Microphotograph of section 2E

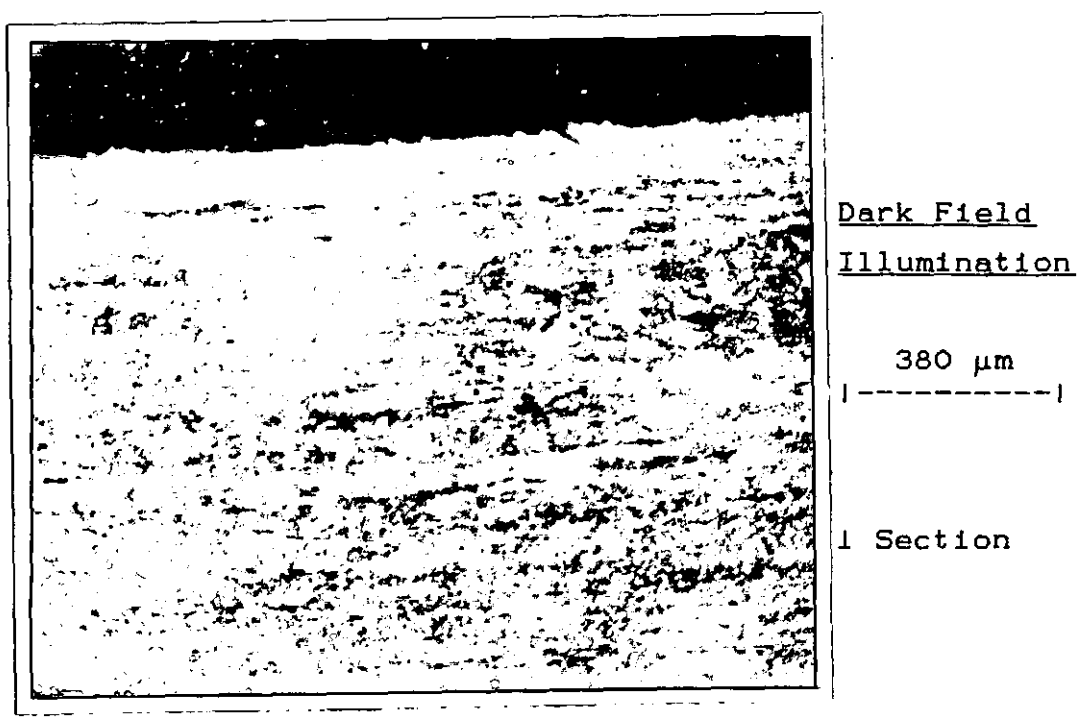

FIGURE 4.16: Microphotograph of section 5A

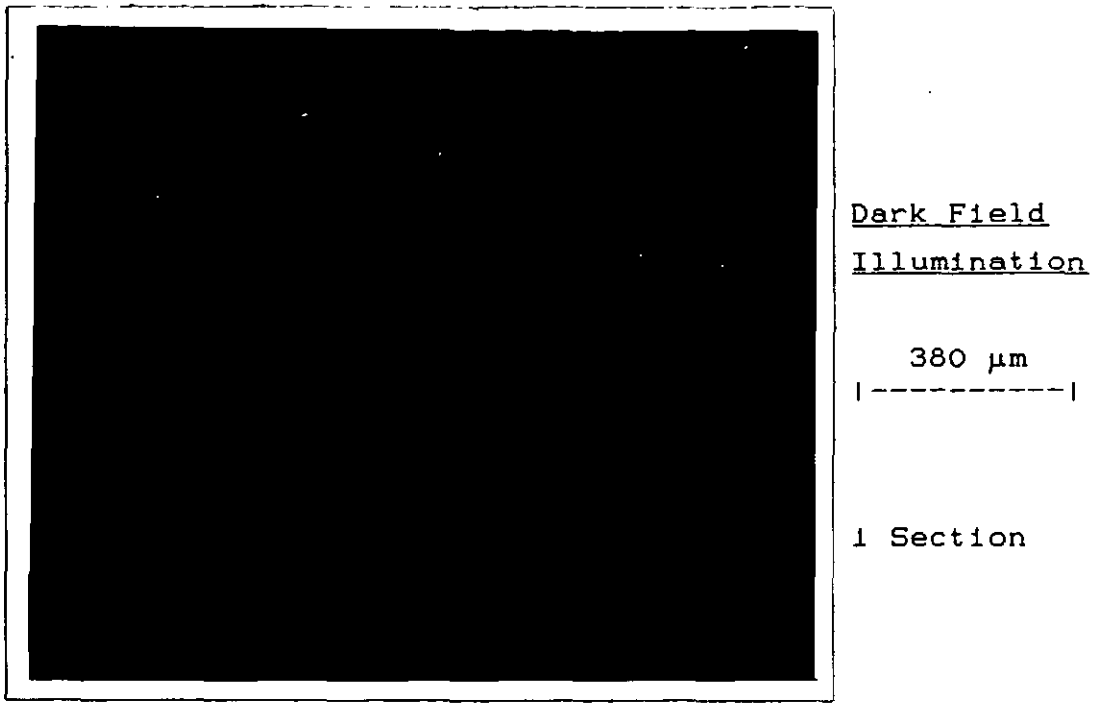

FIGURE 4.17: Microphotograph of section 5C

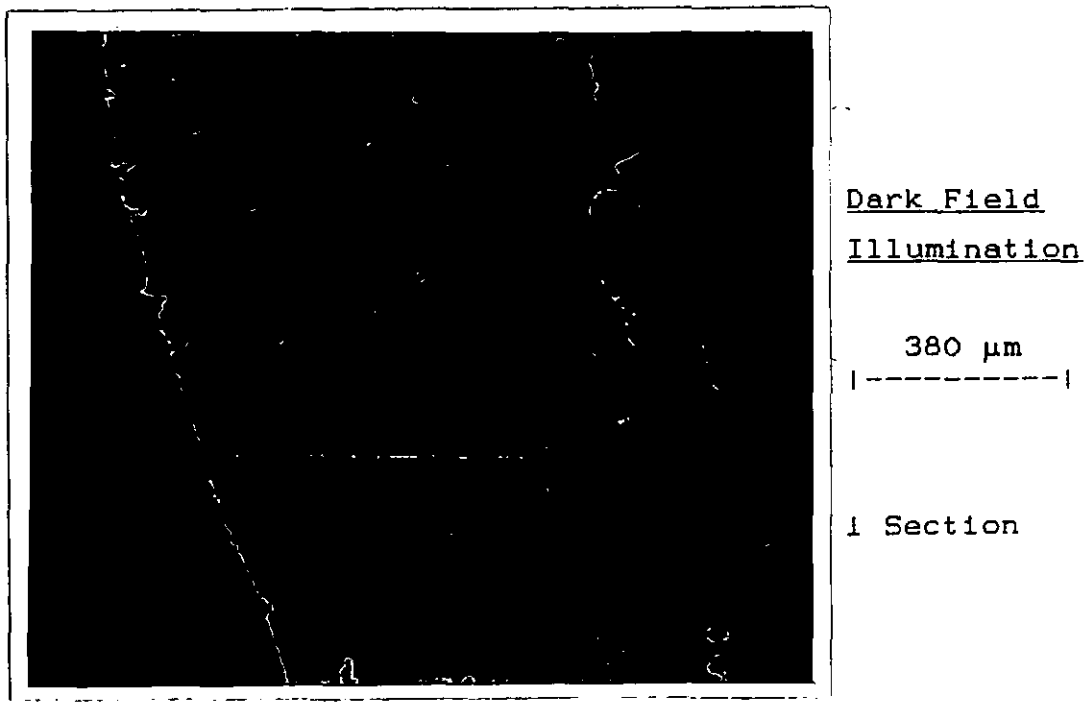

FIGURE 4.18: Microphotograph of section 5F

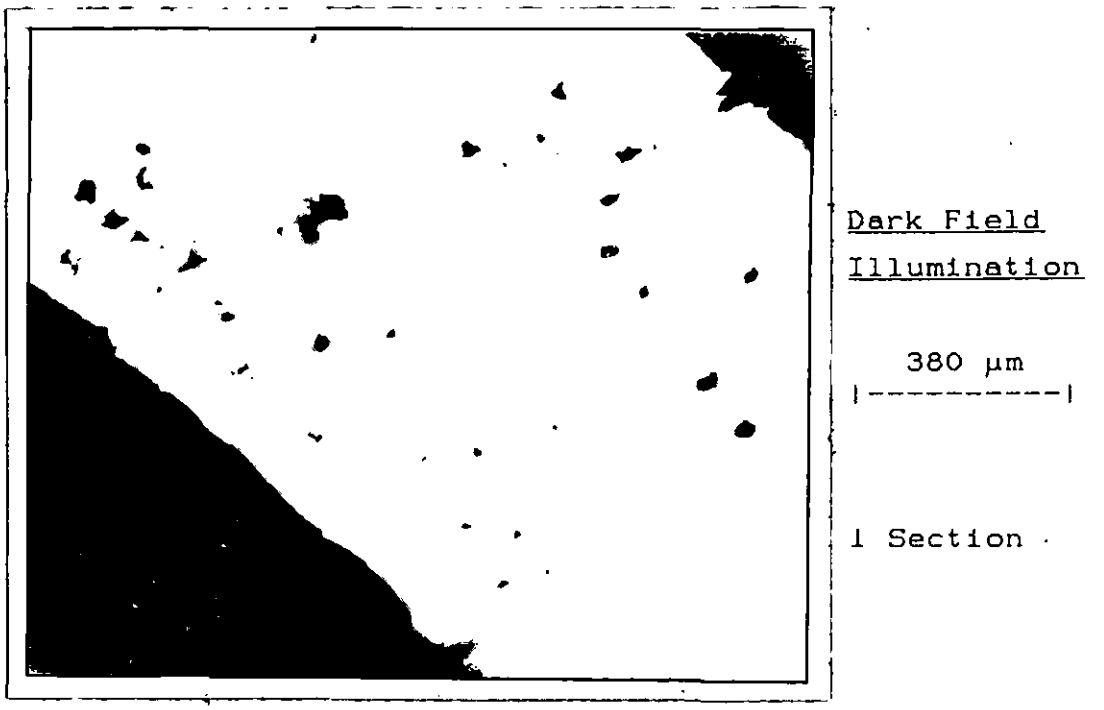

The presence of residual grains was also verified by the UV fluorescence technique described in §2.8. Here the grains are identified as bright areas of fluorescence within a additive-rich matrix exhibiting little or no fluorescence. Figure 4.19 illustrates the presence of a few highly elongated grains in a extrudate, 1F, processed at relatively high extrusion temperatures. The technique complements the inferences gained from the dark field microscopy sections, however the level of fluorescence at lower extrusion temperatures does not allow easy identification of the residual grains and therefore limits the application of UV fluorescence in this case.

Figure 4.20 illustrates a section using the UV fluorescence technique for a highly filled extrudate, 5A. The filler fluoresces and thus enables the presence and distribution of the filler to be examined. The results again confirm the dark field microscopy technique as an appropriate method to examine filler distribution.

FIGURE 4.19: Microphotograph of section 1F

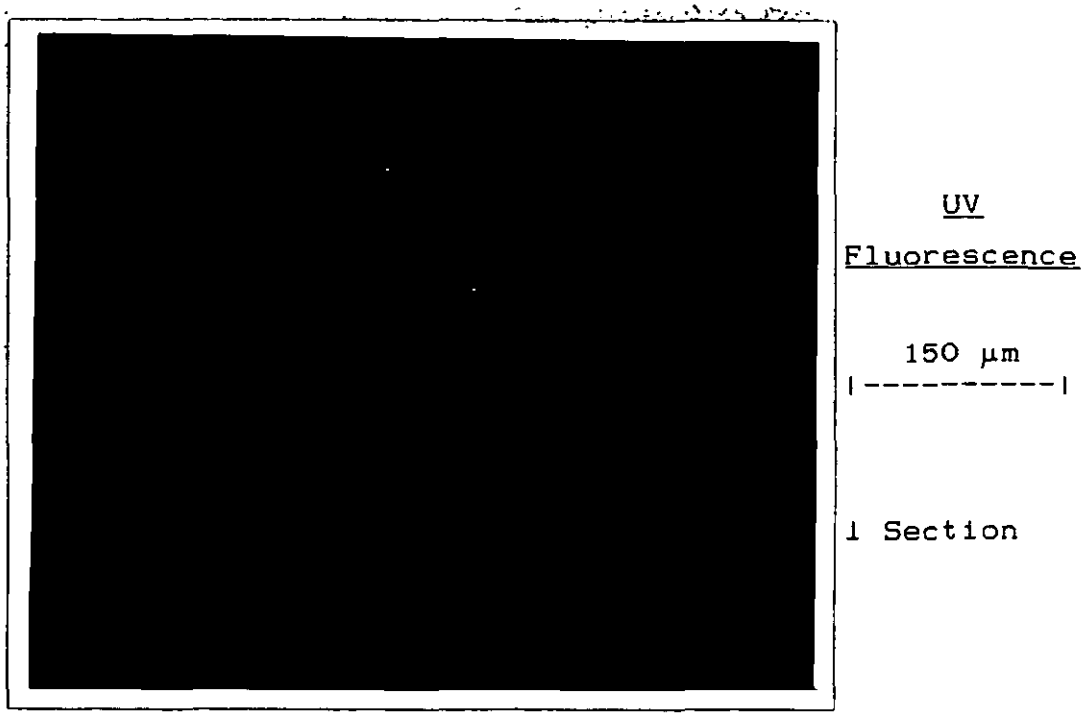

FIGURE 4.20: Microphotograph of section 5A

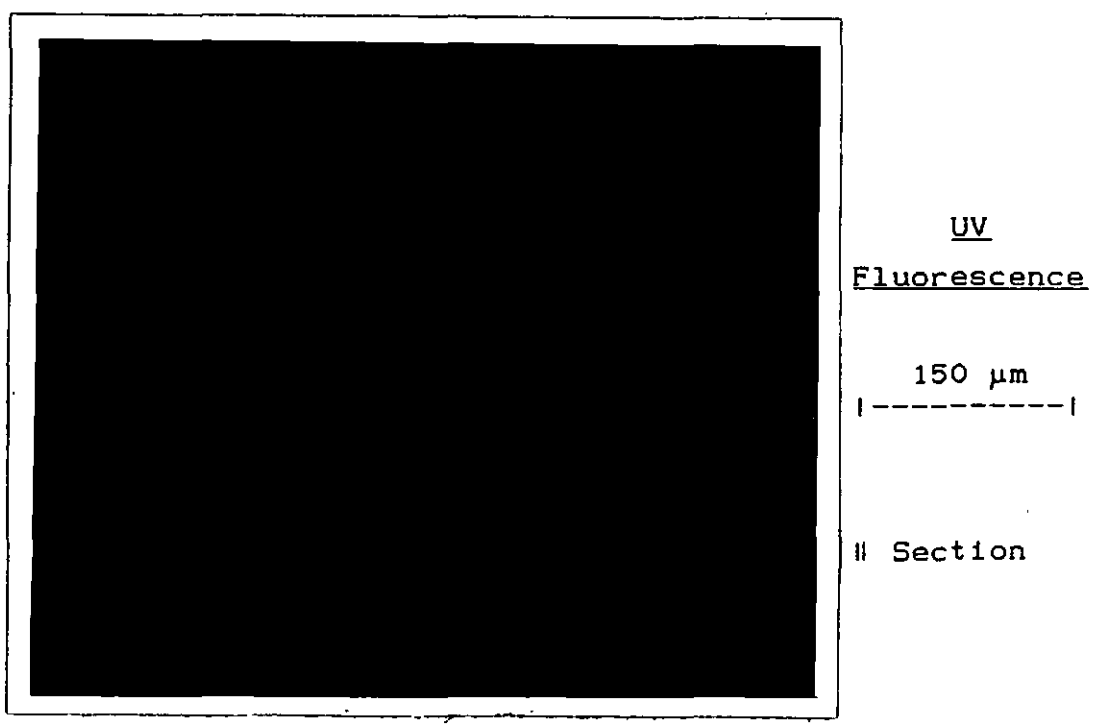

4.3.2 ACETONE SWELLING TEST

The swelling of PVC in acetone, shearing between glass slides and observation under a common light microscope has been reported in a number of publications [109-110, 130]. This simple and convenient test is applied to provide information upon the fusion level of processed PVC. In this project, small samples of the pipes were assessed and micrographs taken of the sheared fragments. Figures 4.21-4.23 provide examples of the results for all the filled blends produced. Extrudate samples processed at profiles A and B under the acetone shearing test were easily broken down to primary particles with little discernible cohesion between the particles. Figure 4.21 demonstrates this poor cohesion strength and can be considered to represent all blends with a filler range 0-40 phr.

FIGURE 4.21: Acetone shearing of OA

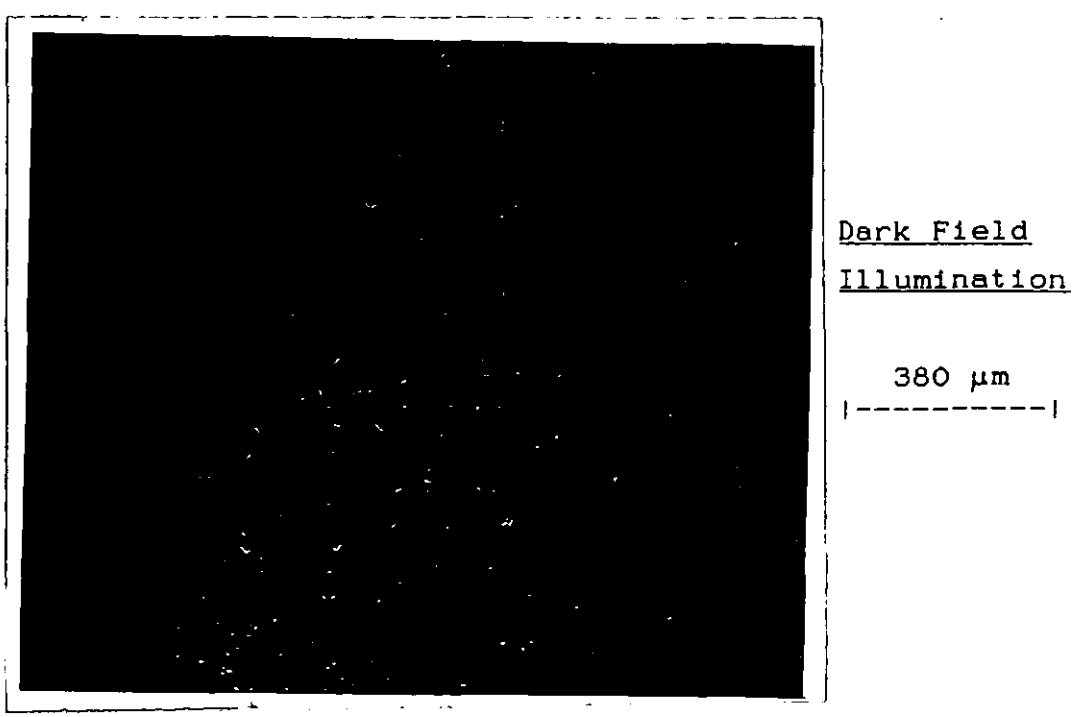

Higher profile temperatures, C and D, resisted particulate breakdown and the micrograph, figure 4.22, clearly shows that primary particles existed albeit with a degree of cohesion; the agglomerates can still be disrupted into smaller units via shearing.

The last microphotograph, figure 4.23, represents the filled blends processed at the profile temperatures beyond D, i.e. E and F; here the primary particles are not readily observed and the breakdown of the swollen fragments is prevented. The cohesion strength within the specimen is significantly greater which results in fibrillar tearing during acetone shearing.

Although the technique does provide a useful approach to quickly assess the quality of fusion, the qualitative method does not quantify the extent of fusion nor is it able to distinguish between relatively large steps in the degree of fusion. Thus the test does not provide significant information of the consequences upon fusion when large amounts of filler are added, but it does provide complementary evidence to the thermal analysis data discussed earlier in this chapter.

4.3.3 ELECTRON MICROSCOPY OF PIPE SURFACE

The surface of the pipe was viewed via electron microscopy (§2.7) and the results, in general, provide complementary evidence to the visual examination of the pipe surface. The electron micrographs provide a convenient technique to observe the detail of the outer surface and thus the pipes can be easily grouped according to their surface quality. Table 4.3 lists the pipes in terms of surface quality and is almost comparable with the previous classification given in table 3.4; also an example of each group is given in the electron micrograph figures 4.24-4.29.

FIGURE 4.22: Acetone shearing of OD

FIGURE 4.23: Acetone shearing of OF

TABLE 4.3

Micro-surface of pipe series 0-5

GROUP †					
I	II	III	IV	V	VI
5A, B	5C-E	3A-D	3E	3F	1F
4A, B	4C-E	2A-C	2D	2E	0F
		1A, B	1C	1E	
		0A, B	0C	0E	
		5F		**2F**	
		4F		**0D**	
				1D	

† Where I = poor surface finish and VI = best

Reformatted pipes are highlighted in **bold** text

FIGURE 4.24: Micro-surface of pipe 4B

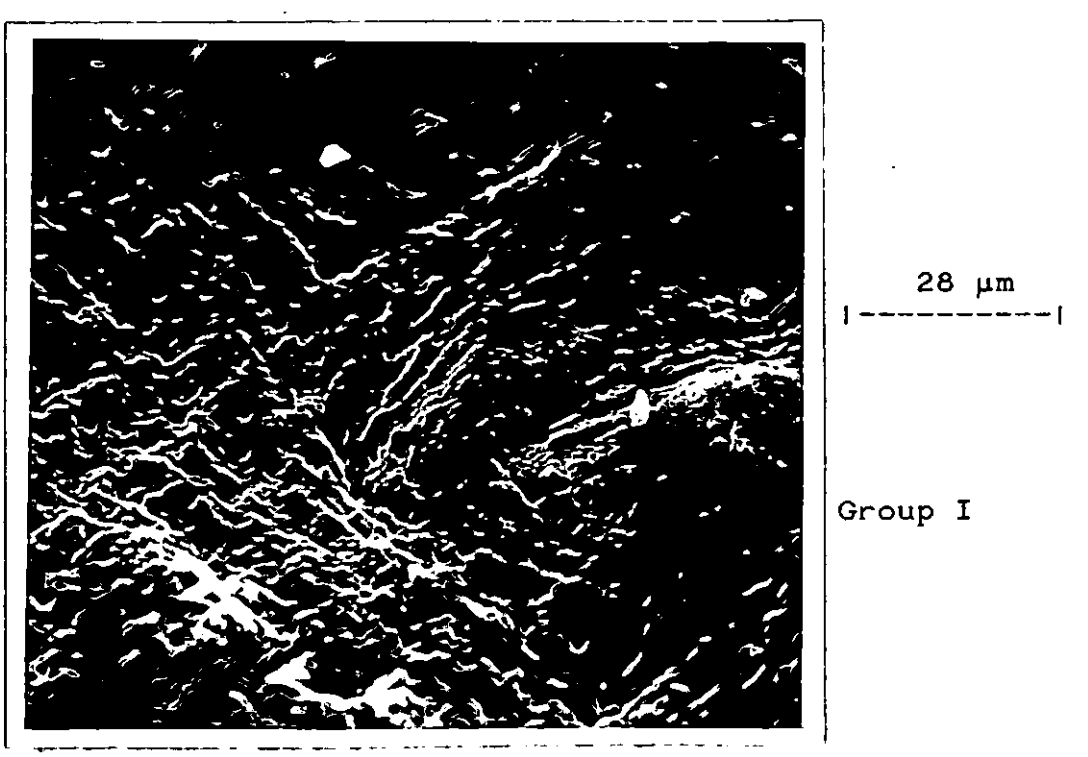

FIGURE 4.25: Micro-surface of pipe 4E

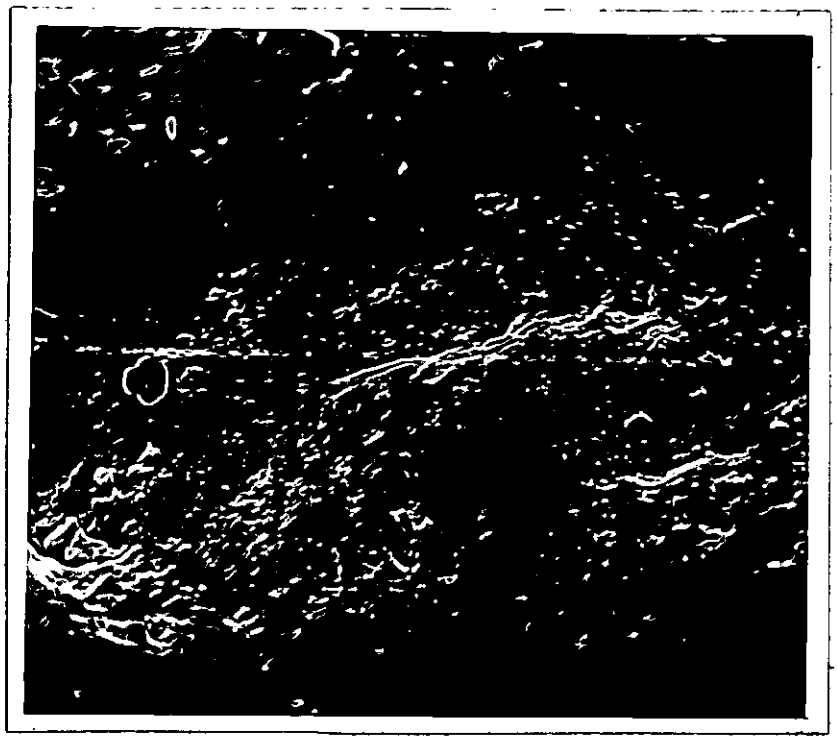

FIGURE 4.26: Micro-surface of pipe 3C

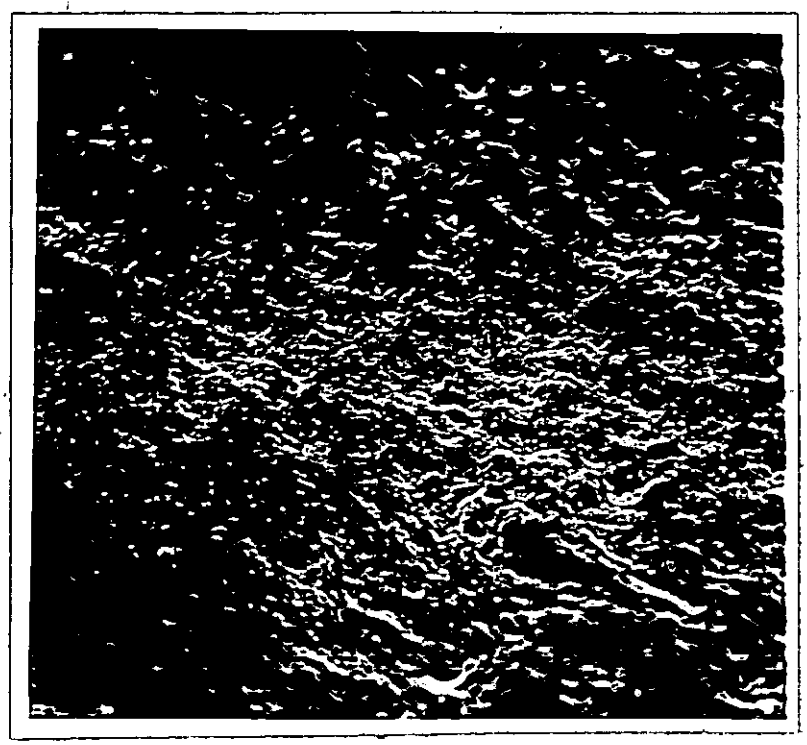

FIGURE 4.27: Micro-surface of pipe 3E

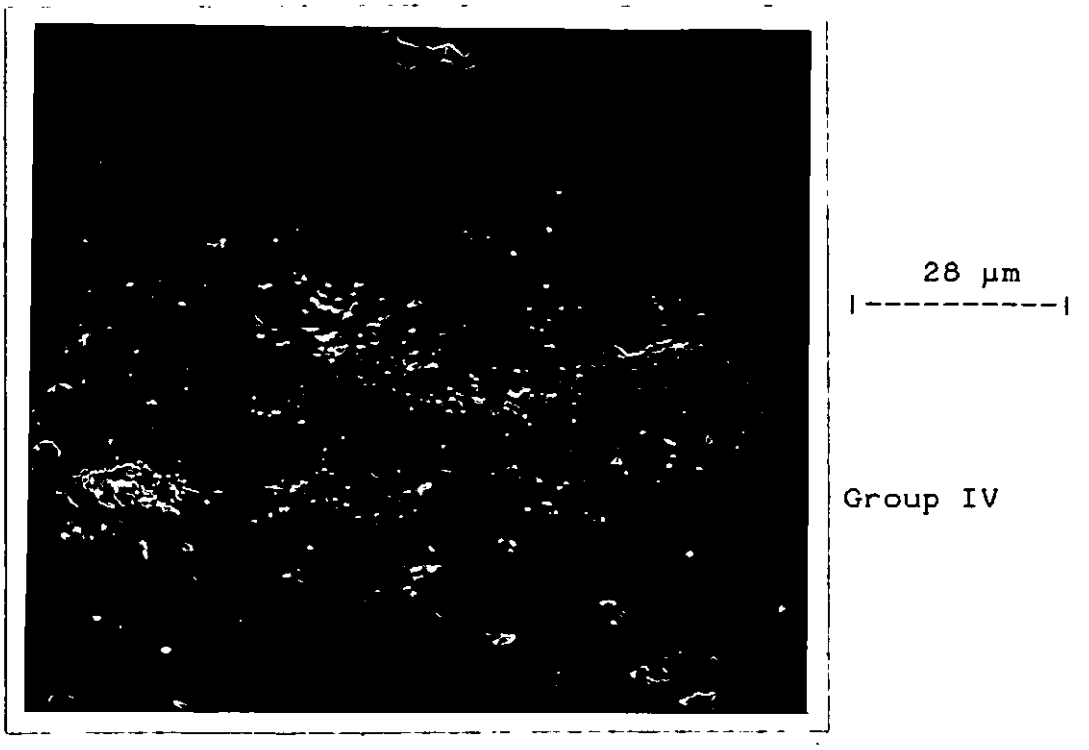

FIGURE 4.28: Micro-surface of pipe 1E

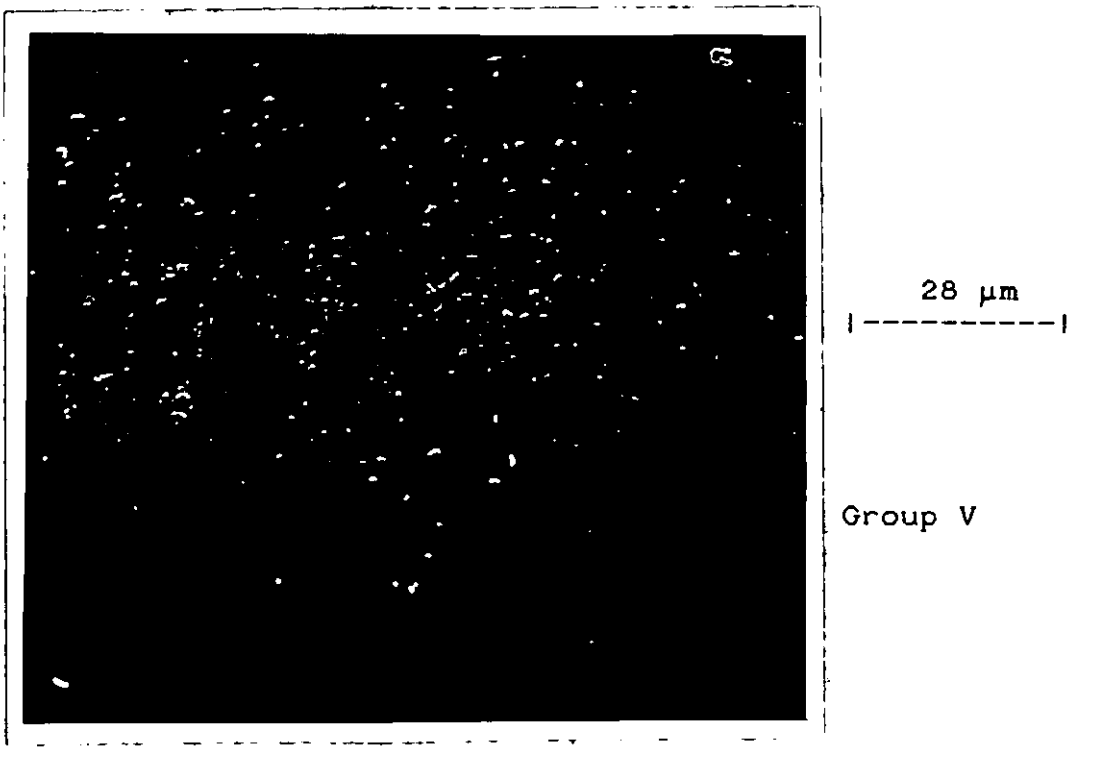

FIGURE 4.29: Micro-surface of pipe OF

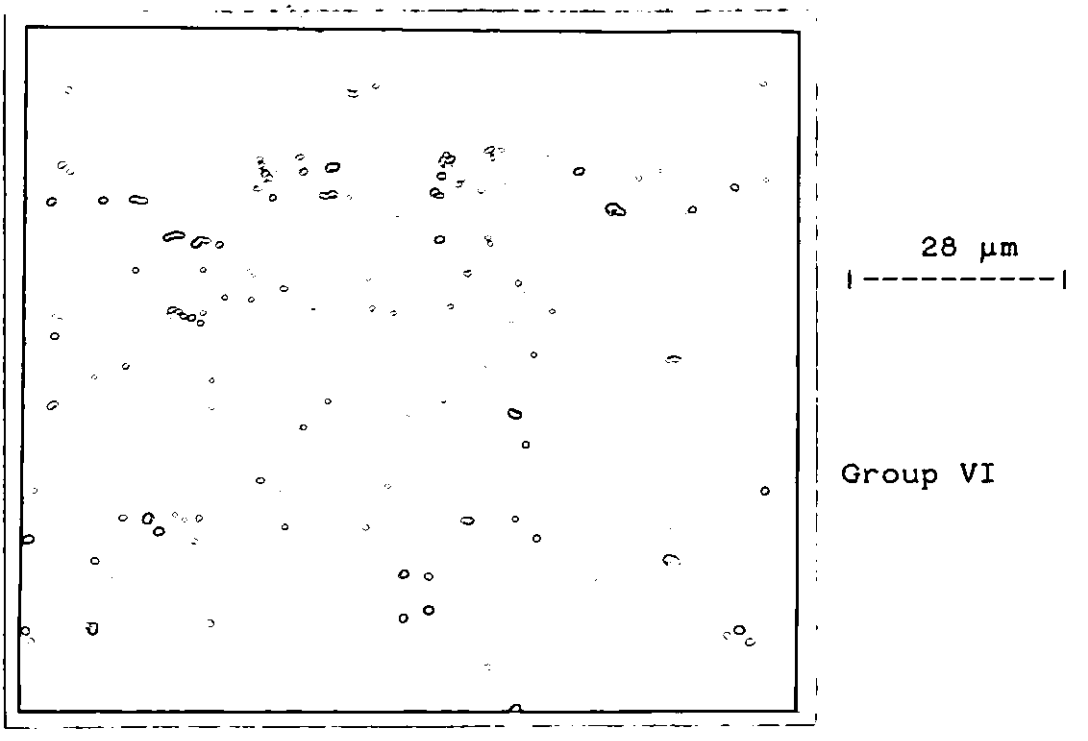

An increase in filler content not only leads to a general deterioration in the surface quality of the pipe as discussed in §3.3.1 but also leads to an increase in the amount of deposited filler on the surface. These deposits can be qualitatively assessed by mapping calcium, detected via x-ray analysis, within the electron microscope; figures 4.30-4.32 demonstrates the increase in detected calcium with increasing filler loading.

FIGURE 4.30: Micro-surface of pipe 1F

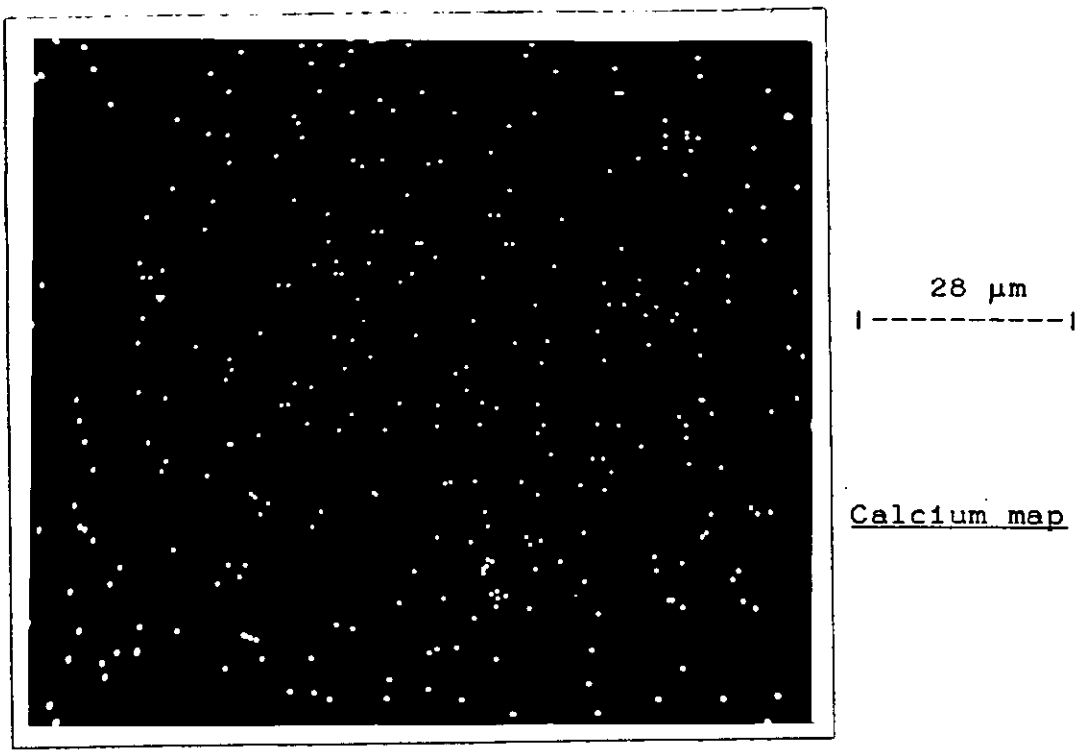

FIGURE 4.31: Micro-surface of pipe 2F

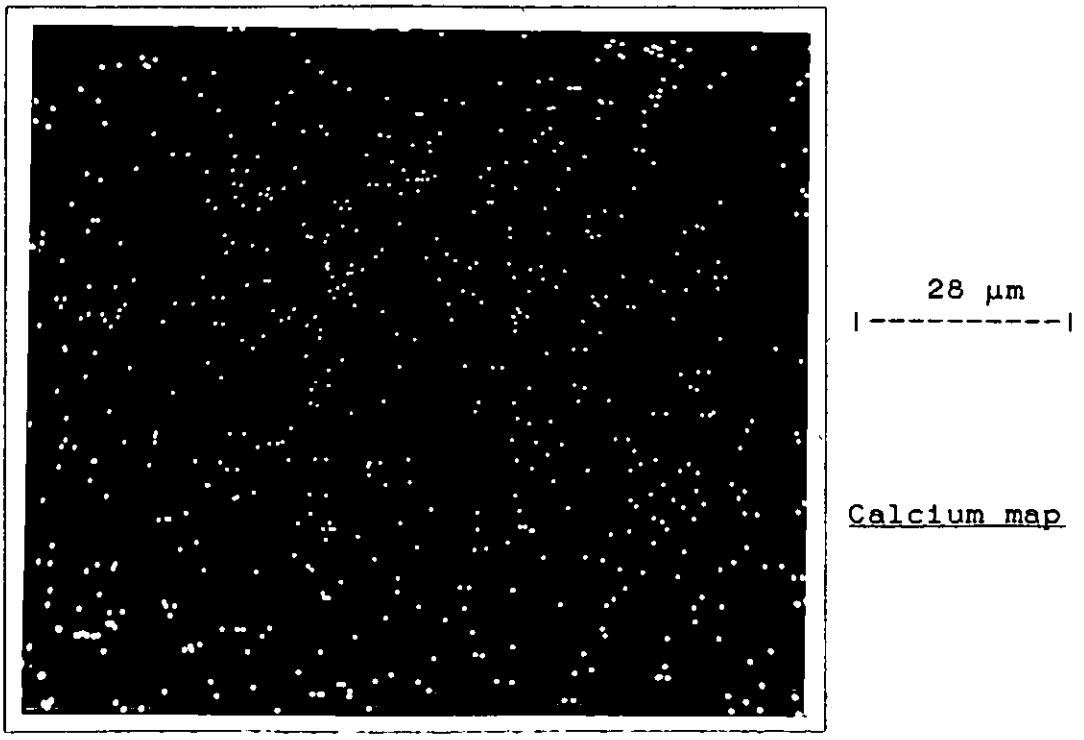

FIGURE 4.32: Micro-surface of pipe 5F

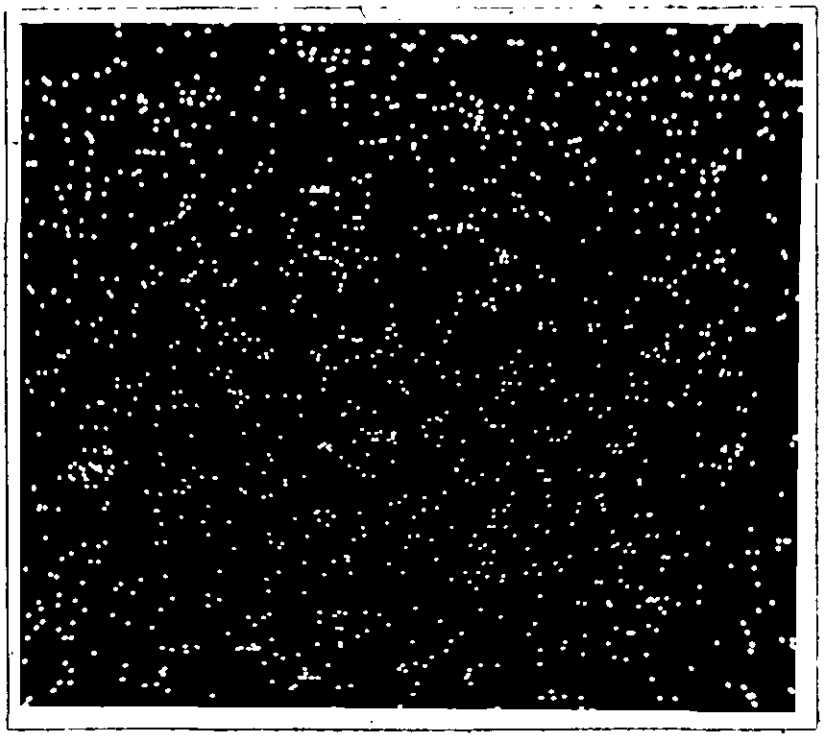

4.4 MICROSCOPY OF ADDITIVE SERIES

4.4.1 OPTICAL MICROSCOPY

The blends containing the range of additives discussed in §2.3 were also sectioned and viewed via light microscopy. The micrographs of these extrudates yielded significant differences between the filled and unfilled additive series; the unfilled additive series in a similar manner to the unfilled extrudate series OA⇒OF revealed a residual grain structure. The occurrence of these grains was dependent upon the type and level of additive incorporated and an order of decreasing residual grain content can be presented as follows:

POOR ◄ ----- grain content ----- ► GOOD

OEG OEB OEF · OE- OEC OEE OEH

OEA OED

Figures 4.33-4.37 present a number of micrographs to illustrate the gross differences in residual grain content. Again no subtle differences were observed between sections taken parallel or transverse to the direction of extrusion

Figure 4.33 shows a high distribution of residual grains. OEG being clearly the worst of all extrudates in this series. Extrudates OEB and OEF show a marked improvement in terms of residual grain content and similarly extrudates OE- and OEA are next in the series with few grain inclusions. Pipes OEC, OED and OEE are very similar and suggest an almost homogenous section; OEE reveals slightly fewer inclusions than its similar counterparts. The best extrudate in terms of homogeneity was OEH; few inclusions were observed with the additives well dispersed to yield a homogeneous section.

FIGURE 4.33: Microphotograph of section OEG

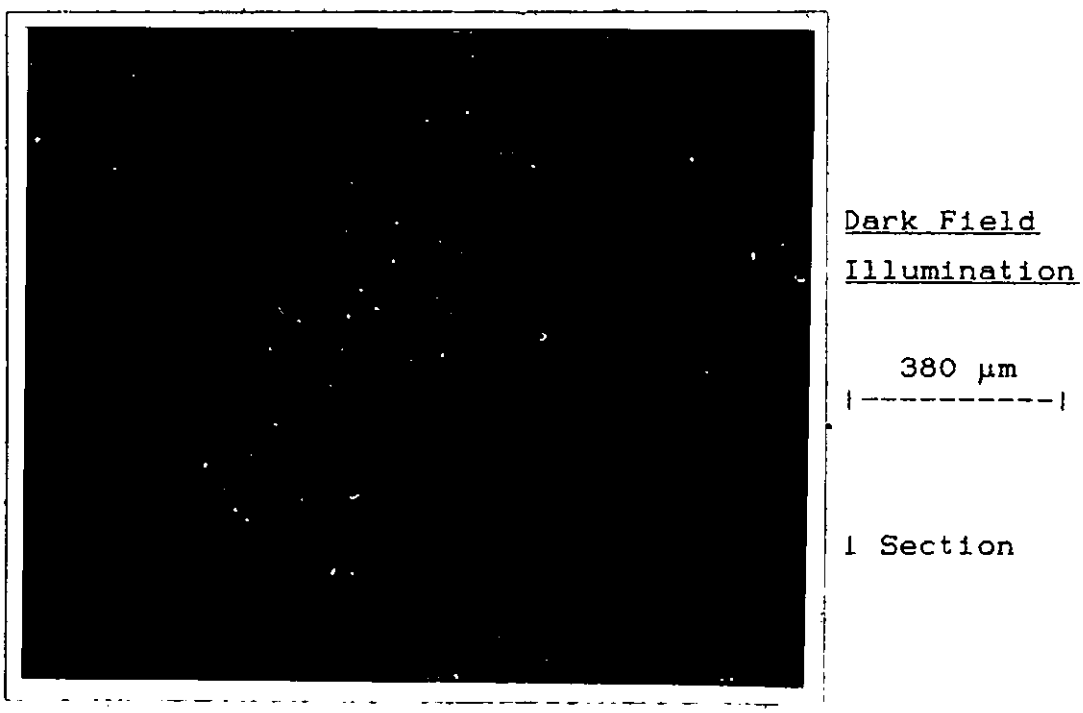

FIGURE 4.34: Microphotograph of section OEB

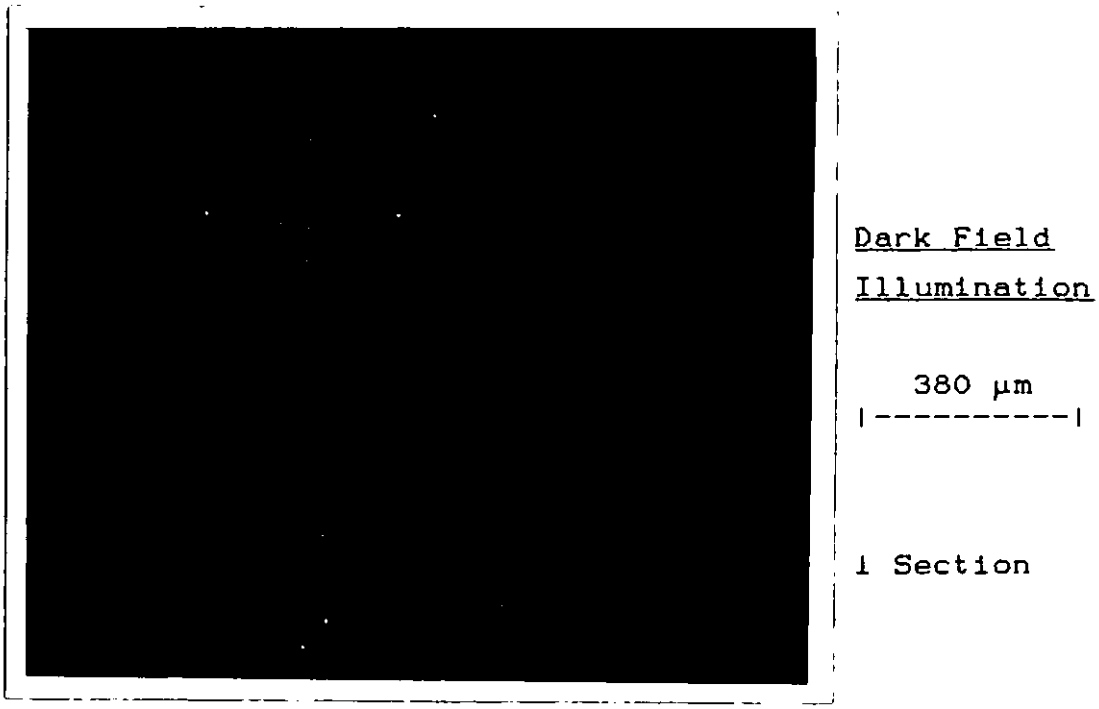

FIGURE 4.35: Microphotograph of section OE-

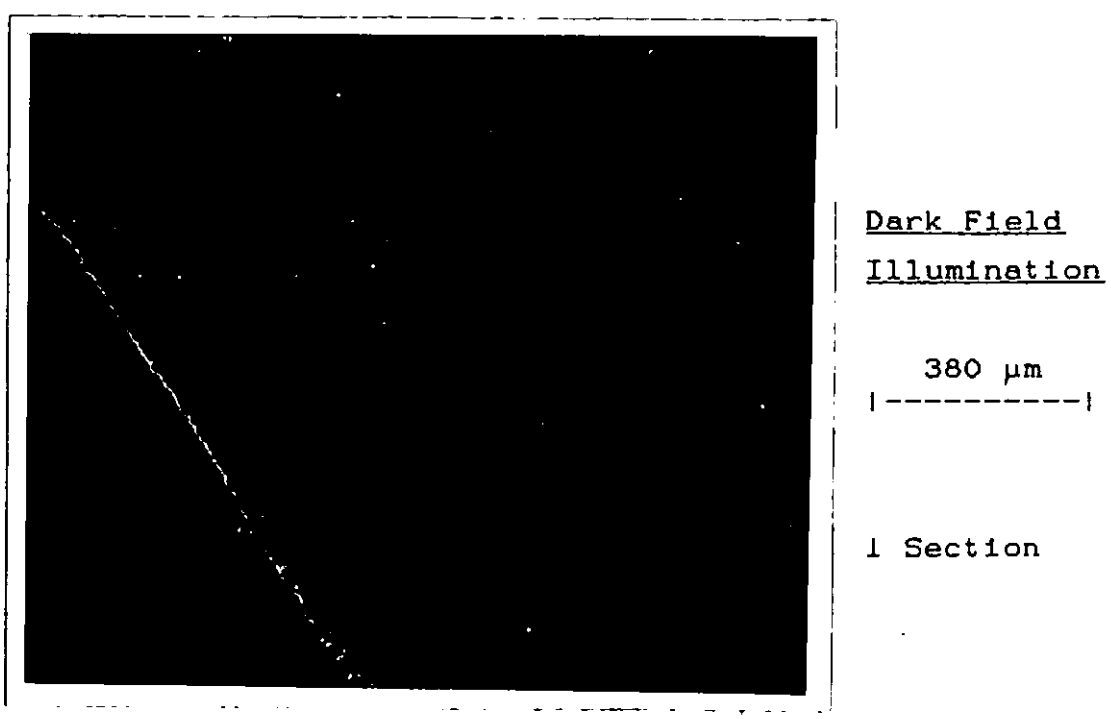

FIGURE 4.36: Microphotograph of section OEE

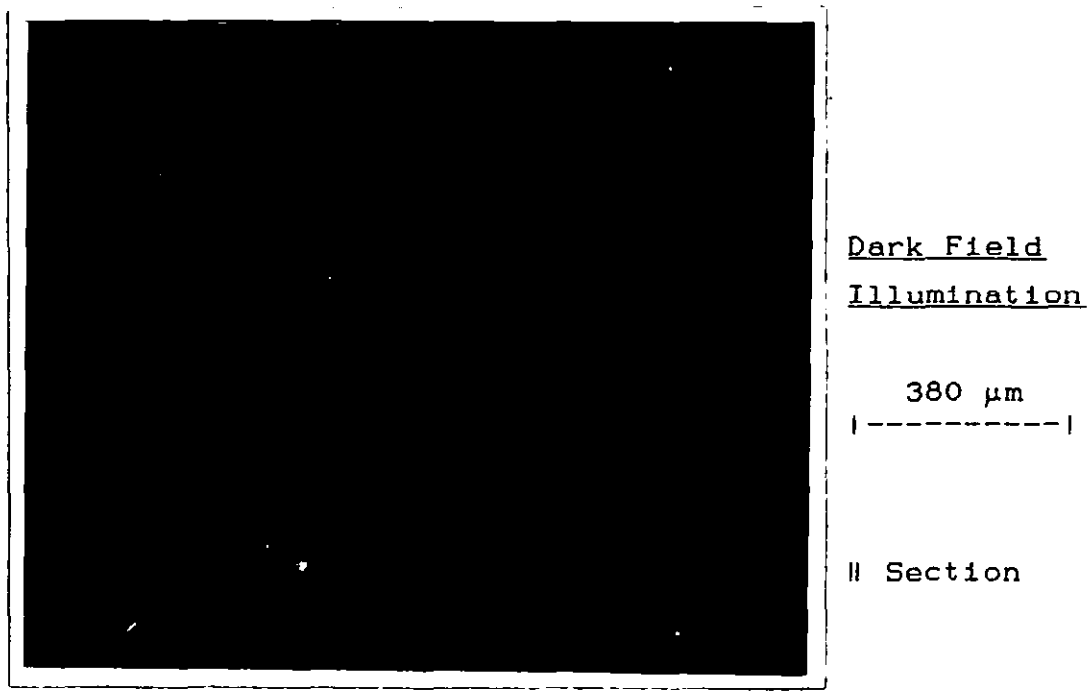

FIGURE 4.37: Microphotograph of section OEH

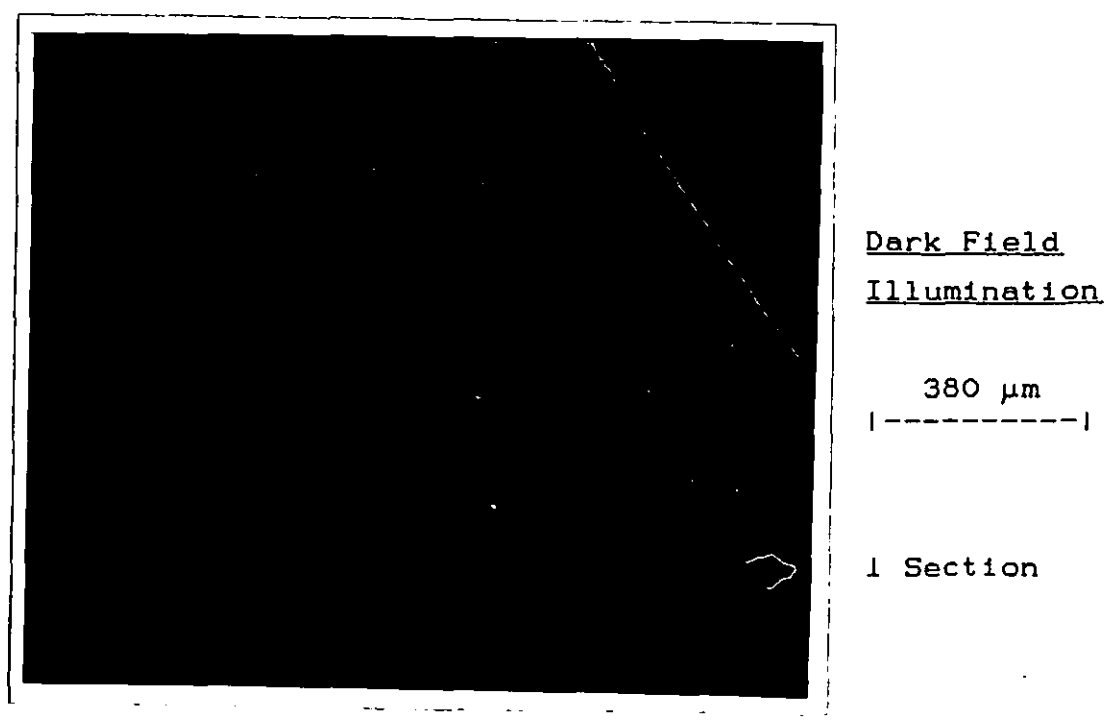

The additive series containing approximately 27 phr of Polcarb S filler differed in that residual grain distribution was not a prominent feature, here the dispersion of the filler was the significant factor and the distribution of the filler was affected by the type and level of additive. The series can be ranked in terms of increasing filler dispersion, from a poor distribution in which quite large agglomerates (20-30 μm) can be seen to a homogeneous section which does not indicate filler separation. Figures 4.38-4.42 illustrate the trend shown in the list below:

POOR ◄ --- filler dispersion --- ► GOOD

3EA	3EE	3E-	3EC	3EB	3EF	3EH
3ED					3EG	

FIGURE 4.38: Microphotograph of section 3EA

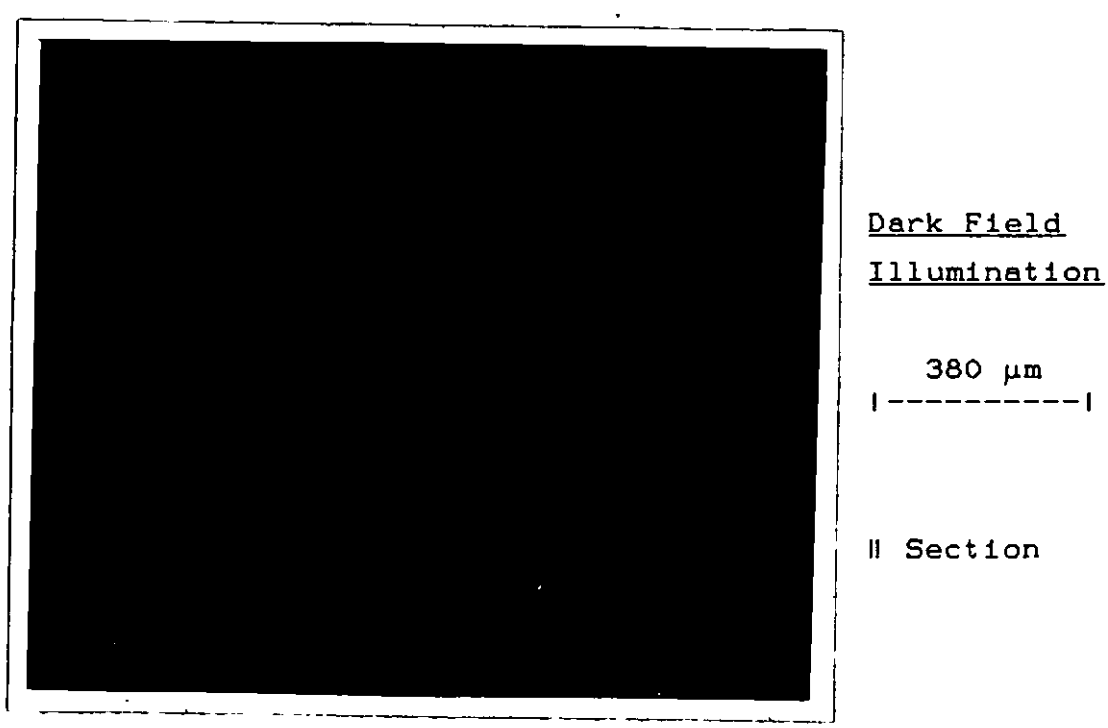

FIGURE 4.39: Microphotograph of section 3EC

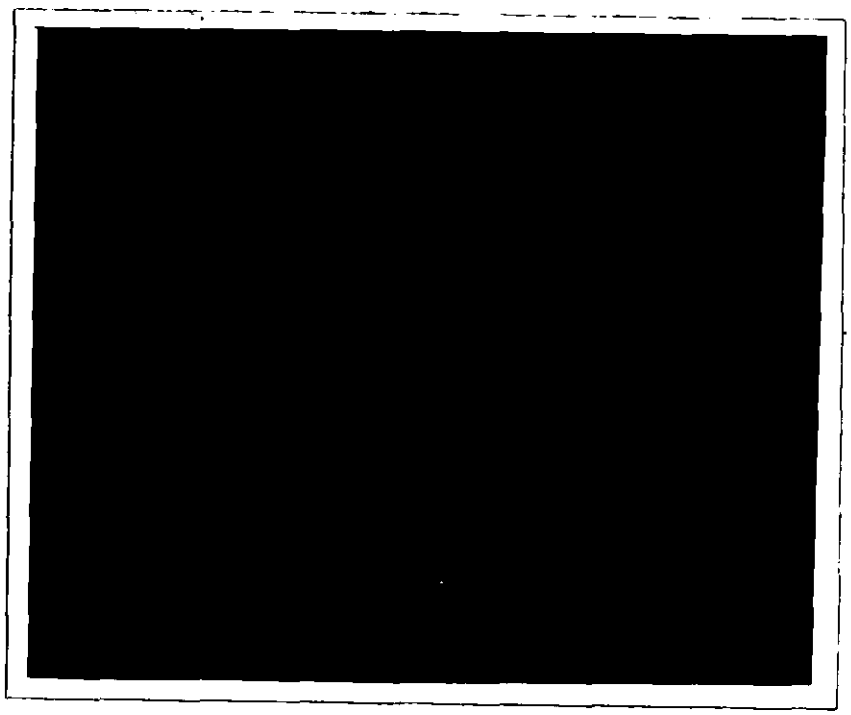

FIGURE 4.40: Microphotograph of section 3EB

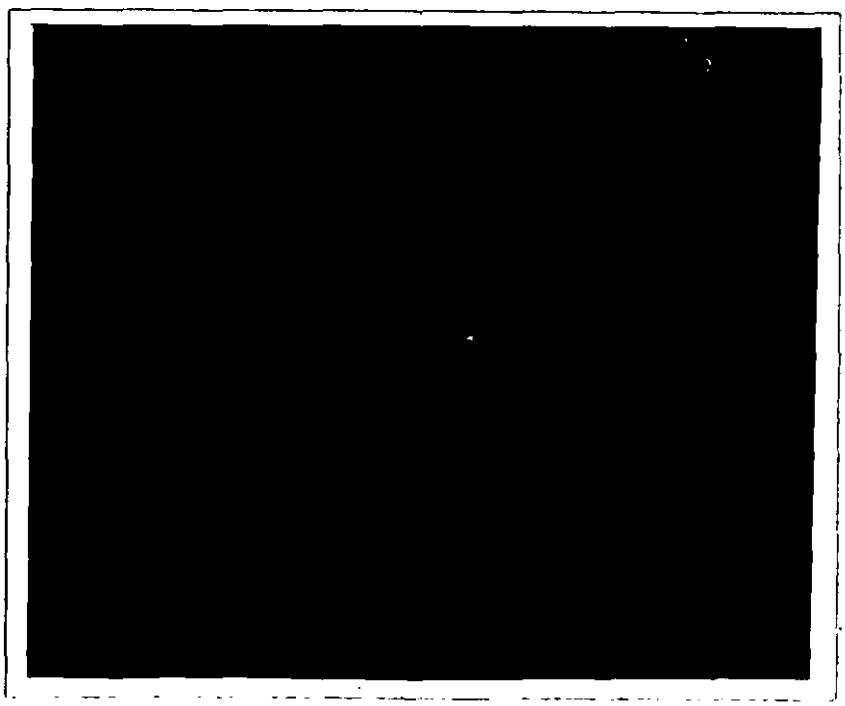

FIGURE 4.41: Microphotograph of section 3EF

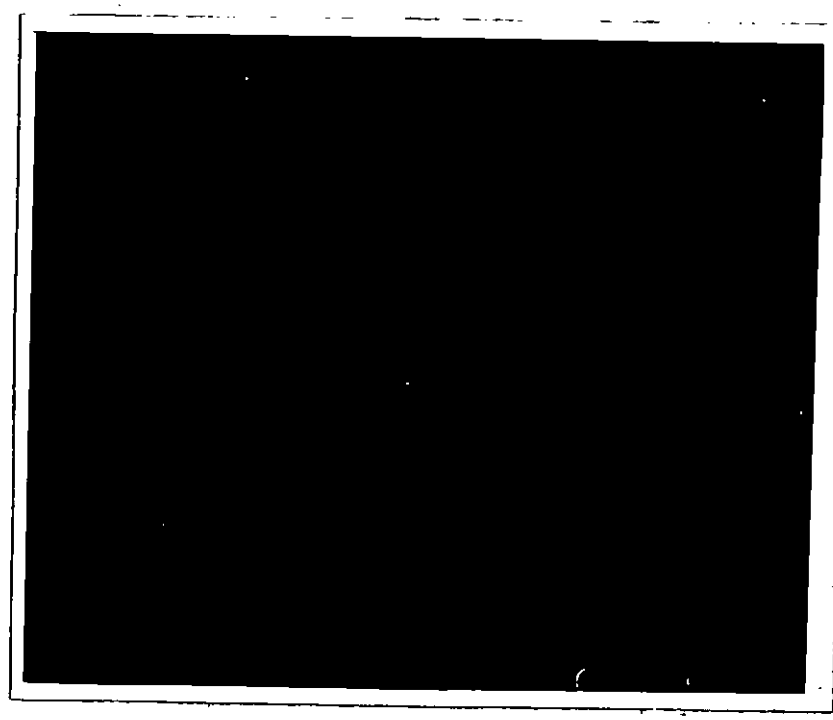

FIGURE 4.42: Microphotograph of section 3EH

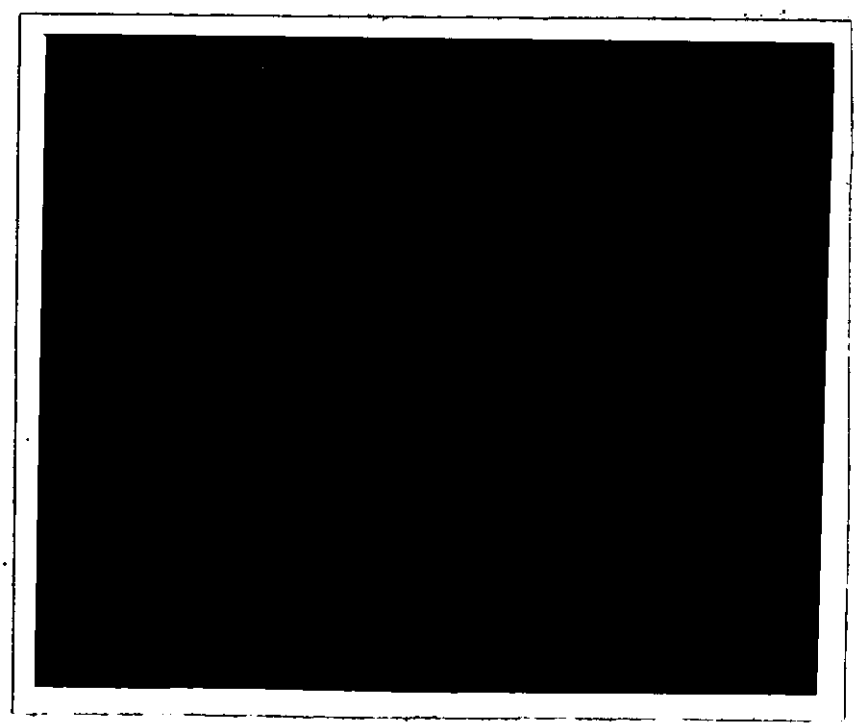

4.4.2 ACETONE SHEARING TEST FOR ADDITIVE SERIES

The extrudates incorporating the range of additives were also subject to the acetone shearing test in a similar manner to §4.3.2. In this case, few discernible differences were observed between the pipe specimens, that is, the test did not identify poorly fused specimens and the limited discriminating power of the test suggested that all the extrudates were of approximately equal fusion level. The pipes were extruded at the same profile (E) and therefore gross changes in fusion level might not be expected and, indeed, the solvent shearing test did not distinguish between the extrudates. The original series processed at a wide temperature range revealed an approximate correlation between fusion level obtained via thermal analysis and the acetone shearing test. However the extrudates for the additive series were, at least, moderately fused (table 4.2) and the test was unable to provide further evidence to indicate or measure the degree of fusion involved.

4.4.3 MICRO-SURFACE OF ADDITIVE SERIES

Scanning electron microscopy of the surface of these extrudates provided evidence to support the trends observed via visual examination i.e. table 3.5. The same order of increasing surface quality was suggested by the photomicrographs obtained via this technique.

CHAPTER FIVE

RESULTS OF MECHANICAL PROPERTY TESTS

5.1 TENSILE PROPERTIES OF FILLED EXTRUDATES

The pipes containing 0⇒40 phr of the mineral filler, Polcarb S, were subject to uniaxial tensile testing as described in §2.10.1. The low temperature extruder profiles did not produce regular pipe section which prevented preparation of tensile specimens; thus results are presented for pipes processed at extruder profiles C, D, E and F. These results can be summarised in table 5.1:

It can be seen from the results that, in general, the measure of experimental scatter (s.d) is quite high, particularly for elongation at break values where reproducible failure was not always evident. However the test does identify a number of trends which can highlight the influence of filler loading and fusion level. Figures 5.1 and 5.2 consider the influence of filler content upon yield and failure tensile properties; a steady decrease in yield stress is observed with increasing filler content with some deviation between profile temperatures at the higher filler loadings i.e. extrudates containing 35·6 phr of filler processed at E and F profiles resulted in a lower σ_Y value then profiles C and D.

The influence of filler loading upon failure characteristics can be seen in figure 5.2; again a decrease in ultimate stress is observed with increasing filler content, however the results differentiate between extruder temperature profiles. Profiles C and D produce similar σ_B values while profiles E and F illustrate that an increase in processing temperature leads to a reduction in ultimate stress values. It was observed in §4.1 that the estimated processing temperature determined by thermal analysis for profiles C and D were similar, while an approximate 10°C

TABLE 5. 1

Tensile properties of filled extrudates

Pipe code	Yield stress (MN/m²)		Ultimate stress (MN/m²)		Yield elongation (%)		Ultimate elongation (%)	
	σ_Y	s.d†	σ_B	s.d	ε_Y	s.d	ε_B	s.d
0C	52·1	0·7	41·2	0·5	10·7	0·5	90	21
0D	51·8	0·3	41·9	0·4	10·0	0·0	124	4
0E	52·7	0·2	40·3	0·7	11·0	0·8	114	24
0F	52·3	0·4	38·6	0·4	17·0	0·8	61	23
1C	48·8	1·0	41·2	1·4	10·8	0·8	128	7
1D	47·1	0·5	41·7	0·6	11·7	0·5	135	4
1E	46·8	0·4	38·5	0·9	14·3	0·5	133	7
1F	48·2	0·3	36·2	0·4	15·0	0·0	67	12
2C	43·3	0·3	40·2	1·6	10·0	0·0	121	8
2D	44·1	0·1	40·1	2·0	11·0	0·0	140	6
2E	43·5	0·3	37·3	0·8	16·0	0·8	136	6
2F	43·8	0·2	36·0	0·2	15·0	1·3	60	4
3C	42·3	0·5	37·1	0·6	4·7	0·9	41	4
3D	41·4	1·2	36·3	1·2	4·0	0·0	29	1
3E	39·8	0·2	34·3	0·1	10·7	0·9	33	4
3F	37·5	0·8	33·6	0·2	13·3	0·5	27	2
4C	37·3	0·9	35·0	0·2	10·3	1·2	20	3
4D	37·5	1·2	34·7	0·9	8·7	0·5	26	4
4E	36·4	0·6	34·7	0·1	8·0	0·0	15	3
4F	35·0	1·0	32·4	0·2	10·3	0·5	23	3
5C	35·7	1·0	34·5	0·7	10·0	0·0	26	3
5D	37·4	0·2	35·1	0·4	9·0	0·8	29	15
5E	37·1	0·5	34·8	0·3	10·3	0·5	23	3
5F	35·0	0·2	33·0	0·3	9·3	0·9	14	0

† s.d = Sample standard deviation

FIGURE 5.1

Yield stress versus Filler content

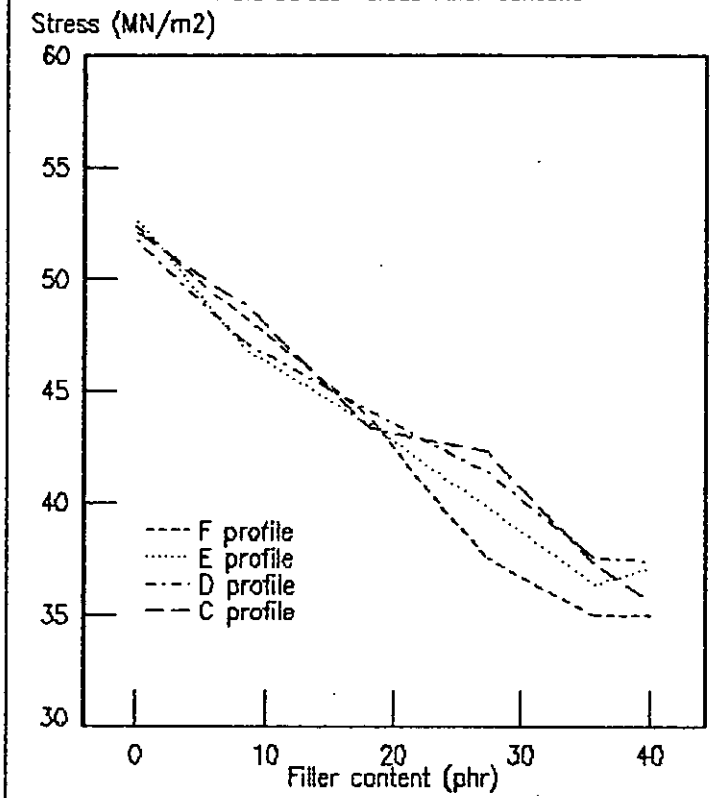

FIGURE 5.2

Ultimate stress versus Filler content

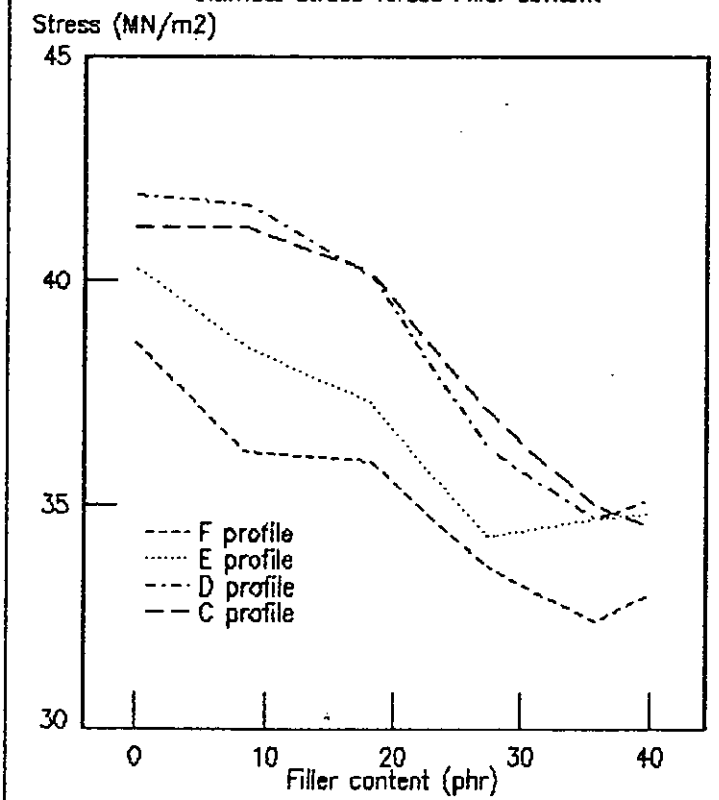

increase in processing temperature was measured between profiles D & E and E & F.

The measured values can be replotted against the approximate processing temperature ('B' onset temperature) as shown in figures 5.3 and 5.4. Similar figures would be obtained if σ_Y and σ_B were plotted against fusion level because of the strong relationship obtained in §4.1.3.

Figure 5.3 presents the yield values as a family of curves which are dependant upon filler loading; a higher filler loading results in a series of data which is substantially lower than the preceding filler loading, however the yield values remain constant, albeit at different base levels, with increasing 'B' onset temperature until a filler level of approximately 27 phr is reached. At this filler loading and beyond an increase in 'B' onset produces a decrease in yield stress. Little difference is observed for the data collected upon the 35·6 and 40 phr filled extrudates and the results of 5C (□ symbol) seem unreliable.

The second figure (5.4) again provides sets of data which distinguish between filler loadings, although, unlike yield values, an increase in 'B' onset temperature for all the filler loadings leads to a decrease in ultimate stress. The results are not as precise as for the yield stresses, especially for the testing of extrudates processed at low temperatures, and this fact may account for the crossover observed between the unfilled extrudates and the lightly filled grades (8·5 and 18·1 phr). The extrudates containing a relatively large amount of filler (35·6 and 40 phr) were very similar with a spurious result noted for 5C as seen for the yield values.

If the values measured for ε_Y and ε_B are considered, then it can be seen that yield elongation differs slightly with perhaps a small increase with increasing processing temperature for the lightly filled extrudates; whereas elongation at yield measurements for the heavily filled pipes seem unaffected by the processing temperature.

FIGURE 5.3

Yield stress versus 'B' Onset

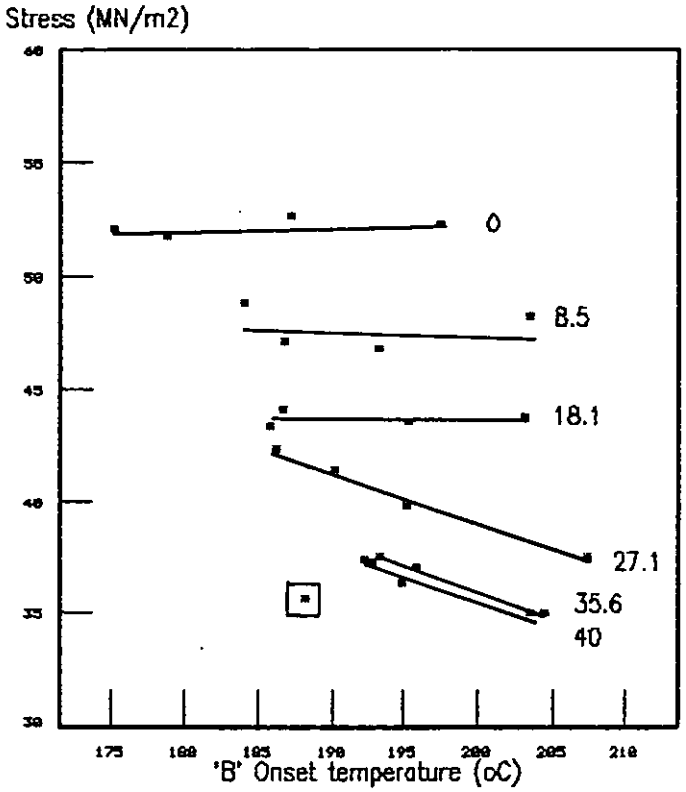

FIGURE 5.4

Ultimate stress versus 'B' Onset

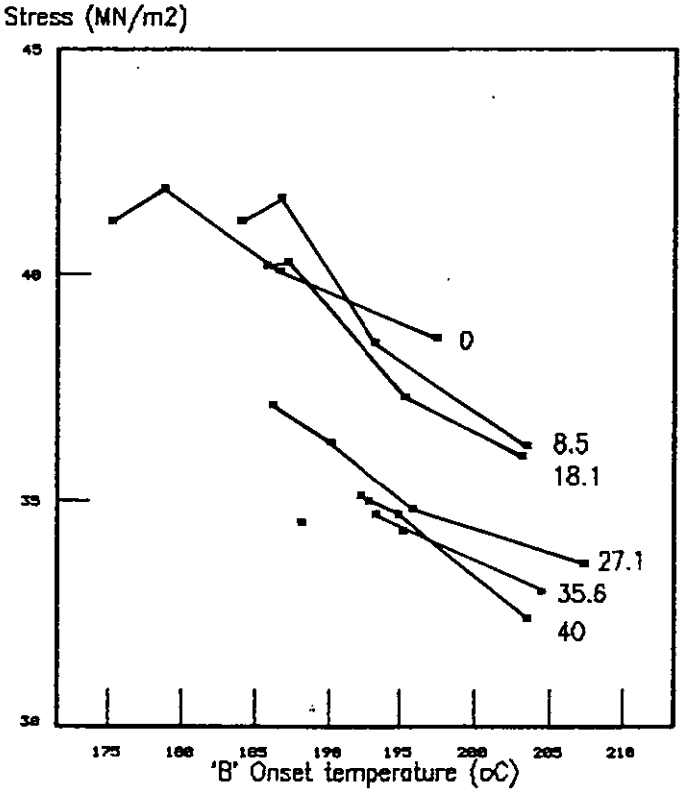

Tensile extension at failure was dependent upon filler content and processing temperature as shown in figure 5.5. The scatter of results should be taken into consideration and may account for some variation in the trends observed. σ_B values for extrudates containing 27·1 phr filler and above seem relatively independent of the processing temperature and remain at a low value. In contrast, the lightly filled extrudates achieved a high extension value at low processing temperatures but this value sharply diminished at the highest temperature profile, F. The elongation at break measurements mimic the trends observed for ultimate stress and it is interesting to note ultimate elongation values were higher for the lightly filled extrudates (8·5 and 18·1 phr) at intermediate extrusion temperatures than the unfilled series.

FIGURE 5.5

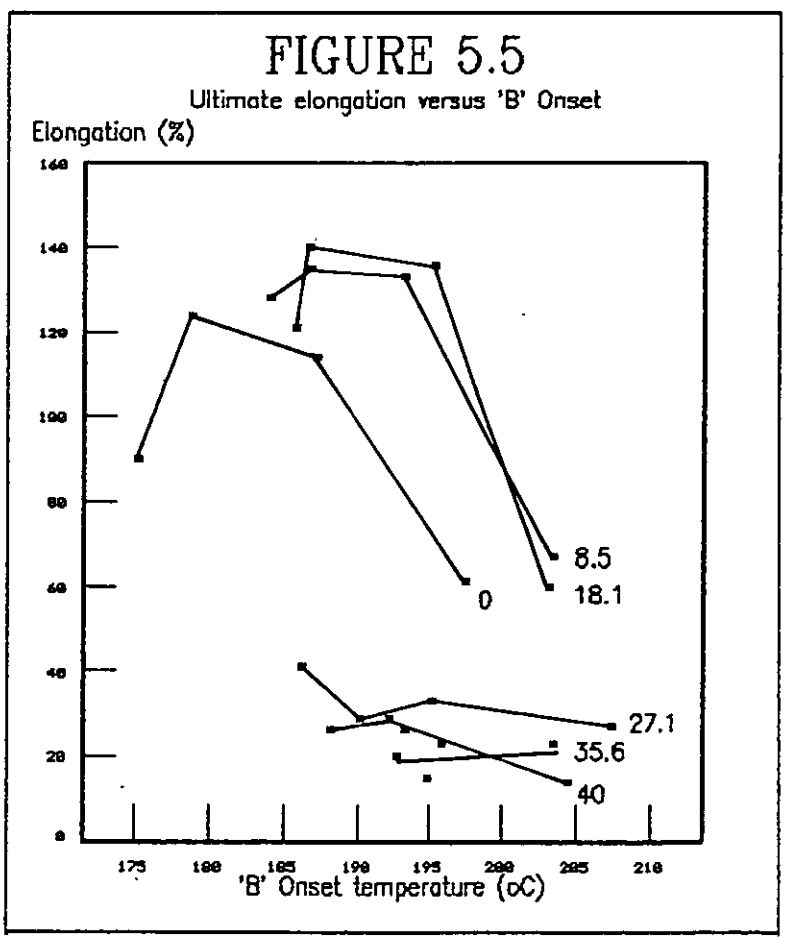

5.2 TENSILE PROPERTIES OF ADDITIVE SERIES

The unfilled and filled (≈27 phr) pipes containing the wide range of additives were also assessed for tensile properties and a summary of results is presented in table 5.2:

TABLE 5.2

Tensile properties of additive series

Pipe code	Yield stress (MN/m²)		Ultimate stress (MN/m²)		Yield elongation (%)		Ultimate elongation (%)	
	σ_Y	s.d†	σ_B	s.d	ε_Y	s.d	ε_B	s.d
0E-	53·4	0·3	46·9	2·4	6·0	0·0	165	18
0EA	51·8	0·5	44·4	1·9	4·8	0·8	179	14
0EB	52·2	0·9	43·0	1·8	5·8	0·4	157	9
0EC	53·9	0·5	42·1	1·2	10·0	0·0	158	22
0ED	54·7	0·9	41·7	1·0	8·0	0·0	83	5
0EE	54·4	0·4	44·1	2·0	8·0	0·0	169	12
0EF	53·8	0·6	42·7	0·7	9·0	1·0	148	18
0EG	42·4	0·5	44·5	1·7	10·0	0·0	191	8
0EH	49·3	0·7	51·5	2·1	10·0	0·0	206	17
3E-	45·4	0·4	41·5	1·9	10·0	0·0	154	9
3EA	45·3	0·3	41·0	0·8	11·7	0·7	148	9
3EB	44·9	0·4	44·3	1·2	10·3	1·3	180	12
3EC	44·4	1·0	42·1	0·8	11·1	1·8	149	7
3ED	44·8	0·4	40·5	0·7	9·2	1·0	122	18
3EE	44·7	0·9	39·9	1·3	9·7	0·7	145	10
3EF	44·7	0·9	42·2	2·3	9·0	1·0	162	16
3EG	42·9	0·5	47·9	1·4	11·0	0·0	194	12
3EH	41·1	0·8	45·5	2·1	10·0	0·0	196	7

† s.d = Sample standard deviation

Figure 5.6 illustrates yield stress for the additive blends and it can be seen that the type or concentration of additive has little effect upon yield properties with the exception of impact modifier addition. In this case the yield stress is lowered by the incorporation of an impact modifier and the extent of the reduction depends upon the type and whether the material is filled. The CPE modifier

(additive code G) in an unfilled system significantly reduces yield stress while the all acrylic modifier (additive code H) has a moderate lowering effect. In the filled system the roles are reversed in that the acrylic modifier has a greater lowering effect.

The ultimate tensile properties are depicted by figure 5.7 and a relationship between elongation at break and ultimate stress is observed i.e. a large amount of drawing, in general, produces a higher tensile stress. The results indicate a dependence upon the type and concentration of the additive and the consequences of these results will be discussed fully in §6.3.2.1 when complementary evidence is also considered.

5.3 IMPACT PROPERTIES OF HIGHLY FILLED SYSTEMS

The impact properties of the extrudates were determined via an instrumented falling impact tester as described in §2.10.2.

The extrudates produced at the lowest temperature profiles (A and B) were not a regular shaped pipe and thus presented problems of sampling as a split pipe, however for the purpose of impact testing these samples were hot pressed to produce flat plaques (§2.10.2.1). The flattened specimens were supported and clamped onto a DIN ring anvil and tested using the same test variables as described for the split pipe. The geometry of the test piece is a well known testing variable in impact testing and this must be considered when comparing with results for the split pipe.

The thickness of the pipe varied slightly between extruder runs and in order to provide a comparable test value the results were 'normalised' by dividing the individual results by the thickness of the specimen. Differences in specimen thickness can produce disproportionate impact results even after normalising, however the thickness variation in this study was relatively

FIGURE 5.6

Yield stress for Additive series

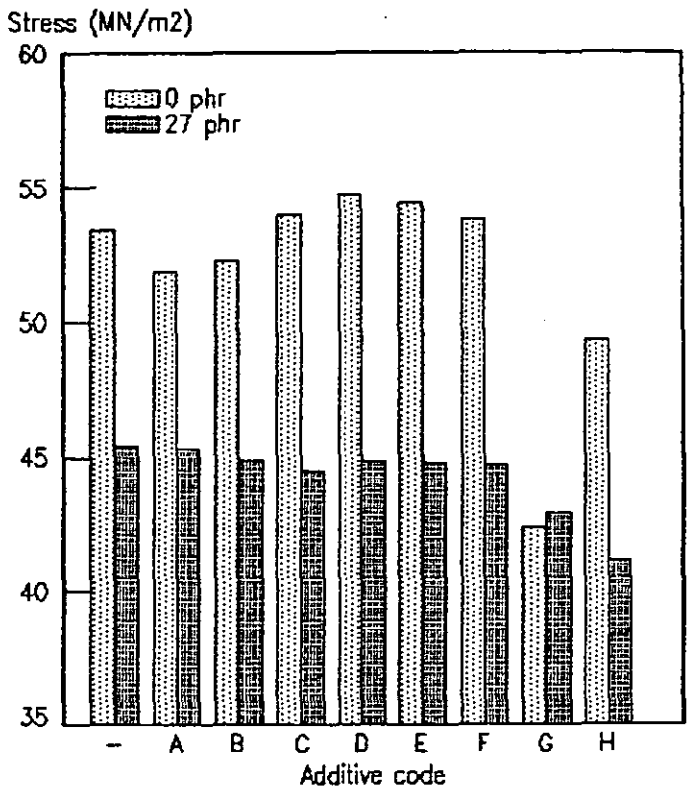

FIGURE 5.7

Ultimate stress for Additive series

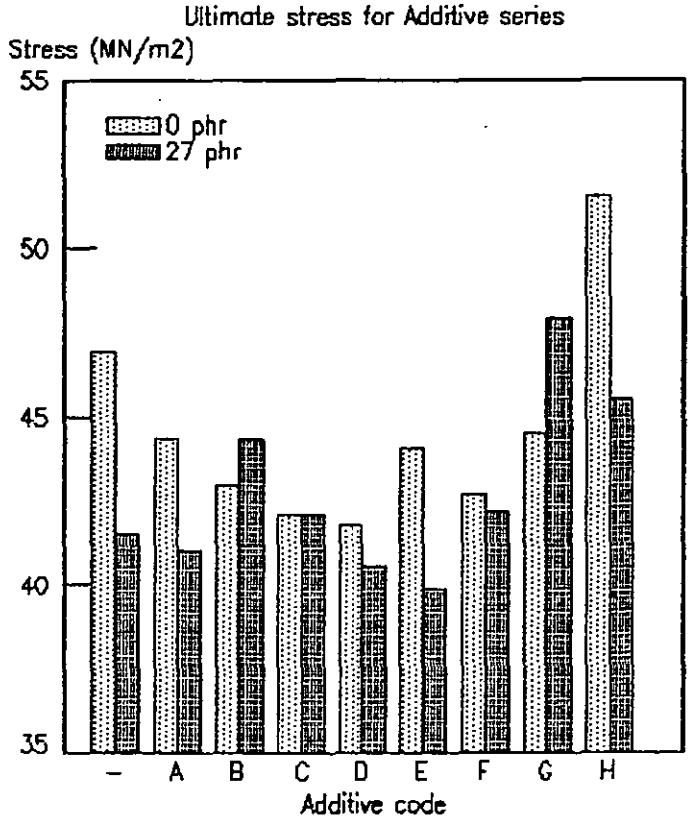

low and an extensive trial study indicated that normalised values were constant for a given pipe.

Another test feature which should be considered in high strain rate tests is the application of filters. Filtering is normally required to yield practicable results and overcome excessive 'noise to signal' spikes, especially for testing of brittle materials. The impact tester is fitted with a digital filter which can post-filter the signal with a number of available filters. The effect of filtering a brittle material can be illustrated in the figures shown in Appendix E. Figure E.1 effectively demonstrates the unfiltered brittle failure of a split pipe in the rig described in Appendix C; the trace is difficult to analyse and complicated by signal artefacts. In the opposing case of extreme filtering, figure E.2 illustrates the same impact data of E.1 but with a high powered filter. Over-filtering can lead to a reduction in peak response and therefore is a source of variability. The final trace, E.3, indicates the application of an intermediate filter which eliminates the spikes of a noisy signal while retaining a true representation of the fracture behaviour. The criterion suggested for the sensible application of a filter is a maximum deviation in peak value of less than 3%. A series of trials for each set of extrudates provided the appropriate post-filter value.

The salient fracture characteristics as shown in figure 2.7 for the filled extrudates are summarised in table 5.3:

The results indicate a strong interrelationship between the major characteristics of impact fracture; that is, the general trends are similar for the measures of force, deflection and energies. The exception is maximum gradient (maximum value of slope in a force-deformation trace) which remains relatively insensitive within a pipe series (C⇒F) and increases slightly with increasing filler loading. The ability to measure the slope is complicated by

TABLE 5.3

Impact properties of filled extrudates

Pipe code	Peak Force (N/mm)	Peak Deflection (mm)	Peak Energy (J/mm)	Failure Deflection (mm)	Failure Energy (J/mm) E_F	Failure Energy (J/mm) s.d†	Maximum Gradient (KNmm/m)	Type of Failure
0A	240	3·41	0·4	7·51	0·7	0·4	-	B
0B	165	2·54	0·2	5·82	0·4	0·1	-	B
0C	1223	14·00	8·3	15·40	9·0	0·5	123	B/D
0D	1248	15·07	9·8	16·41	10·5	1·1	114	B/D
0E	1192	14·68	8·8	20·31	11·0	0·7	116	D
0F	1261	14·90	9·9	20·64	12·5	0·7	119	D
0G	1216	14·35	8·6	19·83	10·9	0·5	113	D
1A	964	7·51	3·1	8·88	3·6	1·5	-	B/D
1B	822	6·65	2·3	7·75	2·6	1·2	-	B/D
1C	1263	12·90	8·3	14·40	8·9	1·2	130	B/D
1D	1343	14·66	9·5	15·78	10·1	1·0	142	B/D
1E	1258	14·19	8·7	15·48	9·4	0·8	123	B/D
1F	1293	15·46	10·4	17·89	12·1	0·7	125	D
2A	174	2·47	0·2	8·28	0·7	0·1	-	B
2B	117	1·94	0·1	7·69	0·6	0·1	-	B
2C	219	6·36	0·9	10·98	1·5	0·3	126	B
2D	295	5·98	1·0	7·70	1·2	0·3	108	B
2E	262	7·17	1·2	10·13	1·6	0·2	131	B
2F	1034	11·84	5·8	13·05	6·3	0·7	116	B/D
3A	103	1·91	0·1	9·65	0·6	0·3	-	B
3B	66	1·62	0·1	7·85	0·5	0·1	-	B
3C	185	5·07	0·8	9·54	1·2	0·2	204	B
3D	256	4·99	0·9	8·68	1·4	0·2	211	B
3E	180	4·43	0·6	7·18	0·9	0·1	158	B
3F	198	5·39	0·7	7·75	1·0	0·2	137	B
4A	94	2·24	0·1	8·69	0·7	0·2	-	B
4B	91	2·39	0·1	10·31	0·8	0·3	-	B
4C	184	4·20	0·5	9·64	1·2	0·2	150	B
4D	191	5·21	0·7	7·71	1·0	0·2	149	B
4E	194	6·50	1·1	7·76	1·1	0·2	168	B
4F	180	5·71	0·8	8·03	1·1	0·1	166	B
5A	91	2·44	0·1	11·11	0·8	0·3	-	B
5B	89	2·33	0·1	8·34	0·5	0·1	-	B
5C	203	6·22	1·0	8·42	1·3	0·2	187	B
5D	178	5·85	0·6	8·12	1·1	0·4	166	B
5E	212	5·15	0·8	7·78	1·2	0·1	198	B
5F	184	6·15	0·9	9·00	1·2	0·3	155	B

B = Brittle. B/D = Brittle/Ductile. D = Ductile

† s.d = Sample standard deviation

the differing impact traces encountered and some variation might be expected. It was not possible to accurately measure the maximum gradient for the flat hot pressed specimens because of the small deflection at peak, which did not provide a sufficient number of points for the automatic calculation of slope.

It is also evident that the peak impact characteristics obtained from the testing of the flat plaques (profiles A & B) are considerably lower than the split pipe specimens. This can be accounted for by the different deformation behaviour involved when deforming a flat specimen compared to hemispherical pipe. However the failure impact characteristics seem reasonably comparable between the two sampling techniques, especially if the failure deformation values for the moderately filled pipes are considered. The results obtained for profiles A and B with a filler content of 0 and 8.5 phr are vastly different from their counterparts; however it is suggested that these values are related to impact performance rather than a possible specimen geometry factor since a brittle-ductile transition is observed i.e. failure mechanism changes from brittle or ductile/brittle to ductile on increasing processing temperature.

Since the results indicate similar trends for the analysis of the force-deformation traces, then failure energy can be used to represent the relationships between filler loading and processing conditions and impact performance. The measure of scatter (s.d) within the data is indicated and can be considered quite acceptable for this type of test; a larger degree of variation is observed for extrudates which fail in a brittle manner and some samples which exhibit a brittle/ductile behaviour. The criterion for classifying the mechanism of failure is described in 2.10.2 and shown in figure 5.8, which superimposes representative data for three different extrudates and clearly identifies the main modes of fracture: ductile, brittle/ductile and brittle.

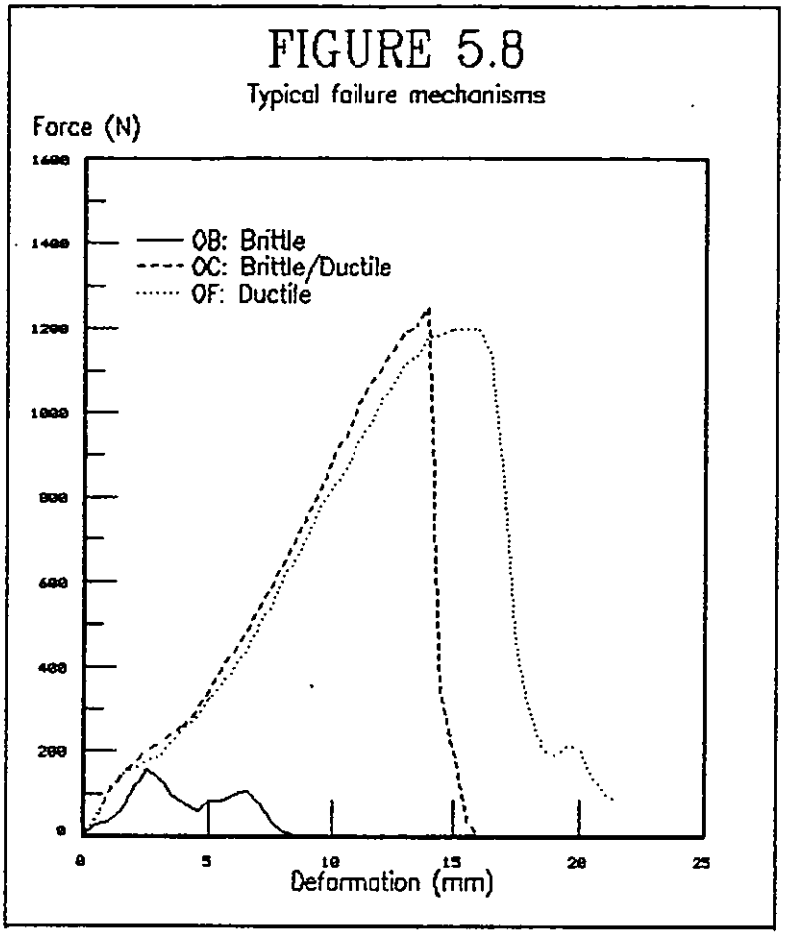

Brittle fracture is visually observed as a crack running a considerable length parallel to the direction of extrusion or an area of the pipe wall which is sheared out. A crack running in the direction of extrusion may be 'capped' at either end by further cracks transverse to the original propagated crack. The length of the crack can vary but can be in the order of 100 mm. Brittle failure via shear out results in approximate circular sections of the pipe wall being 'pushed out'; the area of the holes are at least the size of the impactor probe and can be considerably greater (upto 3×).

Brittle/ductile failure is generally characterised by a complete shattering of the specimen which is associated

with crack propagation in many directions.

Ductile failure is observed as gross deformation of the pipe, local yielding at point of impact with attributed stress whitening, continued deformation and finally tearing of drawn yield area. Therefore a puncture hole of similar dimensions to the impactor probe is seen which can lead to a continued force signal, due to further penetration of the probe through a restricted puncture.

The effects of filler loading and extruder profile can be seen in figure 5.9; the impact performance is sensitive to processing conditions at a low filler content; Here a higher profile temperature, in general, produces a higher impact resistance. The values obtained for extruder profiles A and B are very low and are reversed to the general trend in that profile A yields nominally higher values than profile B. Profile F is clearly distinct from the moderately processed extrudates (C, D and E) with a slightly higher impact energy. At filler levels greater and including 18.1 phr then all profiles, with the exception of F, produce equally poor impact resistance. Profile F at an intermediate filler loading of 18·1 phr retains a modicum of resistance but is approximately halved when compared to the unfilled grade.

Figure 5.10 presents failure energy versus fusion levels for the extrudates implied via thermal analysis (§4.1). A similar graph would be observed if the fusion level axis was replaced by the estimated processing temperature ('B' onset temperature) also derived from thermal analysis.

If the highly filled extrudates (≥27·1 phr) are considered first; then fusion level has no effect upon the poor impact resistance obtained. A similar trend is seen for the extrudates containing 18·1 phr of filler until a dramatic increase in impact resistance is observed for the most fused member; the improvement is dramatic with the specimens failing in a brittle/ductile manner as opposed to a brittle mode.

FIGURE 5.9

Failure energy versus Filler content

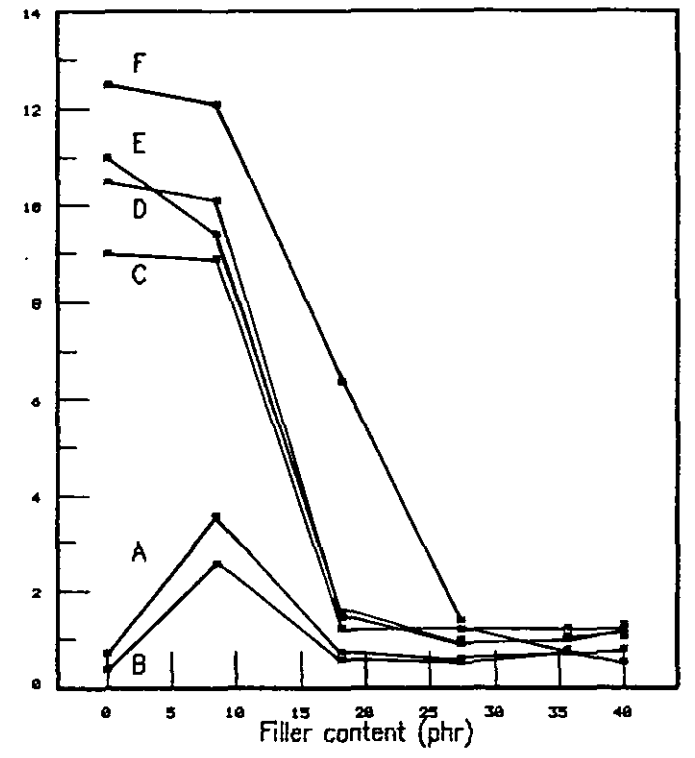

FIGURE 5.10

Failure energy versus Fusion level

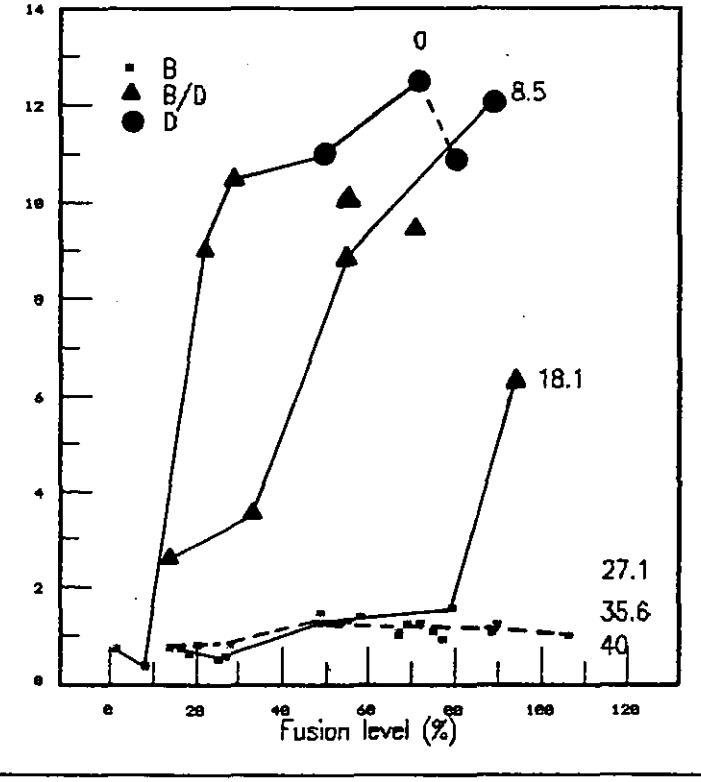

The unfilled and lightly filled extrudates (0 and 8·5 phr) illustrate a transition from poor brittle behaviour to 'high' impact, ductile characteristics with increasing fusion level. The lightly fused extrudates of these two series (extrudates processed at A and B) indicate poor impact, although 1A and 1B do exhibit some impact resistance which might be associated with their higher level of fusion (c.f. low fusion levels of 0A and 0B). It is interesting to note that figure 5.9 demonstrated that impact properties for 1A and 1B were reversed in terms of extruder profile; while fusion levels for these two extrudates are also reversed and thus might account for the impact values obtained. Higher fusion levels result in considerably higher impact properties until a levelling off or maximum is obtained; the lightly filled series (8.5 phr) is shifted to the right indicating the requirement of a higher fusion level to obtain the same level of impact performance. The impact resistance of the 0 phr series, after passing through a sharp transition at an approximate fusion level of 20%, increases until ductile failure mode is reached where a levelling off or actual decrease is observed. The last member of this series (joined via a dotted line) is pipe 0G, which is included to demonstrate the possible existence of a maximum in impact energy. 0G is a pipe extruded at high profile temperatures (§2.6.1) which has traces of degradation due to hot spots within the processing equipment; thermal analysis indicates a fusion level of 80% ('B' onset temperature = 201.2°C) and impact testing suggests ductile failure but with a reduced impact energy.

Therefore impact testing of the filled extrudate series illustrated the poor impact properties of the highly filled pipes and the transition from poor to a maximum impact value with increasing fusion level.

5.3.1 IMPACT PROPERTIES: INFLUENCE OF TEST TEMPERATURE

The influence of environmental temperature upon impact performance was assessed for the unfilled and filled extrudates processed at extruder profile temperature F (§2.10.2.1). The samples were carefully conditioned at the appropriate test temperature and then quickly transferred to the pre-conditioned impact rig for testing. The results are presented in table F.1 of Appendix F.

Failure impact energy can again be used to illustrate impact performance, although deflection characteristics show an increase with increasing test temperature and is not strictly related to failure energy as in the above case. It should be appreciated in the analysis of these results that the extrudates have different fusion levels. Figure 5.11 illustrates the dependence of impact energy upon test temperature.

FIGURE 5.11

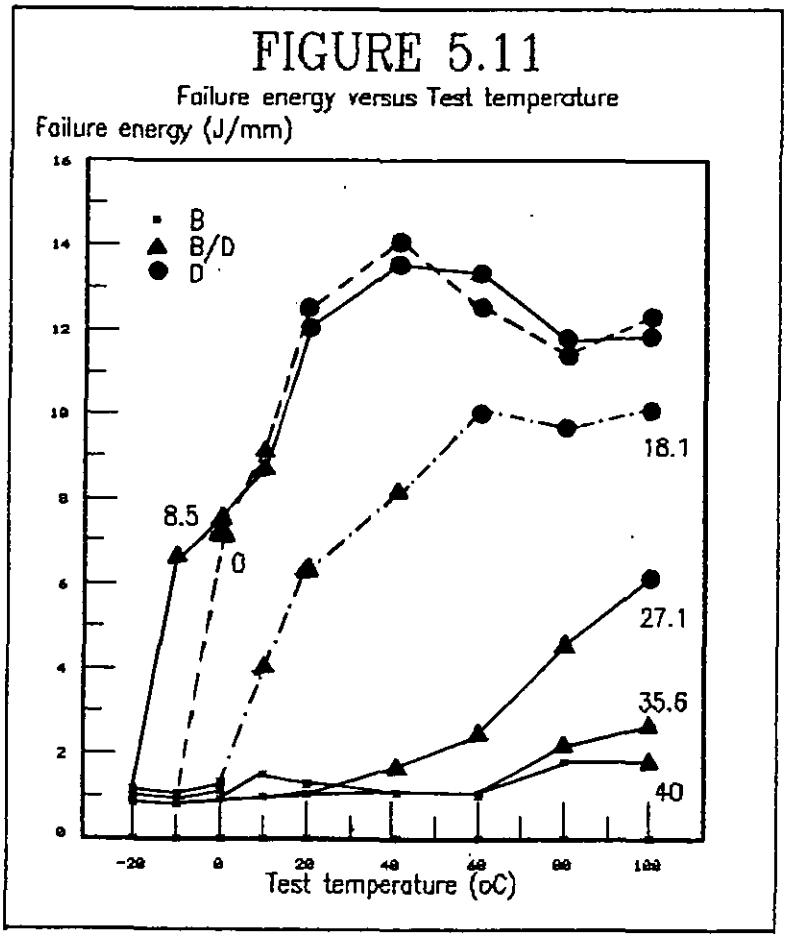

The highly filled specimens, 35·6 and 40·0 phr, are unaffected by test temperature until a conditioning temperature of 80°C and 100°C respectively, where the specimen undergoes a hot tearing mechanism which can be seen as a small brittle/ductile impact trace.

The testing of 3F produces a broad brittle-ductile transition that begins at 40°C and ends with a ductile trace at 100°C. Although a ductile fracture is obtained, the impact value is relatively small.

The moderately filled pipe, 2F, again produces a broad brittle-ductile transition beginning at 10°C and levelling off at 60°C. The impact value obtained for ductile failure is substantially higher than 3F and a further increase in test temperature did not improve the energy value.

The unfilled and lightly filled pipes produced similar failure energies with the onset of a narrower brittle-ductile transition beginning at -10°C for 1F versus 0°C for 0F and finally ending in ductile failure at 20°C. The better low temperature properties of 1F are probably related to the substantially higher level of fusion compared to 0F (c.f. 88·7% versus 71·7%) and the consequences of fusion upon ductility will be discussed in chapter six. The values obtained for impact energy are quite high but the level appears to decrease beyond 40°C.

Therefore the influence of test temperature distinguishs between filler levels, determines any brittle-ductile transitions, indicates a levelling off of impact property with increasing temperature and suggests that fusion level can cause a shift to ductile behaviour.

5.4 IMPACT PROPERTIES OF ADDITIVE SERIES

The pipes containing the range of additives were tested in a similar manner and the properties can be listed as given in table 5.4:

TABLE 5.4

Impact properties of additive blends

Pipe code	Peak Force (N/mm)	Peak Deflection (mm)	Peak Energy (J/mm)	Failure Deflection (mm)	Failure Energy (J/mm) E_F	s.d†	Maximum Gradient (KNmm/m)	Type of Failure
OE-	1124	12·05	6·1	13·29	6·7	1·3	124	B/D
OEA	1067	12·64	6·2	14·53	6·9	0·7	117	B/D
OEB	929	11·57	4·8	13·39	5·3	0·6	107	B/D
OEC	1094	14·48	7·8	22·17	10·2	0·6	115	D
OED	1211	15·21	9·2	21·33	11·4	0·8	116	D
OEE	1175	15·04	8·8	22·24	11·2	0·4	118	D
OEF	1052	12·56	6·1	14·26	6·7	1·3	111	B/D
OEG	1108	16·11	8·6	21·47	10·3	0·5	98	D
OEH	1279	16·74	10·8	21·20	12·4	0·7	118	D
3E-	848	10·47	3·9	11·76	4·4	0·6	100	B/D
3EA	615	8·53	2·3	9·76	2·7	0·2	99	B/D
3EB	1064	13·36	6·6	14·65	7·3	0·7	100	B/D
3EC	915	11·28	4·6	12·53	5·1	0·5	104	B/D
3ED	676	9·13	2·8	10·46	3·2	0·4	99	B/D
3EE	753	9·80	3·3	11·05	3·7	0·7	103	B/D
3EF	1062	13·14	6·3	14·44	7·0	0·6	104	B/D
3EG	1079	15·17	7·5	16·94	8·3	0·4	102	B/D
3EH	1065	14·57	7·0	15·84	7·7	1·0	102	B/D

B/D = Brittle/Ductile. D = Ductile
† s.d = Sample standard deviation

The values for failure energy are illustrated in figure 5.12; it should be noted that the extrusion conditions between the two additive series are not strictly comparable (§2.6.2) and thus comparisons should be made within each series. It is evident from the bar graph that sizeable differences can be obtained in impact properties with a small change in type of additive or, in the case of pipes OEA and OEB, an increase in the concentration of the

same lubricant (§2.3). In fact a two fold increase can be obtained with an accompanying change in fracture mode from brittle/ductile to ductile behaviour. Possible explanations will be discussed when factors such as ease of processing, fusion level and microscopy results are presented (§6.3.2.2).

Figure 5.12

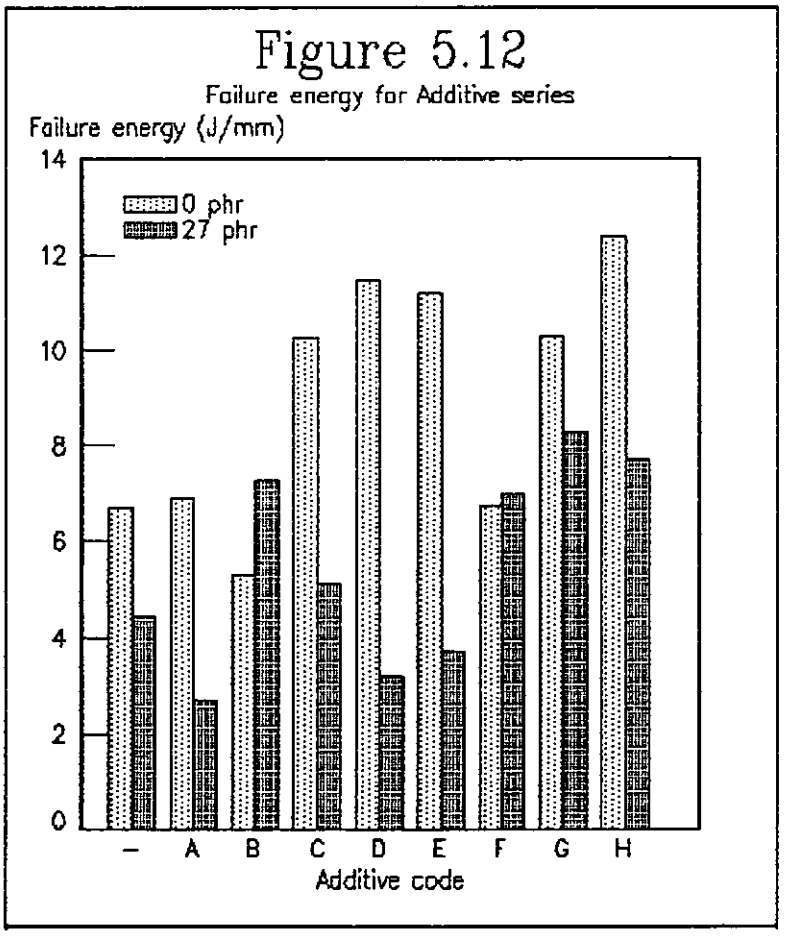

CHAPTER SIX

DISCUSSION OF RESULTS

6.1 INTRODUCTION

The preceding chapters, 3-5 inclusive, have presented the results obtained from dry blending, extrusion and the subsequent tests as a series of brief discrete sections. It is intended in this chapter to discuss the data in detail and compile the results to evaluate the possible interactions.

In order to simplify the following discussion, the chapter is divided into three parts; firstly the filled pipes processed over a wide range of extrusion conditions will be considered. Secondly the extrudates incorporating subtle differences in formulation for an unfilled and a relatively highly filled grade will be reviewed. Lastly the general inferences gained from the above two sections will be presented to provide a general overview of the complete process from powder additives to finished pipe.

6.2 DISCUSSION OF FILLED EXTRUDATES

6.2.1 DRY BLENDING AND DRY BLEND CHARACTERISTICS

The dry blending results outlined in §3.1 revealed that dry blending time was unaffected by filler loading until the addition of high loadings of filler (original filler loading of 40 and 50 phr respectively). At these high filler loadings longer blending times were observed which can be attributed to filler loss as seen in the heater mixer as mixer fouling; filler loss, in effect, reduces the material available to generate frictional heating between the particles and the high speed rotor and also between the particles themselves. Thus a longer time was required to achieve the required discharge temperature [138, 177].

The resultant filler loss is also shown quantitatively by the estimated ash content, which shows a significant variation between expected and actual filler content for original filler contents of 40 and 50 phr. In fact an original loading of 50 phr yielded only 40 phr after dry blending, even though the dry blending operation was carefully optimised to prevent excessive filler loss (§2.4). The relatively high filler loss appears to be related to the surface adhesion of filler to the surface of the polymer grains (§3.1.1.3). It is not possible to relate the surface area of filler (7·0 m^2/g) directly to that of the polymer grain (1 m^2/g) since it is unlikely that a monolayer of filler is involved at the surface, filler is shown to be preferentially located at the polymer folds, and only a portion of the filler surface is involved in its attachment to the grain surface. High filler loadings (blends 4 & 5) appear to saturate the surface of the polymer grains and possibly produce either a layer of filler which weakly adheres to the polymer grain surface or yields 'free' unassociated filler particles. Since fine powders are subjected to higher frictional forces than coarse particles and are more likely to stick to metal surfaces [178], then the tendency of mixer fouling by 'free' or easily removed filler particles can be explained.

The SEM micrographs (figures 3.5, 3.6 & 3.8) indicate that the mineral filler adheres to the polymer surface initially by electrostatic and possibly chemisorption forces [42] and that the filler is also preferentially situated in the folds of the irregular shaped polymer grains as described in similar dry blending studies [136, 176]. Hancock [42], using the same grade of filler and similar blending temperatures, illustrated micrographs which indicated the partial adsorption of the filler; however in this study the micrographs (figures 3.6 and 3.8) provide little support to this suggestion, and instead the filler is shown to adhere to the grain surface in a similar manner to other solid, high melting point additives [176, 180].

The level of adhesion is probably related to the filler particle size/surface area and the surface treatment of the filler [42, 51, 177].

The micrographs also illustrate that the introduction of filler, particularly at levels greater than 8·5 phr, produces polymer grains which appear more rounded, i.e. attrition of the non-rounded fragments associated with the original PVC grains and the preferential filling of the folds with filler. A slight decrease in the average grain diameter can be observed if micrographs 3.3 and 3.5 are compared. Similar observations have been made by an interim report from TNO [176] and a more recent report from Hancock [42], where the dry blending of filled grades produced more spherical shaped grains and a slightly lower average particle size.

Bulk density values generally increase with increasing blend temperature [137, 139, 168, 176-177, 180] and obtain maximum values after relatively short periods of blending [136, 177], although the rate of heat generation and increase in bulk density depends to a large extent on the type and operation of the high speed mixer. In this study, the discharge temperature remained constant and increases in bulk density measurements were dependent upon increases in filler content (figure 3.1). Higher tap densities might be expected due to the incorporation of a higher specific gravity material and particles which can pack more efficiently i.e. they are more spherical, however the highly filled grades (blends 4 & 5) yielded disproportionate increases. At these high loadings the filler particles which are unattached or loosely associated with the grain surfaces can fill the interstices between the polymer grains to yield exceptionally high tap density values as seen in the bar graph of figure 3.1.

The implications of the dry blending results suggest that in order to produce filled dry blends which are representative of the original formulation and have good powder characteristics, then the filler should ideally

adhere to the large polymer grains. The problem of filler segregation for highly filled blends may be less significant in a commercial dry blending process since the mixer is not cleaned out after each batch and thus a steady state situation might occur where filler loss is minimalised. Ash content provides an accurate means to determine the filler level whereas bulk density can provide a quick check upon composition, i.e. tap density is commonly used for quality control measurements on site.

6.2.2 PROCESSING OF FILLED EXTRUDATES

6.2.2.1 EXTRUSION CHARACTERISTICS

The instrumented twin screw extruder, Krauss Maffei KMDL-25, enabled the important extrusion characteristics to be monitored, i.e. powder flow properties, mass throughput, mechanical processing energy, extrusion pressures and 'melt' temperatures. The complexity of twin screw extruders presents many problems when attempting to relate results from one machine to another, or even attempt to predict the likely extrusion characteristics from a laboratory machine to a full scale production model. The KMDL-25 is a scaled down production model for use in the laboratory and has proven useful in predicting extrusion behaviour on larger machines, on which trials would be economically prohibitive, and for the evaluation of formulation and processing aspects [131, 142, 154, 179].

Hopper flow properties

The introduction of substantial amounts of filler can lead to various material handling problems, i.e. surging of extruder [177], poor powder flow properties [168, 177], filler segregation [42] and high bulk densities leading to high extruder torque values [177]. These problems were originally observed during preliminary extruder trials with

filled blends containing more than 18·1 phr filler; these blends (3, 4 & 5) exhibited poor dry-flow properties ultimately resulting in bridging of the extruder. During the experimental runs these problems were controlled or minimalised by the fitting of a multi-pronged agitator to the hopper which gently agitates the dryblend to aid flow characteristics to a horizontal screw dosing unit (§2.6.1). The dosing unit accurately metered the dry blend to prevent surging and excessive torque values.

Mass throughput

It is generally reported for twin screw extruders that an increase in output is obtained by increasing screw speed [131, 141, 142, 179] and higher bulk densities [136-138, 138, 154, 177]. However since the screw speed was kept constant and the machine starve fed, then the output rate was controlled by the rate at which the material was introduced [142, 179, 181, 183]. The machine was starve fed as opposed to flood fed since high filler loadings (high bulk densities) and low extruder temperature profiles induced overloading of the extruder (§2.6.1). Therefore the output was dependant upon the rate of the dosing feed unit, which was kept constant, and thus seen to be independent of bulk density. The values obtained for mass throughput (Appendix D: table D.2) were also independent of the wide array of processing conditions indicating the positive conveying behaviour of the extruder and the design of the screw zones [131, 141-142, 179].

'Melt' temperature

Processing temperature was measured by two methods; a thermocouple situated in the die head and secondly the indirect method of thermal analysis (§1.4.2.5). A linear relationship was observed between the two methods (figure 4.1) as also shown in a number of reports [114, 131, 179, 182],

however, the inability to accurately calibrate the thermocouple resulted in the measurements being offset when compared to the thermal analysis measurements, i.e. thermocouple reading high or low depending upon day's calibration. Therefore it was suggested in §4.1.1 that the estimated processing temperature obtained via thermal analysis produced a better measure of melt temperature and thus further mention of extrusion melt temperature refers to this method of determination.

It was shown that 'B' onset temperature increased with increasing set head temperature (figure 4.1), in fact a 10°C rise in set head temperature resulted in an approximate 10°C increase in 'B' onset temperature. Profiles which involved an increase in barrel temperatures and not further increases in die head temperatures did not increase 'B' onset temperature (A & B and C & D), thus suggesting that 'B' onset indicates the effective processing temperature which is dominated by the die head conditions [131].

The influence of filler addition upon processing temperature was almost negligible (figure 4.2). A slight increase in value at intermediate extruder temperature profiles (C & D) with little effect at higher or lower temperature profiles (E & F and A & B respectively). §4.1.1 suggested that the unfilled blend was extruded at lower extruder set temperatures and figure 4.4 illustrated the difference between the 'B' onset temperatures for this series and the rest of the blends. The good control over the processing temperature even when significant amounts of filler are added can be attributed to low mass throughput, low screw speed, low shear rates for this type of conical extruder [131, 181] and accurate proportional temperature controllers (Appendix D: table D.1).

Extrusion pressures

The twin screw extruder was fitted with pressure transducers which measured the extrusion pressure at three positions within the extruder; beginning of discharge zone

(P1), adaptor zone (P2) and die head (P3). These transducers could not be calibrated *in situ* and thus gave comparative results.

Extrusion pressures at P1 were only measured in such cases where high adaptor and head pressures were also present (Appendix D: table D.3). A measurable response was obtained by high die resistances induced by low extrusion temperature profiles (A & B) and the value increased with increasing filler content. A value is also obtained for 5C indicating the effect of high filler content upon die resistance. The high die resistance (high back pressure) for these conditions increased the length of the 'gel column' (numbers of chambers full of solid or melted material) to the position of the transducer and thus a measurable response was obtained [131, 142]. Although under certain conditions a pressure value was measured by P1 it was not possible to predict the position of melting within the extruder. Covas [131] conducted an extensive processing study on the same machine and concluded that the position of melting (within one 'C' shaped chamber) remained constant at the beginning of the discharge zone under a wide variety of conditions. However his study used flood feeding and a pressure response was always registered at P1 indicating a full chamber of compacted unmelted material. In this study, due to the starve feed conditions, a full chamber was not always obtained at P1 and thus it is questionable whether the melting mechanism would have occurred in the same position for all the blends under the wide processing and composition range chosen. Therefore the P1 transducer provides information upon the 'Gel column' and the value is dependant upon the extruder temperature profile (increases with decreasing barrel temperatures) and increases with increasing melt viscosity (increasing filler content). Low extrusion pressures are generally reported in the feed section of the screw and it is usually suggested that pressure build-up becomes measurable in the last third of the screw [131, 141, 143].

Adaptor/inlet pressure response for the filled blends is illustrated in figure 6.1 (from §3.2.2). The values increase linearly with increasing filler content and depend upon the extruder temperature profile. Stephenson [142] evaluated the KMDL-25 as a processing tool and suggested that adaptor pressure was dependant upon output rate, geometry of flow in the head and die, output temperature and rheological properties of the material. He concluded that at constant output and constant adaptor temperature, the adaptor pressure would indicate 'genuine' melt viscosity differences. In this study, throughput rate remained constant, the flow geometry in the pipe die was constant and it is also suggested that the temperature control in the barrel zones was good (§3.2). Therefore the adaptor transducer seems to indicate the rheological properties of the material at that point [131, 142]. An increase in filler content provides a roughly linear increase in P2 which suggests that the loading of an inert low aspect ratio filler, such as Polcarb S, has a linear effect upon melt viscosity [184, 185]. The effect of extruder temperature profile is more difficult to establish since the transducer does not provide a material temperature at that point and sampling for thermal analysis is not possible without stripping the pipe head and adaptor assembly; thus inlet/adaptor pressure could not be plotted against temperature.

The last transducer was positioned in the pipe die and resultant head pressure was shown to be dependant upon filler content and extruder temperature profile (§3.2.2). Head pressure increased with filler content and decreased with increasing set head temperature as might be expected. In section 4.1.2 multiple regression analysis was applied to predict head pressure response due to the components of processing temperature (measured by thermal analysis) and filler content. A mathematical relationship was obtained which clearly shows that the two components control the pressure response and figure 6.2 illustrates the acceptable

FIGURE 6.1

Inlet pressure versus Filler content

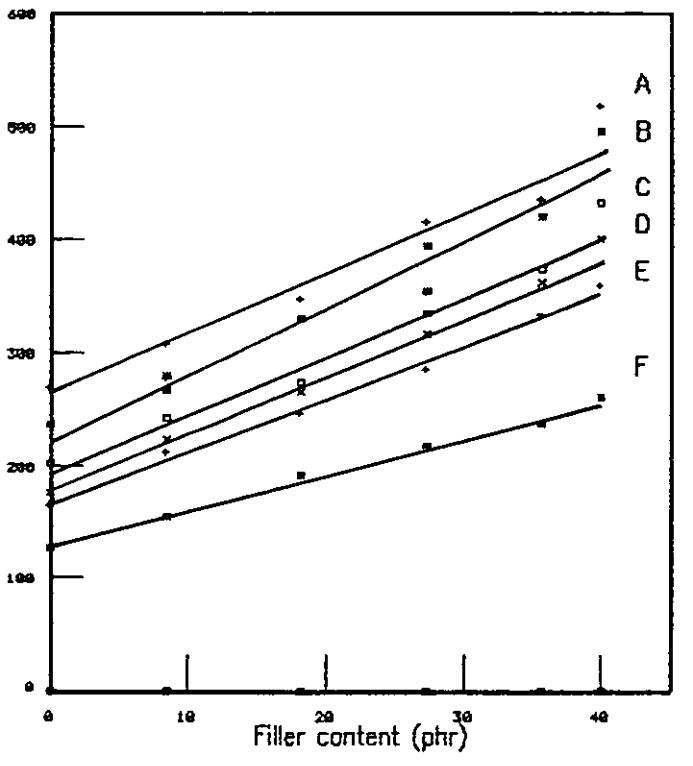

FIGURE 6.2

Analysis of Head pressure

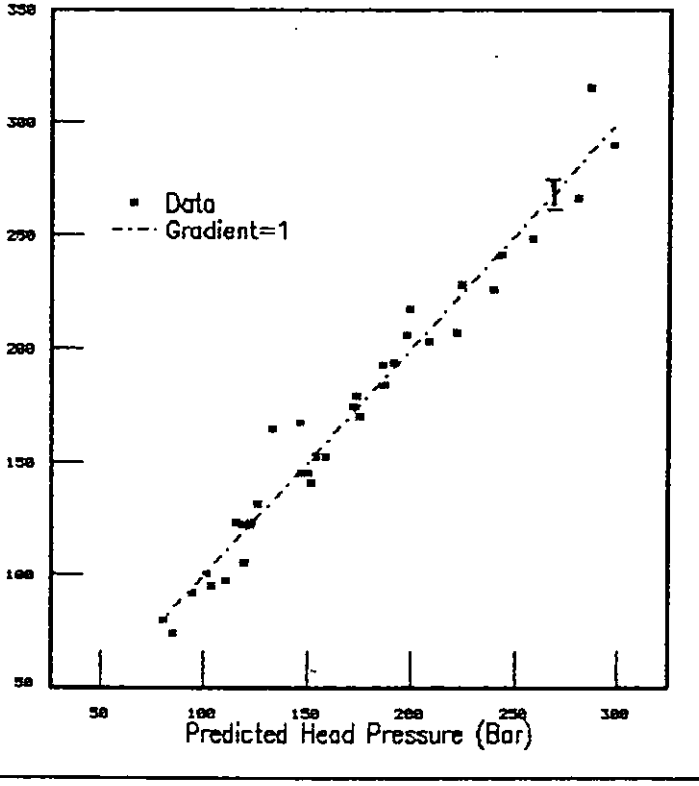

straight line relationship obtained from the regression analysis (equations 4.2 and 4.3). Thus for the base composition containing 0⇒40 phr of Polcarb S processed over a wide range of processing conditions, the transducer response in the head could be well defined.

Torque

The final extrusion characteristic monitored by the twin screw extruder is motor torque (TQ); this value can be related to output by the expression given in equation 3.1 to give specific energy consumption (Q). Q is perhaps a better method of evaluating the mechanical work involved in extrusion since Q is a measure of mechanical energy per unit mass. In this case, where the mass throughput is almost constant, the figures 3.9 and 3.10 which depict torque and Q data respectively are very similar. Thus it is intended to refer to Q data for further discussion and these values are replotted in figure 6.3 for ease of reference.

Specific energy consumption (Q) is dominated by the metering zone, in a similar manner to pressure build-up, since resistance to flow is generated late relative to the screw length. Also the value of Q is dependant on a large number of parameters; set temperatures [142], rheological properties of material [131,142], length of 'Gel column' [131] and extent of backpressure assuming that output remains constant. Thus the value of Q provides information upon the melting behaviour of the material within the melting zone. Rauwendaal [181] evaluated two twin screw extruders and concluded that Q was an important process parameter for the analysis of such extruders. He considered Q to be a 'measure of the total deformation that the material is exposed to during the extrusion process and the stress that is required to bring about this deformation'.

i.e.

$$Q \propto \bar{\tau} \cdot \bar{\dot{\gamma}} \qquad (6.1)$$

Where $\bar{\tau}$ = Average shear stress

$\bar{\gamma}$ = Average shear strain

Also average shear strain can be considered as the product of average shear strain rate and residence time.

These components are virtually impossible to compute [131] but have a significant effect upon mixing properties; shear stress is reported to be an important parameter in dispersive mixing [186] and shear strain is an important parameter in distributive mixing [187]. Rauwendaal [181] also demonstrated that under certain conditions a large increase in specific energy consumption involved a significant increase in minimum residence time.

The extrusion data does not include melt temperature within the discharge zone and thus Q can not be related to melt zone temperature. However the effect of processing temperature ('B' onset temperature) is shown in figure 4.4. As might be expected Q falls with increasing extrusion temperature and the influence of filler is to produce a series of curves depending upon the level of filler content (§4.1.2) i.e. a family of curves with the highest filler content producing the largest torque.

Figure 6.3 presents the influence of filler content upon Q; as suggested in §3.2.1, Q increases with increasing filler content and the temperature profiles clearly differentiate between the curves with the higher profiles requiring substantially less mechanical energy input. The figure highlights a number of anomalies, namely profiles A & B yield exceptionally high values and secondly a tendency for the curves to level off when highly filled blends are extruded at high profile temperatures. The large value of Q associated with profiles A & B might be related to a significant increase in residence time, i.e. long residence time invokes a large value for specific energy consumption [181]. The pressure data for P1 complements this suggestion since a substantial increase in 'Gel column' (increase in residence time) was noted whereby a response at P1 was

obtained. The levelling off tendency appeared to be commensurate with poor dispersion. Poor dispersion was obtained for extrudates containing 35·6 and 40 phr of filler at extruder profile temperatures D, E and F (§4.3.1). Figures 4.17 and 4.18 illustrate the dispersion of Polcarb S for the extrudates 5C and 5F respectively (40 phr); the microphotographs indicate a degree of mixing for 5C while 5F has poor filler dispersion resulting in filler dropout upon microtoming. An explanation for the levelling off of the Q curve (figure 6.3) and the increased likelihood of poor dispersion might be that the high extrusion temperatures of profiles D, E and F reduce the component of shear stress (equation 6.1) substantially resulting in lower than expected Q values and reduced dispersive mixing efficiency.

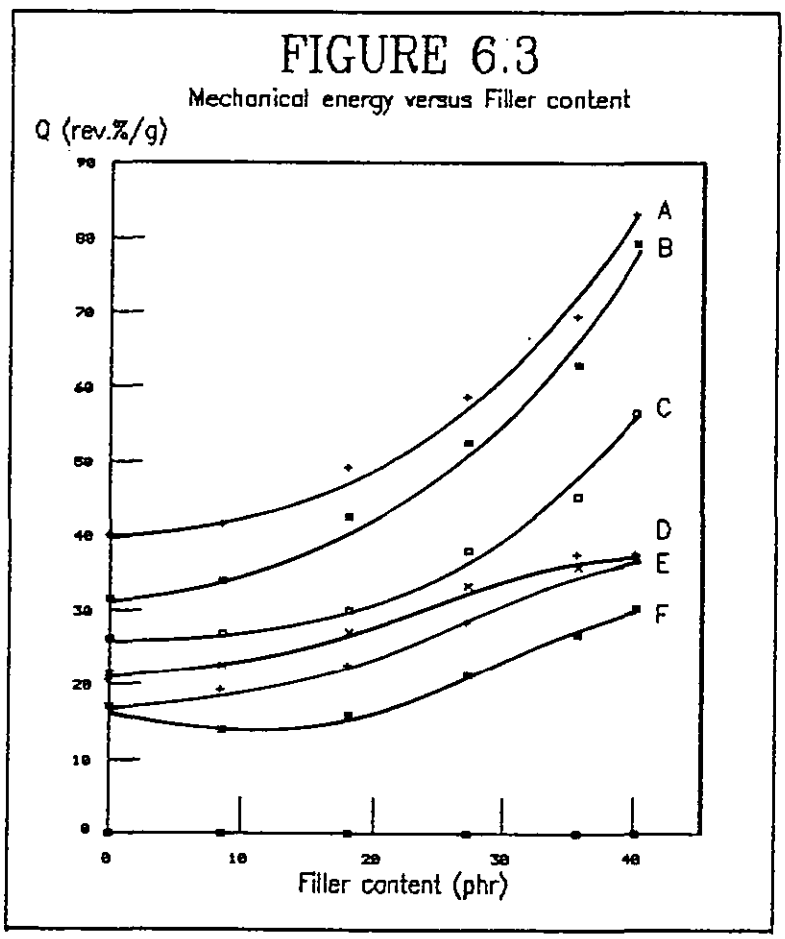

6.2.2.2 EXTRUDATE HOMOGENEITY

Optical microscopy of the filled extrudates revealed two main features; unfilled and lightly filled extrudates contained residual grains, and secondly moderate to highly filled grades differed in terms of filler dispersion.

Grain content

Residual grains were detected in extrudates containing 0 and 8·5 phr of filler (§4.3.1); the presence and consequences of residual grain content has been noted in the literature [112, 116, 137, 142, 170, 188–189]. Residual grains were present in extrudates processed at low processing temperatures as spherical entities, approximately the same diameter as the original polymer grains, within a flow band (figure 4.11). However when the processing temperature was increased the grain content was reduced and the grains became highly elongated (figure 4.12). The existence and shape of the grains were therefore dependant upon the processing temperature. Terselius *et al* [116] observed a similar behaviour and extended this approach by quantifying the grain content of a pipe cross-section via a series of micrographs. They obtained a value of approximately 30% for a poorly processed pipe at a low processing temperature (176°C), while the grain content decreased to virtually negligible amounts when the processing temperature was increased to 205°C. The microphotograph shown in figure 4.11 reveals a relatively high level of residual grain content attributed to the low processing temperature (172·7°C) but the total content does not approach a value of 30% mentioned above i.e. the machine type and/or composition plays an important role in the level of mixing. Stephenson [142] suggested that the level of mixing was dependant upon leakage flows and position of gelling within the extruder i.e. backpressure determined by the processing conditions and composition.

Backpressure accounts for the lower residual content of OA and 1A pipes when compared to OB and 1B extrudates (§4.3.1). Little difference in processing temperature was measured between the respective profiles (A and B), however the higher pressures developed by the extrudates processed via profile A (§3.2.2) yielded pipes with an appreciably lower residual grain content than extrudates processed at profile B. The presence and shape of residual grains supports the 'compaction, densification, fusion and elongation' (CDFE) mechanism proposed by Allsopp [112] for this type of machine (§1.4.1). Similarly Covas [131] and Obande [179] conducting more fundamental studies upon this particular extruder also suggested the 'CDFE' mechanism.

Filler dispersion

Extrudates containing ⩾18·1 phr did not contain significant amounts of residual grains and those present are highly elongated (figure 4.14), which suggests that the compositions invoke sufficient extruder backpressures to ensure almost complete breakdown of the grains. However these blends did show different levels of filler dispersion in the finished extrudate depending upon the processing conditions (§4.3.1). The lightly filled grade of 8·5 phr presented no problems of dispersion but the slightly higher level of 18·1 phr contained agglomerates of filler at the higher processing temperatures (figure 4.15). These agglomerates were approximately 10-20 μm in diameter and were quite well distributed. Higher filler loadings were characterised by a degree of dispersion at low processing temperatures (<180°C), a deterioration at intermediate temperatures (upto ≈190°C) and then very poor dispersion at high processing temperatures (>195°C). The exceptionally poor dispersion obtained with the highly filled blends at high processing temperatures produced agglomerates of approximately 30-40 μm in diameter which lead to filler dropout upon microtome sectioning (figure 4.18). Thus filler

dispersion is dependent upon processing conditions and, in general, an increase in processing temperature leads to a deterioration in the quality of dispersion. The effect of high processing temperatures upon highly filled blends was noted in the discussion upon torque characteristics as discussed in §6.2.2.1. Thus filler dispersion is dependent upon the amount of mechanical energy input and the filler level.

Surface appearance

The aesthetic appearance of the pipe's outer surface was assessed by visual examination (§3.3.1) and also via scanning electron microscopy (§4.3.3). Both arbitrary assessments reveal similar results as shown in table 4.3; any differences between the two examinations are highlighted in **bold** text. The SEM micrographs produced a more detailed viewing area than visual examination, however only a few differences were noted which were no more than one group apart (cf. table 3.4 with table 4.3).

The results possibly confirm what might be expected, that is, high processing temperatures and low filler contents produce the best surface finish while high filler contents and low processing temperatures produce a poor quality surface, the quality of the surface being a function of the ability for the material in the die head/tip to flow and reproduce the dimensions of the pipe die [148]. Table 4.3 (§4.3.3) separates the extrudates into three main groupings according to the filler loading, i.e. 0 & 1, 2 & 3 and 4 & 5. The highly filled blends (4 & 5) produced very poor surface finish even at quite high processing temperatures (upto ≃195°C). The highest extruder temperatures (≃204°C) improved the finish of the pipes but surface quality was only equivalent to the worst of the other two groups (≡Group III: table 4.3). The next filler group (2 & 3) at the lowest processing temperature had a surface finish equivalent to the more highly filled blends

at their maximum processing temperatures, while the moderately filled blends at higher extrusion temperatures produced pipe of acceptable appearance (2E, 2F and 3F). Lastly the unfilled and lightly filled blend (0 & 1) yielded an acceptable finish at lower processing temperatures (i.e. 0D, 0E, 1D and 1F) and at the highest extrusion temperatures produced a separate classification group (Group VI) containing extrudates having a good aesthetic appearance (0F and 1F).

None of the micrographs exhibited signs of melt fracture nor evidence of filler agglomeration on the surface. An increase in filler loading does yield a greater amount of filler particles on the pipe surface (figures 4.30-4.32), however the filler particles are not present as agglomerates.

The inner surface finish of the pipes was also examined (§3.3.2) and, in this case, less discrimination between samples was observed. A better finish was obtained for those extrudates containing substantial amounts of filler and/or processed at low extrusion temperatures. Table 3.6 ranked the unfilled extrudates processed within a wide temperature range (≃173-197°C) and also the lightly filled extrudates processed at high processing temperatures (≃193-204°C) as having the worst inner surface. The quality of the inner surface is probably related to molecular relaxation which is reduced by the introduction of filler and/or extrusion processing at low temperatures thus maintaining the finish of the inner core pin of the die.

6.2.2.3 ASSESSMENT OF THE DEGREE OF FUSION

Fusion has been studied, as discussed in §1.4.2, by a number of workers who have applied a range of techniques in an attempt to quantify the level of fusion in processed articles. Common techniques include capillary rheometry, solvent testing and more recently thermal analysis. The application of capillary rheometry (§1.4.2.4) relies on the

measurement of elastic pressure losses in a short capillary [103, 108, 123-126, 181]. However the resultant 'standard gelation curve' has been shown to be sensitive to changes in formulation/processing technique [113, 124-125, 179] and the introduction of fillers is reported to have a diluting effect upon the elastic response [124]. Figure 6.4 illustrates the entrance pressure results for a series of extrudates which contain increasing amounts of calcium carbonate filler [190]; the entrance pressure is initially higher for the more highly filled compositions due to the higher resistance to flow. However the increase in entrance pressure with increasing processing temperature indicates a distinct levelling off with higher filler contents. Thus increasing filler content appears to mask the elastic pressure response and therefore reduces the discriminating power of the technique.

FIGURE 6.4

Entrance pressure versus 'B' Onset

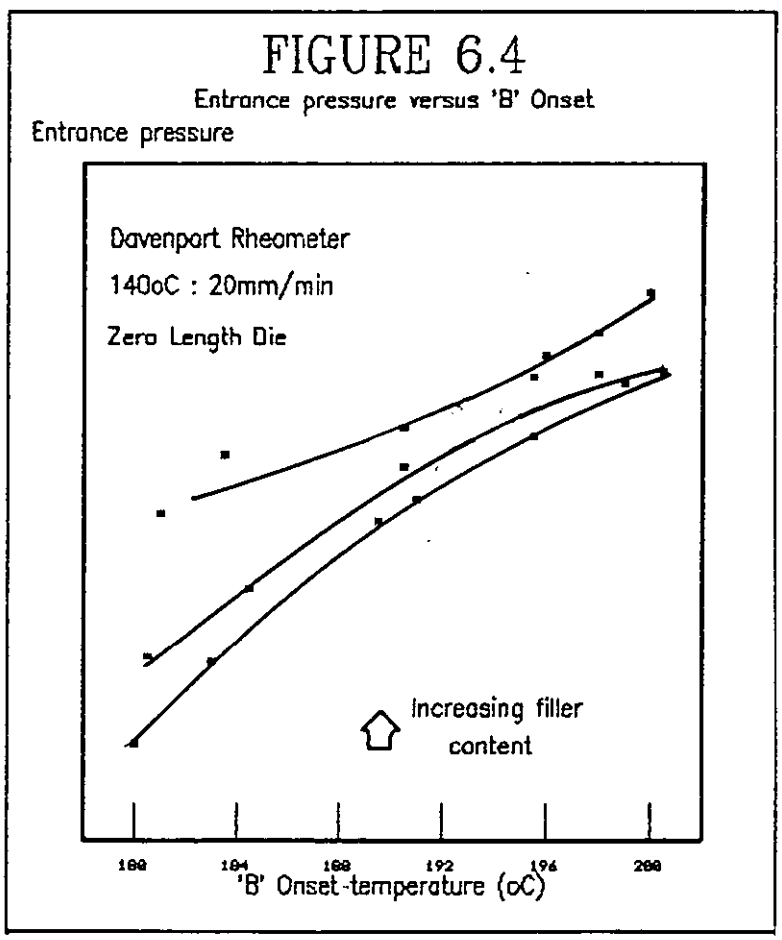

The techniques applied in this study to indicate the extent of fusion included the methylene chloride test (§3.4), acetone swelling test (§4.3.2) and differential thermal analysis (§4.1).

Methylene chloride test

The methylene chloride test provided a quality control type test indicating a pass or fail result. All the extrudates after immersion in methylene chloride passed with the exception of those pipes processed at the lowest extrusion temperatures, profiles A & B, (i.e. ≈<180°C) where excessive swelling, splitting and surface delamination was observed.

Thermal analysis

The application of thermal analysis as a potential technique for the measure of fusion has been discussed in §1.4.2.5 and a typical thermogram for a moderately processed pipe is redrawn in figure 6.5 (figure 2.3: §2.9.2). The features are similar in appearance and location to other thermal analysis studies [115, 128, 131, 179];

a) An endothermic baseline shift corresponding to the glass transition temperature (T_G) of the material.

b) A small endothermic peak at approximately 100°C due to a reduction in free volume during storage [128, 129].

c) The onset of the 'B' endotherm provides a good indicator of the maximum processing temperature (§6.2.2.1).

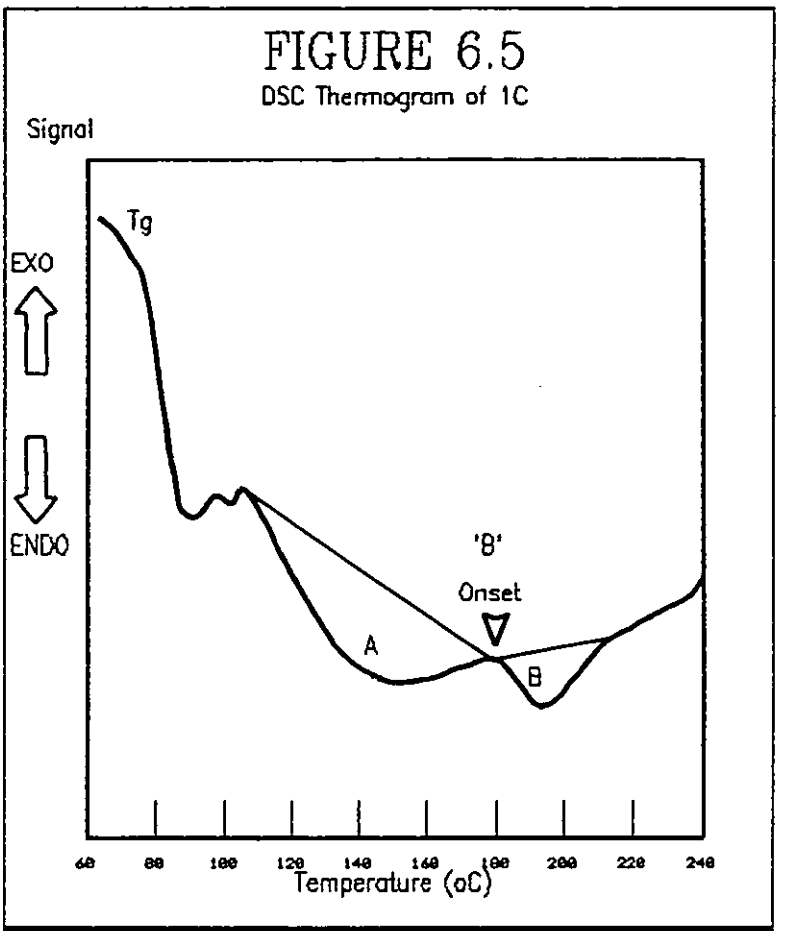

FIGURE 6.5
DSC Thermogram of 1C

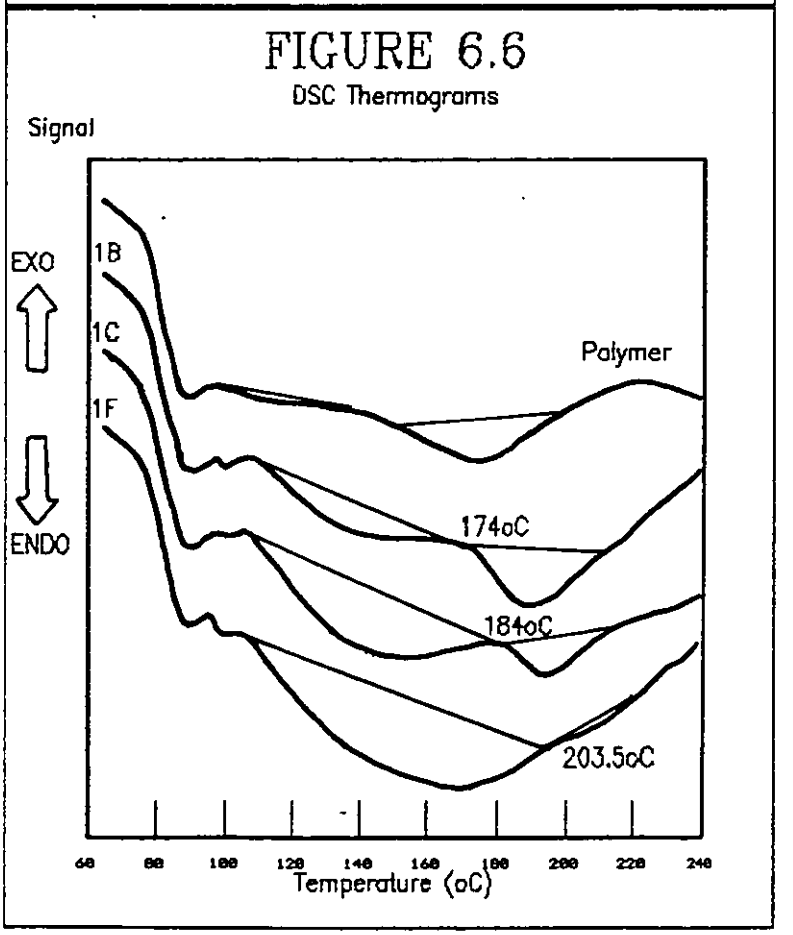

FIGURE 6.6
DSC Thermograms

d) A 'B' endotherm representing the melting of crystallites of various sizes and degrees of perfection [128]. A broad endotherm is shown in figure 6.6 for the virgin polymer and this endotherm progressively decreases in size and shifts to a higher temperature due to the melting of low temperature crystallites and annealing of high temperature crystallites.

e) A broad endotherm 'A' peak develops at low processing temperatures attributed to the recrystallisation of the primary crystallites to provide secondary crystallites of a lower order.

Figure 6.6 illustrates the influence of processing temperature upon these features for a few members of the lightly filled extrudate series (8·5 phr). A negligible ΔH_A value is noticed for the virgin polymer (0·28 J/g) which also exhibits a broad 'B' endotherm. A value for ΔH_A is measured even at low processing temperatures, i.e. ≈170°C (§4.1: Table 4.1), and increases progressively with increasing processing temperature. The 'B' peak is distinctive at low processing temperatures but at higher temperatures the peak becomes more difficult to detect and almost disappears (1F: figure 4.6). Although the value of ΔH_B becomes increasing more difficult to measure, the thermograms in this study allowed identification and measurement of this peak where appropriate. Terselius *et al* [116] concluded in a thermal analysis study that the 'B' peak was difficult to determine and refrained from quoting ΔH_B values because of excessive scatter. The thermal analysis data for the large number of extrudates considered and the major peaks identified generally agree with previous results [113, 115, 116, 128, 131, 179]. However a recent study by Potente *et al* [182] provided a different interpretation of the major peaks; it was concluded that the development of the endothermic peaks depended upon the particulate nature

of the material and whether the material had been processed above a 'critical gelation temperature'. The two peaks, 'A' and 'B', were referred to as gelation and post-gelation peaks and were related to the destruction of the grain structure, if the the PVC blend was not compounded then neither 'A' or 'B' was observed. In the case of compounded PVC below the 'critical gelation temperature' then a single peak, 'B', was observed; while processing above this temperature split this peak into two, 'A' & 'B'. The area of 'B' endotherm was measured by drawing a baseline from the 'B' onset temperature to the onset of an endothermic peak associated with decomposition (ca. 245°C). This interpretation yields a large energy value for 'B' of similar proportions to a well developed 'A' peak until at high processing temperatures (ca. 220°C), the peak disappears. No explanation is offered to the existence or development of these peaks in terms of molecular or crystallinity structure. In this project, a number of important differences from the above publication are noted; the existence of a 'B' endotherm is clearly shown in figure 6.6 for the virgin polymer, albeit broad and ill defined, and thus it is not related to the destruction of the grain structure. Secondly the measurement of 'B' for the processed specimens differs since the baseline is drawn from the 'B' onset temperature to a second inflection in the trace at ca. 205-220°C. This peak is related to the melting of primary crystallites and complete melting is envisaged at these high temperatures.

The introduction of filler did not affect the main characteristics of the thermograms and T_G seemed unaffected by the filler level [53] which suggests little molecular interaction [191]. However the introduction of filler obviously reduced the size of the endotherms proportional to the level of filler; if this effect is taken into account by appropriate normalising (§4.1), then the size of 'A' and 'B' are not dependant upon filler content.

Master fusion curves are shown in figures 4.6 and 4.7 and these can be described mathematically as in §4.1.3. These normalised fusion curves which describe all the extrudates, both filled and unfilled, are redrawn in figures 6.7 and 6.8. It can be seen from these graphs that the introduction of an inert mineral filler did not appear to affect the level of fusion. Any slight increases in fusion level with increasing filler content (table 4.1) were also associated with increases in processing temperature and thus these data points continued to fit the polynomial curve. A maximum value of approximately 10.53 J/g was estimated for ΔH_A from the best fit curve at an approximate processing temperature of 207°C; this value agrees well with a maximum range of 10-12 J/g suggested by Gilbert *et al* [114]. Thus a broad range of fusion levels were obtained from very low levels of fusion, i.e. OA @ 0·43 J/g (1·4%), to high ΔH_A values. The fusion curves comprised of discrete groups of data points according to the extruder profile/head temperature (§6.2.2.1) and although the curves are beginning to level off, a further increase in ΔH_A may be obtained at higher processing temperatures.

Therefore the application of thermal analysis provided a convenient and apparently accurate method to determine the fusion level of the pipe specimens, even when the composition was significantly altered by the incorporation of large amounts of an inert filler.

Acetone shearing test

The acetone shearing test (§1.4.2.2) does not yield quantitative information but provides a qualitative assessment of the level of cohesion within the polymer network. The test divided the extrudates into groups (§4.3.2) according to the original extruder profile temperatures and appeared to be independent of filler content in a similar manner to thermal analysis. A similarity was observed between the groups obtained by this

FIGURE 6.7

Master Fusion Curve:- Energy

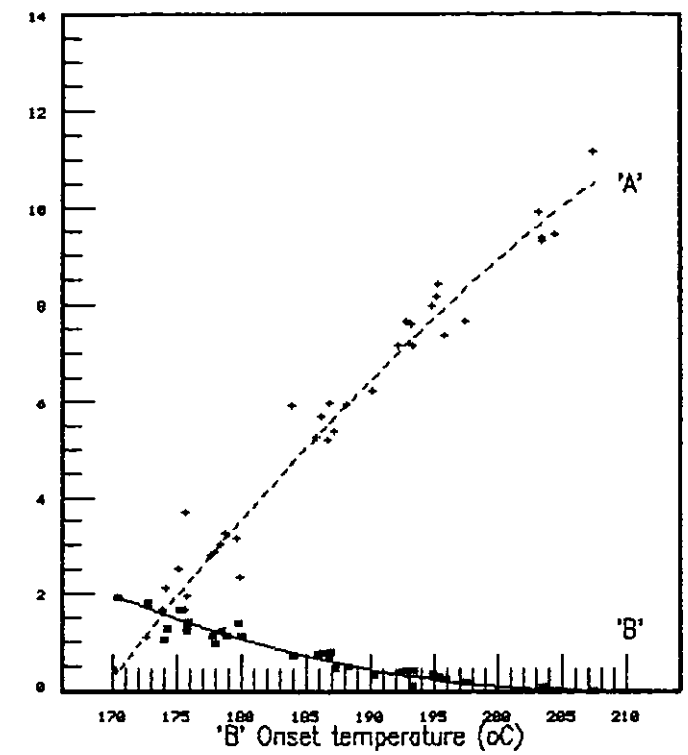

FIGURE 6.8

Master Fusion Curve:- % Fusion

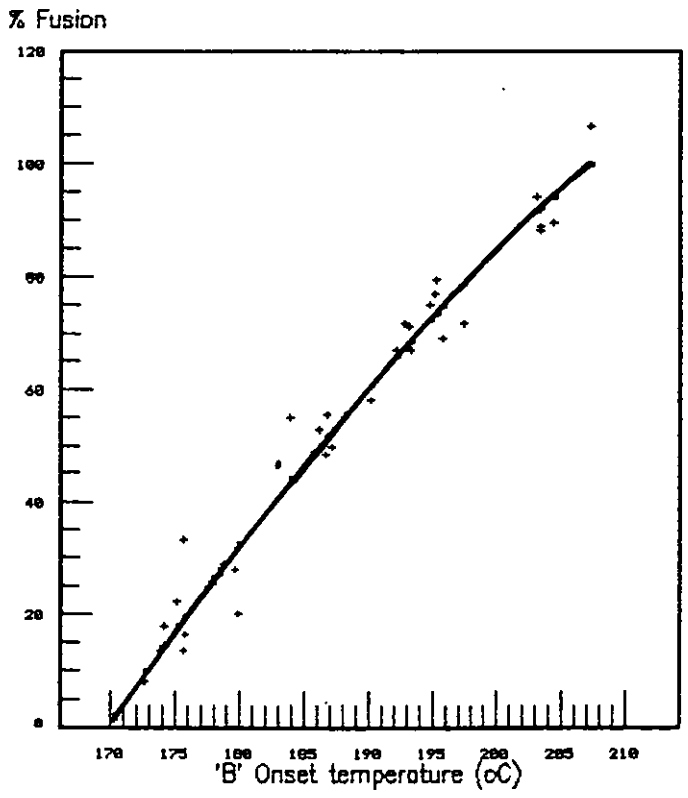

assessment and those revealed by thermal analysis (figure 6.8). Extrudates processed at profiles A and B yielded fusion levels less than ≈30% (via thermal analysis) and the optical microscopy of the acetone swelled specimens indicated very poor cohesion of the network resulting in easy fragmentation to primary particles or particle agglomerates (figure 4.21). Pipes processed at moderate extruder temperatures indicated a fusion level of approximately 30-65% and resisted breakdown during the acetone shearing test (figure 4.22). Lastly the group comprising of the extrudates processed at profiles E and F, i.e. >65% fusion, produced a strong cohesive network which resisted breakdown and under sufficient shear resulted in fibrillar ligaments between large agglomerates (figure 4.23). The subjective test did not distinguish between the higher extrusion temperatures (E and F), even though there is an approximate 10°C difference in 'melt' temperature (table 4.1). However the test does provide easy examination of poorly fused specimens and complements thermal analysis and the methylene chloride test in establishing the extent of fusion of processed products.

At low processing temperatures (<190°C), primary particles are clearly evident, via the acetone test, which confirms the relationship between primary particle loss and the development of the 'A' peak [116, 131]; similarly at these low fusion levels (<35%) the poor cohesive strength of the network offers little resistance to the methylene chloride test. At higher processing temperatures the loss of primary particles is evident [67, 77, 92] and the development of secondary crystallites well defined. At the highest processing temperatures no primary crystallisation (ΔH_B) is detected together with fewer primary particles (figure 4.23) and also the ΔH_A/% fusion curve begins to level off.

6.2.3.1 TENSILE PROPERTIES

The tensile properties of the unfilled and filled extrudates with varying degrees of fusion are described in §5.1; the results can be discussed with reference to yield and post-yield deformation.

Yield parameters

Yield properties are listed in table 5.1 and it can be seen from this table that elongation at yield (ε_Y) appears independent of extrusion profile and filler content. However yield stress (σ_Y) is dependent upon filler content; figure 6.9 illustrates yield stress versus fusion level (similar to figure 5.3). At low filler contents (upto 18·1 phr), σ_Y remains independent of fusion level although the load bearing characteristics at yield are clearly dependent on the level of filler. At higher loadings, σ_Y decreases with increasing fusion level; the reduction is concurrent with poor dispersion obtained at higher filler loadings and higher processing temperatures (§4.3.1). Poor dispersion resulted in large filler agglomerates (§4.3.1) which is analogous to a larger particle size filler; increasing filler particle size has been shown to have a detrimental effect upon properties [52, 193].

Thus yield parameters appear relatively insensitive to changes in fusion level as suggested by a number of workers [75, 131, 151, 153]. The negligible response to the level of secondary crystallites and number of entanglements suggest that yield properties are dependant on 'flow units' smaller than the spacing of entanglement couplings [131, 151].

The influence of filler content on yield stress is illustrated in figure 6.10; a dilution effect is observed with increasing volume fraction (similar to figure 5.1) resulting in a decrease in yield stress [52,53]. The reduction is almost linear although deviations are observed

due to poor dispersion in extrudates containing substantial amounts of filler. Nielsen [192] presented a simple theory for the stress-strain properties of filled polymers; the theory accounted for the consequences of perfect adhesion of the filler to the polymer matrix and alternatively the situation where all the load must be carried by the polymer. In the no adhesion case the predicted relative tensile stress can be estimated by the following relationship:

$$\sigma_{REL} \simeq (1-\phi_F^{2/3})S \qquad (6.2)$$

Where σ_{REL} = Relative tensile stress
ϕ_F = Volume fraction of filler
S = Stress concentration function (=1)

Figure 6.10 illustrates the no adhesion model and that the relative tensile stress at yield values generally follow a similar relationship [52]. The simple model does not accurately predict the actual observations since the value for the stress concentration function is unlikely to be one and may differ according to the level of dispersion.

Post-yield parameters

The preceding section suggested that yield parameters were insensitive to the level of fusion while yield stress was strongly influenced by the level of filler. Post-yield values, however, were strongly dependant upon the ability of the test specimen to neck and then cold draw. High extensions produced higher breaking stresses (σ_B) while rupture during the necking mechanism resulted in low values. This relationship between elongation at break (ε_B) and σ_B can be seen if figures 5.4 and 5.5 are compared (§5.1). A high degree of scatter was observed for these post-yield parameters (table 5.1) due to the instability of the necking mechanism. The transition between the formation of a stable neck (cold drawing) and necking rupture has been examined in

FIGURE 6.9

Yield stress versus Fusion level

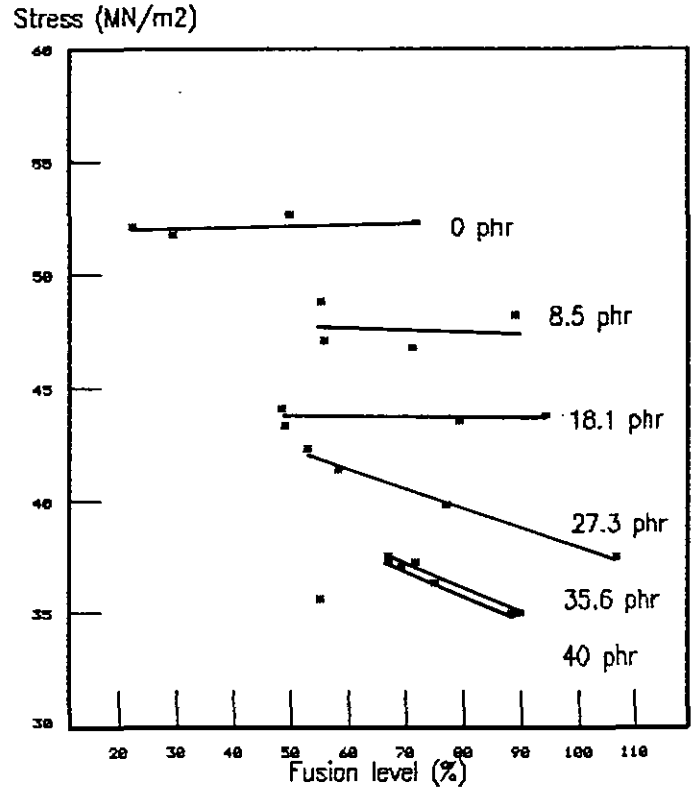

FIGURE 6.10

Yield stress versus Volume fraction

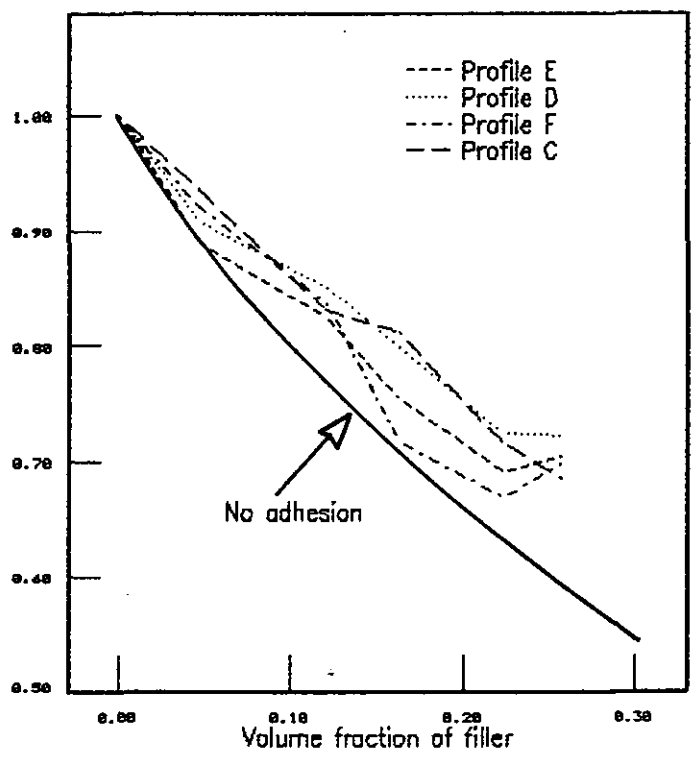

a number of previous reports [151, 194-197] and its occurrence related to tensile strain rate, geometrical aspects of the test specimen, test temperature and material characteristics. It would appear from table 5.1 that neck instability gave raise to poor reproducibility in the drawing region and thus high standard deviation values for ε_B & σ_B.

Figure 6.11 illustrates σ_B versus fusion level (DTA technique) and similar trends are observed when compared with figures 5.4 and 5.5. The influence of filler content divides the tensile response into two groups of data according to the level of filler. The highly filled extrudates exhibited low ε_B values and similarly low σ_B responses. The low values might be related to a dilution effect upon the load bearing characteristics of the polymer being replaced by an inert particulate filler and/or a consequence of poor dispersion (§4.3.1). Chauffoureaux [53] also reported the reduction of σ_B with increasing filler content and in one case of poor dispersion the value for σ_B was severely reduced. The second set of data incorporating low levels of filler reveal similar values and the relationship between σ_B and filler levels is not as straightforward as in the case for yield behaviour.

The influence of fusion level is more difficult to ascertain; figure 6.11 suggests that σ_B decreases with increasing fusion level with a possible broad maximum at low fusion levels (cf. figure 5.5). A maximum has indeed been observed by various workers [67, 108, 131] as discussed in §1.5.3. However since neck instability was a prevalent feature then it is perhaps inappropriate to consider the true influence of fusion level. Terselius *et al* [151] and Covas [131] conducted tensile tests above T_G and demonstrated that the extent of cold drawing (ε_B) provides a good indication of the influence of fusion level.

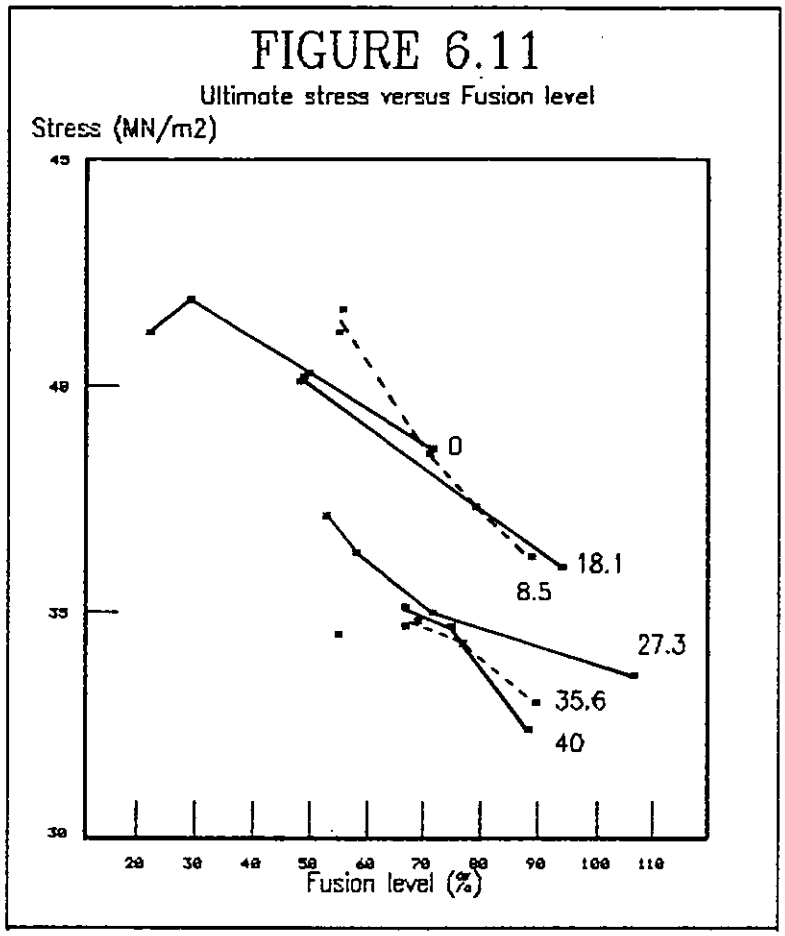

6.2.3.2 IMPACT PROPERTIES

The impact performance of UPVC extrudates and its interrelation with fusion level has been examined in numerous reports (§1.5.3). However meaningful comparisons are complicated since impact testing is critically dependent on the method of testing, i.e. type of test, notched or unnotched, test temperature, specimen preparation, specimen holder, specimen thickness, filtering etc. In this project, an instrumented falling weight impact tester was used (§2.10.2); the design of the test procedure was discussed in §2.10.2 and §5.3.

Three types of failure were observed (§5.3) and were arbitrarily defined as brittle, brittle/ductile and ductile according to visual examination and the resultant fracture trace (figure 5.3). Brittle failure resulted in low force and energy values with fracture occurring over short fracture periods. Brittle/ductile and ductile failures produced similar peak characteristics such as force and deflection gradient (slope of force-deformation trace), but varied in yield behaviour to produce considerable differences in fracture energy values. Although the instrumented tester produced an accurate fracture trace which could be analysed to yield relevant information on the main features discussed in §2.10.2; failure energy was found to be the best method of distinguishing between the extrudates. The influence of filler and extent of fusion is summarised in figure 5.10 and is reproduced in figure 6.12 for ease of reference.

The influence of fusion level can be seen to have a dramatic effect upon performance and is also critically dependent upon filler content. The unfilled series exhibited a sharp transition from brittle failure (• symbol) of very poorly fused pipes to a brittle/ductile fracture (▲ symbol) of pipes with a fusion level of approximately 20-30%. Impact performance continued to improve, passing through a ductile mode of failure (● symbol), and a maximum was obtained at an approximate fusion level of 70-75% ('B' onset temperature ≈193-196°C). A further increase in fusion level indicated a significant drop in impact energy. A maximum and its approximate location is well supported by a number of publications [67, 108, 113, 115, 150, 179, 198], however the exact position and breadth of peak is not well defined.

Obande [179] observed a maximum in notched Izod testing using different compositions processed on two twin screw extruders; he concluded that the development of a maximum depended upon the existence of an inhomogeneous network, which, in turn was related to the shear regime during processing and the nature of the composition.

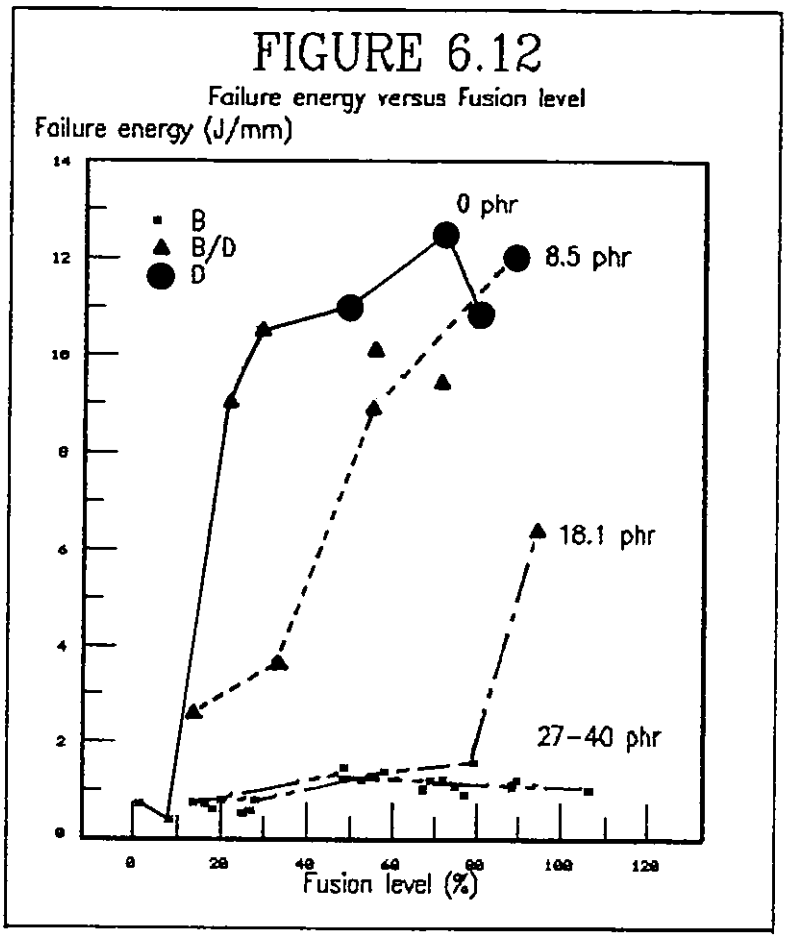

Terselius *et al* [150] refer to an 'interparticulate entanglement network' theory which, in the case of an optimised network produces a maximum performance in unnotched falling weight tests; on the other hand, they did not obtain a maximum for the Charpy testing of notched pipe specimens. Similarly Menges *et al* [67] proposed a mechanism whereby a particulate network system could enhance performance (figure 1.2).

Summers *et al* [149] also observed a maximum impact peak with falling weight impact tests; but on press polishing the reduction at high processing temperatures was eliminated to yield a monotonic increase in performance with increasing extrusion temperature. It was concluded that

surface stress concentrators due to melt fracture at high processing temperatures resulted in poor impact. In this work, no evidence of melt fracture was observed from the SEM micrographs (§4.3.3) and thus neither melt fracture nor surface roughness was considered responsible for the decrease observed for OG.

It is suggested that impact behaviour of the O series is attributed to the development of a coherent particulate network structure; low fusion levels retained a primary particle structure with little cohesive or entanglement strength (§4.3.2) resulting in poor resistance to failure, also, the proportionally high level of residual grains may have a detrimental effect. Increasing fusion levels increased the cohesive strength of the network and thus impact performance, while retaining some residual primary particles. The final processing regime (T_M ≈201°C) produced a strong coherent structure but with the possible absence of residual primary particles leading to reduced impact energies. The presence of a few primary particles in a strong network provides well distributed, discrete weak regions whereby energy dispersive mechanisms are invoked by localised yielding and voiding (cf. UPVC modified by discrete rubbery additives; figure 1.2). It is also interesting to note that the value for primary crystallinity (ΔH_B) measured by thermal analysis is virtually zero at this processing temperature (§4.1), and the progressive loss of residual grains with increasing processing temperature results in virtually no residual grains at this temperature (§4.3.1).

The introduction of filler had a dramatic effect upon failure energy (figure 6.12); filler contents greater than 27·3 phr (≥0.163 % volume fraction) exhibited poor impact resistance with the failure energy value reduced to approximately 10% of the maximum for the unfilled series. This level of reduction was also observed by Zolotor [52]; who concluded that samples containing 0·34 % volume fraction of filler, irrespective of filler particle size, had an

impact resistance of only 5-15% of an unfilled grade. The poor resistance can be attributed to the level and dispersion of filler; the number and size of stress concentration loci offers easy crack initiation and crack propagation. The influence of fusion has little effect upon the consequences of the test due to the extent of the critical flaws.

The moderately filled series containing 18·1 phr of Polcarb S was similar in behaviour to the highly filled members until a brittle/ductile failure was obtained for the highest fused member. The failure energy of this pipe (2F) is still considerably lower than for the brittle/ductile failures of the unfilled or lightly filled extrudates which might be expected due to the dilution effect of an inert filler. However it would appear that a stronger network developed at high extrusion temperatures overcomes the detrimental effect of stress concentrators. It was also observed that the level of dispersion at the highest processing temperature was considerably better than the more highly filled series (§4.3.1) which suggests that poor dispersion behaves in a similar manner to oversize particles (i.e. increases stress concentrators effect) [53].

The lightly filled series (8·5 phr) behaved in a similar manner to the unfilled pipes; a transition was observed from poor impact at low fusion levels to much improved failure energies at approximately 50% (20% higher than unfilled). Further increases in fusion level resulted in improved impact behaviour until the final member of the series failed in a ductile mode. The measured values were similar to the unfilled series and the complete curve appears to be shifted to higher fusion levels. The introduction of filler is more likely to incur brittle or brittle/ductile failures since the filler stiffens the matrix and thus reduces the critical flaw size [199]. Indeed the lightly filled grades had a greater tendency to fail in a brittle/ductile manner than the unfilled series and the failure value was slightly lower as might be expected from

the incorporation of an inert particulate additive ('dilution effect'). The 8·5 phr series did not show a tendency to peak at high extrusion temperatures which might be explained by the general shift of the curve to higher fusion levels (i.e. maximum not reached at highest extrusion temperature), or if a particulate network is a prerequisite for high failure energy then the introduction of a well dispersed small amount of mineral filler satisfies this criterion.

Thus the impact performance of the pipes was seen to be highly dependent upon filler level/dispersion and the level of fusion.

The influence of test temperature was also considered (§5.3.1) and the results are replotted in figure 6.13 (from figure 5.11). The test temperature affects the mode of failure and also the measured impact value. Table 6.1 summarises the range of brittle to ductile transitions observed for all the pipes.

It can be seen that increasing filler level results in a broader transition with the onset of the transition beginning at higher test temperatures. The most highly filled pipes (35·6 and 40 phr) did not exhibit a transition but a slight improvement in failure characteristics at temperatures corresponding to the T_G of UPVC. The moderately filled pipes (18·1 and 27·3 phr) revealed broad transitions with the final ductile failure energy commensurate with the level of inert filler added.

The unfilled and lightly filled pipes were similar in their response to test temperature; the transition range occurring close to 0°C and involving a range of 30-40°C [195]. A maximum in failure energy occurs at 41°C whereupon the values decrease slightly due to the softening of the polymer (table F.1). The slightly lower onset of the brittle-ductile transition observed for the pipe containing 8·5 phr (1F) may be accounted by the higher level of fusion measured for this pipe versus the unfilled pipe (88·7% versus 71·7%).

TABLE 6. 1

Brittle-ductile transitions

Filler level (phr)	Brittle-ductile transition (°C)	Maximum impact value (J/mm)
0	-10→20	14·1@ 41°C
8·5	-20→20	13·6@ 41°C
18·1	0→60	10·1@ 60°C
27·3	20→100	6·1@100°C
35·6	60→>100	N/A
40	80→>100	N/A

FIGURE 6.13

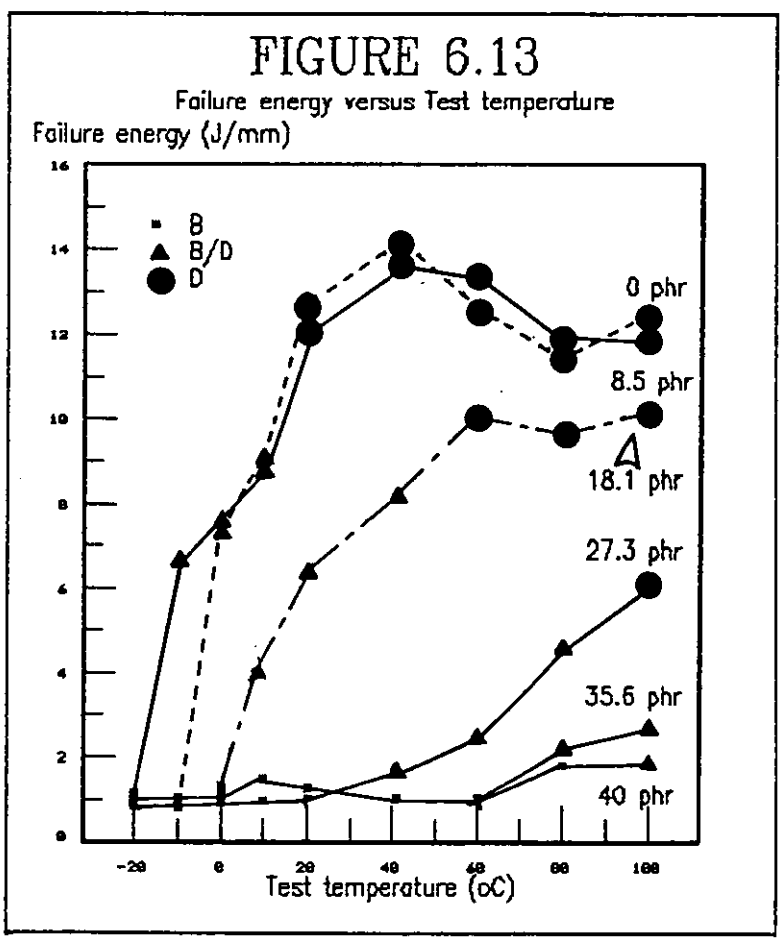

Thus figure 6.13 illustrates the presence of brittle-ductile transitions. Filler addition generally increases and broadens the transition to ductile failure, reduces impact energy even when ductile failure is observed, and above critical filler levels and/or cases of poor dispersion; impact performance is not improved by higher test temperatures.

6.3 DISCUSSION OF ADDITIVE SERIES

The previous section discussed the extrudates containing a wide range of filler levels; in this section, the results of an unfilled and a filled (≈27 phr) base composition containing a range of primary lubricants and impact modifiers will be considered (§2.3).

The base composition (§2.2) contains two additives which are considered to have a lubricating function; normal lead stearate and calcium stearate. Therefore the addition of a primary lubricant affects the overall 'lubricant system' and should not be viewed in a singular manner. With this point in mind, it should also be noted that the concentrations used for the component lubrication system may not necessarily achieve the optimum system; further experimentation may reveal a better combination or perhaps the existence of synergistic interrelationships. The choice and levels of the primary lubricant was based on practical experience where the base lubrication package is tailored by the choice of the third component to suit machine/die head design or to overcome specific processing problems such as melt fracture, weld lines etc.

6.3.1 DRY BLENDING AND PROCESSING OF ADDITIVE SERIES

6.3.1.1 DRY BLENDING AND DRY BLEND CHARACTERISTICS

The dry blending of these compositions was described in §3.1 and it can be seen that no significant differences

in dry blending times were observed.

Similarly, the dry blend characteristics, tap density and ash content, remained insensitive to varying additive type and the values were comparable to the original series (0-5). The ashing technique suggested a filler content of ≈27-28 phr for the 3E-⇒3EH series which agrees well with the original blend containing an estimated 30 phr of filler (3). Tap density values depended on filler content and the values differed slightly with variation in filler content.

Thus the dry blending results of these compositions confirm the trends observed for the original series; no difference in dry blending time upto moderate filler levels, filler content agrees well with expected values upto moderate filler levels and tap density is dependant upon filler level (§6.2.1). The apparent insensitivity of dry blending behaviour to composition can be related to the size/design of the high speed mixer which ensures good distribution and uniform heat generation to produce similar mix times and similar bulk densities per given filler loading.

6.3.1.2 PROCESSING CHARACTERISTICS

The processing results for the additive series are presented in §3.2.3 and, in general, it can be seen that the measured processing parameters (torque, Q and extrusion pressures) have similar trends, that is, an increase in, say, head pressure is commensurate with an increase in values for Q and torque. The temperature control of the extruder was considered good since little difference was observed between the extrudates except that the filled extrudates (3E-⇒3EH) were generally processed at a slightly higher processing temperature (§4.2) and also the acrylic modified blends resulted in marginally higher processing temperatures. The dry flow properties of the blends did not present any problems in the feeding of the extruder even at

30 phr filler levels. The results for the unfilled and the filled series can not be compared directly due to significant differences in mass output and screw design (§3.2.3).

The unfilled additive series indicated dramatic differences in processibility when the base primary lubricant was substituted by a different lubricant. If the first five members are considered (OE-⇒OED), then the extrusion results clearly differentiate between the so-called internal and external lubricants. Little difference was observed between OE- and OEA where the high m.pt. paraffin wax (≈95°C) was substituted by a higher level of a low m.pt. paraffin wax (≈60°C). These lubricants are generally classed as external [19, 27, 37-38, 200] and thus the overall lubricant package was more external in nature producing low Q and extrusion pressure values.

When the level of the low m.pt. wax was increased to 1·0 phr (OEB), the external lubrication efficiency of the component system was enhanced further leading to very low torque and pressure values.

Conversely the introduction of internal lubricants (OEC & OED) such as GMS (fatty acid ester of glycerine) and hydrogenated castor oil [19, 27, 146] lead to a significant increase in extrusion characteristics; the introduction of these compatible lubricants required a significant increase in mechanical energy input when compared to similar proportions of a non-polar, non-compatible lubricant.

The next member (OEE) incorporated a high m.pt. (≈105-110), low concentration polyethylene wax. Although this is considered an external type additive, high torque and pressures were observed. An explanation for this behaviour might be related to the late action of the lubricant due to its high m.pt. and/or the addition level being sufficiently low to have low external lubrication efficiency.

The final member which involved lubricant substitution was OEF, where 1·0 phr of stearic acid was

introduced. The processing behaviour of this blend resembled that of the highly lubricated blend containing 1·0 phr of the low m.pt. paraffin wax except that the stearic acid did not appear as efficient in terms of external lubrication, i.e. Q was low but not as low as OEB while values of head/inlet pressures were comparable to extrudates containing low levels of paraffin wax (OE- & OEA). Thus stearic acid is predominantly external but the more compatible material is not as efficient in reducing mechanical energy input as, say, the non-polar paraffin wax at equivalent proportions.

The introduction of impact modifiers (OEG & OEH) in conjunction with the lubricant system of OE- yielded high melt viscosities [146, 201] and thus high Q and pressure values (cf. OEG & OEH with respect to OE-), the acrylic modifier (ACR) system resulting in substantially higher torques than the chlorinated polyethylene (CPE) system. Thus the instrumented twin screw extruder provides useful comparative information upon the efficiency of lubricants to reduce melt viscosity and mechanical energy input, and it is envisaged that further experimentation would allow optimisation of the lubricant system.

The extrusion results for the filled additive series vary less and do not differentiate between low levels of external lubricant or comparatively high levels of internal lubricant (§3.2.3 and Appendix D.4). Blends 3E-, 3ED, 3EC and 3EE incorporate vastly different lubricant systems as indicated by the unfilled series, and yet the extrusion characteristics remain remarkably similar. The blend 3EA (0·2 phr low m.pt. paraffin wax) was similar to the above group but produced slightly higher extruder results.

The remaining two blends, 3EB and 3EF, incorporated 1·0 phr of a strongly external lubricant (low m.pt. paraffin wax) and a moderately efficient external lubricant (low m.pt. stearic acid) respectively. These processed blends dramatically increased processibility, i.e. Q reduced by ≈50% and the paraffinic wax appeared to reduce Q to a

greater extent than the stearic acid while extrusion pressures remained similar.

Therefore the introduction of a substantial level of filler appears to upset the lubricant balance and a higher proportion of external lubricant is required to achieve acceptable processing conditions. The introduction of quite high levels of an internal lubricant has little beneficial effect and the under-lubricated systems do not discriminate between external lubricant types at low proportions. The gross differences between the processibility of these filled extrudates can be related to the level of filler dispersion which will be discussed in §6.3.1.3.

The impact modified, filled grades did not significantly increase Q as in the case of the unfilled series. The CPE system (3EG) was similar to 3E- while the ACR modified blend had slightly higher torque characteristics.

6.3.1.3 EXTRUDATE HOMOGENEITY

The optical microscopy of the additive series again revealed that residual grains were an important feature for the unfilled series, while filler dispersion varied significantly for the filled extrudates (§4.4.1).

Grain content

The residual grain structure for these extrudates varied significantly between the additive series and since the processing temperature remained virtually constant throughout the series at ≈185-189°C (§4.2), then the level of residual grains must be explained by another process variable. A relationship was observed between the extrusion characteristics such as Q and head pressure versus the quantity of residual grains. High pressures and mechanical energy inputs resulted in low levels of residual grains as shown in the following comparison:

POOR ◄ ----- grain content ----- ► GOOD
OEB OEF OEA ≡ OE- OEC ≡ OED OEE
OEB OEF OEA OE- OEC OED OEE
LOW ◄ ----- head pressure ----- ► HIGH

A high external lubrication efficiency has a tendency to retain a high proportion of residual grains in the pipe extrudate, while reduced external efficiency involves greater mechanical energy, higher backpressures and a tendency for a more homogeneous extrudate. Gale [146] also observed that increasing levels of a non-compatible lubricant (external: stearic acid) lead to a greater proportion of 'unfused grains'. He referred to these entities as unfused since intergrain fusion is clearly not developed, but the effect of intragrain fusion was not considered.

The influence of impact modifier produced extremes with respect to grain memory; the CPE modified extrudate exhibiting the highest proportion of grains for the unfilled additive series (figure 4.33), whilst the ACR modified system exhibited a few highly elongated grains (figure 4.37) and was clearly the most homogeneous extrudate for this series. The gross differences can be considered a consequence of the type of network produced by each modifier. The ACR system should exist as discrete crosslinked rubbery particles distributed in a homogeneous network; the well distributed rubbery particles increase impact energy through dispersive mechanisms such as cavitation and shear yielding (§1.2.5.2). Since higher melt pressures and torque were required to process this blend (cf. other members of the series), then the extrudate resulted in a low level of residual grain content. The CPE system is considered to form a continuous phase of CPE which encapsulates inhomogeneities such as primary particles or, in this case, residual grains and the improvement in impact performance is related to enhanced deformation mechanisms. A slight increase in melt viscosity is observed on processing,

however the grains are encapsulated in a continuous network resulting in lower intergrain frictional contact and thus a higher retention of grain memory. This behaviour is analogous to external lubrication where a coating of the lubricant prevents frictional forces at the grain boundaries.

Filler dispersion

In a similar manner to the earlier extrudate study, the microscopy of these extrudates revealed that the level of dispersion was an important feature and that no measurable traces of grain content were observed. The level of filler dispersion varied greatly from distinct agglomerates of ≈20-30 μm for 3EA and 3ED to virtually a homogeneous system with few agglomerates for 3EF (§4.4.1). The order of improving filler dispersion can be ranked as follows and also compared with the resultant head pressure observed during processing:

POOR ◄ ----- filler dispersion ----- ► GOOD

(3EA ≡ 3ED) (3EE 3E- 3EC) (3EB) (3EF)

3EA 3ED 3EC 3E- 3EE 3EB 3EF

HIGH ◄ ----- head pressure --------- ► LOW

The visual examination of these microscopy sections indicated little difference in dispersion between 3EA & 3ED and also the group, 3EE, 3E- & 3EC. Thus four groups are indicated by the brackets and a micrograph of each group is shown in figures 4.38-4.41 inclusive.

The interaction of head pressure can be clearly seen, high head pressures were concurrent with poor dispersion. Again these results can be attributed to the amount of external lubricants; a high level of external lubricant (3EF & 3EB) ensures that a sufficient amount is available to coat the filler particles and prevent the fine particle size filler from agglomeration. The well lubricated

blends exhibit good flow properties with low torques and low pressure build-up.

For other lubricant systems, the values of head pressure vary less, however 3EA yields high head pressure which is attributed to poor dispersion and low level of efficient external lubricant. The incorporation of a moderate level of internal lubricant (3EC & 3ED) has some effect but is not equivalent to a low level of a high m.pt. paraffin wax (3E-). The values obtained for Q generally bear out the above trends with the notable exception that 3EB and 3EF are reversed. This would suggest that 3EF is more efficiently lubricated in the head region than 3EB. A possible interaction is envisaged between the calcium stearate surface treated filler and the chemically similar lubricant stearic acid producing a more efficient system at high temperatures.

The introduction of impact modifiers resulted in extrudates with the filler being well dispersed (§4.4.1); the acrylic modifier system produced the best dispersion of filler for all the series (figure 4.42) and the CPE extrudate was equivalent to 3EF. The good filler dispersion for the ACR modified system can be related to the significant increase in mechanical energy input (Q) when compared to 3E- (base lubricant composition). The high level of energy input leads to a better dispersive action (§6.2.2.1). The reason for the good dispersion in the CPE system is analogous to that for the behaviour of the unfilled system given above, that is, the CPE continuous phase encapsulates the fine particles of the filler ensuring that the particles remain discrete and 'well lubricated' from other particles.

Surface appearance

The aesthetic appearance of the pipes outer surface was assessed by visual examination (§3.3.1) and also via scanning electron microscopy (§4.4.3). The results of both

techniques confirm the groups obtained in table 3.5 (§3.3). Little difference in surface quality was observed with the exception of the blends containing the ACR modifier. These two blends (unfilled and filled) produced the best surface finish which might be explained by the slightly higher melt temperature observed during processing (§4.2) and/or good dispersion of inhomogeneities (see above discussion). As for the original extrudates, no evidence was observed to suggest melt fracture, lubricant plate-out or poor filler agglomeration on the surface.

The inner surface was also visually examined and the results listed in table 3.7. The introduction of ≃27 phr of filler produced a better inner surface which may be attributed to a decrease in melt elasticity in a similar manner to the earlier extrudate series (§6.2.2.2). The introduction of the acrylic modifier also reduces melt elasticity while the CPE modifier increases melt elasticity (§1.2.5.1).

6.3.1.4 ASSESSMENT OF THE DEGREE OF FUSION

In a similar manner to the original series of filled extrudates, the level of fusion for the additive extrudates were assessed by thermal analysis and solvent tests.

Thermal analysis

The thermograms for the additive series are similar in appearance and characteristics to those obtained for the filler series (figure 6.5), and no effect upon T_G was observed [27]. Table 4.2 lists the thermal analysis results obtained and it can be seen that the processing temperature (as indicated by the 'B' onset temperature) is well controlled within the extruder, even though a wide difference in lubricant composition is considered. The exception to good melt control can be seen for the blends containing the acrylic modifier; these have slightly higher

melt temperatures due to higher levels of work input [201].

The ΔH_A values are compared to the maximum obtained in the original series, 3F≡10·53 J/g, to yield comparative % fusion values, and the last column of table 4.2 estimates the predicted % fusion using the measured 'B' onset temperature in equation 4.6. Comparing the last two columns suggests a reasonable agreement between values with a few notable exceptions. The general agreement infers that the master curve plotted in figure 6.7 is also indicative of the blends containing appreciable differences in the composite lubricant system. This suggestion differs from previous reports on fusions studies and their interactions with lubricants; most workers report a decrease in fusion level with increasing external lubricant content [22-24, 29, 37-38, 137, 200-202] and therefore, all things being equal, the fusion level of OEB should have been lower than OEA. However the common processing method used to assess fusion is the Brabender™ torque rheometer. This uses the torque generated by the material to raise melt temperature and thus enable the fusion process to progress. Since the introduction of an external acting lubricant reduces the magnitude of the initial torque [22, 29], this, in effect, reduces the amount of work input via frictional forces leading to a decrease in the rate of heat build-up. The ultimate effect of the decrease in the rate of work input is a lengthening of the fusion time. The use of a less externally lubricated system does not have such a dramatic reduction upon initial torque, alternatively, calcium stearate is reported to increase initial torque [22, 38] and thus these lubricants have less effect upon fusion time. The application of results from a Brabender torque rheometer to a process such as twin screw extrusion is questionable since: firstly the mechanism of particulate breakdown may differ from comminution as seen in a high shear regime of a torque rheometer (§1.4.1) to the 'CDFE' mechanism reported in this study and many others [112-116]; secondly the twin screw extruder offers good temperature control which ensures that the melt achieves the

correct processing temperature mainly by conduction [131, 181] without the prerequisite of a high degree of work input.

Thus it can be seen that for many of the extrudates the level of fusion can be related to the original master curve at the appropriate processing temperature within the bounds of experimental error. Obande [203] reported similar ΔH_A values (3-3·7 J/g) for a range of compression moulded plaques containing substantial differences in external lubricant (1·0-4·5 phr) at moulding temperatures appropriate to this study (≈190°C), although at higher 'B' onset temperatures (>200°C) discernible differences were obtained which indicated that a higher external lubricant content lead to lower ΔH_A values.

The unfilled series, in general, had fusion levels between ≈50-60% with the exception of OEF and OEH. The strong dependence on processing temperature controlled the level of primary crystallite breakdown and the degree of secondary crystallisation (ΔH_A). Thus considering the CDFE mechanism considerable intragrain fusion may develop before complete destruction of the grains. The high level of residual grains observed in some of these blends (§6.3.1.3) does not indicate that the entities are 'unfused', as suggested by Gale [137], but that insufficient extrusion pressures/mechanical energy are available to enable grain elongation and eventual destruction. Therefore although residual grains were obtained for these blends, the level of intragrain fusion was similar.

The higher value of OEH (≈82%) may be explained by the high shear regime as indicated by the high value of Q and extrusion pressures (§6.3.1.2 & §3.2.3); these values were considerable higher than for the other members of the group and it may be envisaged that these conditions enhance pressure transfer and heat conduction leading to early breakdown of the grains and possibly the primary particles. The partial removal of boundaries would enhance chain interdiffusion between primary particles and, possibly grain

boundaries, to allow further secondary recrystallisation and hence higher values of ΔH_A.

The other anomaly was the extrudate OEF. This pipe yielded a higher ΔH_A value than might be expected from the processing temperature. It is difficult to account for this variance since the extrusion conditions were not harsh in comparison to the acrylic modified blend (OEH), however it is interesting to note that the high level of lubricant used in this blend (1·0 phr: stearic acid) gave low values of Q as might be predicted but retained comparable pressure results to blends containing considerable lower levels of external lubricant. It may be possible that the stearic acid may interact with the similar lubricant, calcium stearate, to produce a higher fusion level at the moderate processing temperature [22, 38].

The filled systems, in general, produced fusion levels of approximately 60-70% which were attributed to slightly higher average processing temperatures of ≃190-193 °C (§4.2). Again the fusion level can be related to the extrusion temperature but also a number of anomalies are observed (3EB, 3ED and 3EG). These can not easily be related to processing conditions, lubrication effects, filler dispersion or melt temperature differences. 3EB and 3ED had considerable higher ΔH_A values than might be expected which may involve substitution of the calcium stearate coating on the filler and thus allowing 'free' calcium stearate to interact, however no evidence is available to support this speculation and further work is necessary to ascertain whether these blends can be fitted to the original master fusion curve in a similar manner to the majority of the filled additive series. 3EG (10 phr CPE modifier) had a lower than expected fusion level and also the acrylic modified system did not enhance the level of fusion as indicated in the unfilled series. These differences may be due to the filler diluting the high extrusion characteristics of these modified systems (Appendix D.4) and thus reducing the expected benefit in fusion level.

Therefore the thermal analysis technique appears to be less dependent upon the composition and allows a single fusion curve for a particular processing machine to be used to predict fusion levels for a range of vastly different materials. A number of mismatches were obtained which did not fit the original master curve, these results may need to be verified.

Acetone shearing test

The acetone shearing test (§4.4.2) confirmed the results observed for the original filled series (§6.2.2.3), that is, at moderate levels of fusion the technique is unable to distinguish between quite large increments in % fusion. Thus the test provides complementary evidence to support thermal analysis and the methylene chloride tests (§3.4) but does not yield any further information other than that the pipes are not poorly fused.

6.3.2 MECHANICAL PROPERTIES

6.3.2.1 TENSILE PROPERTIES

The tensile properties are listed in table 5.2 and illustrated graphically in figures 5.6 and 5.7.

Yield parameters

The yield properties of the unfilled series appear relatively independent of additive type (with the exception of OEG & OEH) and of similar values to the original unfilled series (§6.2.3.1). The two impact modifiers reduce yield stress [59] with the CPE system (soft CPE phase) having a greater effect than the ACR blend.

The filled additive series is also insensitive to yield measurements, *albeit* at a lower value, with the modifiers again causing a decrease in yield stress. However,

in this case, the ACR blend has a lower yield stress than the CPE modified system (cf. OEG & OEH) and also the level of reduction is not as great as the unfilled extrudates. The value of yield stress for 3EG (10 phr CPE modifier) is approximately the same as for the OEG and thus is possibly related to the CPE network phase retaining properties even though the effective cross sectional area of the polymer is reduced by the introduction of the filler.

Post-yield parameters

It is evident from table 5.2 that the ultimate elongation values (ε_B) are significantly higher than the original series (cf. table 5.1). These high extension values are induced by a more stable neck formation with the filled extrudates (3E-⇒3EH) having comparable extension values as the unfilled. The improved behaviour at failure for the filled additive series compared to the original ≃27 phr extrudates can be related to improved dispersion (cf. §4.4.1 with §4.3.1) allowing substantial drawing before failure. The modified systems exhibited high neck stability and thus high elongation at break [67]. The tentative relationship observed in §6.2.3.1 between breaking stress (σ_B) and ultimate elongation (ε_B) was again apparent, i.e. high extensions (esp. modified blends) lead to high σ_B measurements.

Therefore tensile properties did not distinguish, with any certainty, between the members of each series unless modified by a rubbery additive such as CPE and ACR, and secondly, the introduction of approximately 27 phr of filler produced a step reduction in yield stress.

6.3.2.2 IMPACT PROPERTIES

The instrumented impact testing of the pipes containing the range of additives revealed gross differences (table 5.4) and failure energy derived from the impact trace

provided a good indicator of the overall impact performance (figure 5.12).

The results of the additive series differed from the original series since the approximately 30 phr filled pipes had far greater impact properties than the original 3E pipe and also OE- has a lower value than OE. The better overall performance of the filled additive series is attributed to better dispersion, but there is still considerable variation between members; the earlier series at this filler level had very poor dispersion compared to the series discussed here (§4.4.1 & §4.3.1).

The impact performance of the original unfilled extrudates (OA-OG) was shown to be dependent upon the level of fusion, however the additive series indicates gross differences whilst fusion level (via thermal analysis) is apparently constant. The behaviour of these extrudates was shown to be critically dependent on the homogeneity of the extrudates which, in turn, can be related to the measured extrusion characteristics (§6.3.1.3) and hence the external efficiency of the composite lubricant system.

The impact behaviour of the unfilled extrudates can be compared to the level of residual grains assessed during optical microscopy (§4.4.1):

LOW ◄ ----- impact energy ---- ► HIGH
OEB OEF ≡ OE- OEA OEC OEE ≈ OED
OEB OEF OE- ≈ OEA OEC ≈ OED OEE
HIGH ◄ ----- grain content ---- ► LOW

A clear relationship is observed between residual grain content and failure energy. §6.3.1.3 identified the link between processibility and grain retention, similarly the ease of processing was related to the composition. Thus higher levels of external lubricant (eg. OEB & OEF) resulted in low head pressures giving poor residual grain content and ultimately poor impact resistance and brittle/ductile failure. Therefore impact performance is dependent upon the

level of processing and the external lubrication efficiency. Thermal analysis (§4.2) suggested that, in general, fusion level did not dramatically differ between blends (excluding OEF) and therefore the presence of high levels of grain inclusions does not necessary imply poor fusion.

The influence of residual grains upon impact resistance has been observed: Mai *et al* [204] measured the fracture toughness of a well processed (low level of residual grains) versus a poorly processed extrudate (high level of 'unmixed PVC granules'); it was proposed that the poorly processed pipe resulted in a low toughness value. Gale [35] also considered that impact strength was directly due to the presence of 'unfused' material.

A number of reports have investigated the effect of high levels of external lubricant upon impact properties and most agree that a detrimental effect is obtained [33-35, 113, 179]. Marshall *et al* [113] suggested that a higher level of external lubricant delays the fusion process and also delays the development of maximum impact performance. Shaw *et al* [34] also attributed the observed decrease in impact performance with increasing levels of lubricant to the fusion delaying effect of the external lubricant.

The impact results for the additive series in this study were directly attributable to the presence of residual grains acting as stress concentrators, and the concentration of these grains was related to the level of processing. Fusion level, as measured by thermal analysis, varied slightly between the blends and was not associated with high residual grain content.

The introduction of impact modifiers produced a significant increase in performance over the poorly processed pipes (OEB, OEF, OE- OEA). The ACR blend (OEH) produced the best properties of all the blends; since no residual grains were detected and, secondly, the effect of the rubbery additive (§1.2.5.2). The CPE extrudate (OEG) gives good impact performance compared to the blends containing high levels of external lubricant, yet the value

of OEG is marginally lower than for the well processed pipes (OED & OEE). Optical microscopy (§4.4.1) revealed that the grain content of this system is the worst of all the extrudates and thus the observed impact behaviour may be related to its energy absorbing phase (§1.2.5.2) which encapsulates the poorly mixed residual grains.

The testing of the filled additive series also indicated that the instrumented tester is a viable machine for detecting differences in the quality of processed UPVC. In this case, a relationship was observed between filler dispersion (§4.4.1) and impact behaviour:

LOW ◄ ----- impact energy ---- ► HIGH						
3EA	3ED	3EE	3E-	3EC	3EF	3EB
3EA ≈	3ED	3EE	3E-	3EC	3EB	3EF
POOR ◄ --- filler dispersion -- ► GOOD						

It is clear from the above comparison that the level of filler dispersion is the main factor controlling impact performance, the failure energy values varying considerably but, as might be expected, always remaining significantly lower than the unfilled series due to the substitution in effective polymer area by inert filler. The agglomerates of poorly dispersed filler may act as stress concentrator loci which assists crack initiation and crack propagation [53]. §6.3.1.3 attributed the level of filler dispersion to the processing characteristics and proposed that good dispersion is related to the external nature of the lubricants present. 3EB and 3EF contain relatively high levels of external lubricant and can be seen to yield more homogeneous extrudates in terms of filler dispersion.

In a similar manner to the unfilled series, the impact properties of the filled series were also related to product homogeneity and highly dependant upon the lubricants. Again the influence of fusion (esp. 3EA & 3ED) was not observed.

The introduction of a modifier resulted in good

impact results and, as discussed in §6.3.1, produced extrudates exhibiting good dispersion. It is difficult to ascertain whether the inherent mechanism of the modifier system also has a tangible effect upon impact performance in conjunction with good filler dispersion.

6.4 INTERACTION OF FILLERS AND LUBRICANTS IN RIGID PVC

The discussion to-date has considered each major stage of work in detail; the following discussion reviews some of the major similarities between the stages of work.

The dry blending process and dry blend characteristics revealed little effect upon the addition of filler or primary lubricant substitution with the exception of highly filled blends; these systems lead to poor powder handling, filler loss, high tap density and longer blending times.

The processing characteristics of blends containing variations in filler concentration and additives differed appreciably. Figure 6.14 illustrates the behaviour of an unfilled or lightly filled system (≤8·5 phr) in terms of the fusion mechanism and final extrudate homogeneity. Figure 6.15 depicts the differences observed in this mechanism with the addition of moderate to high levels of filler. This simplistic approach is based upon Allsopp's compaction, densification, fusion and elongation (CDFE) mechanism [112] which can be extended to explain the observations obtained.

Figure 6.14 describes the basic CDFE mechanism (§1.4.1) with intragrain fusion occurring before breakdown of the grains. The level of intragrain fusion was estimated by the development of secondary crystallinity and was shown to be highly dependant upon the processing temperature (§6.2.2.3). Low processing temperatures retained a primary particle structure within the grain which was easily fragmented during the acetone shearing test (§6.2.2.3). The elongation and grain retention depended upon the processing regime and composition. High processing temperatures, high

torque characteristics and an appropriate lubricant system tended to produce a homogeneous matrix with few residual grains (A). These components acting singularly or in addition to one another. If the opposing conditions are involved i.e. low processing temperature, low level of mechanical energy input and high external lubricating efficiency, then, in general, a high level of residual grains were obtained. The filled extrudates series at moderate temperatures were characterised by few grain inclusions and fusion level had an important role in determining properties (§6.2.3.2). If situation B prevails, as observed in a number of lubricant modified extrudates, then properties such as impact are reduced due to stress concentrators, and fusion level is not envisaged as a controlling influence.

Figure 6.15 illustrates the case for moderate to highly filled blends. A similar fusion mechanism is envisaged and intragrain fusion is unlikely to be affected by the addition of an inert filler. The elongation and destruction of the grain takes place quickly but the level of filler dispersion is dependent upon processing conditions and composition as illustrated. Good dispersion was related to adequate dispersive energy forces, sufficient external lubrication and low processing temperatures. While filler agglomeration was observed with blends processed at high extrusion temperatures, low dispersive energy forces, increasing filler loadings and compositions which have a low external lubricating nature. Again these effects are likely to interact. Impact performance was related to filler agglomeration and the influence of fusion level is not well defined.

The two figures discussed previously (figures 6.14 & 6.15) demonstrated that properties and product quality are critically dependent upon formulation and processing aspects. The significant effect of lubricant composition can be highlighted in both unfilled and filled extrudates; suitable formulation in unfilled blends can yield properties

FIGURE 6. 14

Schematic mechanism of fusion for unfilled or lightly filled extrudates

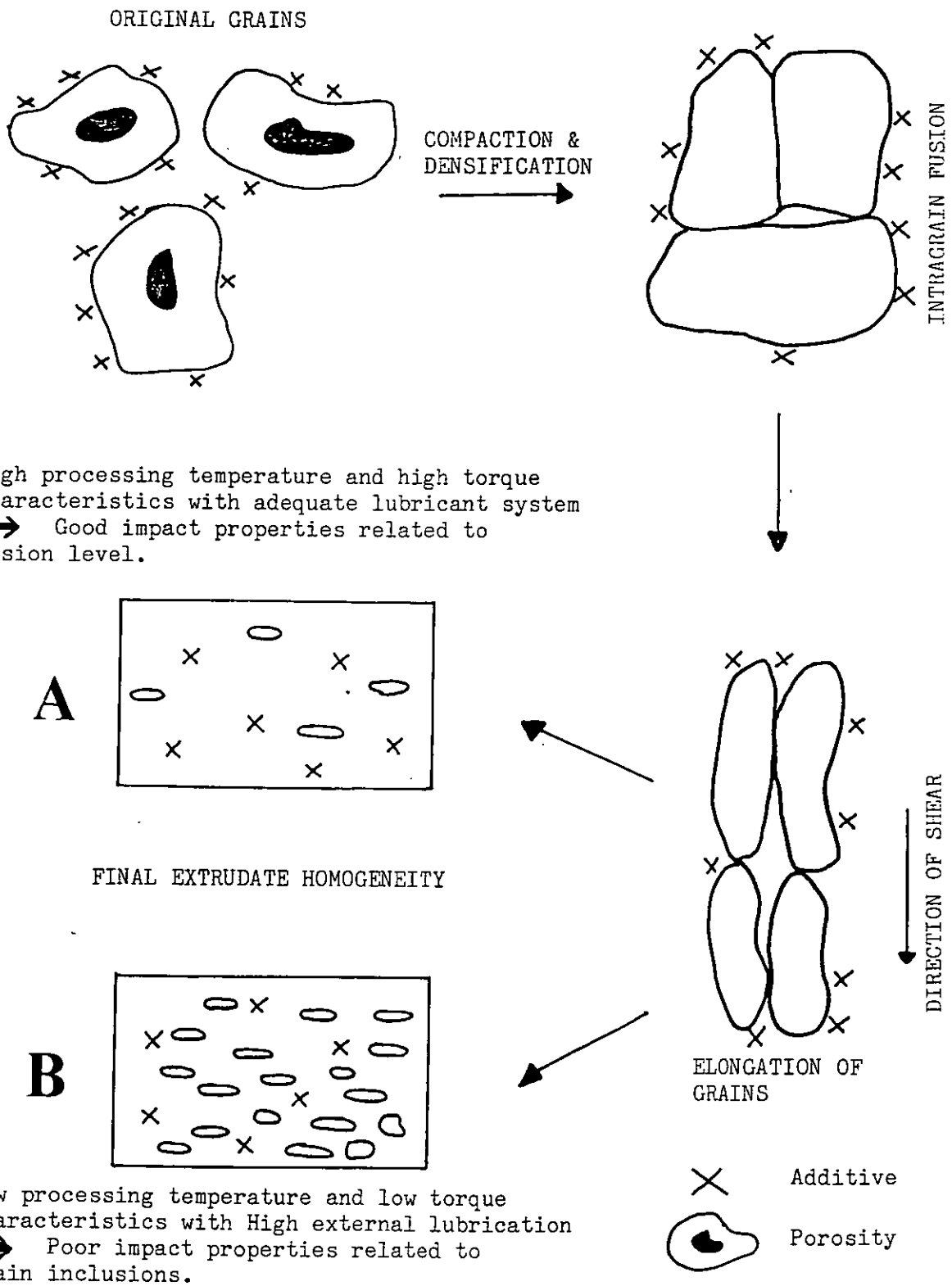

FIGURE 6. 15

Schematic mechanism of fusion for highly filled extrudates

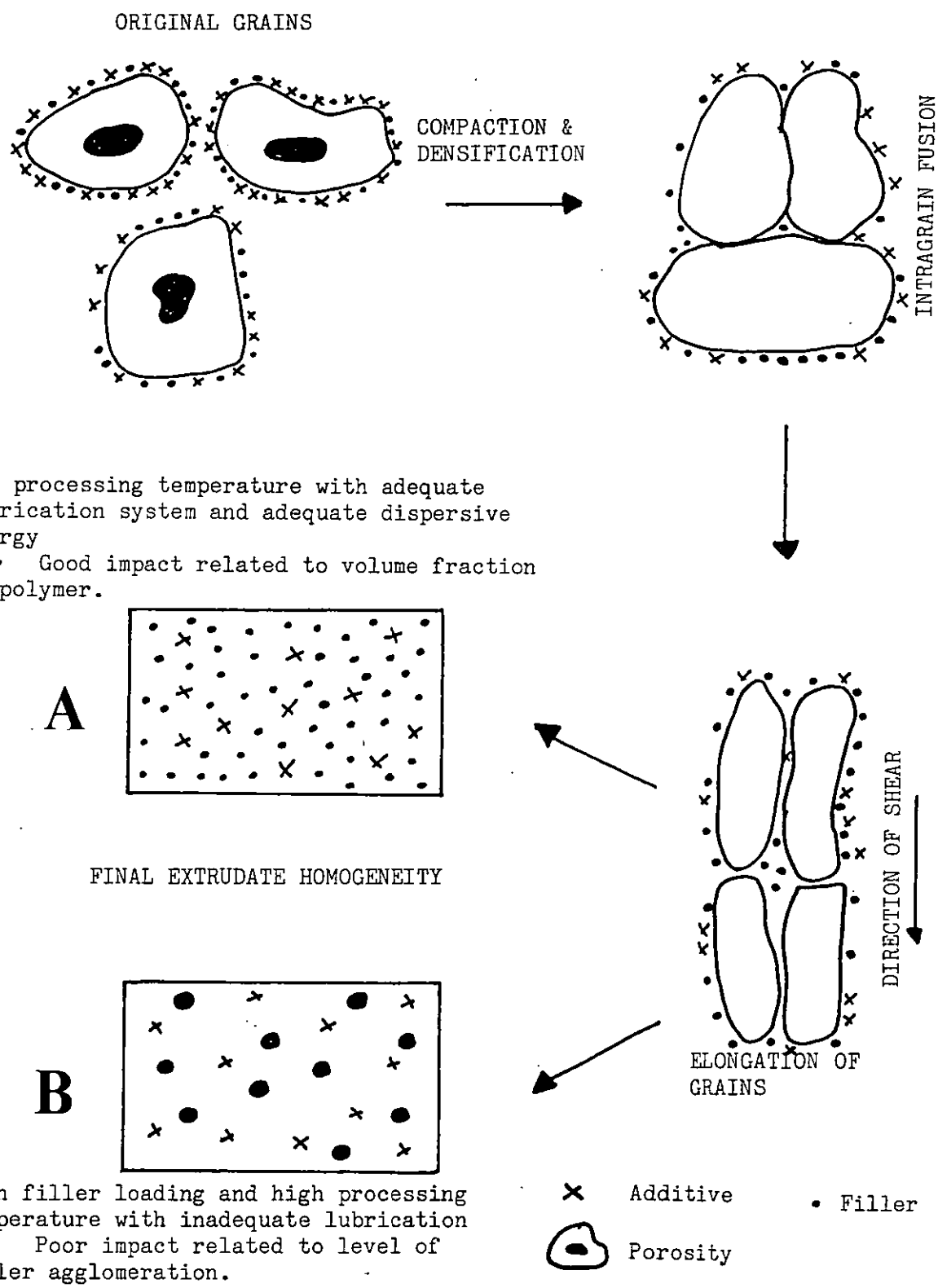

which approach those extrudates containing traditional impact modifiers such as CPE and ACR. In the case of quite highly filled blends, the interaction between lubricant system and filler level can be developed to prevent serious reduction in impact performance which generally occurs with the addition of substantial levels of an inert filler. In some instances, optimisation of the formulation induced better impact performance for a quite highly filled grade (≈27 phr) when compared with an unfilled extrudate produced under similar extrusion conditions.

Thus it can be seen for a given filler level and processing regime, the lubricant system must be tailored (i.e. modification of primary lubricant) to optimise the level of filler dispersion and ease of processing. It is likely that each system is machine specific, however the techniques outlined above can be used to assess the quality of the final extrudate.

CHAPTER SEVEN

CONCLUSIONS AND SUGGESTIONS FOR FURTHER WORK

7.1 CONCLUSIONS

Dry blending

- *Dry blending time remained constant until, at high filler loadings, filler loss reduced the charge weight and increased blending time. Ash content provided accurate filler content values and confirmed the resultant filler loss at high filler loadings.*

- *Filler loss in the mixer appeared to coincide with the polymer grains being completely covered by filler particles and leaving 'free' filler particles.*

- *Dry blending of the filled blends lead to slight attrition of the original polymer grains to produce more spherical grains with the inherent folds in the pericellular membrane preferentially filled with filler.*

- *Bulk density measurements progressively increased with increasing filler content until at filler levels beyond 30 phr the value increased disproportionately due to 'free' filler yielding an efficiently packed powder.*

- *Modification to the composite lubricant system did not significantly affect dry blending characteristics or bulk density values.*

- *The free flowing properties of the dry blends were disrupted by the introduction of the calcium carbonate filler; high loadings of filler prevented powder flow and feeding modification were required to aid conveyance in hoppers.*

Twin screw extrusion

From the extruder results a number of general conclusions were obtained:

- *The extruder attained steady state conditions quickly and mass throughput was apparently unaffected by processing conditions or formulation aspects.*

- *Acceptable pipe was produced for all blends with the exception of those extruded at extrusion profiles, A & B; at these low extrusion temperatures the pipe could not be formed into pipe.*

- *All extrudates passed the methylene chloride test with the exception of pipe processed at temperature profiles, A & B; these extrudates showed signs of excessive swelling and disintegration.*

- *The instrumented extruder can be used to compare the processibility of different compositions including filler and lubrication aspects.*

- *Pressure values were measurable only in the last zone of the extruder; these values increased with increasing filler content, decreasing extrusion temperature and decreasing external lubricant efficiency*

- *Torque and Q measurements followed a similar trend as was exhibited in the head pressure results.*

From the extruder results of the filled extrudate series it was concluded that:

- *Extrusion characteristics were critically dependent upon composition; the incorporation of filler lead to an increase in torque and pressures, with the pressure transducer at the adaptor showing an approximate linear relationship between pressure and filler content.*

- *A levelling off in torque values with high filler loadings at high extrusion temperatures was related to poor dispersion.*

- *Surface appearance improved with increasing extruder temperatures and was lowered by the introduction of moderate levels of filler (>8·5 phr).*

- *A mathematical relationship was obtained to describe head pressure as a function of melt temperature and filler content.*

From the extruder results for the additive extrudate series it was concluded that:

- *Extrusion characteristics confirmed the behaviour of some common lubricants as external or internal lubricants; for example paraffin wax has a strong external lubricating efficiency compared to, say, GMS.*

- *The extrusion results indicated the external behaviour of the composite lubricant system, a high external nature leading to low torque and pressure values.*

- *A high proportion of external lubricant was required to counteract the effect of filler addition.*

- *The incorporation of an impact modifier, in general, lead to an increase in melt viscosity and thus an increase in extrusion characteristics.*

- *Lubricant modification had little effect upon surface quality, however the incorporation of an impact modifier improved surface appearance in both filled and unfilled extrudates.*

Microscopy

From the microscopy study of the filled extrudate series it was concluded that:

- *Optical microscopy of the lightly filled and unfilled extrudates revealed residual grains which decreased in number with increasing extrusion temperature; the grains were distributed in a flow band and at high processing temperatures became highly elongated.*

- *The presence of residual grains supports the CDFE mechanism and the final stage of this mechanism, elongation of intrafused grains, depended upon backpressure and extrusion temperature.*

- *Moderately filled extrudates did not exhibit significant traces of residual grains, but revealed that filler dispersion was dependent upon filler level and extrusion temperature; high filler contents at high processing temperatures produced poorly dispersed filler agglomerates within the polymer matrix.*

- *UV fluorescence microscopy supports the presence of residual grain entities and filler agglomerates as indicated by optical microscopy.*

From the microscopy study of the additive extrudate series it was concluded that:

- *The unfilled additive series also illustrated a grain memory which was related to the head pressure characteristics, these extrusion characteristics being a function of the external nature of the lubricant. A highly external lubricated system yielded low torque and head pressures to produce a extrudate containing a high level of residual grains.*

- *The ACR modified unfilled blend produced the lowest level of residual grains whilst the CPE system indicated the highest level of grain inclusions for the series.*

- *The filler dispersion of the filled additive series was related to the external nature of the lubricant; highly external lubricants produced a well dispersed extrudate.*

- *Both impact modified pipes containing filler yielded well dispersed filler particles.*

Fusion

From the fusion assessment of the filled extrudate series it was concluded that:

- *Thermal analysis measurements indicated that secondary crystallinity increases with increasing extrusion temperatures and that the amount of primary crystallinity decreases with increasing processing temperatures.*

- *'B' onset temperature provided an accurate measure of the maximum melt temperature achieved during processing.*

- *The 'B' onset temperature was strongly dependent upon the setting of pipe head temperature; the barrel temperatures had little effect upon the final 'B' onset temperature.*

- *A linear relationship was obtained between 'B' onset and the temperature indicated by a thermocouple situated in the pipe head, however the latter method relied upon accurate calibration as opposed to the thermal analysis technique.*

- *A master fusion curve of secondary crystallinity versus 'B' onset temperature was obtained for the filled extrudates processed within a wide processing window.*

- *The introduction of substantial amounts of filler did not appear to influence the level of fusion attained by the extrudates.*

- *The acetone shearing test provides qualitative evidence to support the inferences gained from thermal analysis, but lacks discriminating power for more fused extrudates.*

From the fusion assessment of the additive extrudate series it was concluded that:

- *The pipes incorporating a range of additives, in general, seem insensitive to changes in fusion level. In cases in which high extrusion characteristics were obtained, the level of fusion increases slightly.*

- *The thermal analysis technique appears useful in estimating fusion level from a fusion curve and seems relatively insensitive to changes in formulation and processing conditions. However significant differences in processing behaviour may require modification of the original master curve.*

Mechanical properties

From the tensile testing of the filled extrudate series it was concluded that:

- *Yield parameters were insensitive to variations in fusion level.*

- *Yield stress was dependent upon filler level; a reduction in stress with increasing filler level was attributed to a dilution effect of the inert filler.*

- *Yield stress of highly filled extrudates decreased with increasing processing temperature due to poor filler dispersion.*

- *Post-yield properties were sensitive to neck instability during cold drawing. Poor neck stability was observed for most pipe specimens leading to substantial scattering of results.*

- *High filler loadings reduce ultimate stress due to poor filler dispersion affecting neck stability and promoting premature failure*

From the tensile testing of the additive extrudate series it was concluded that:

- *Yield and post-yield parameters were not significantly affected by changes in the primary lubricant.*

- *The introduction of impact modifiers reduced yield stress, especially for the unfilled pipes.*

From the impact testing of the filled extrudate series it was concluded that:

- *The testing of the unfilled extrudates suggested a maximum at a fusion level of approximately 70-75%. Low fusion levels gave poor resistance to failure while at intermediate levels, a ductile behaviour was noted giving improved impact performance. At high processing temperatures, the destruction of a particulate network reduces impact resistance due to the elimination of energy absorption mechanisms at the interfaces of the particulate structures.*

- *The introduction of filler delayed the attainment of ductile behaviour, requiring high levels of fusion to promote ductile failure.*

- *High loadings of filler with poor filler dispersion yielded brittle behaviour with very low impact strengths of approximately 10% of the maximum obtained for the unfilled pipes at optimum fusion levels.*

- *At high filler loadings, impact properties were insensitive to fusion level.*

- *Impact properties of filled pipes which failed in a ductile manner were considerably lower than for unfilled pipes failing in a similar manner.*

- *Impact testing at a wide range of test temperatures indicated different brittle-ductile transitions for the unfilled and filled extrudates. The introduction of an inert filler increased the brittle-ductile temperature and this transition occurred over a wider temperature range.*

- *A higher fusion level lowered the brittle-ductile transition temperature.*

- *Pipes with high filler loadings, exhibited poor filler dispersion; a brittle-ductile transition was not observed.*

From the impact testing of the additive extrudate series it was concluded that:

- *The presence of a residual grain structure had a significant effect upon performance for the unfilled pipes. High levels of residual grains caused poor properties; thus impact performance was directly linked to processing and formulation aspects.*

- *Impact modification of the unfilled pipes lead to a dramatic increase in performance with the ACR system showing better improvement than the CPE additive.*

- *The impact behaviour of the filled additive series was dependent upon the quality of the filler dispersion. Poor dispersion yielded poor properties; therefore the resistance to impact was again related to processing and formulation aspects.*

• *Modification of the lubricant system can play an important role in determining end performance properties.*

• *Impact modification of the filled extrudates again improved impact resistance, the CPE modifier producing slightly better improvement than the ACR modifier in this case.*

7.2 SUGGESTIONS FOR FURTHER WORK

This investigation considered the influence of a single particle size coated filler upon processing and properties. A fuller understanding might be gained by considering:

a) The influence of the particle size distribution.

b) The influence of coating and coating level.

These factors are presently under investigation at IPTME.

The lubricant study suggested the importance of the composite lubricant package upon the processing and performance of unfilled and filled extrudates; the application of factorial design experimentation might enable optimum lubricant systems to be identified.

Preliminary work (§4.1) indicated that thermal analysis testing provided a master fusion curve which was valid for a relatively large number of compositions. Further work might confirm these observations and relate the fusion levels to mechanical properties.

The instrumented extruder provided a convenient method to investigate the processing behaviour of extruded pipe. It is envisaged that a processing window might be identified from the extruder characteristics which would ensure a good quality extrudate.

The application of an instrumented falling weight impact tester demonstrated that this type of test could establish the quality of the extrudate; further investigations might consider the suitability of this type of test as a on-line quality control technique.

REFERENCES

1. Anon *Euro. Plast. News.*, 14 1, (1987)
2. Anon *Mod. Plast. Int.*, 17 1, 21 (1987)
3. Stephenson, R C, *J. Vinyl Techn.*, 5 1, 13-19 (1983)
4. Tester, D A, *Plast. & Rubb. Int.*, 8 4, 137-140 (1983)
5. Saunders, K J, *'Orangic Polymer Chemistry'*, Chapman & Hall (1973)
6. Viola, P I, *Med. law*, 61 174 (1970)
7. Maltoni, C, Lefemine, S, *Environ. Res.*, 7 387 (1974)
8. Burgess, R H, *'Manufacture and Processing of PVC'*, Appl. Sci. Publ. (1982)
9. Menges, G, Berndtsen, N, *Pure & Appl. Chem.*, 49 597-613 (1977)
10. Saechtling, H J, *Kunststofftaschenbuch, C. Hanser-Verlag, Munchen*, (1974)
11. ASTM D1755-78
12. Breon PVC Resins *BP Monograph*, TM1 BP Chem. Int. (1973)
13. Hoff, A, *Industrial Hazards of plastics and synthetic elastomers*, 141 91-98 (1984)
14. Matthews, G A R, *'Vinyl and Allied Polymers'*, Butterworths Ltd Volume 2 (1970)
15. Nass, L I, *'Encylopedia of PVC'*, Marcel Dekker, New York Volume 2 (1977)
16. Chevassus, F, DeBroutelles, R, *'The Stabilisation of Polyvinyl chloride'*, Edward Arnold (1963)
17. Logan, M S, Chung, C I, *Polym. Eng. Sci.*, 19 15, 1110-1116 (1979)
18. Jacobson, U, *Brit. Plast.*, 34 328-333 (1961)

19. King, L F, Noël, F, *Polym. Eng. Sci.*, 12 2, 112-119 (1972)

20. Illman, G, *SPE J.*, 23 71 (1967)

21. Souma, I, *Conf. Prog. Sci. Eng. Composi. 4th*, 179-186 (1982)

22. Pedersen, T C, *J. Vinyl Techn.*, 6 3, 104-109 (1984)

23. Hartitz, E, *Polym. Eng. Sci.*, 14 5, 392-398 (1974)

24. Oakes, V, Hughes, B, *Plast.*, 31 1132-1134 (1966)

25. Hatt, B W, *J. Vinyl Techn.*, 6 3, 120-124 (1984)

26. Marshall, B I, *Brit. Plast.*, 42 8, 70-78 (1969)

27. Rabinovitch, E B, Lacatus, E, Summers, J, *J. Vinyl Techn.*, 6 3, 98-103 (1984)

28. Sieglaff, C L, *Polym. Eng. Sci.*, 9 2, 81-85 (1969)

29. Krzewki, R J, Collins, E A, *J. Macrom. Sci.-Phys.*, B(20) 4, 465-478 (1981)

30. Khanna, R K, *Plast. & Polym.*, 42 80-82 (1974)

31. Guignard, J, *SPE-ANTEC*, 12 112 (1972)

32. Gross, R C, Coaker, A W M, Hinchen, J D, *SPE-ANTEC*, 27 425-429 (1969)

33. Bower, D, Heffner, M H, *J. Vinyl Techn.*, 5 3, 116-120 (1983)

34. Shaw, L G, Diluciano, A R, *J. Vinyl Techn.*, 5 3, 100-103 (1983)

35. Gale, G M, *RAPRA J.*, 105-107 (1974)

36. Jones, D R, Hawkes, J C, *Trans. J. Plast. Inst.*, 35 12, 773-781 (1967)

37. Clark, D, Woodley, T, *J. Vinyl Techn.*, 6 3, 114-116 (1984)

38. Yu, A J, Boulier, P, Sandhu, A, *J. Vinyl Techn.*, 6 3, 110-113 (1984)

39. Fredriksen, O, *J. Appl. Polym. Sci.*, 13 69-80 (1969)

40. Ritchie, P D, *'Plasticisers, Stabilisers and Fillers'*, Iliffe (1972)

41. Whissen, R R, Chapter 2 of Wake W C (ed) *'Fillers for Plastics'*, Iliffe (1971)

42. Hancock, M, *PVC Symp. 'Current Trends in PVC Technology'*, Loughborough University of Tehnology (1986)

43. Penn, W S, *'PVC Technology'*, Appl. Sci. Publ. (3rd Ed.) (1971)

44. Ferrigno, T H, Chapter 2 of Katz H S & Milewski J V (eds) *'Handbook of Fillers and Reinforcements for Plastics'*, Van Nostrand Reinhold, New York (1978)

45. Macturk, H M, Phillips, I, *Brit. Plast.*, 28 463-467 (1955)

46. McMurrer, M C, *Plast. Compound.*, 5 1, 88-96 (1982)

47. Fradon, J, *Plast. Compound.*, Red Book 75-78 (1981/82)

48. Gibson, P R S, *Plast.*, 31 1121-1124 (1966)

49. Wright, P J, *Patent: WO85/03715*, (1985)

50. Miller, W G, *Brit. Plast.*, 42 99-102 (1969)

51. Schlumpf, H P, Bilogan, W, *Kunstst.*, 73 5, 255-257 (1983)

52. Zolator, A M, *Mod. Plast.*, 48 84-88 (1971)

53. Chauffoureaux, J C, *Pure & Appl. Chem.*, 51 1125-1147 (1979)

54. Bilogan, W, Schlumpf, H P, *Kunstst.*, 70 6, 331-336 (1980)

55. Naik, S H, *M.S. Plastics Engineering Thesis*, University of Lowell, U.S.A (1978)

56. Danyliuk, I M, *Plast. Compound.*, 4 6, 47-52 (1981)

57. Kiefer, M, *J. Vinyl Techn.*, 5 2, 57-62 (1983)

58. Breuer, H, Haaf, F, Stabenow, J, *J. Macrom. Sci.-Phys.*, B(14) 3, 387-417 (1977)

59. Siegmann, A, English, L K, Bauer, E, Hittner, P, *Polym Eng. Sci.*, 24 11, 877-885 (1984)

60. Pezzin, G, *Plast. & Polym.*, 37 295-299 (1969)

61. Mooney, J, Rozkuska, K, *PVC Symp. 'Current trends in PVC technology'*, Loughborough University of Technology (1986)

62. Rabinovic, I S, *J. Vinyl Techn.*, 5 4, 179-182 (1983)

63. Fleischer, D, Fischer, E, *J. Macrom. Sci.-Phys.*, B(14) 1, 17-27 (1977)

64. Fleischer, D, Brandup, J, Heinzmann, D, *Kunstst.*, 67 6, 312-316 (1977)

65. Fleischer, D, Sherer, H, Brandup, J, *Angew Makromol Chem.*, 62 121-132 (1977)

66. Fleischer, D, Kloos, F, Brandup, J, *Angew Makromol Chem.*, 62 69-84 (1977)

67. Menges, G, Berndtsen, N, Opfermann, J, *J. Plast. & Rubb. Proc.*, 4 156-164 (1979)

68. Siegmann, A, Hiltner, A, *Polym. Eng. Sci.*, 24 11, 869-876 (1984)

69. Berens, A R, Folt, V L, *Trans. Soc. Rheol.*, 11 95-111 (1967)

70. Hori, Y, *Japan Plast.*, 3 2, 48 (1969)

71. Clark, M, Chapter 1 of Butters G (ed) *'Particulate Nature of PVC: Formation, Structure and Processing'*, Appl. Sci. Publ. (1982)

72. Allsopp, M W, Chapter 7 of Burgess R H (ed), *'Manufacture and Processing of PVC'*, Appl. Sci. Publ. (1982)

73. Hattori, T, Tanaka, K, Matsuo, M, *Polym. Eng. Sci.*, 12 3, 199-203 (1972)

74. Singleton, C, Isner, J, Gezovich, D M, Tsou, P K C, Geil, P H, Collins, E A, *Polym. Eng. Sci.*, 14 5, 371-381 (1974)

75. Uitenham, L C, Geil, P H, *J. Macrom. Sci.-Phys.*, B(20) 4, 593-622 (1981)

76. Munstedt, H, *J. Macrom. Sci.-Phys.*, B(14) 2, 195-213 (1977)

77. Sieglaff, C L, *Pure & Appl. Chem.*, 33 509-520 (1981)

78. Mandell, J F, Darwish, A Y, McGarry, F J, *J. Vinyl Techn.*, 4 3, 95-100 (1982)

79. Rosenthal, J, *J. Vinyl Techn.*, 5 3, 104-109 (1983)

80. Faulkner, P G, *J. Macrom. Sci.-Phys.*, B(11) 2, 251-279 (1975)

81. Krzewki, R J, Collins, E A, *J. Macrom. Sci.-Phys.*, B(20) 4, 443-464 (1981)

82. Geil, P H, *J. Macrom. Sci.-Phys.*, B(14) 1, 171 (1977)

83. Maddams, W F, Chapter 3 of Butters G (ed) *'Particulate Nature of PVC: Formation, Structure and Processing'*, Appl. Sci. Publ. (1982)

84. Vyvoda, J C, Gilbert, M, Hemsley, D A, *Polymer*, 21 109-115 (1980)

85. Pham, Q T, Millan, J, Madruga, E L, *Makromol Chem.*, 175 945 (1974)

86. Lemstra, P J, Keller, A, Cudby, M E A, *J. Polym. Sci.-Phys.*, 16 1507-1514 (1978)

87. Pezzin, G, *Pure & Appl. Chem.*, 26 241-254 (1971)

88. Gray, A, Gilbert, M, *Polymer*, 17 44-50 (1976)

89. Soni, P L, Geil, P H, Collins, E A, *J. Macrom. Sci.-Phys.*, B(20) 4, 479-503 (1981)

90. Wenig, W, *J. Polym. Sci.-Phys.*, 16 1635-1649 (1978)

91. Natta, G, Corradini, P, *J. Polym. Sci.*, 20 251-266 (1956)

92. Summers, J W, *J. Vinyl Techn.*, 3 2, 107-110 (1981)

93. Nakajima, A, Hamada, H, Hayashi, S, *Macrom. Chem.*, 95 40-51 (1966)

94. Ohta, S, Kajiyama, T, Takayanagi, M, *Polym. Eng. Sci.*, 16 7, 465-472 (1976)

95. Straff, R S, Uhlmann, D R, *J. Polym. Sci.-Phys.*, 14 353-365 (1976)

96. Singleton, C J, Stephenson, T, Isner, J, Geil, P H, Collins, E A, *J. Macrom. Sci.-Phys.*, B(14) 1, 29-86 (1977)

97. Ballad, D G H, Burgess, A N, Dekoninck, J M, Roberts, E A, *Polymer Papers*, 28 3-9 (1987)

98. Mammi, M, Nardi, V, *Nature*, 199 247 (1963)

99. Baker, C, Maddams, W F, Preedy, J E, *J. Polym. Sci.-Phys.*, 15 1041 (1977)

100. Brady, T E, Jabarin, S A, *Polym. Eng. Sci.*, 17 9, 686-690 (1977)

101. Parey, J, Menges. G, *J. Vinyl Techn.*, 3 3, 152-156 (1981)

102. Vidyikina, L I, Okladnov, N A, *Vysokomol Soedin*, 7 214 (1965)

103. Gonze, A, *Plast.*, 24 2, 49-53 (1971)

104. Rabinovitch, E B, *J. Vinyl Techn.*, 4 2, 62-66 (1982)

105. Berens, A R, Folt, V L, *Polym. Eng. Sci.*, 9 1, 27-34 (1969)

106. den Otter, J L, Wales, J L S, *PVC Technical Report (final)*, Centraal Laboratorium TNO, Delft (1976)

107. Portingell, G C, Chapter 4 of Butters G (ed) *'Particulate nature of PVC: Formation, Structure and Processing'*, Appl. Sci. Publ. (1982)

108. Benjamin, P, *Plast. & Rubb. Mat. & Appl.*, 5 151-160 (1980)

109. Summers, J W, Isner, J D, Rabinovitch, E B, *Polym. Eng. Sci.*, 20 2, 155-159 (1980)

110. Summers, J W, Rabinovitch, E B, *3rd Int. Symp. PVC*, P. 127 (1980)

111. Collins, E A, Metzger, A P, *Polym. Eng. Sci.*, 10 2, 57-65 (1970)

112. Allsopp, M W, Chapter 8 of Burgess R H (ed), *'Manufacture and Processing of PVC'*, Appl. Sci. Publ. (1982)

113. Marshall, D E, Higgs, R P, Obande, O P, *PVC Proc. II Int. Conf.*, P. 13 (1983)

114. Gilbert, M, Hemsley, D A, Mladonye, A, *Plast. & Rubb. Proc. Appl.*, 3 343-351 (1983)

115. Covas, J A, Gilbert, M, Marshall, D E, *To be published in Plast. & Rubb. Int: Proc. & Appl.*, (1988)

116. Terselius, B, Jansson, J F, *Plast. & Rubb. Proc. Appl.*, 5 3, 193-201 (1985)

117. Patel, S V, *PhD Thesis*, Loughborough University of Technology (1983)

118. Chartoff, R P, *Polymer*, 16 470-471 (1975)

119. Katchy, E M, *Kunstst.*, 71 9, 585-586 (1981)

120. BS3505 (1986)

121. ASTM D2152-67

122. Gilbert, M, Mulla, M I, *Polym. Test.*, 3 171-182 (1983)

123. Lamberty, M, *Plast. Mod. et Elastom.*, 26 10, 82-89 (1974)

124. Gray, A, *PVC Proc. Int. Conf.*, P. 10 (1978)

125. Terselius, B, Jansson, J F, Bystedt, J, *J. Macrom. Sci.-Phys.*, B(20) 3, 403-414 (1981)

126. Moore, D R, *PVC Proc. Int. Conf.*, P.11 (1978)

127. Han, C D, *'Rheology in Polymer Processing'*, Academic Press, New York (1976)

128. Gilbert, M, Vyvoda, J C, *Polymer*, 22 1134-1136 (1981)

129. Illers, K H, *J. Macrom. Sci.-Phys.*, B(14) 4, 471-482 (1977)

130. Patel, S V, Gilbert, M, *Plast. & Rubb. Proc. Appl.*, 5 1, 85-93 (1985)

131. Covas, J A, *Phd Thesis*, Loughborough University of Technology (1985)

132. Krüger, E, Menges, G, *'From A Theoretical PVC Processing Model To New Practical Processing Equipment'*, Institut For Kunststoffverarbeitung, Aachen (1984)

133. Berens, A R, Folt, V L, *Polym. Eng. Sci.*, 8 1, 5-10 (1968)

134. Tordella, J P, *J. Appl. Phys.*, 16 6 (1945)

135. den Otter, J L, *Rheologica Acta*, 8 355 (1969)

136. Krüger, E, *Adv. Polym. Techn.*, 5 1, 9-17 (1985)

137. Gale, G M, *Plast. & Polym.*, 38 183-191 (1970)

138. Guimon, C, *SPE-ANTEC*, 13 1085-1092 (1967)

139. Miadonye, A, *Phd Thesis*, Loughborough University of Technology (1983)

140. Hawkins, T, *J. Vinyl Techn.*, 5 2, 66-68 (1983)

141. Menges, I G, Klenk, P, *Plastverab.*, 17 791-800 (1966)

142. Stephenson, R C, *Kunstst.*, 71 9, 546-551 (1981)

143. Marhenkel, H, *Plast.*, 30 57-59 (1965)

144. Klenk, P, *Plastverab.*, 21 642-648, 723-730, 819-821, 881-888 (1970)

145. Reber, D, *SPE-ANTEC*, 708-710 (1974)

146. Gale, G M, *RAPRA J.*, 68-72 (1974)

147. Berndtsen, N, *Phd Thesis*, TH Aachen (D82) (1978)

148. Summers, J W, Rabinovitch, E B, Quisenberry, J, *J. Vinyl Techn.*, 7 **1**, 32-35 (1985)

149. Summers, J W, Rabinovitch, E B, Quisenberry, J G, *J. Vinyl Techn.*, 4 **2**, 67-69 (1982)

150. Terselius, B, Jansson, J F, Bystedt, J, *Plast. & Rubb. Proc. Appl.*, 5 **1**, 1-7 (1985)

151. Terselius, B, Jansson, J F, *Plast. & Rubb. Proc. Appl.*, 4 291-299 (1984)

152. Terselius, B, Jansson, J F, *Plast. & Rubb. Proc. Appl.*, 4 **4**, 285-290 (1984)

153. Pezzin, G, Ajroldi, G, Casiraghi, T, Garbuglio, C, Vittadini, G, *J. Appl. Polym. Sci.*, 16 1839-1849 (1972)

154. Humphreys, J, Volkmar, K, *PVC Proc. Int. Conf.*, P.4 (1978)

155. Ditto, P E, *J. Vinyl Techn.*, 4 **3**, 124-127 (1982)

156. Patrick, S G, McKenna, M P, *PVC Symp. 'Current trends in PVC technology'*, Loughborough University of Technology (1986)

157. Corvic Data Sheet: S68/173

158. Polcarb Data Sheet: Polcarb S

159. Associated Lead Manufacturers Ltd: Data Sheet: TBLS

160. Associated Lead Manufacturers Ltd: Data Sheet: Lead Stearate

161. Associated Lead Manufacturers Ltd: Data Sheet: Calcium Stearate

162. Sasol Marketing Ltd: Data Sheet: Sasolwaks H1

163. Hoechst: Data Sheet: PE520 (1977)

164. Henkel: Data Sheet: Loxiol G15 (1982)

165. Henkel: Data Sheet: Loxiol G12 (1982)

166. Pristerene: Data Sheet: Stearic acid 4903

167. Oletec: Data Sheet: Oletec 6009

168. Pepper, S T, *MSc Thesis*, Loughborough University of Technology (1984)

169. Barth, H J, *Kunstst.*, 71 **10**, 636-642 (1981)

170. Hemsley, D A, Higgs, R P, Miadonye, A, *Polymer Comm.*, 24 103-106 (1983)

171. BS 903 **Part A2**, (1971)

172. Rosand Instrumented Impact Test Systems *Company Manual for Drop Weight Tester 5A*, (1986)

173. ISO/DP 6603/2.3: Draft (1987)

174. Gutteridge, P A, Hooley, C J, Moore, D R, Turner, S, Williams, M J, *Kunstst*, 72 **9**, 543-547 (1982)

175. Bowerman, H H, McKelvey, J M, *Polym. Eng. Sci.*, 8 **4**, 310-318 (1968)

176. den Otter, J L, *PVC Technical Report (No 2)*, Centraal Laboratorium TNO, Delft (1974)

177. Lead Industries Group Ltd. Report *'Calcium Carbonate Fillers, And Their Effect On The Fusion, And Impact Strength Of PVC For Pipe'*, PM/25/82 Perivale, London (1982)

178. Strijbos, S, *Powder Techn.*, 18 209-214 (1977)

179. Obande, O P, *Phd Thesis*, Loughborough University of Technology (1983)

180. Katchy, E M, *J. Appl. Polym. Sci.*, 28 1847-1869 (1983)

181. Rauwendaal, C J, *Polym. Eng. Sci.*, 21 **16**, 1092-1100 (1981)

182. Potente, H, Schultheis, S M, *Kunstst.*, 77 **4**, 401-404 (1987)

183. Janssen, L P B M, *'Twin Screw Extrusion'*, Elsevier Sci. Publ. Corp. (1978)

184. Cogswell, F N, *'Polymer Melt Rheology'*, George Godwin (1981)

185. Zolotor, A M, *Mod. Plast.*, 47 12, 68-72 (1970)

186. Tadmor, Z, *Ind. Eng. Chem. Fundam.*, 15 346 (1976)

187. McKelvey, J M, *'Polymer Processing'*, John Wiley & Sons, New York (1962)

188. ICI Tech. Service Note W 121 ICI Vinyls group (1980)

189. Gotham, K V, Hitch, M J, *Brit. Polym. J.*, 10 47-52 (1978)

190. Pepper, S T, *Unpublished results* (1986)

191. Howard, G J, Shanks, R A, *J. Appl. Polym. Sci.*, 26 3099 (1981)

192. Nielsen, L E, *J. Appl. Polym. Sci*, 10 97-103 (1966)

193. Alter, H, *J. Appl. Polym. Sci.*, 9 1525-1531 (1965)

194. Oberst, H, Retting, W, *J. Macrom. Sci.-Phys.*, B(5) 3, 559-590 (1971)

195. Gonze, A, Chauffoureaux, J C, *Pure & Appl. Chem.*, 35 317-351 (1973)

196. Cross, A, Haward, R N, Mills, N J, *Polymer*, 20 288-294 (1979)

197. Vincent, P I, *Polymer*, 1 7 (1960)

198. Parey, J, Kruger, E, *Kunstst.*, 74 1, 39-42 (1984)

199. Marshall, G P, *Plast. & Rubb. Proc. Appl.*, 2 2, 169-182 (1982)

200. Stapfer, C H, Hampson, D G, Dworkin, R D, *SPE-ANTEC*, 14 276 (1968)

201. Collins, E A, Hartitz, E, *Plast. Design & Proc.*, 15-20 (1978)

202. Cookson plc Central Research Laboratories Report *'Performance of Hydrocarbon Lubricants in a High Speed Mixer in Filled and Unfilled PVC Formulations'*, PM/5/84 Perivale, London (1984)

203. Obande, O P, Gilbert, M, *To be published* (1988)

204. Mai, Y W, Kerr, P R, *J. Vinyl Techn.*, 7 **4**, 130-139 (1985)

APPENDIX A

FORMULATION DETAILS

A1.1 COMPOSITE STABILISER/LUBRICANT SYSTEM

TABLE A. 1

Properties of TBLS, NLSt and Cast

Property	TBLS [159]	NLSt [160]	Cast [161]
Formula	$3PbO.PbSO_4.H_2O$	$Pb(CH_3(CH_2)_{16}COO)_2$	$Ca(CH_3(CH_2)_{16}COO)_2$
Appearance	cream/white	soft white	white
Specific gravity	6·3	1·4	1·05
PbO content (%)	82-84	27-29	-
Safe PbO (%)	61-63	27-29	-
Melting point (°C)	-	102-108	121 †
Moisture content (%)	0·2	0·25	3·0

† Determined by DSC

A1.2 LUBRICANT DETAILS

TABLE A.2

Primary lubricant properties

	Sasol H1 [162]	Hoechst PE520 [163]	Loxiol G15 [164]	Loxiol G12 [165]	Pristerene 4903 [166]	Oletec 6009 [167]
Manufacturer	Sasol	Hoechst	Henkol	Henkol	Pristerene	Oletec
Description	High M.pt Paraffin	Polyethylene wax	Hydrogenated castor oil	Fatty acid ester of glycerine	Stearic acid	Low M.pt paraffin
Addition (phr)	0·1	0·2	1·0	1·0	1·0	0·2 & 1·0
Solidification point (°C)	98	118-123	-	-	-	59
Drop point (°C)	-	≈108	64-90	57-60	53-55	-
Melting point †	95	105	82	60	54	56
Acid value (mg KOH/g)	<0·1	0	<5	<2	≈2	-
S.G/Density (-/gcm³)	0·94 @25°C	0·92-0·94 @20°C	0·895 @100°C	0·5-0·915 @80°C	-	-
Viscosity (m.pa.s/cs)	-	≈1000 @140°C	24 @100°C	25-35 @80°C	-	4·25 cs @100°C

† DSC measurement (°C)

APPENDIX B

ASH ANALYSIS

B1.1 CALIBRATION GRAPH FOR ASH CONTENT

A number of blends with a filler content ranging from 0⇒120 phr were hand mixed and ashed as described in §2.5.1. The resultant graph and fitted curve was then used to calculate the filler content of the Henschel dry blended samples.

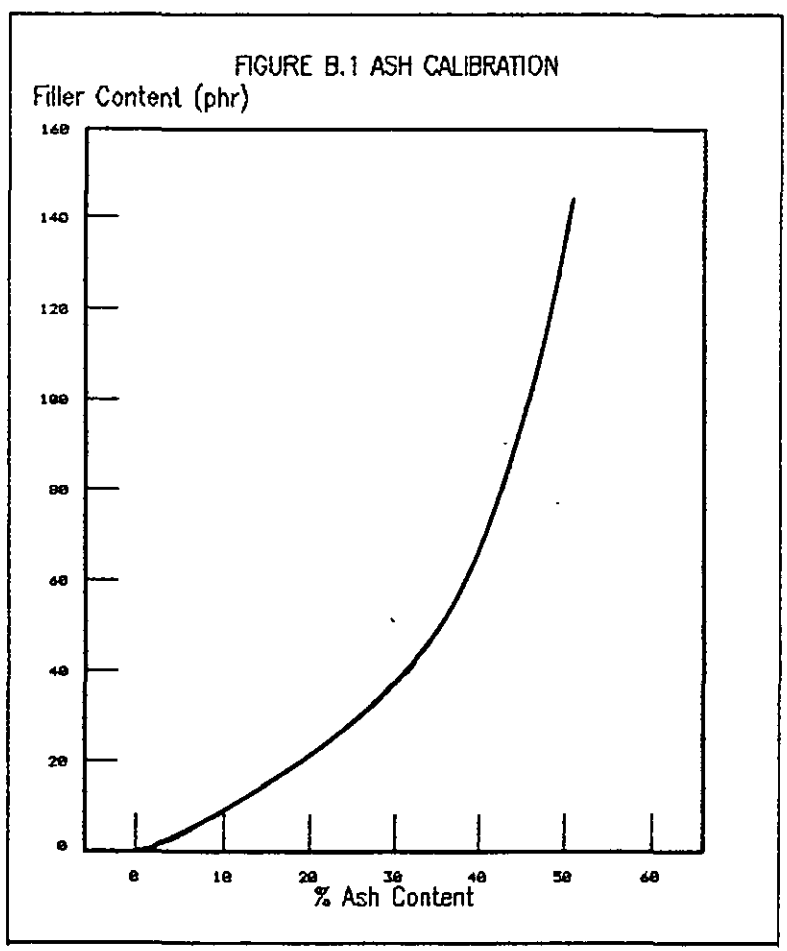

Polynomial regression equation:

$Y = 0{\cdot}078 + 0{\cdot}353x + 0{\cdot}0792x^2 - 0{\cdot}0032x^3 + 0{\cdot}0000051x^4$

Correlation [r] = 0·9987

Standard deviation of errors [sde] = 1.886

APPENDIX C

SKETCH OF SPLIT PIPE IMPACT RIG

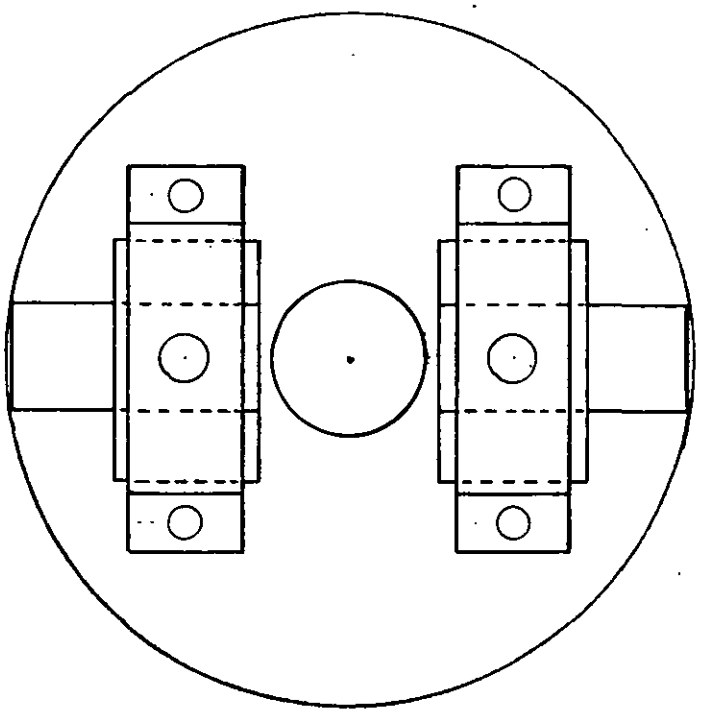

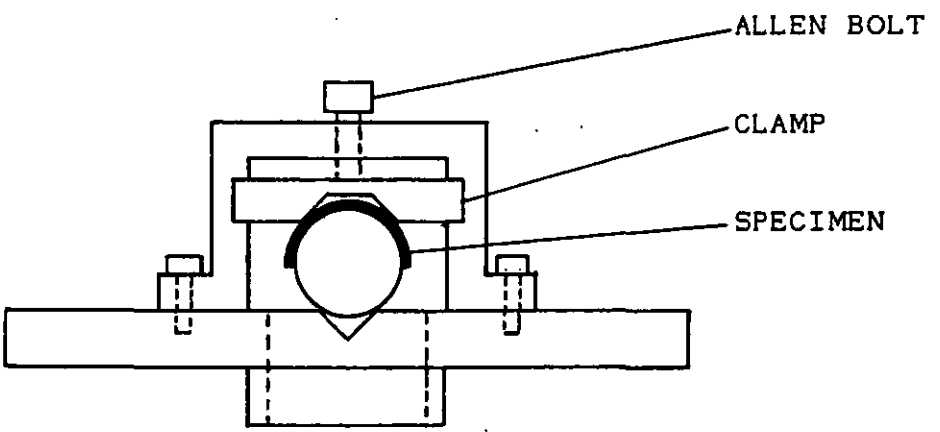

TITLE : Roeand impact rig
SCALE : 1:2 (mm)
DRAWN : S. T. Pepper IPT
MATERIAL: Mild steel

APPENDIX D

EXTRUDER RESULTS

TABLE D. 1

Extruder temperatures

Pipe code	EXTRUDER TEMPERATURES				
	Zone one (°C)	Zone two (°C)	Oil reservoir (°C)	Adaptor TM1 (°C)	Head TM2 (°C)
0A	160	160	142	156	170
1A	158	160	141	153	168
2A	158	161	141	152	164
3A	158	160	141	157	168
4A	158	161	141	159	164
5A	158	162	141	152	165
0B	160	160	142	156	175
1B	158	160	141	153	170
2B	158	161	141	158	168
3B	158	160	141	157	168
4B	158	162	142	160	169
5B	159	162	141	155	169
0C	160	160	142	156	183
1C	159	161	141	158	176
2C	158	161	141	158	177
3C	159	161	141	158	177
4C	159	161	141	158	178
5C	159	162	141	160	177
0D	173	173	142	168	183
1D	172	175	141	165	180
2D	173	176	142	165	181
3D	172	176	141	165	182
4D	172	175	142	166	183
5D	173	175	142	167	182
0E	173	173	142	168	192
1E	173	175	142	169	187
2E	173	175	141	169	186
3E	173	175	142	170	187
4E	173	175	142	171	187
5E	173	175	142	171	188
0F	193	191	142	184	203
1F	191	193	142	185	194
2F	190	193	142	185	197
3F	191	193	143	186	197
4F	191	193	143	186	198
5F	191	193	143	187	198

TABLE D. 1 (cont)

Extruder temperatures

Pipe code	EXTRUDER TEMPERATURES Zone one (°C)	Zone two (°C)	Oil reservoir (°C)	Adaptor TM1 (°C)	Head TM2 (°C)
0E-	172	172	142	169	187
0EA	172	172	142	169	187
0EB	172	172	142	170	186
0EC	172	172	142	170	186
0ED	173	173	142	169	187
0EE	173	173	142	170	186
0EF	173	173	142	170	187
0EG	173	173	142	169	187
0EH	173	173	142	170	187
3E-	173	173	143	171	189
3EA	173	173	143	171	189
3EB	173	173	143	171	190
3EC	172	172	143	170	188
3ED	173	173	144	171	189
3EE	172	172	143	170	188
3EF	173	173	143	170	189
3EG	173	173	143	170	189
3EH	173	173	143	171	190

TABLE D. 2

Mechanical energy: filler content

Pipe code	EXPERIMENTAL VALUE Torque TQ (%)	Output $\dot{m}$ (g/min)	Q (rev.%/g)	Pipe code	EXPERIMENTAL VALUE Torque TQ (%)	Output $\dot{m}$ (g/min)	Q (rev.%/g)
0A	62	130	40·1	1A	65	130	42·0
0B	53	130	31·4	1B	57	127	34·0
0C	47·5	130	26·1	1C	48·5	131	26·9
0D	43	131	21·6	1D	45	136	22·6
0E	42	131	20·6	1E	42	136	19·3
0F	38	130	16·9	1F	35·5	136	13·9
2A	74	133	49·1	3A	84	127	62·8
2B	66	134	42·7	3B	78	129	56·0
2C	51	128	29·9	3C	59	127	38·1
2D	47·5	125	27·1	3D	54	126	33·4
2E	44·5	134	22·5	3E	51	135	28·4
2F	37·5	135	15·8	3F	42·5	130	21·3
4A	94	133	69·4	5A	109	134	83·0
4B	91	141	62·8	5B	105	134	79·2
4C	67	129	45·3	5C	83	139	56·5
4D	59	135	35·8	5D	62	140	37·2
4E	60	132	37·6	5E	62	138	37·8
4F	48·5	132	26·7	5F	53	135	30·2

TABLE D. 3

Extrusion pressure: filler content

Pipe code	EXPERIMENTAL VALUE P1 pressure (Bar)	Inlet pressure (Bar)	Head pressure (Bar)	Pipe code	EXPERIMENTAL VALUE P1 pressure (Bar)	Inlet pressure (Bar)	Head pressure (bar)
0A	31	269	164	1A	39	307	167
0B	2·5	236	131	1B	6	280	141
0C	0	202	105	1C	0	242	123
0D	0	175	97	1D	0	223	123
0E	0	165	92	1E	0	212	100
0F	0	127	80	1F	0	154	74
2A	62	348	192	3A	77	415	226
2B	27	329	170	3B	49	394	207
2C	0	274	145	3C	0	334	184
2D	0	265	145	3D	0	317	174
2E	0	246	122	3E	0	286	152
2F	0	191	95	3F	0	217	122
4A	87	436	266	5A	139	518	315
4B	73	420	248	5B	120	496	290
4C	0	374	217	5C	27	432	241
4D	0	362	206	5D	0	400	228
4E	0	333	193	5E	0	360	203
4F	0	237	152	5F	0	260	179

TABLE D. 4

Extrusion results: additive study

Pipe code	EXTRUDER RESULTS Torque TQ (%)	Output ṁ (g/min)	Q (rev.%/g)	P1 pressure (Bar)	Inlet pressure (Bar)	Head pressure (Bar)
OE-	39	118	19·7	0	112	85
OEA	38	117	18·8	0	113	85
OEB	30·5	117	10·7	0	100	74
OEC	38	113	19·5	0	127	106
OED	39·5	112	21·3	0	135	110
OEE	49	118	30·2	6	179	142
OEF	35	117	15·6	0	123	84
OEG	39	107	21·7	0	126	100
OEH	60	112	44·1	30	228	190
3E-	33·5	50	32·7	0	131	119
3EA	36	50	39·0	0	154	136
3EB	27	52	15·6	0	77	75
3EC	34	52	32·9	0	143	125
3ED	35	57	32·0	0	134	127
3EE	35	55	33·0	0	138	119
3EF	28	50	18·9	0	74	70
3EG	31	41	32·2	0	79	101
3EH	33	41	38·5	0	114	105

APPENDIX E

FILTERING OF IMPACT TRACES

FIGURE E. 1

Impact trace of 5C: unfiltered

Drive: 3
Sample:
Details:
Date: 07/05/86
Time: 23:39:08
Mass: 25Kg
Temp: 20'C

PEAK INFORMATION
Force=275.2 N
Deflection=1.587 mm
Energy=0.196 J
Gradient=21.92 KN/m

FAILURE INFORMATION
Deflection=44.68 mm
Energy=4.265 J

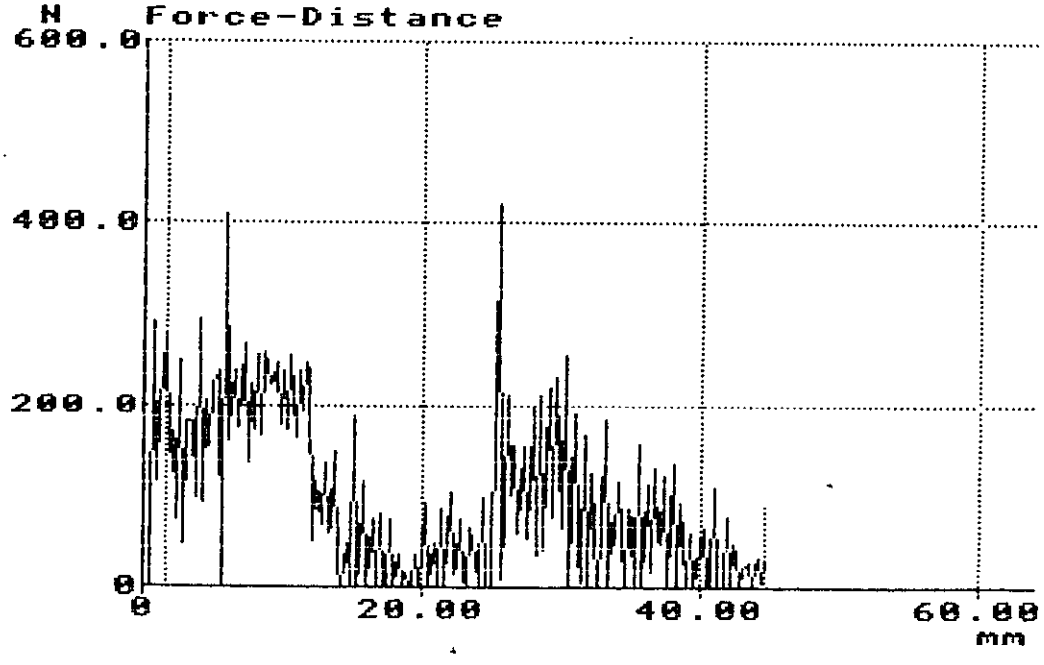

FIGURE E. 2

Impact trace of 5C: Over-filtered

Drive: 3
Sample:
Details:
Date: 07/05/86
Time: 23:39:08
Mass: 25Kg
Temp: 20'C

PEAK INFORMATION
Force=173.5 N
Deflection=2.117 mm
Energy=0.235 J

FAILURE INFORMATION
Deflection=49.80 mm
Energy=4.382 J

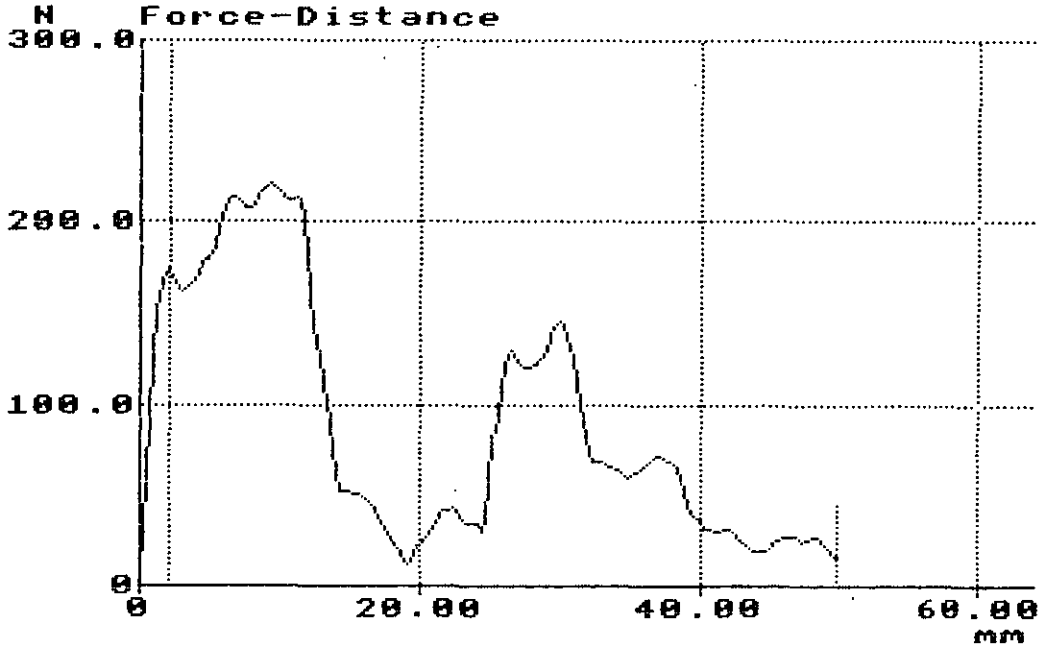

FIGURE E. 3

Impact trace of 5C: Moderate filter

Drive: 3
Sample:
Details:
Date: 07/05/86
Time: 23:39:08
Mass: 25Kg
Temp: 20'C

PEAK INFORMATION
Force=211.0 N
Deflection=1.588 mm
Energy=0.198 J

FAILURE INFORMATION
Deflection=43.62 mm
Energy=4.242 J

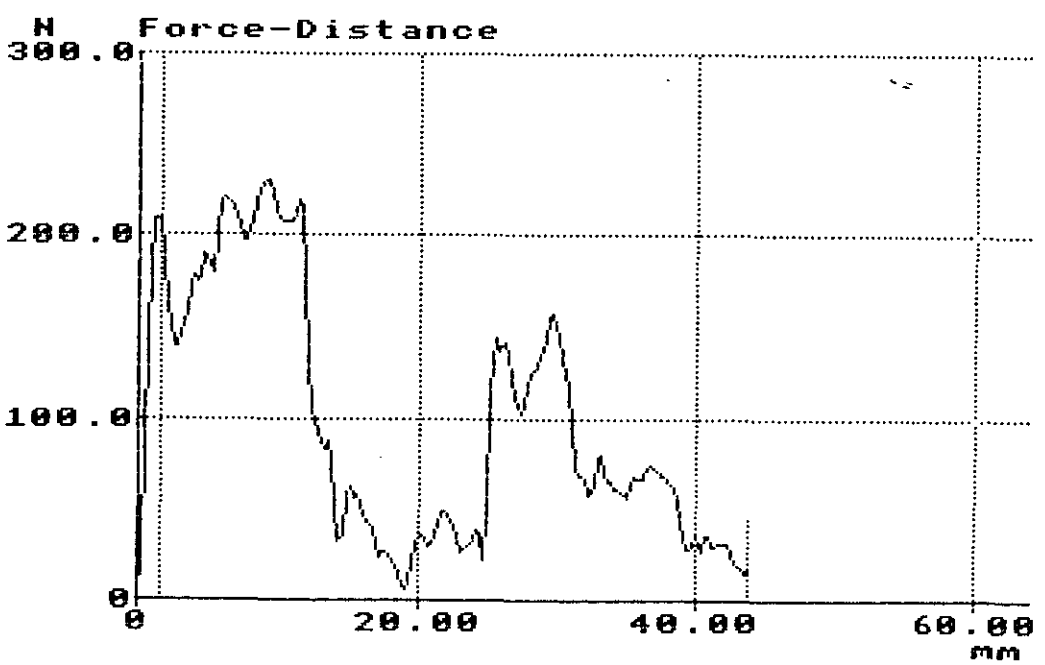

APPENDIX F

IMPACT PROPERTIES

TABLE F. 1

Impact properties: Influence of test temperature

Test temp (°C)	Peak Force (N/mm)	Peak Deflection (mm)	Peak Energy (J/mm)	Failure Deflection (mm)	Failure Energy (J/mm) E_F	s.dt	Maximum Gradient (KNmm/m)	Type of Failure
0F: 0 phr								
-20	166	1·54	0·1	7·21	0·8	0·1	152	B
-10	198	3·19	0·4	8·41	1·0	0·2	161	B
0	1117	11·63	6·0	14·43	7·6	1·6	150	B/D
10	1170	12·67	7·1	15·97	9·1	0·8	130	B/D
20	1261	14·90	9·9	20·64	12·5	0·7	119	D
41	1317	16·45	11·2	19·79	14·1	0·9	117	D
60	1140	16·57	10·1	20·05	12·5	1·0	110	D
80	994	17·15	9·5	20·74	11·8	0·4	96	D
100	921	18·37	9·4	23·98	12·3	1·2	76	D
1F: 8·5 phr								
-20	217	2·11	0·3	6·33	0·9	0·2	162	B
-10	1134	10·57	5·7	12·12	6·6	1·2	144	B/D
0	1117	11·76	6·2	13·51	7·3	1·2	126	B/D
10	1182	12·78	7·2	15·35	8·7	1·0	123	B/D
20	1293	15·46	10·4	17·89	12·1	0·7	127	D
41	1250	17·31	11·7	19·82	13·6	0·5	105	D
60	1158	17·27	10·6	21·11	13·3	0·2	99	D
80	937	17·86	9·5	21·31	11·4	0·6	84	D
100	869	18·40	9·1	23·14	11·9	0·5	72	D
2F: 18·1 phr								
-20	191	4·51	0·6	7·18	0·9	0·1	131	B
-10	203	5·44	0·8	7·22	1·0	0·1	148	B
0	180	3·08	0·4	9·26	1·2	0·3	142	B
10	829	9·26	3·6	10·45	4·1	1·0	119	B/D
20	1034	11·84	5·8	13·05	6·3	0·7	116	B/D
41	1059	13·86	7·2	15·85	8·1	1·3	100	B/D
60	1002	16·82	8·8	19·88	10·1	0·6	81	D
80	908	16·84	8·3	20·21	9·7	0·3	78	D
100	876	17·88	8·7	21·11	10·1	0·5	72	D

B = Brittle. B/D = Brittle/Ductile. D = Ductile

† s.d = Sample standard deviation

TABLE F. 1 Cont.

Impact properties: Influence of test temperature

Test temp (°C)	Peak Force (N/mm)	Peak Deflection (mm)	Peak Energy (J/mm)	Failure Deflection (mm)	Failure Energy (J/mm) E_F	s.dt	Maximum Gradient (KNmm/m)	Type of Failure
3F: 27·3 phr								
-20	163	5·80	0·7	8·57	1·0	0·2	113	B
-10	161	5·59	0·6	7·44	0·8	0·1	107	B
0	188	5·04	0·7	7·48	0·9	0·1	119	B
10	185	5·12	0·7	7·70	1·0	0·1	107	B
20	198	5·39	0·7	7·75	1·0	0·2	137	B
41	402	6·62	1·4	8·62	1·7	0·4	96	B/D
60	467	8·32	2·0	10·36	2·4	1·0	71	B/D
80	624	12·06	3·8	14·81	4·5	0·8	66	B/D
100	691	15·12	5·2	18·11	6·1	0·8	60	D
4F: 35·6 phr								
-20	214	3·54	0·5	7·94	1·2	0·2	238	B
-10	172	5·84	0·7	8·90	1·1	0·2	114	B
0	195	6·15	0·9	9·45	1·3	0·3	120	B
10	183	6·74	0·9	11·86	1·5	0·4	101	B
20	166	5·71	0·9	8·03	1·3	0·1	155	B
41	180	6·96	0·8	10·30	1·1	0·2	107	B
60	191	5·91	0·8	8·49	1·1	0·1	87	B
80	371	7·70	1·5	11·61	2·2	0·1	60	B/D
100	344	8·55	1·5	17·14	2·6	0·5	48	B/D
5F: 40 phr								
-20	188	1·11	0·1	7·00	1·0	0·1	254	B
-10	166	5·39	0·7	8·30	1·0	0·1	110	B
0	168	5·95	0·7	9·09	1·1	0·2	108	B
10	167	6·12	0·7	8·48	1·0	0·1	99	B
20	184	6·15	0·9	9·00	1·2	0·3	151	B
41	180	6·60	0·9	12·57	1·6	0·3	102	B
60	183	5·44	0·6	8·52	1·0	0·3	81	B
80	194	5·84	0·7	15·00	1·8	0·2	37	B
100	238	5·99	0·8	13·90	1·8	0·2	44	B/D

B = Brittle. B/D = Brittle/Ductile. D = Ductile
† s.d = Sample standard deviation